

AD\_\_\_\_\_

Award Number: DAMD17-00-1-0194

TITLE: Exploiting and NQ01-Directed, Calpain-Medicated Apoptotic  
Pathway for Breast Cancer Therapy

PRINCIPAL INVESTIGATOR: Mark W. Wagner  
David A. Boothman, Ph.D.

CONTRACTING ORGANIZATION: Case Western Reserve University  
Cleveland, Ohio 44106-7015

REPORT DATE: April 2003

TYPE OF REPORT: Annual Summary

PREPARED FOR: U.S. Army Medical Research and Materiel Command  
Fort Detrick, Maryland 21702-5012

DISTRIBUTION STATEMENT: Approved for Public Release;  
Distribution Unlimited

The views, opinions and/or findings contained in this report are those of the author(s) and should not be construed as an official Department of the Army position, policy or decision unless so designated by other documentation.

20031003 070

REPORT DOCUMENTATION PAGE			Form Approved OMB No. 074-0188	
Public reporting burden for this collection of information is estimated to average 1 hour per response, including the time for reviewing instructions, searching existing data sources, gathering and maintaining the data needed, and completing and reviewing this collection of information. Send comments regarding this burden estimate or any other aspect of this collection of information, including suggestions for reducing this burden to Washington Headquarters Services, Directorate for Information Operations and Reports, 1215 Jefferson Davis Highway, Suite 1204, Arlington, VA 22202-4302, and to the Office of Management and Budget, Paperwork Reduction Project (0704-0188), Washington, DC 20503				
1. AGENCY USE ONLY (Leave blank)		2. REPORT DATE April 2003		3. REPORT TYPE AND DATES COVERED Annual Summary (6 Mar 2000 - 5 Mar 2003)
4. TITLE AND SUBTITLE Exploiting and NQ01-Directed, Calpain-Medicated Apoptotic Pathway for Breast Cancer Therapy			5. FUNDING NUMBERS DAMD17-00-1-0194	
6. AUTHOR(S) Mark W. Wagner David A. Boothman, Ph.D.				
7. PERFORMING ORGANIZATION NAME(S) AND ADDRESS(ES) Case Western Reserve University Cleveland, Ohio 44106-7015  E-Mail: mww4@po.cwru.edu			8. PERFORMING ORGANIZATION REPORT NUMBER	
9. SPONSORING / MONITORING AGENCY NAME(S) AND ADDRESS(ES) U.S. Army Medical Research and Materiel Command Fort Detrick, Maryland 21702-5012			10. SPONSORING / MONITORING AGENCY REPORT NUMBER	
11. SUPPLEMENTARY NOTES				
12a. DISTRIBUTION / AVAILABILITY STATEMENT Approved for Public Release; Distribution Unlimited				12b. DISTRIBUTION CODE
13. ABSTRACT (Maximum 200 Words)  The purpose of this proposal was to further understand the molecular mechanisms of $\beta$ -lap-induced apoptosis, and its ability to target cancer over normal cells. We believe that $\beta$ -lap induces apoptosis through changes in intracellular calcium homeostasis and $\mu$ -calpain activation. This will be tested via two specific aims using NQ01-expressing and non-expressing ( $\beta$ -lap sensitive and resistant, respectively) MDA-MB-468 breast cancer cells as a model system. The first aim was to determine changes in intracellular calcium homeostasis before and after $\beta$ -lap exposure. Fluorescence calcium dye indicators will be used to determine changes in intracellular calcium levels, as well as GFP-calmodulin calcium indicators (cameleons, that are targeted to intracellular organelles), for a more accurate determination of where calcium changes are occurring. Analysis of apoptosis via flow cytometric analyses will be performed in breast cancer cells in the presence of extracellular calcium chelators, to determine if changes in intracellular calcium concentrations are critical for DNA fragmentation and cell death. The second aim will be to determine the role of calpain and its downstream targets in $\beta$ -lap-induced apoptosis. Calpain activation will be assessed using fluorogenic substrates. Substrate cleavage analyses, <i>in vitro</i> , will be performed using specific downstream targets, as determined from western blot timecourse analyses (PARP, lamin B, and p53). Confocal microscopy with indirect immunofluorescence and Green Fluorescent Protein (GFP)-tagged $\mu$ -calpain will be used to examine calpain translocation and co-localization studies with downstream targets.				
14. SUBJECT TERMS Therapeutics; apoptosis; NQ01/DT-deaphorase; calpain; calcium				15. NUMBER OF PAGES 92
				16. PRICE CODE
17. SECURITY CLASSIFICATION OF REPORT Unclassified	18. SECURITY CLASSIFICATION OF THIS PAGE Unclassified	19. SECURITY CLASSIFICATION OF ABSTRACT Unclassified	20. LIMITATION OF ABSTRACT Unlimited	

## FOREWORD

Opinions, interpretations, conclusions and recommendations are those of the author and are not necessarily endorsed by the U.S. Army.

XX Where copyrighted material is quoted, permission has been obtained to use such material.

XX Where material from documents designated for limited distribution is quoted, permission has been obtained to use the material.

XX Citations of commercial organizations and trade names in this report do not constitute an official Department of Army endorsement or approval of the products or services of these organizations.

   In conducting research using animals, the investigator(s) adhered to the "Guide for the Care and Use of Laboratory Animals," prepared by the Committee on Care and use of Laboratory Animals of the Institute of Laboratory Resources, national Research Council (NIH Publication No. 86-23, Revised 1985).

N/A For the protection of human subjects, the investigator(s) adhered to policies of applicable Federal Law 45 CFR 46.

XX In conducting research utilizing recombinant DNA technology, the investigator(s) adhered to current guidelines promulgated by the National Institutes of Health.

XX In the conduct of research utilizing recombinant DNA, the investigator(s) adhered to the NIH Guidelines for Research Involving Recombinant DNA Molecules.

XX In the conduct of research involving hazardous organisms, the investigator(s) adhered to the CDC-NIH Guide for Biosafety in Microbiological and Biomedical Laboratories.

Mark Wynn  
PI - Signature

7/15/03  
Date:

## Table of Contents

Cover.....	i
SF 298.....	1
Foreword.....	2
Table of Contents.....	3
Introduction.....	4
Body.....	5
Key Research Accomplishments.....	24
Reportable Outcomes.....	25
Conclusions.....	28
References.....	29
Appendices.....	35



## INTRODUCTION:

$\beta$ -Lapachone ( $\beta$ -lap, 3,4-dihydro-2,2-dimethyl-2H-naphto [1,2b] pyran-5,6-dione) is a novel agent used by our laboratory to kill a number of breast cancer cell lines through an unique apoptotic pathway. It is a naturally occurring product present in the bark of the Lapacho tree native to South America.  $\beta$ -Lap has antitumor activity against a variety of human cancers, including colon, prostate, promyelocytic leukemia and breast.  $\beta$ -Lap kills cells exclusively by apoptosis and independently of p53 status, which is critical since many cancers exhibit loss of p53 tumor suppressor function.  $\beta$ -Lap appears to be activated by DT-diaphorase (NQO1), and cells deficient for this enzyme are less sensitive to  $\beta$ -lap's downstream effects, and ultimately cell death. Furthermore, NQO1-expressing MCF-7 breast cancer cells co-treated with dicumoral, a specific inhibitor of NQO1, are protected against  $\beta$ -lap-induced cytotoxicity and apoptosis. Importantly, NQO1 appears to be more abundantly expressed in a number of breast tumors compared with surrounding normal tissue. This observation, more than any other, suggests that drugs that are activated by NQO1 may show significant tumor specific activity against human breast cancer.

The purpose of this proposal was to further understand the molecular mechanisms of  $\beta$ -lap-induced apoptosis, and its ability to target cancer cells over normal cells. **We believe that  $\beta$ -lap induces apoptosis through changes in intracellular calcium homeostasis and calpain activation. This was tested via two specific aims using NQO1-expressing and non-expressing ( $\beta$ -lap sensitive and resistant, respectively) MDA-MB-468 breast cancer cells as a model system.**

The first aim is to determine changes in intracellular calcium homeostasis before and after  $\beta$ -lap exposure. Alterations in intracellular calcium homeostasis are commonly observed in apoptosis. Fluorescent calcium dye indicators will be used to determine changes in intracellular calcium levels, as well as GFP-calmodulin calcium indicators (cameleons, that are targeted to intracellular organelles), for a more accurate determination of where calcium changes are occurring. Analysis of apoptosis via flow cytometric analyses will be performed in breast cancer cells after  $\beta$ -lap treatment in the presence of extracellular calcium chelators, to determine if changes in intracellular calcium concentrations are critical for DNA fragmentation and cell death.

The second aim will be to determine the role of  $\mu$ -calpain and its downstream targets in  $\beta$ -lap-induced apoptosis.  $\mu$ -Calpain activation will be assessed using fluorogenic substrates. Substrate cleavage analyses, *in vitro*, will be performed using specific downstream targets, as determined from western blot timecourse analyses (PARP, lamin B, and p53). Confocal microscopy with indirect immunofluorescence and Green Fluorescent Protein (GFP)-tagged  $\mu$ -calpain will be used to examine calpain translocation and co-localization studies with downstream targets.

Understanding the molecular mechanisms of  $\beta$ -lap-induced apoptosis will help better target this agent for breast cancer therapy, as well as provide a rationale for future drug development and/or modulation of existing agents. In addition, a novel  $\mu$ -calpain-mediated apoptotic pathway will be elucidated using  $\beta$ -lap as an initiating agent.

## BODY OF GRANT UPDATE:

### **Aim 1: To determine the effect of $\beta$ -lap on intracellular calcium homeostasis and apoptosis**

#### *Task 1:*

1. Determine changes in intracellular calcium homeostasis using the fluorescent dye indicator, fura-2, in MDA-MB-468 (plus vector alone) compared to MDA-MB-468 breast cancer cells transfected with NQO1 expression vectors. Several clones will be tested as well as a variety of breast cancer cell lines treated with  $\beta$ -lap, +/- dicumarol, a specific inhibitor of NQO1 (*months 1-12*).

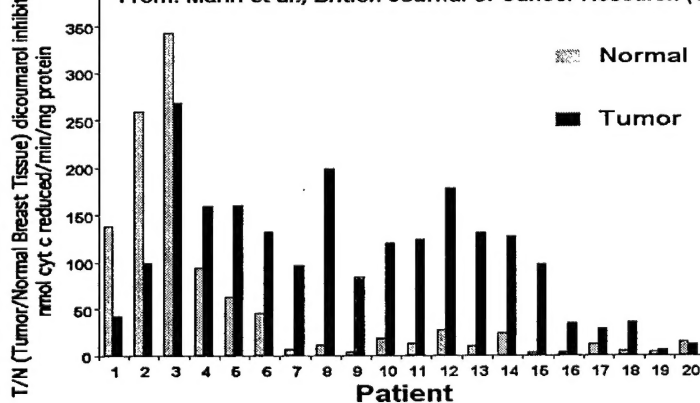
This task was completed and the data published by Dr. Colleen Tagliarino, who received her Ph.D. in 2001. Publications resulting from these studies demonstrated a role for NQO1 (Pink et al., JBC, 2000; Planchon et al., Exp Cell Res., 2001) and calcium (Tagliarino et al., J. Biol. Chem., 2001) in  $\beta$ -lap-mediated apoptotic responses. These results are briefly summarized below:

**NQO1 as an intracellular determinant of quinone xenobiotic toxicity.** NQO1 (NAD(P)H:quinone oxidoreductase, E.C. 1.6.99.2, a.k.a., xip3) is a flavoprotein found in most eukaryotic cells. The human NQO1 gene encodes a 30 kDa protein that is expressed in a tissue-dependent manner. NQO1 is abundant in the liver of most mammals, except humans (1-4). More importantly, NQO1 is over-expressed up to 20-fold in a majority of breast (Fig. 1) v. adjacent normal tissue (1-4). This observation, more than any other, suggests that drugs activated by NQO1, (e.g., mitomycin C (MMC), streptonigrin, or EO9) should show significant anti-tumor activity against NQO1-overexpressing breast cancers.  $\beta$ -Lap and its derivatives belong to this class of quinones (see below).

NQO1 catalyzes a two-electron reduction of various quinones, using NAD(P)H as electron donors, resulting in hydroquinones. This reaction bypasses the unstable and highly reactive semiquinone intermediate. Semiquinones are excellent free radical generators, initiating a redox cycle causing superoxide formation (5). Superoxide can dismutate to hydrogen peroxide, and hydroxyl radicals are then formed by the iron-catalyzed reduction of peroxide via Fenton reactions (6). All of these highly reactive species may directly react with DNA or other cellular macromolecules, such as lipids and proteins, causing damage to the cell. NQO1-mediated production of the hydroquinone, which can be readily conjugated with glutathione and excreted from the cell, constitutes a protective mechanism against quinone-mediated damage (7, 8). NQO1 activity, thus, protects cells from the toxicity of naturally occurring xenobiotics containing quinone moieties, and may be the evolutionary reason for the damage-inducibility of this gene (7-13). NQO1 knock-out (KO) mice show enhanced sensitivity to cytotoxic

**Figure 1. Elevated NQO1 in human tumor v. normal breast tissue.**

From: Marin et al., British Journal of Cancer Research (1997)



(e.g., menadione) and carcinogenic quinones, reinforcing the notion that NQO1 detoxifies quinone xenobiotics (14).

Unfortunately for the cell, NQO1 also reduces certain quinones to toxic products, causing 'activation' of these drugs (8, 15). The alkylating activity of MMC is revealed through a two-electron reduction by NQO1, or through two separate one-electron reductions by other reductases (e.g., NADH:cytochrome-b<sub>5</sub> reductase (b<sub>5</sub>R) and NADPH:cytochrome P450 reductase (P450R)) (10, 16-19). A correlation between MMC sensitivity and NQO1 activity in the sixty-nine cell lines from the NCI human tumor cell panel was noted (20). Thus, NQO1 is a critical activator of MMC, and other quinone-containing antitumor agents. Streptonigrin and EO9 are also activated by NQO1-reduction (12, 13). Although  $\beta$ -lap belongs in this class of quinones, the mechanism of cell death occurs exclusively by apoptosis. The drug does not appear to alkylate DNA or cause strand breaks (21), as does MMC, EO9 or Streptonigrin (7, 13, 22-24).

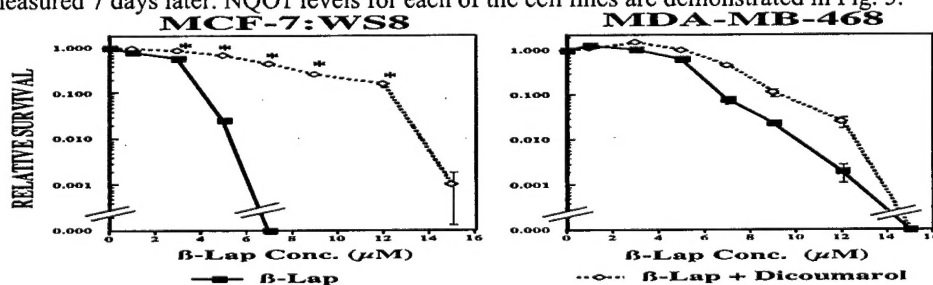
Dicoumarol {3-3'-methylene-bis(4-hydroxycoumarin)} is a commonly used NQO1 inhibitor that competes with NAD(P)H for binding to the oxidized form of NQO1, preventing reduction of various target quinones (25-27). Thus, dicoumarol addition enhances the toxicity of a number of quinones (e.g., menadione) by preventing their detoxification (7, 28). In contrast, dicoumarol significantly prevents the toxicity of quinones that require NQO1 for activation, e.g., MMC, Streptonigrin, or EO9.

**Dicoumarol prevents  $\beta$ -lap lethality.** Structural similarities between  $\beta$ -lap and other naphthoquinones (e.g., menadione (Vitamin K3, 2-methyl-1,4 naphthoquinone)) suggested that NQO1 may be involved in the activation or detoxification of this drug. The IR-inducible properties of NQO1 (xip3) were consistent with this compound's ability to radiosensitize cells (29, 30). Accordingly, co-administration of 50  $\mu$ M dicoumarol concomitant with  $\beta$ -lap caused a significant enhancement in MCF-7:WS8 (MCF-7) cell survival (Fig. 2). While this protection was dramatic at  $\beta$ -lap doses of 4-12  $\mu$ M, the protective effects of 50  $\mu$ M dicoumarol were overcome by >14  $\mu$ M  $\beta$ -lap. In contrast, NQO1<sup>-</sup> 468 cells were relatively resistant to  $\beta$ -lap (LD<sub>50</sub> ~12  $\mu$ M, compared with an LD<sub>50</sub> of ~2  $\mu$ M for MCF-7 cells), and these cells were not protected by dicoumarol. Since 468

cells do not express NQO1 (31) and dicoumarol protected MCF-7 cells (Fig. 2), these data suggested that NQO1 activity was a critical determinant in  $\beta$ -lap-mediated lethality. Further studies showed that  $\beta$ -lap undergoes a futile redox cycle that drains NAD(P)H levels from NQO1<sup>+</sup> cells, resulting in ATP depletion in 30 mins of  $\beta$ -lap exposure; for every mole of  $\beta$ -lap used by NQO1, up to 60 moles of NAD(P)H were used (31).

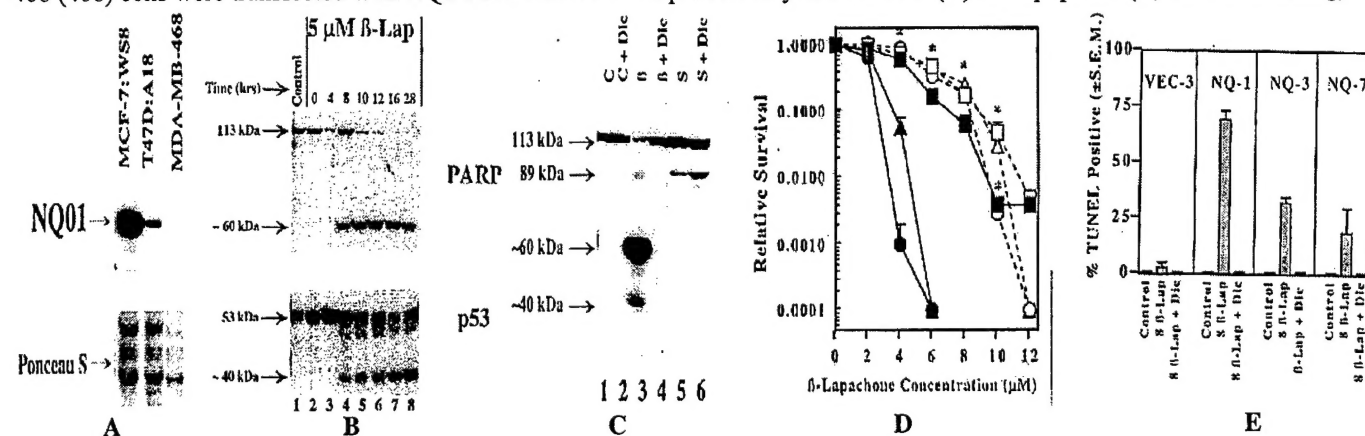
**Dicoumarol prevents  $\beta$ -lap-mediated proteolysis.** We showed that apoptosis in various human breast cancer cell lines induced by  $\beta$ -lap was unique, causing a pattern of PARP and p53 cleavage events *in vivo*, that were distinct from events caused by caspase-activating agents (Figs. 3B, 5C). After  $\beta$ -lap exposure, we observed concomitant unusual PARP (yielding an ~60 kDa fragment, Fig. 3) and p53

**Figure 2. Dicoumarol inhibits  $\beta$ -lap-mediated cytotoxicity in NQO1-expressing MCF-7, but not NQO1-deficient, MDA-MB-468 cells.** Log-phase MCF-7 or 468 cells were exposed to various doses of  $\beta$ -lap at indicated doses,  $\pm$ co-administration of 50  $\mu$ M dicoumarol for 4 h. Colony forming ability (shown) and relative growth inhibition were measured 7 days later. NQO1 levels for each of the cell lines are demonstrated in Fig. 5.



proteolysis (yielding an ~40 kDa fragment) that was likely due to the activation of the neutral,  $\text{Ca}^{2+}$ -dependent protease,  $\mu$ -calpain (32, 33). A similar calpain-mediated cleavage of p53 was reported (34, 35), and activation of  $\mu$ -calpain was explored below. To examine the effect of dicoumarol on  $\beta$ -lap-mediated PARP and p53 proteolysis in MCF-7 cells, we treated cells with a 4 h pulse of 8  $\mu\text{M}$   $\beta$ -lap ( $\beta$ ),  $\pm 50$   $\mu\text{M}$  dicoumarol (D or Dic) (Fig. 3). Dicoumarol abrogated atypical PARP or p53 cleavage after  $\beta$ -lap exposure, but had no effect on 1.0  $\mu\text{M}$  staurosporin (S)-induced classic PARP cleavage (i.e., formation of an 89 kDa PARP fragment (36) in MCF-7 cells, (Fig. 5C)). The fact that dicoumarol significantly protected NQO1-expressing cells from  $\beta$ -lap-mediated apoptosis strongly suggested a role for NQO1 in this compound's toxicity. However, previous studies indicated that dicoumarol may also inhibit other redox enzymes at high concentrations (37).

**Figure 3.  $\beta$ -Lap-mediated, NQO1-dependent proteolysis in human breast cancer cells.** In A, NQO1 levels in human breast cancer cells. In B,  $\beta$ -Lap-treated MCF-7 cells show atypical poly(ADP-ribose)polymerase (PARP) and p53 cleavage during apoptosis. In C, MCF-7 cells were exposed to medium alone (C), 4  $\mu\text{M}$   $\beta$ -lap ( $\beta$ ) or staurosporin (S), with or without dicoumarol (D) and PARP (shown) and p53 cleavage events were observed. In D & E, NQO1 expression sensitizes to  $\beta$ -lap. Open triangles and circles are  $\beta$ -lap-treated, NQO1<sup>+</sup> 468 cells co-treated with dicoumarol. Closed squares are vector alone 468 cells. MDA-MD-468 (468) cells were transfected with NQO1 and tested for  $\beta$ -lap sensitivity for survival (D) and apoptosis (E, TUNEL staining).

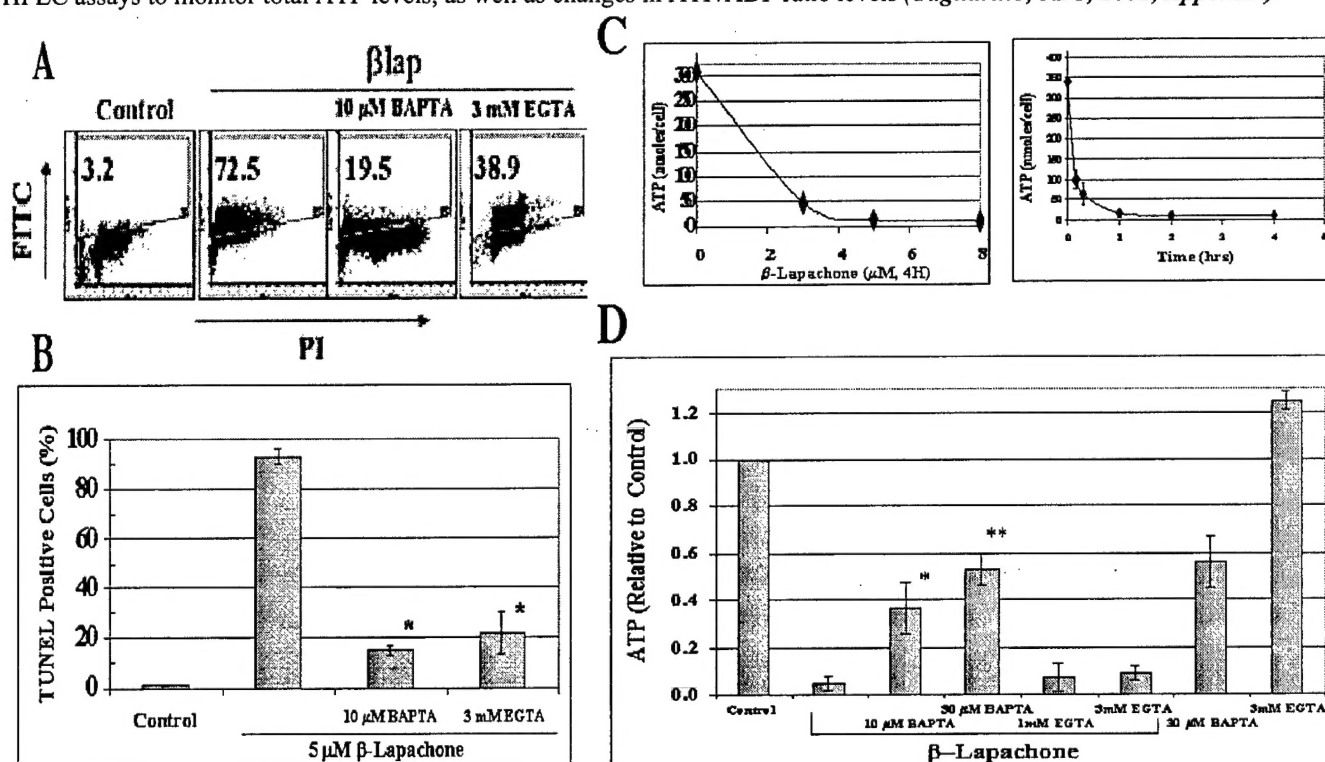


**Transfection of NQO1 sensitizes cells to  $\beta$ -lap.** To examine the role of NQO1 in  $\beta$ -lap cytotoxicity, we used the drug resistant, NQO1-deficient, 468 cell line to determine if exogenous expression of NQO1 could sensitize these cells to  $\beta$ -lap. NQO1 expression in isolated clones was determined by Western blot and enzyme assays. Enzyme activity correlated with NQO1 protein expression. Vector alone clones, as in parental 468 cells, did not express NQO1. Of the ten clones isolated, nine expressed NQO1. NQO1 transfectants were then tested for sensitivities to  $\beta$ -lap or menadione (31). Growth inhibition and survival were assessed after 4 h pulses of drugs,  $\pm 50$   $\mu\text{M}$  dicoumarol (Fig. 3D). The relative growth of  $\beta$ -lap-treated v. control (T/C) cells was examined 7 days after drug exposure, and responses correlated well with clonogenic assays. In all cases, NQO1 expression led to a marked increase in  $\beta$ -lap sensitivity (31, 38). Co-addition of 50  $\mu\text{M}$  dicoumarol inhibited  $\beta$ -lap toxicity in all NQO1<sup>+</sup> clones (Fig. 3D). Dicoumarol did not affect the  $\beta$ -lap-resistant NQO1<sup>-</sup> Vec-3 clones. Opposite results were observed after menadione exposure. NQO1<sup>+</sup> cells were more resistant to menadione than NQO1<sup>-</sup> clones. Resistance was ameliorated by dicoumarol (31, 38). To confirm that cell death occurred due to apoptosis in NQO1 transfectants, we used TUNEL and flow cytometric assays to measure DNA fragmentation after  $\beta$ -lap exposures (Fig. 3E). Vec-3 cells showed <2% apoptosis after  $\beta$ -lap treatment. NQO1<sup>+</sup> clones showed 30-70% apoptosis, whereas NQO1<sup>-</sup> 468 Vec3 cells did not show TUNEL staining (Fig. 3E). Dicoumarol prevented DNA fragmentation in all NQO1<sup>+</sup> 468 clones. NQO1<sup>+</sup> 468



clones were then used to determine if lethality corresponded with increased atypical PARP and p53 cleavage. NQO1<sup>+</sup> clones (NQ-1, NQ-3, NQ-6 & NQ-7) showed ~60 kDa PARP cleavage, 24 h after a 4 h, 8  $\mu$ M  $\beta$ -lap treatment (32, 33, 39). p53 cleavage was also noted. These data showed that while certain aspects of  $\beta$ -lap lethality were unique (e.g., atypical PARP cleavage), other aspects conformed to classic apoptosis (e.g., DNA fragmentation) (40, 41). Cells exposed to 10  $\mu$ M menadione  $\pm$  dicoumarol showed opposite survival responses and p53 and PARP cleavage. Dicoumarol enhanced p53 cleavage. NQO1 expression also led to resistance to menadione-induced p53 cleavage, which was reversed by dicoumarol. Near identical results were found using human prostate cancer cells, (31-33, 38). These data established that NQO1 activity was critical for the acute cytotoxicity of  $\beta$ -lap. Apoptosis elicited by this agent was unique, resulting in the atypical cleavage of PARP and p53.

**Figure 4.  $\text{Ca}^{2+}$  changes required for  $\beta$ -lap-mediated ATP losses and apoptosis.** MCF-7 cells were treated with 5  $\mu$ M  $\beta$ -lap at times or other concentrations as indicated. Some cells were pretreated for 30 mins with BAPTA-AM or EGTA,  $\pm$  4 h 5  $\mu$ M  $\beta$ -lap as indicated. Cells were then monitored for apoptosis by TUNEL (A,B) and losses in ATP (C,D), using luciferase and HPLC assays to monitor total ATP levels, as well as changes in ATP/ADP ratio levels (Tagliarino, JBC, 2001, Appendix).



**Role of  $\text{Ca}^{2+}$  signaling in apoptosis after  $\beta$ -lapachone ( $\beta$ -lap).** NQO1-directed,  $\beta$ -lap-mediated apoptosis (>60% apoptosis, 8-10 h after a 4 h pulse of 4-5  $\mu$ M  $\beta$ -lap) was accompanied by: (a) rapid dephosphorylation of the pRb protein, 3 h after exposure of MCF-7 cells to 2-4  $\mu$ M  $\beta$ -lap (40); (b) atypical cleavage of p53 and PARP (39); and (c) apparently 'typical' apoptosis-associated lamin B cleavage that was not prevented by zVAD, DEVD or other global caspase inhibitors. Similar responses did not occur in NQO1-deficient cells, nor in NQO1-expressing cells exposed to dicoumarol. According to reports in the literature, p53 cleavage during apoptosis (as in Fig. 3) is indicative of  $\mu$ -calpain-mediated apoptosis (32, 42, 43). These data suggest that  $\mu$ -calpain was activated in NQO1-expressing cells by  $\beta$ -lap. Since we suspected  $\mu$ -calpain activation by  $\beta$ -lap, and since this zymogen was specifically activated by  $\text{Ca}^{2+}$  binding, alterations in intracellular  $\text{Ca}^{2+}$  stores

in an NQO1-dependent fashion after  $\beta$ -lap exposure were explored (33). Consistent with our theory, we found that ATP losses and TUNEL responses (apoptosis) in cells exposed to 5  $\mu$ M  $\beta$ -lap for 4 h were prevented by  $\text{Ca}^{2+}$  chelators (Fig. 4). Administration of EDTA (or EGTA) also partially prevented apoptosis and intracellular proteolysis of PARP, p53 or lamin B in  $\beta$ -lap-exposed cells (32, 33). BAPTA-AM partially blocked ATP losses (Fig. 4, lower right panel) and partially prevented  $\beta$ -lap-mediated apoptosis (Fig. 4, left panels) proteolysis, and lethality (not shown); BAPTA-AM is a specific  $\text{Ca}^{2+}$  chelator that concentrates in cells and sequesters cytosolic  $\text{Ca}^{2+}$  released from ER stores, as well as from other internal organelles. Thapsigargin (TG, an irreversible ER SERCA pump inhibitor) or ionomycin, known stimulators of  $\text{Ca}^{2+}$  release, were used as positive controls. BAPTA-AM prevented TG- or ionomycin-induced  $\text{Ca}^{2+}$  releases (by fluo4-AM staining and confocal microscopy) and apoptosis (not shown, (33)).

We then confirmed that  $\text{Ca}^{2+}$  alterations occurred in NQO1-expressing,  $\beta$ -lap-exposed MCF-7 or 468-NQ3 cells using fluo4-AM dye staining and confocal microscopic evaluation of exposed or non-exposed single cells (Fig. 7, (33)). Dramatic  $\text{Ca}^{2+}$  increases (3-10 mins post-treatment) in  $\beta$ -lap-exposed, NQO1-expressing human breast cancer cells were measured (33).  $\text{Ca}^{2+}$  increases were prevented by dicumarol in NQO1<sup>+</sup> breast cancer cells (not shown), but not in NQO1<sup>-</sup> cells (33). Although these data suggested that  $\text{Ca}^{2+}$  changes were important for  $\beta$ -lap-mediated cell death,  $\text{Ca}^{2+}$  chelation did not completely abrogate these responses, **at least when cells were exposed to 4  $\mu$ M  $\beta$ -lap for 4 h.**

*Task 2:*

1. Stably transfect MDA-MB-468 vector and NQO1 breast cancer cells with cameleons, GFP-calcium indicators (*months 1-12*).

**We determined that this line of investigation was not feasible, since the cameleons are not reliable. This line of research yielded little useable data due to instability of the cameleons and very strong noise within the data. All experiments using the cameleons were, therefore, terminated.**

2. Determine the localization of intracellular calcium changes in the above stably transfected cells after  $\beta$ -lap, +/- dicumarol treatments, via confocal microscopy (*months 12-36*).

**See the data above published in Tagliarino et al., JBC, 2003. These studies were completed as discussed above.**

*Task 3:*

3. Determine whether blocking intracellular calcium with EGTA/EDTA prevents  $\beta$ -lap-induced apoptosis and downstream apoptotic events (i.e., p53 and lamin B cleavage, nuclear condensation, DNA fragmentation) via flow cytometric and western blot analyses. Vector alone 468 cells will be compared to 468 clones expressing NQO1, and cells will be treated +/- DMSO (drug vehicle), +/-  $\beta$ -lap, and +/- dicumarol in various combinations (*months 1-24*).

**See the data above published in Tagliarino et al., JBC, 2003. These studies were completed and published as discussed above.**

## **Aim 2:**

### **To determine the role of calpain and its downstream targets in $\beta$ -lap-induced apoptosis**

#### *Task 1:*

1. Determine  $\mu$ -calpain activation using flurogenic substrates (i.e., Suc-LY-MNA), inhibitors (i.e.,  $\mu$ -calpain inhibitor I, PD15606, etc), and observe  $\mu$ -calpain autolysis via western blot analyses. Similar treatments as described in Aim 1 using 468 vector and NQ01 expressing cells, +/- DMSO, +/-  $\beta$ -lap, and +/- dicumarol in various combinations, will be used (*months 1-24*).

#### *Task 2:*

1. Develop mammalian expression plasmids which produce  $\mu$ -calpain-GFP fusion proteins via TOPO cloning (Invitrogen) (*months 1-12*).
4. Transiently transfect MDA-MB-468 vector or NQ01 breast cancer cells with the  $\mu$ -calpain-GFP expression vector and determine  $\mu$ -calpain translocation after treatment with  $\beta$ -lap via confocal microscopy. Endogenous  $\mu$ -calpain levels will be simultaneously assessed via confocal microscopy as described in preliminary results (*months 12-36*).

#### *Task 3:*

- Determine calpastatin levels and localization before and after  $\beta$ -lap treatment via indirect immunofluorescence and confocal microscopic analyses (*months 1-24*).

#### *Task 4:*

2. *In Vitro* transcription/translation of key downstream targets implicated in  $\beta$ -lap-induced apoptosis (i.e., PARP, p53, and lamin B). Incubate these substrates with purified  $\mu$ -calpain to determine calpain cleavage sites and fragment sizes to compare with those observed *in vivo*, after  $\beta$ -lap treatment. The goal is to then sequence the  $\mu$ -calpain cleavage site(s), make specific fmK-cleavage site peptide inhibitors, and use these to potentially block  $\beta$ -lap-mediated apoptosis (*months 1-36*).

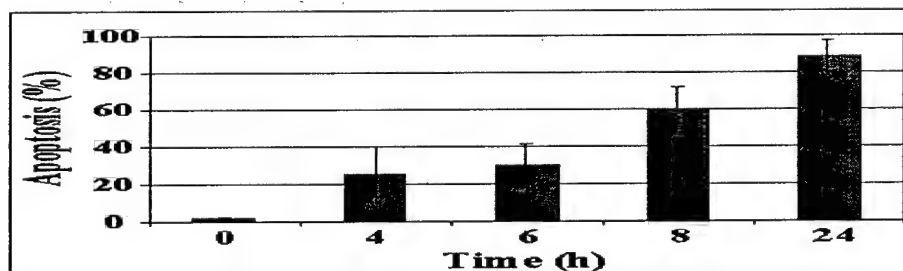
Tasks 1-4 were complete and published in Tagliarino et al., Cancer Biology and Therapy, 2003. Briefly, these results are described below:

***Exposure of MCF-7 cells to  $\beta$ -lap resulted in  $\mu$ -Calpain activation in a temporal manner corresponding to cell death-*** Log-phase MCF-7 cells were treated for 4 h with 5 mM  $\beta$ -lap, at which time fresh medium was added. Cells were harvested at the indicated times and analyzed for substrate proteolysis, calpain activation  $\mu$ - and m- calpain (via western blot analyses), and apoptosis. Treatment of MCF-7 cells with  $\beta$ -lap resulted in ~25% apoptotic cells, at 4-6 h post-treatment, ~60% apoptosis at 8 h, and >90% apoptotic cells by 24 h, as measured by TUNEL analyzes (Fig. 1A). TUNEL data was correlated with morphological analyses via phase contrast microscopy and Hoechst staining for nuclear condensation as described(38), indicating that TUNEL data was representative of apoptotic cells. Treatment of MCF-7 cells with  $\beta$ -lap also resulted in PARP and p53 proteolysis 8 h post-treatment, and complete loss of full-length PARP protein by 16 h post-treatment (Fig. 1B). Proteolysis of the 113 kDa full-length PARP protein to an ~60 kDa cleavage fragment was distinct from that observed after caspase activation (e.g., 89 and 24 kDa fragments) and occurred at the same time p53 was cleaved

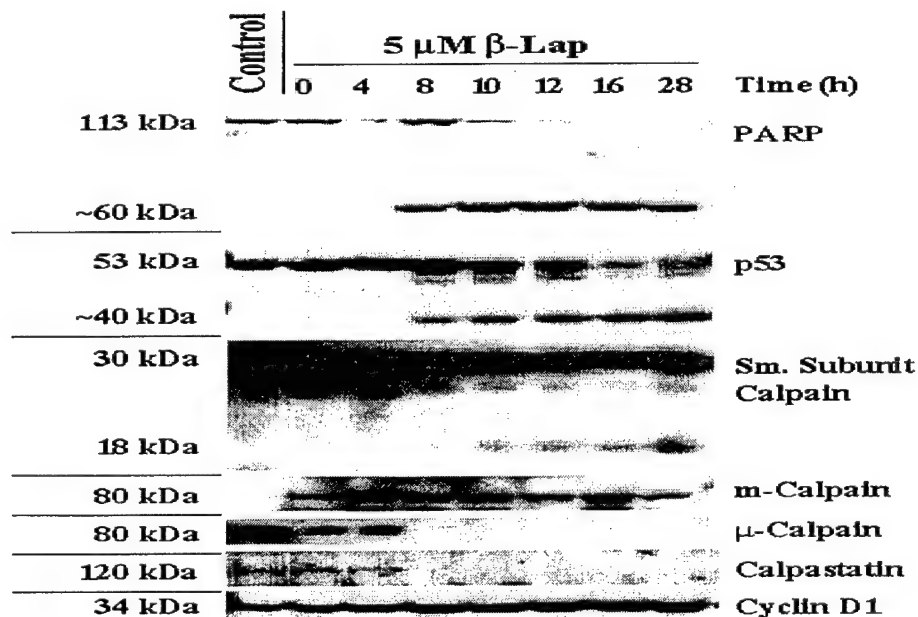
to a characteristic calpain cleavage fragment of ~40 kDa (Fig. 1B) (34, 43, 44). Calpain activation was assessed using autolysis of the regulatory (30 kDa full-length protein to an 18 kDa fragment) as well as the catalytic subunit of  $\mu$ -calpain (80 kDa full-length protein to 76 or 78 kDa fragments) (34, 45). PARP and p53 underwent proteolysis in a temporal manner corresponding to autolysis of the regulatory subunit of calpain and loss of full-length  $\mu$ -calpain (Fig. 1B). Calpastatin, an endogenous inhibitor of calpains, was degraded by 8 h post-treatment at the same time the small subunit of calpain underwent autolysis and full-length  $\mu$ -calpain was cleaved (Fig. 1B), further implicating calpain activation in  $\beta$ -lap-induced apoptosis. Apoptotic and calpain substrate proteolysis were observed at the same time >50% of cells exposed to  $\beta$ -lap exhibited apoptosis (8 h), as determined by DNA fragmentation measured by the TUNEL assay (Fig. 1A). The other ubiquitously expressed form of

**Figure 1.  $\mu$ -Calpain activation in  $\beta$ -Lap-mediated apoptosis.** (A) TUNEL assays were performed to monitor DNA fragmentation at times indicated in MCF-7 cells after a 4 h pulse of 5  $\mu$ M  $\beta$ -lap. Results are graphically summarized as the average of at three independent experiments, mean  $\pm$  S.E. (B) Apoptotic proteolysis was measured in MCF-7 cells exposed to a 4 h pulse of 5  $\mu$ M  $\beta$ -lap, under identical conditions described in 1A. Whole cell extracts were prepared at the indicated times and analyzed using standard Western blotting techniques with antibodies to PARP, p53, the small subunit of calpains, m-calpain,  $\mu$ -calpain, calpastatin, and cyclin D1. Shown is a representative Western blot of whole cell extracts from experiments performed at least three times.

**A.**



**B.**



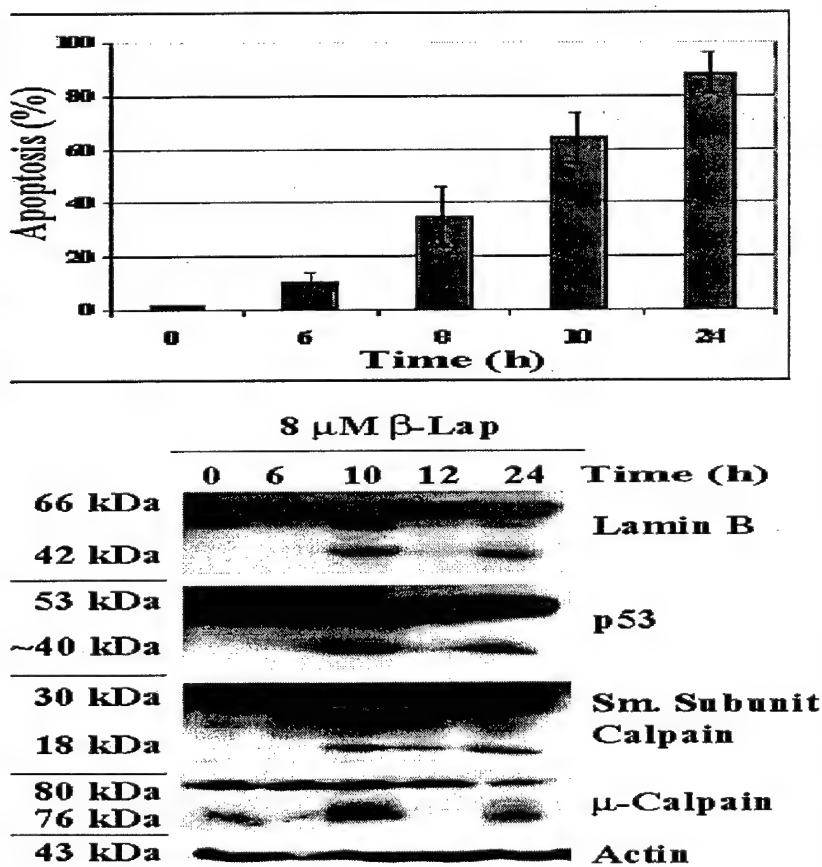


calpain, m-calpain, was not lost (80 kDa) nor cleaved to a fragment (76 kDa) indicative of activation. These data indicate that m-calpain was not activated in NQO1-expressing cells after  $\beta$ -lap exposures (Fig. 1B). Similarly, cyclin D1 levels remained unchanged in  $\beta$ -lap-treated MCF-7 cells, as previously described (40). Consistent with previous results, neither  $\mu$ -calpain activation nor cell death (loss of survival) occurred in NQO1-deficient cells following a 4 h, 8 mM  $\beta$ -lap exposure (data not shown, ref. (39)).

***$\mu$ -Calpain activation occurred independent of caspases, in NQO1-expressing breast cancer cells after  $\beta$ -lap exposure-***

Caspase activation was assessed, as previously described, using SDS-PAGE western immunoblot analyses via the formation of the active fragment from the full-length pro-enzyme (Table 1) (46). Since MCF-7 cells lack caspase 3, caspase 3-containing MDA-468 cells transfected with NQO1 to sensitize them to  $\beta$ -lap were used, as described. A nominal level of apoptosis (~15%) was observed 6 h after exposure to 8  $\mu$ M  $\beta$ -lap (for 4 h) as described, increasing to ~38% by 8 h, and ~65% by 10 h (Fig. 2A). By 24 h, >80% apoptotic cells were noted (Fig. 2A). Furthermore, MDA-468-NQ3 cells elicited the same apoptotic proteolysis as MCF-7 cells, but at a later time, 10 h vs. 8 h in MCF-7 cells (Fig. 2B and 1B, respectively and data not shown). Lamin B, as well as p53, cleavages were observed 10 h after  $\beta$ -lap treatment (Fig. 2B). Autolysis (i.e., activation) of  $\mu$ -calpain corresponded in a temporal fashion to proteolysis (Fig. 2B), as well as to the level of apoptosis: at 10 h > 60% of the cells were apoptotic when  $\mu$ -calpain activation and substrate proteolysis were observed (Fig. 2A). It was interesting to note that lamin B and p53 proteolysis occurred concurrent with  $\mu$ -calpain activation in Fig. 2 B, further suggesting that the apoptotic proteolysis observed in cells after exposure to  $\beta$ -lap was indeed due to

Figure 2. .  $\mu$ -Calpain activation, but not caspase activation, during  $\beta$ -Lap-mediated apoptosis in NQO1-expressing MDA-468-NQ3 cells. (A) TUNEL assays were performed to monitor DNA fragmentation in MDA-468-NQ3 cells at the times indicated after a 4 h pulse of 8  $\mu$ M  $\beta$ -lap. Results are graphically summarized as the average of at three independent experiments, mean  $\pm$  S.E. (B) Apoptotic proteolysis was measured in MDA-468-NQ3 cells exposed to a 4 h pulse of 8  $\mu$ M  $\beta$ -lap. Whole cell extracts were prepared at the indicated times and analyzed using standard Western blotting techniques using antibodies to lamin B, p53, the small subunit of calpains,  $\mu$ -calpain and actin. Shown is a representative Western blot of whole cell extracts from experiments performed at least three times.



$\mu$ -calpain activation: lamin B and p53 proteolysis were diminished concurrently with decreased  $\mu$ -calpain activation at 12 h. The inactivation of  $\mu$ -calpain at 12 h was not observed in all experiments, but the absence of proteolytic cleavages at 12 h in this experiment further supports the role of  $\mu$ -calpain in substrate cleavages in these cells in response to  $\beta$ -lap.

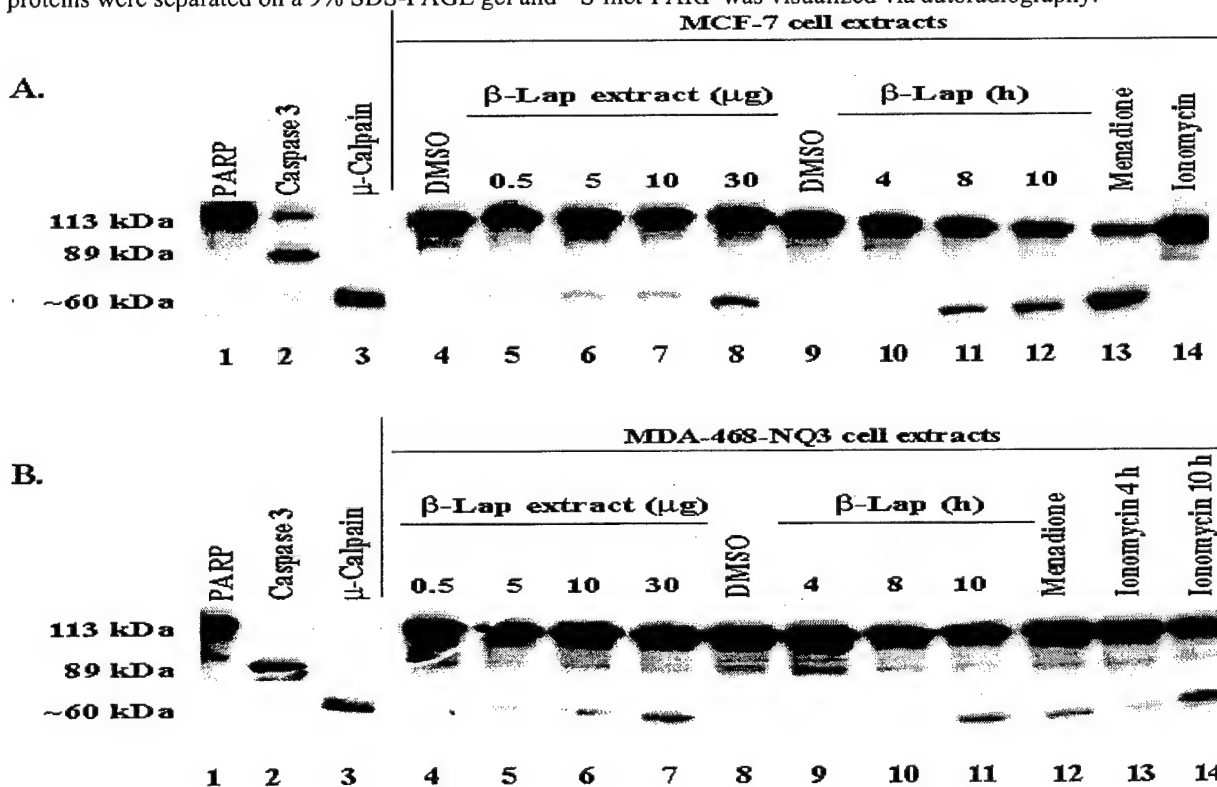
We then examined activation of known apoptotic caspases in MDA-468-NQ3 cells 8-24 h following a 4 h pulse of 8 mM  $\beta$ -lap. Known apoptotic-inducing agents, topotecan (TPT) and staurosporine (STS), were used as positive controls for caspase activation. None of the caspases examined (3, 6, 7, 8, 9, 10, and 12), nor  $\mu$ -calpain, were activated in MDA-468-NQ3 cells following  $\beta$ -lap treatment (Table 1). In contrast,

Table 1. Exposure of MCF-7 human breast cancer cells to  $\beta$ -lap does not lead to the activation of caspases.

Table 1

Protease	STS	TPT	$\beta$ -Lap
$\mu$ -Calpain	-	-	+
m-Calpain	-	-	-
Caspase 3	+	+	-
Caspase 6	-	+	-
Caspase 7	+	+	-
Caspase 8	+	+	-
Caspase 9	+	+	-
Caspase 10	+	+	-
Caspase 12	-	-	-

Figure 3. Purified  $\mu$ -calpain cleaved PARP to the same fragment size as did NQO1-expressing breast cancer cells exposed to  $\beta$ -lap. PARP protein was translated using an *in vitro* transcription and translation TNT-coupled Reticulocyte Lysate system.  $^{35}$ S-methionine-labeled protein was incubated with 100  $\mu$ M  $\text{CaCl}_2$ , and either 0.05 U of recombinant human erythrocyte  $\mu$ -calpain, 20 U of recombinant caspase 3, or 30  $\mu$ g of cell lysate, unless otherwise indicated. The reaction mix was incubated at 37  $^{\circ}\text{C}$  for 1 h. (A) MCF-7 cells were treated for 4 h with 5  $\mu$ M  $\beta$ -lap, 25  $\mu$ M menadione, or 10  $\mu$ M ionomycin, and harvested at 8 h, unless otherwise indicated. (B) MDA-468-NQ3 cells were treated for 4 h with 8  $\mu$ M  $\beta$ -lap, 25  $\mu$ M menadione, or 10  $\mu$ M ionomycin, and harvested at 10 h post-treatment, unless otherwise indicated. Sample proteins were separated on a 9% SDS-PAGE gel and  $^{35}$ S-met-PARP was visualized via autoradiography.



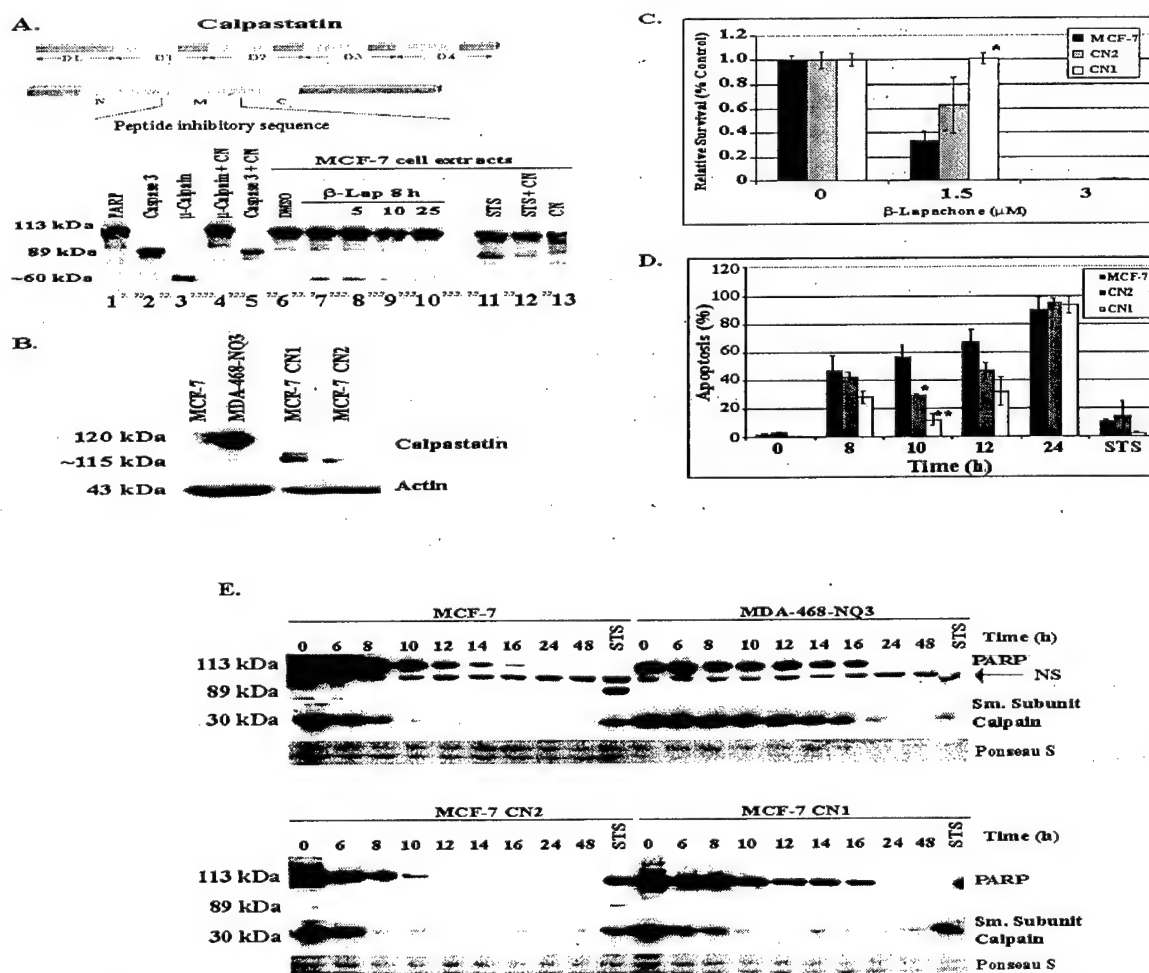
$\mu$ -calpain was cleaved to its active form following  $\beta$ -lap exposures (Fig 2B and Table 1). Additionally, the proteolytic events (lamin B, PARP and p53 cleavage events) observed after  $\beta$ -lap treatment were not blocked by pan-caspase peptide inhibitors, zVAD, DEVD, or YVAD (Refs. (38, 39) and data not shown). Thus,  $\mu$ -calpain, but not caspase, activation was the predominant event in NQO1-expressing breast cancer cells after  $\beta$ -lap treatment.

**Purified  $\mu$ -calpain elicited the same PARP cleavage fragment as noted in NQO1-expressing breast cancer cells exposed to  $\beta$ -lap-** It was previously reported that  $\mu$ -calpain could cleave PARP yielding an ~40 kDa fragment *in vivo* in SH-SY5Y human neuroblastoma cells during maitotoxin-induced necrosis (47, 48), or when using purified  $\mu$ -calpain isolated from calf thymus yielding ~42 kDa, 55 kDa and 67 kDa cleavage fragments (49). However, the proteolysis of PARP was not reported to be accompanied by p53 cleavage nor apoptosis, nor was it identical to proteolysis observed in NQO1-expressing cells after  $\beta$ -lap exposure (~60 kDa) (39). To directly observe  $\beta$ -lap-mediated activated  $\mu$ -calpain activity from treated cells using PARP as a substrate,  $^{35}$ S-methionine-labeled PARP was generated by coupled *in vitro* transcription and translation of full-length human PARP cDNA, and then incubated with various cell extracts or purified enzymes. Using this *in vitro* cleavage assay, we examined whether purified  $\mu$ -calpain could cleave *in vitro* transcribed/translated  $^{35}$ S-met-PARP to similar polypeptide fragments as observed in NQO1-expressing breast cancer cells exposed to  $\beta$ -lap. Log-phase MCF-7 or MDA-468-NQ3 cells were treated with  $\beta$ -lap for 4 h and harvested at 8 or 10 h, respectively (corresponding to Western blot analyses of  $\mu$ -calpain activation and proteolysis after exposure to  $\beta$ -lap, Fig. 1B and 2B), to assess enzymatic activity using  $^{35}$ S-met-PARP. Cell extracts or purified enzyme ( $\mu$ -calpain or caspase 3, used as controls) were incubated with  $^{35}$ S-met-PARP for 1 h at 37 °C. Caspase 3 cleaved PARP to the expected 89 and 24 kDa fragments (Figs. 3A-B, lane 2 and data not shown). Purified  $\mu$ -calpain cleaved PARP to ~60 kDa and ~50 kDa fragments (Figs. 3A-B, lane 3 and data not shown). The PARP cleavage fragment observed after  $\beta$ -lap-treated cell extracts were incubated with  $^{35}$ S-met-PARP were the same as that elicited by recombinant  $\mu$ -calpain (Figs. 3A, lanes 3 and 6-8, 11-12 and 3B, lanes 3 and 4-7 and 11). This was most apparent when  $^{35}$ S-met PARP substrate was cleaved by purified  $\mu$ -calpain and analyzed with  $\beta$ -lap-treated cell extracts on the same gel (Fig. 3B lanes 3-7).  $\beta$ -Lap-treated cell extracts cleaved PARP in a protein concentration-dependent (Fig. 3A lanes 5-8 and Fig. 3B lanes 4-7) and time-dependent (Fig. 3A lanes 10-12 and Fig. 3B lanes 9-11) manner, further implicating  $\mu$ -calpain activation in  $\beta$ -lap-induced apoptosis. DMSO-treated cell extracts did not exhibit any cleavage of PARP in this assay (Figs. 3A lane 4 and lane 8). Proteolytic activity in cell extracts (control or  $\beta$ -lap-treated conditions) could not be stimulated by addition of 100  $\mu$ M  $\text{Ca}^{2+}$  alone, suggesting that the enzymatic activity was inherent to the  $\beta$ -lap-treated extract upon harvest (data not shown).

To further support the role of  $\mu$ -calpain in  $\beta$ -lap-induced apoptosis, menadione-treated cells, the only other known agent to stimulate a similar cell death pathway as  $\beta$ -lap, were also examined. In contrast to extracts from untreated cells, extracts from menadione-exposed cells elicited cleavage of  $^{35}$ S-met-PARP resulting in fragments similar to those generated by purified  $\mu$ -calpain or  $\beta$ -lap-treated cell extracts (~60 kDa) (Figs. 3A, lanes 3, 6-8 and 11-13 and Fig. 3B, lanes 3, 4-7, and 11-12). Ionomycin is a calcium ionophore reported to activate  $\mu$ -calpain (50-53). Ionomycin-treated MDA-468-NQ3 cell extracts also elicited the same PARP cleavage pattern (Fig. 3B, lanes 13-14), as did  $\mu$ -calpain, menadione, and  $\beta$ -lap-exposed cell extracts (Fig. 3B, lanes 3, 12, and 4-7 and 11). Interestingly, ionomycin did not elicit PARP cleavage in MCF-7 cells (Fig. 3A, lane 14).

**Calpastatin, a modulator of  $\beta$ -lap-mediated apoptosis involving calpain activation-** We noted that MDA-468-NQ3 cells expressed higher levels of endogenous calpastatin than MCF-7 cells (Fig. 4B).

**Figure 4.** Calpastatin inhibits or delays substrate proteolysis, apoptosis and survival after exposure to  $\beta$ -lap. (A)  $^{35}$ S-methionine-labeled protein was incubated with 0.05 U recombinant  $\mu$ -calpain, 20 U recombinant caspase 3, or 30  $\mu$ g cell lysate. MCF-7 cells were treated for 4 h with 5  $\mu$ M  $\beta$ -lap or continuously with 1  $\mu$ M STS and where indicated, with a calpastatin peptide inhibitor, and harvested at 8 h. Samples were run on a 9% SDS-PAGE gel and  $^{35}$ S-met-PARP was visualized via autoradiography. Shown is a representative experiment from experiments performed at least twice. (B) Whole cell extracts were collected and Western blot analyses performed using a calpastatin primary antibody to determine relative calpastatin levels in MCF-7, MDA-468-NQ3, and MCF-7 cells stably-expressing full-length calpastatin. (C) Cells were seeded into 60-mm dishes (2000 cells/dish in duplicate) and allowed to attach overnight. Cells were then exposed to a 4 h pulse of  $\beta$ -lap. Medium was removed, fresh medium was added, and cells were allowed to grow for 7 days. Plates were then washed and stained with crystal violet in 50% methanol. Colonies of >50 normal-appearing cells were then counted. Results were graphically summarized as the average of at two independent experiments performed in duplicate, mean  $\pm$  S.E. Student's *t* test for paired samples, experimental group compared to MCF-7 cells treated with  $\beta$ -lap were indicated (\*,  $p < 0.01$ ). (D) At times indicated, TUNEL assays were performed to monitor apoptotic DNA fragmentation in cells after a 4 h pulse of 5  $\mu$ M  $\beta$ -lap, or 24 h after 1  $\mu$ M STS continuous treatment. Results were graphically summarized as the average of at two independent experiments, mean  $\pm$  S.E. Student's *t* test for paired samples, experimental group compared to MCF-7 cells treated with  $\beta$ -lap were indicated (\*,  $p < 0.1$  and \*\*,  $p < 0.05$ ). (E) Apoptotic proteolysis was measured in the various cell lines exposed to a 4 h pulse of 5  $\mu$ M  $\beta$ -lap, or continuous exposure of 1  $\mu$ M STS (harvested at 24 h). Whole cell extracts were prepared at the indicated times and analyzed using standard Western blotting techniques with antibodies to PARP and the small subunit of calpains. Shown is a representative Western blot of whole cell extracts from experiments performed at least three times with Ponceau S staining of the membrane for protein loading. NS= nonspecific protein banding.



We hypothesized that levels of this endogenous calpain inhibitor may explain the slower responses of MDA-468-NQ3 cells (in terms of substrate proteolysis and apoptosis) compared to MCF-7 cells that contained far less calpastatin (10 h vs. 8 hr, Figs. 1 and 2). In addition, the aforementioned data suggested a correlation between PARP and p53 cleavage with m-calpain activation. To further investigate whether calpain was indeed involved in apoptotic substrate proteolysis after  $\beta$ -lap-exposure, we examined the effects of a calpastatin peptide containing the inhibitory sequence of calpastatin, as well as stable over-expression of calpastatin in MCF-7 cells. Calpastatin is a specific endogenous inhibitor of calpains, and does not inhibit other proteases (e.g., cathepsins, caspases). (54, 55) A calpastatin peptide consisting of the sequence of a domain of the calpastatin protein that can inhibit 1 mole of calpain per domain sequence was used (Fig. 4A); calpastatin contains four inhibitory domains and thus is able to inhibit 4 moles of calpain per mole of calpastatin (Fig. 4A) (56-60). In the *in vitro* cleavage assay, the calpastatin peptide inhibitor (CN) blocked purified  $\mu$ -calpain-mediated  $^{35}\text{S}$ -met-PARP cleavage, but not caspase 3-mediated  $^{35}\text{S}$ -met-PARP cleavage (Fig. 4A, lanes 2-5). The CN peptide alone did not have any effect on the integrity of the  $^{35}\text{S}$ -met PARP substrate (data not shown). DMSO-treated cell extracts also did not exhibit any PARP cleavage activity (Fig. 4A lane 6). Cell extracts generated from MCF-7 cells treated with a 4 h pulse of 5  $\mu\text{M}$   $\beta$ -lap and extracted 4 h post-treatment elicited PARP cleavage activity yielding an ~60 kDa fragment (Fig. 4A lane 7). In contrast,  $\beta$ -lap-exposed MCF-7 cell extracts co-incubated with increasing concentrations of the CN peptide, exhibited a decreased amount of the PARP cleavage fragment in a concentration-dependent manner (0-25 mM CN peptide) (Fig. 4A lanes 8-10) compared to  $\beta$ -lap-exposed cell extracts containing no peptide treatment (lane 7). Thus,  $^{35}\text{S}$ -met-PARP cleavage, mediated by  $\beta$ -lap treated cell extracts, was inhibited in a concentration-dependent manner by the calpastatin inhibitory peptide (Fig. 4A, lanes 8-10). Furthermore, in Western blot analyses 8 h after  $\beta$ -lap exposure, the calpastatin peptide inhibitor slightly diminished PARP cleavage and loss of the small subunit of  $\mu$ -calpain in a dose-dependent manner. Interestingly, the peptide had a greater effect on the enzymatic activity in menadione-treated cells (data not shown).

To further support the role of  $\mu$ -calpain activation in  $\beta$ -lap-induced apoptosis, MCF-7 cells were transfected with calpastatin and clones selected by limiting dilution cloning (Figs. 4 B-E). Two clones with varying levels of calpastatin, MCF-7 CN1 (CN1) and MCF-7 CN2 (CN2), were selected for subsequent analyses. The two MCF-7 calpastatin clones selected expressed intermediate levels of calpastatin, compared to MCF-7 or MDA-468-NQ3 cells (Fig. 4B). CN1 cells expressed higher levels of calpastatin than MCF-7 or CN2 cells, but less than MDA-468-NQ3 cells (Fig. 4B). CN2 cells expressed a much lower level of calpastatin than CN1, but a higher level than MCF-7 cells (Fig. 4B). The molecular weight difference between endogenous and exogenous calpastatin in the MCF-7 clones compared to MCF-7 parental cells is presumably due to the lack of exon 1 in exogenous calpastatin (sequence analysis). Exon 1 encodes part of domain L of calpastatin; the function of domain L remains unknown and alternative first exons have been shown to lead to four calpastatin isoforms with distinct amino-terminal sequences resulting in protein sizes ranging from 60-120 kDa via western blot analyses. (61) It is important to note that endogenous calpastatin was detected at the higher molecular weight in these clones (Fig. 4B). Calpastatin contains four repetitive and homologous domains (not encoded by exon 1) that each inhibits both  $\mu$ - and m-calpain; each domain is a functioning unit of calpastatin and can bind one  $\mu$ -calpain molecule and inhibit its activity (56, 58, 62). Other inhibitors have been used to inhibit calpain activity, however, these inhibitors are less useful due to their poor solubilities, intracellular uptake, and non-specific ability to inhibit other proteases and/or the proteasome (e.g., cathepsins B and L, papains, etc.) (63-66). Log-phase MCF-7, MDA-468-NQ3, CN1 and CN2 cells were treated for 4 h with 1.5 mM or 3 mM  $\beta$ -lap, at which time fresh medium was



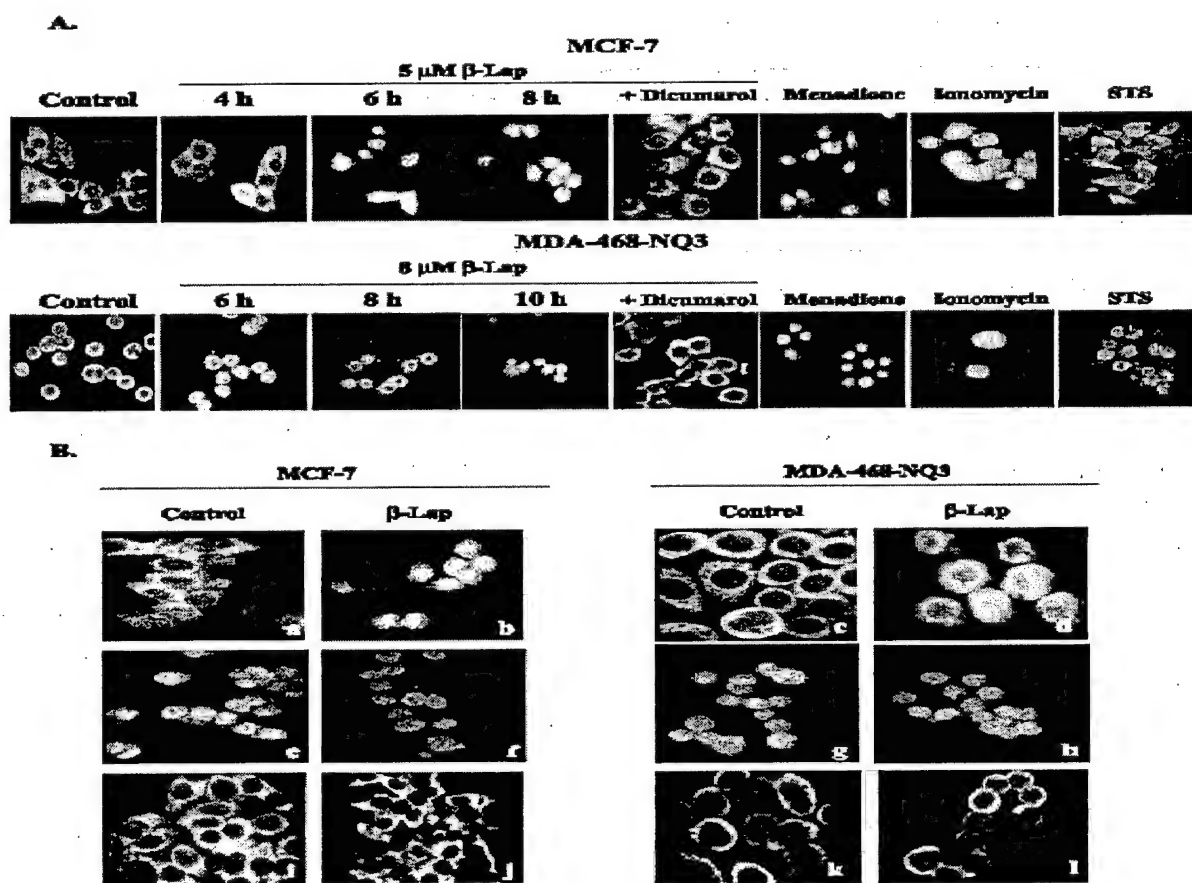
added. Clonogenic survival was determined seven days later. At 1.5 mM  $\beta$ -lap, increasing survival after  $\beta$ -lap exposure correlated with the level of calpastatin expressed in each cell line; MCF-7 cells (low calpastatin) exhibited ~30% survival, CN2 cells (intermediate calpastatin) exhibited ~60% survival, and CN1 cells (high calpastatin) exhibited ~100% survival (Fig. 4C). At 3 mM  $\beta$ -lap, no difference in survival was observed indicating that the inhibitory affects of calpastatin could be overcome with higher drug concentrations (Fig. 4C); binding of calpains to calpastatin is reversible and does not result in any lingering loss of calpain activity.(67) To examine proteolysis during b-lap-mediated cell death in CN1 and CN2 cell clones, cells were harvested at the indicated times for Western blot and apoptosis analyses. MCF-7 cells expressed low levels of calpastatin and exhibited ~50% apoptosis at 8 h, increasing to >90% cells staining TUNEL positive at 24 h. In contrast,  $\beta$ -lap-treated CN1 and CN2 cells that possessed higher levels of calpastatin exhibited less apoptosis than MCF-7 cells at 8, 10 and 12 h after 5 mM  $\beta$ -lap exposures (Fig. 4D). At 24 h, no difference was observed between the cell lines, indicating that the inhibitory affects of calpastatin could be overcome with time following a 4h, 5 mM  $\beta$ -lap exposure (Fig. 4D), and corresponding to cell survival data at 3 mM (Fig. 4C). Specific proteolytic events in cells with varied calpastatin levels were then examined following  $\beta$ -lap exposure.  $\beta$ -Lap-exposed MCF-7 cells expressed low levels of calpastatin and exhibited apoptotic-substrate proteolysis, specifically PARP cleavage to a distinct ~60 kDa fragment at 8 h, with complete loss of full-length protein by 16 h (Fig. 1B). In contrast,  $\beta$ -lap-treated MDA-468-NQ3 cells that possessed higher levels of calpastatin, exhibited apoptotic-substrate proteolysis at 10 h (Fig 2B). Loss of PARP protein also corresponded with cleavage of both the small subunit of calpains and  $\mu$ -calpain (Fig. 1B and 2B and data not shown), indicative of  $\mu$ -calpain activation (34, 45). In MCF-7 clones stably expressing calpastatin, b-lap-induced apoptosis and calpastatin levels were inversely correlated (Fig. 4D and E). CN2 cells expressed low levels of calpastatin and exhibited a similar time-course of PARP and small subunit of calpain proteolysis at 8 h, as that demonstrated in MCF-7 cells (Fig. 4E). In contrast, CN1 cells that expressed high levels of calpastatin showed a more delayed time-course of proteolysis following b-lap exposure similar to that of MDA-468-NQ3 cells; PARP cleavage occurred at 10-12 h (Fig. 4E). Furthermore, the small subunit of calpain was lost much earlier in CN1 cells than in MDA-468-NQ3 cells, but later than MCF-7 or CN2 cells (Fig. 4E, 1B and 2B and data not shown). These data strongly suggest that calpastatin levels can influence the responses of NQO1-expressing cells to b-lap-induced, m-calpain-mediated apoptosis and survival.

***$\mu$ -Calpain translocated to the nucleus in NQO1-expressing breast cancer cells after  $\beta$ -lap exposure-*** PARP and p53 are nuclear proteins and m-calpain is reported to primarily reside in the cytoplasm (68-70). Confocal microscopic analyses were performed to examine  $\mu$ -calpain localization after  $\beta$ -lap treatment. Log-phase MCF-7 or MDA-468-NQ3 cells were treated for 4 h with  $\beta$ -lap (5 mM or 8 mM, respectively) and fixed for indirect immunofluorescent staining at 8 h or 10 h, unless otherwise indicated. Cells were stained with a primary antibody specific for  $\mu$ -calpain and a FITC-conjugated secondary antibody (green). Slides were then mounted in medium containing propidium iodide for DNA/nuclear staining (red). Cells exhibited  $\mu$ -calpain translocation to the nucleus (Fig. 5A;  $\mu$ -calpain staining is green, DNA is red, and nuclear translocation of  $\mu$ -calpain is indicated by yellow fluorescence) at a time concomitant with  $\mu$ -calpain activation after  $\beta$ -lap treatment (Figs. 1B and 2B). In MCF-7 cells,  $\mu$ -calpain exhibited minimal nuclear translocation at 4 h increasing to almost 100% nuclear translocation by 8 h, consistent with substrate proteolysis in Fig.1B (Fig. 5A). In MDA-468-NQ3 cells,  $\mu$ -calpain did not exhibit nuclear translocation until 10 h, corresponding to substrate proteolysis in these cells (Figs. 5D and 2B). In addition, translocation of  $\mu$ -calpain to the nucleus was concomitant with overall loss of calpastatin immunofluorescence and protein expression, as determined by Western blot analyses, after exposure to  $\beta$ -lap (Fig. 1 and data not shown).

Translocation of  $\mu$ -calpain was NQO1-dependent, since it was prevented by co-administration of 50  $\mu$ M dicumarol (Fig. 5B and D), and did not occur in cells that lacked NQO1 enzymatic activity (i.e., in MDA-468 cells not transfected with NQO1 sequence (vector alone, data not shown)).

**Figure 5.  $\mu$ -Calpain translocation to the nucleus after exposure to  $\beta$ -lap.** (A) MCF-7 or MDA-468-NQ3 cells were treated for 4 h with 25  $\mu$ M menadione, 5  $\mu$ M or 8  $\mu$ M  $\beta$ -lap, respectively, or continuously with 1  $\mu$ M STS or 3  $\mu$ M ionomycin. Dicumarol (50  $\mu$ M) was added concomitantly with  $\beta$ -lap for 4 h. MCF-7 or MDA-468-NQ3 cells were fixed at 8 h or 10 h, respectively, for analyses. Indirect immunofluorescent staining of fixed cells was performed using primary antibodies for anti- $\mu$ -calpain, anti-calpastatin and anti-NQO1 with secondary FITC-anti-mouse antibody (green). Slides were coated with mounting medium containing propidium iodide for DNA/nuclear staining (red) and analyzed. Confocal images were collected using dual excitation at 488 nm and 568 nm from a krypton/argon laser. Nuclear translocation was indicated by yellow fluorescence from the merging of red DNA/nuclear staining and green protein staining.

**Figure 5**



Translocation of  $\mu$ -calpain to the nucleus in NQO1-expressing,  $\beta$ -lap-treated cells, was a specific event that did not occur due to nuclear membrane breakdown. Proteins residing in the cytoplasm (NQO1) did not translocate to the nucleus, and proteins that reside in the nucleus (Ku70/Ku80) did not diffuse out into the cytoplasm at the times  $\mu$ -calpain was observed to translocate to the nucleus (Fig. 5C and data not shown); Ku70/Ku80 is a heterodimeric protein required for non-homologous DNA double strand break repair (71). Also, consistent with Western blot analyses in Fig.

1,  $\mu$ -calpain immunoreactivity did not change after exposure of NQO1-expressing breast cancer cells to  $\beta$ -lap (data not shown), further implicating  $\mu$ -calpain activation in  $\beta$ -lap-induced apoptosis.

Other agents (e.g., menadione) that cause the same cell death pathway as  $\beta$ -lap also induced  $\mu$ -calpain translocation to the nucleus at times concomitant with PARP and p53 proteolysis, while agents that elicit caspase-mediated cell death (e.g., staurosporine) did not elicit changes in  $\mu$ -calpain localization (Fig. 5B and D). Ionomycin, a  $\text{Ca}^{2+}$  ionophore, activated  $\mu$ -calpain in some cells (50-52). Consistent with these data,  $\mu$ -calpain translocated to nuclei after treatment with ionomycin in MCF-7 and MDA-468-NQ3 cells (Fig. 5B and D). Translocation of  $\mu$ -calpain after ionomycin was more prominent in MDA-468-NQ3 cells than in MCF-7 cells, corresponding to the ability of each cell line to elicit PARP (Fig. 3A-B, lane 14) or p53 (not shown) cleavage. Menadione elicited a similar cell death pathway as did  $\beta$ -lap, and in a similar manner to  $\beta$ -lap-exposed cells. For example, menadione-treated cells caused translocation of  $\mu$ -calpain to the nucleus at times concomitant with PARP and p53 substrate proteolysis (Fig. 3 and ref. (39)). In contrast to  $\beta$ -lap exposures, there was no observed change in  $\mu$ -calpain localization in staurosporine (STS)-exposed MCF-7 or MDA-468-NQ3 cells (Fig. 5B and D); STS is a protein kinase inhibitor that initiates apoptosis via a caspase-mediated pathway (72). Collectively, these data implicate  $\mu$ -calpain activation in  $\beta$ -lap-mediated apoptosis and  $\mu$ -calpain translocation to the nucleus upon its activation. These data are consistent with the essential role of  $\text{Ca}^{2+}$  release in  $\beta$ -lap-induced apoptosis as previously demonstrated (33, 39).

## Discussion

We previously demonstrated that treatment of NQO1-expressing breast cancer cells with  $\beta$ -lap exposure caused increases in intracellular  $\text{Ca}^{2+}$  levels that were critical for apoptosis and cell death induced by  $\beta$ -lap (33).  $\mu$ -Calpain is a  $\text{Ca}^{2+}$ -activated protease implicated in a number of apoptotic pathways (51, 66, 73-75). Our results indicate that  $\mu$ -calpain is activated after  $\beta$ -lap-induced apoptosis by cleavage of the catalytic subunit, as well as the regulatory subunit of calpains, to fragment sizes indicative of calpain activation (Fig. 1-2). Purified  $\mu$ -calpain was also able to cleave *in vitro*  $^{35}\text{S}$ -met-PARP to the same fragment size as observed in  $\beta$ -lap-treated MCF-7 or MDA-468-NQ3 cell extracts (Fig. 3). Furthermore, extracts from  $\beta$ -lap-treated MCF-7 cells were also able to cleave  $^{35}\text{S}$ -met PARP to the same cleavage fragments as observed with PARP substrate incubated with purified calf thymus  $\mu$ -calpain. Finally, cleavage of p53 in  $\beta$ -lap-exposed cells to fragments indicative of  $\mu$ -calpain activation further suggests  $\mu$ -calpain activation in these cells (34, 43).

We used calpastatin, the specific endogenous inhibitor of  $\mu$ -calpains, to assay calpain's role in  $\beta$ -lap-mediated apoptosis. Since many calpain inhibitors used in earlier work can also inhibit the proteasome, cathepsins, other cysteine proteases, or inhibit entirely different enzymes (for example, a protein tyrosine phosphatase), the use of exogenous calpastatin expression to delay/inhibit  $\beta$ -lap-mediated apoptosis has significant advantages over the exclusive use of inhibitors. A peptide comprised of the inhibitory domain of calpastatin was able to block purified  $\mu$ -calpain-mediated, as well as the activity of  $\beta$ -lap-treated cell extracts to cleave PARP both *in vitro* and *in vivo* (Fig. 4 and data not shown). Furthermore, stable over-expression of the calpastatin protein in MCF-7 cells, which possess low levels of calpastatin compared to MDA-MB-468 cells, delayed  $\beta$ -lap-mediated apoptotic events and protected against cell death at 1.5 mM  $\beta$ -lap in clonogenic assays (Fig. 4C).

$\mu$ -Calpain has two distinct sites for association with calpastatin, one at the active site and another at the EF-hand domain (45); it is believed that calpain interacts with substrates through these same two sites. Binding of  $\mu$ -calpains to calpastatin is reversible and does not result in irreversible loss of  $\mu$ -calpain activity (67). Therefore, the ability of calpain activation to overcome the inhibitory effects of calpastatin was not surprising. The delay of  $\mu$ -calpain activation observed in cells over-



expressing calpastatin after  $\beta$ -lap exposure could be due to the dissociation of calpastatin, or the eventual degradation of calpastatin by initial minimal  $\mu$ -calpain activation, thus explaining the rather moderate survival and apoptotic inhibition caused by this exogenous natural inhibitor. The degradation of calpastatin after calpain activation is supported by the loss of calpastatin protein observed in Western blot as well as confocal analyses (Fig. 1B and data not shown). It is also possible that calpastatin has a lower affinity for  $\mu$ -calpain than for calpain substrates. These data suggest a role for calpain in the effector phase of the apoptotic pathway induced by  $\beta$ -lap.

The role of calpains in apoptosis has been widely discussed, but their patterns of activation are not well characterized (51, 74, 76). Thus, elucidation of  $\mu$ -calpain activation after exposure of NQO1-expressing breast cancer cells to  $\beta$ -lap, and the potential role of caspases in regulating  $\beta$ -lap-mediated apoptosis was critical to evaluate.  $\mu$ -Calpain was activated in a temporal manner corresponding to proteolytic cleavage events, apoptosis, and its apparent translocation to the nucleus from the cytoplasm (Figs. 1-5). Known apoptotic caspases (3, 6, 7, 8, 9, 10 and 12) were not activated after treatment of NQO1-expressing cells with  $\beta$ -lap, suggesting a role for  $\mu$ -calpain in this apoptotic response independent of caspase activation (Table 1). Other caspases (1, 4, 5, 11 and 13) were not assayed for activation after  $\beta$ -lap exposures because they are not associated with most apoptotic pathways, but rather, are implicated in inflammation processes (77-79). Killer/DR5, a death-domain containing pro-apoptotic receptor, mRNA was reported to be up-regulated after  $\beta$ -lap-exposures in colon cancer cell lines, however, neither downstream receptor activation nor caspase activation were assayed in these cells (80). Since caspases 8 and 10 are important for receptor-mediated apoptosis, through their association with death domains (e.g., FADD (81)), and neither caspase was activated after  $\beta$ -lap exposures in MDA-468-NQ3 cells (Table 1), our data would strongly suggest that receptor-mediated pathways are not involved in  $\beta$ -lap-induced apoptosis. Furthermore, pan-caspase inhibitors did not prevent apoptotic proteolytic substrate cleavages, nor cell death induced by  $\beta$ -lap (38, 82). In contrast,  $\text{Ca}^{2+}$  chelators and calpastatin, the endogenous inhibitor of  $\mu$ -calpains, did prevent and/or delay proteolytic cleavage events, as well as apoptosis induced by  $\beta$ -lap (refs. (33, 39) and Fig. 4), further implicating a role for calpains in apoptosis independent of caspase activation. Together with the rather dramatic loss of ATP in  $\beta$ -lap-exposed cells (33), these data strongly suggest that caspases are not involved in cell death induced by this cytotoxic agent.

Determining whether caspases were involved in  $\beta$ -lap induced apoptosis was essential since caspases are known to be involved in a number of the classic apoptotic pathways discussed (83-86). In addition,  $\mu$ -calpain activation in apoptosis is usually linked upstream or downstream of caspase activation, or in a parallel pathway alongside caspase activation (87-89). In studies described above, we demonstrated that calpains were activated in human breast cancer cells during  $\beta$ -lap-mediated apoptosis, while caspase activation was not apparent (Fig. 1-4, Table 1). In addition, caspase inhibitors did not have any effect on the apoptotic morphology or survival of NQO1-expressing cells exposed to  $\beta$ -lap (38, 39). This may suggest a redundancy of apoptotic proteases, as well as a novel proteolytic pathway for calpains. Furthermore, although  $\mu$ -calpain is activated, this protease may either be one of a family of proteases activated in response to  $\beta$ -lap, or simply represent a mechanism for eliminating badly damaged cells. This conclusion is supported by the fact that  $\mu$ -calpain inhibitors (chemicals or endogenous calpastatin expression) only slightly delayed apoptotic responses triggered by  $\beta$ -lap.

Endonuclease activation is a critical step in the apoptotic pathway culminating in DNA fragmentation. Many DNases are known to exist, some of which are involved in apoptosis, consisting of  $\text{Ca}^{2+}/\text{Mg}^{2+}$ -dependent endonucleases (e.g., DNase I, DNase gamma),  $\text{Mg}^{2+}$ -dependent endonucleases (CAD/DFF40), and the cation-independent endonucleases (DNase II) (90). Caspase 3 usually mediates cleavage of DFF45/ICAD (a DNase inhibitor) allowing for translocation and activation of

DFF40/CAD that mediates DNA fragmentation (91). Since caspases were not activated in  $\beta$ -lap-mediated apoptosis and DNA fragmentation was observed via the TUNEL assay (Fig. 1-4 and Table 1), three potential pathways for endonuclease activation in  $\beta$ -lap-mediated apoptosis are possible: (1) Calpains directly activate an endonuclease, (2) Calpains activate another protease that then activates an endonuclease, or (3) Calpains are not involved in endonuclease activation, and  $\text{Ca}^{2+}$  alone may activate an endonuclease. In some apoptotic pathways, calpain inhibitors blocked all aspects of apoptosis, including DNA fragmentation (51, 73). These data imply that  $\mu$ -calpain activation led to endonuclease activation either directly, or indirectly, and it is unclear whether this is through activation of a caspase, another protease, or directly by calpains. Our data suggest that either  $\mu$ -calpain directly activates an endonuclease or that calpain activates another protease (independent of caspases) that then activates an endonuclease, since calpastatin over-expression can delay the onset of DNA fragmentation and calpastatin protein levels were inversely proportional to the time and amount of DNA fragmentation observed after  $\beta$ -lap exposure (Fig. 4). Calpastatin should not affect the levels of  $\text{Ca}^{2+}$  in the cell and thus should not affect endonuclease activation by  $\text{Ca}^{2+}$  alone. However, although calpastatin is not known to inhibit any other proteases, it may inhibit another yet unknown protease that is involved in endonuclease activation. We have preliminary evidence that DFF45 was cleaved concomitantly with PARP and p53 cleavages, as well as calpain activation *in vivo* in MDA-468-NQ3 cells exposed to 8 mM  $\beta$ -lap and by purified  $\mu$ -calpain *in vitro* (Tagliarino *et al.*, unpublished results). These data would suggest that  $\mu$ -calpain might directly activate the DFF40/CAD endonuclease.

Calpains are not only suggested to be involved in DNA fragmentation (via endonuclease activation), but are also effector proteases that cleave cellular proteins involved in DNA repair (e.g., PARP), membrane associated proteins (e.g., a-spectrin and actin) and other homeostatic regulatory proteins (e.g., c-FOS, C-JUN, p53) (43, 45, 48, 51, 92-95). Calpain substrate cleavage does not involve a specific primary cleavage site, but rather, is dependent upon the secondary structure of the substrate, making calpains a class of proteases different from the aspartate-specific caspases (92, 96-100). We demonstrated that  $\beta$ -lap-induced activation of  $\mu$ -calpain in human breast cancer cells mediated cleavage of p53 in a manner similar to that previously reported (34, 43). Loss of p53 may further promote apoptosis by preventing anti-apoptotic pathways or cell cycle arrest to allow for cell repair. PARP is a caspase 3 substrate, and a widely used indicator of apoptosis when cleaved to a characteristic 89 kDa fragment from its 113 kDa full-length protein. PARP was previously reported to be cleaved by  $\mu$ -calpains to a 40 kDa fragment during maitotoxin-induced necrosis (48). PARP was also cleaved by  $\mu$ -calpains purified from calf thymus to ~42 kDa, ~55 kDa (doublet) and ~67 kDa (triplet) fragments (49). Here, we show a novel cleavage of PARP to an ~60 kDa polypeptide fragment, mediated by  $\mu$ -calpain in  $\beta$ -lap-treated, NQO1-expressing breast cancer cells during apoptosis (Fig. 1-4). In our hands, purified active calf thymus  $\mu$ -calpain also cleaved PARP substrate to an ~60 kDa polypeptide fragment.

**Calpain translocated to the nucleus upon activation in  $\beta$ -lap-induced apoptosis-** Both m- and  $\mu$ -calpains are predominantly cytoplasmic (70, 101-103). However, some immunoreactivity towards calpains has been localized at the cell membrane (104), at cell-substrate attachment plaques in cultured cells (105), at the I-band in muscle cells (106), or around and within the nucleus (34, 70, 107-110). Calpains can exhibit diffuse cytoplasmic staining with no change after activation by certain agents (68, 69). Conversely,  $\mu$ -calpains have also been shown to undergo redistribution from the cytosol to the plasma membrane upon activation by other agents (111). This suggests a complex activation process for calpains that is agent- and cell type-specific. While calpains have been reported to cleave a number of nuclear proteins (e.g., p53, PARP) there is negligible data that calpains may be localized to the nucleus, and translocation to the nucleus upon activation has only been suggested (34, 70).

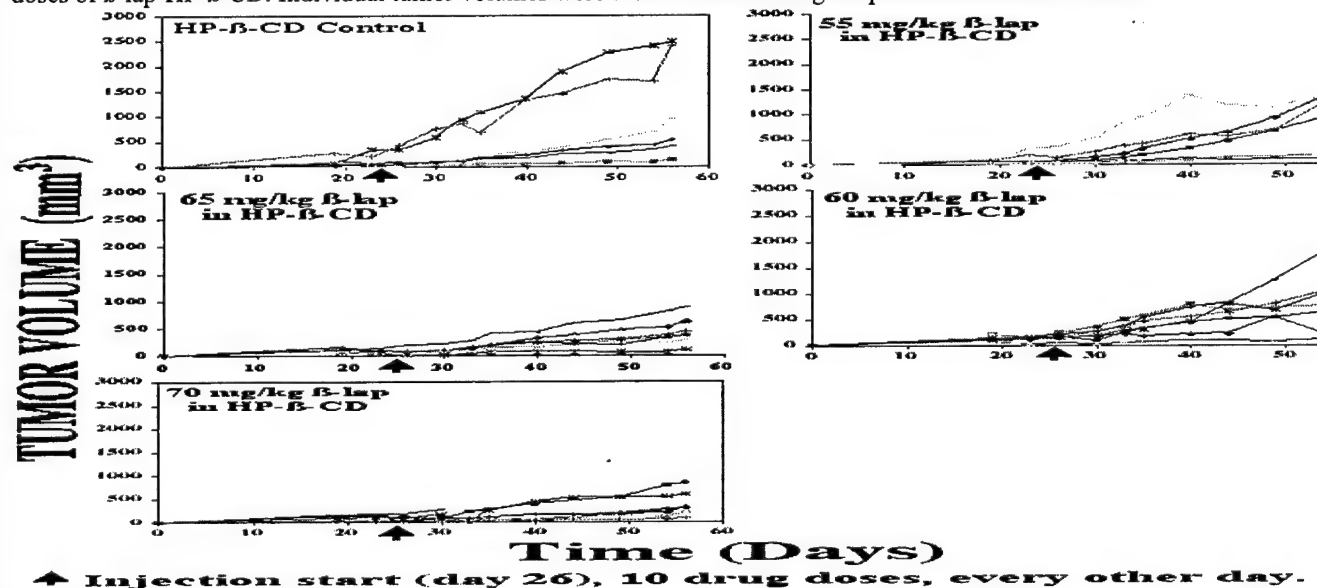
Interestingly, one group showed that  $\mu$ -calpain immunoreactivity transiently accumulated in cell nuclei concomitant with proteolysis of p53 in late G<sub>1</sub> phase (112). Mellgren *et al.*, (109) also demonstrated nuclear transport of purified calpains in permeabilized cells; fluorescein-tagged,  $\mu$ -calpain was transported into nuclei in an ATP-dependent fashion and calpastatin did not block  $\mu$ -calpain translocation. Here, we demonstrate the ability of m-calpain to translocate to the nucleus in NQO1-expressing breast cancer cells after exposure to  $\beta$ -lap (Fig. 5).  $\mu$ -Calpain translocated to the nucleus concomitant with its own activation, apoptotic proteolytic cleavage events, and DNA fragmentation (Figs. 1-2 and 5). This translocation would allow for the ability of calpain to proteolytically cleave the nuclear substrates, PARP and p53, as well as potentially activate an endonuclease.

In conclusion, we demonstrated that  $\mu$ -calpain was activated in NQO1-expressing breast cancer cells exposed to  $\beta$ -lap. Its activation involved an apoptotic signal transduction pathway leading to cell death independent of caspase activation and sensitive to calpastatin expression (Figs. 1-4 and Table 1). We also demonstrated a novel translocation of  $\mu$ -calpain to the nucleus upon its activation in  $\beta$ -lap- and menadione- mediated apoptosis (Fig. 5). However, to unambiguously prove the essential role of calpains in  $\beta$ -lap-induced apoptosis, NQO1-expressing cells deficient in calpain enzymatic activity compared with calpain containing cells after exposure to  $\beta$ -lap would be paramount. Two groups have made calpain knockout mice; Arthur *et al.* disrupted murine *Capn4* (the gene encoding the regulatory subunit of calpains) which eliminated both  $\mu$ - and m-calpain activities (113), and Azam *et al.* deleted *Capn1* ( $\mu$ -calpain) in mice (114).

#### Future Directions (Projects under investigation by Mr. Mark Wagner)

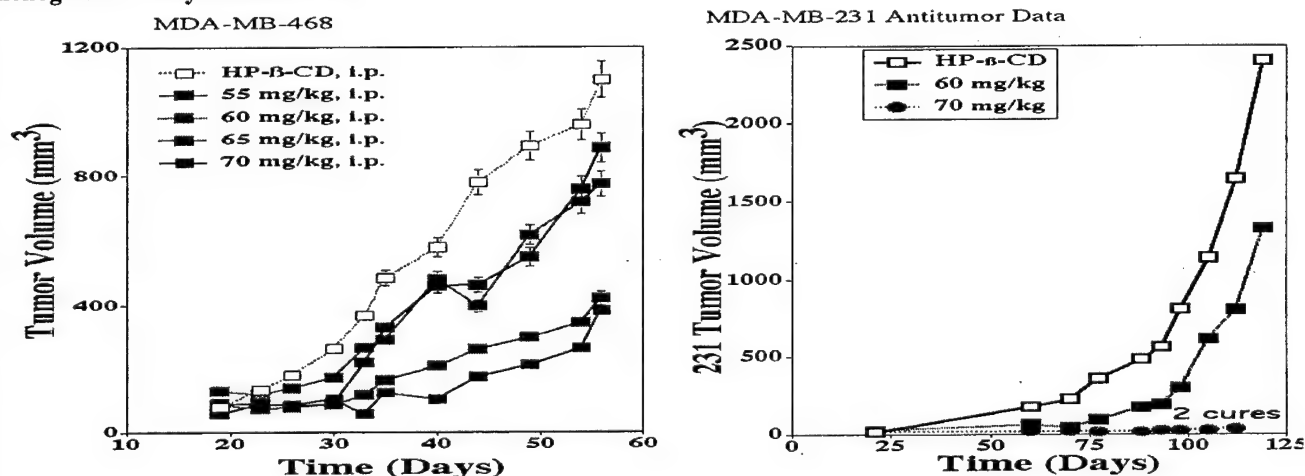
Our future directions with  $\beta$ -lap are focused on the development of efficacious delivery systems for the testing of the antitumor efficacy of  $\beta$ -lap using NQO1+ v. NQO1- human breast cancer xenografts. We have developed three unique delivery methods, including millirods, nanoparticles (which are both made from PLGA polymers), and  $\beta$ -hydroxylpropyl- $\beta$ -cyclodextrin (HP- $\beta$ -CD) complexes. Using HP- $\beta$ -CD we have demonstrated significant antitumor activity against human NQO1+ breast cancer xenografts (Fig. 6).

**Figure 6. Antitumor activity of  $\beta$ -lap-HP- $\beta$ -CD complexes against NQO1+ 468 xenografts in female athymic nude mice.** Mice bearing ~30 mm<sup>3</sup> xenografts from 468 NQO1-expressing human breast cancer cells were treated with various doses of  $\beta$ -lap-HP- $\beta$ -CD. Individual tumor volumes were then measured using calipers and are shown below.



**Antitumor efficacy of  $\beta$ -lap.** Recently, we observed significant antitumor activity of  $\beta$ -lap against NQO1-expressing MDA-MB-468 and MDA-MB-231 human xenograft tumors grown in athymic nude mice. As noted above, we developed a new drug delivery system for  $\beta$ -lap *in vivo*, complexing the drug with hydroxypropyl- $\beta$ -cyclodextrin (HP- $\beta$ -CD). HP- $\beta$ -CD greatly enhanced the solubility and bioavailability of  $\beta$ -lap in athymic nude mice. To investigate the antitumor efficacy of  $\beta$ -lap-HP- $\beta$ -CD complexes, we generated NQO1-expressing xenografts in nude mice from MDA-MB-231, as well as MDA-MB-468 breast cancer cells;  $1 \times 10^6$  231 or 468 cells were injected into both flanks of 40-60 athymic nude mice. Xenografts ( $\sim 30 \text{ mm}^3$ ) formed in  $\sim 30$  days. Animals were then treated i.p. with various doses (40-90 mg/kg)  $\beta$ -lap-HP- $\beta$ -CD once every other day for 10 total injections. Significant antitumor activity was noted in athymic nude mice bearing 231 or 468 xenografts following treatment of mice with 60-70 mg/kg  $\beta$ -lap-HP- $\beta$ -CD. The data are shown in two ways: (A) in Figure 6, individual 468 tumor volumes for control and  $\beta$ -lap treatments were shown; and (B) in Figure 7, average tumor volumes for 231 and 468 experiments are shown.

**Figure 7.  $\beta$ -Lap demonstrates significant antitumor activity against xenografts from 231 or 468 breast cancer xenografts in athymic nude mice.**



**KEY RESEARCH ACCOMPLISHMENTS:**

We have accomplished the following objectives of this grant. We have determined that:

- NQ01 is the key determinant in  $\beta$ -lap-mediated lethality (Pink et al., J. Biol. Chem., 2000 and Planchon et al., Exp. Cell Res., 2001).
- NQ01 is elevated in many human breast cancer cells and should be a useful target for  $\beta$ -lap and its derivatives (Planchon et al., Oncology Reports, 1999).
- $\beta$ -Lap stimulated a unique apoptotic pathway, as measured by TUNEL positive, G0/G1 cells, and specific cleavage of key apoptotic substrates, i.e., PARP, pRb, p53, lamin B and calpain. (Tagliarino et al., Cancer Biology and Therapy, 2003).
- $\beta$ -Lap causes calcium release from endoplasmic reticulum (ER) stores that is sequestered by BAPTA-AM, which subsequently protects cells from  $\beta$ -lap-induced apoptosis and lethality.
- $\beta$ -Lap causes calpain movement from the cytosol to the nucleus at a time concomitant with APRP and p53 cleavage. Apparent movement/activation of calpain is prevented by dicoumarol.
- Atypical PARP and p53 cleavage events are consistent with  $\beta$ -lap-activated calpain-mediated apoptosis as measured *in vivo* and *in vitro* with whole cell extract, <sup>35</sup>S-met-labeled PARP cleavage assays.
- Dicoumarol and calcium chelators protected cells from  $\beta$ -lap-mediated apoptosis and activation of calpain.
- $\beta$ -Lap undergoes NQ01-dependent futile cycling that leads to calcium release and loss of energy (ATP). This combination is thought to prevent ATP-dependent caspase activation and supply the calcium needed to convert the inactive calpain zymogen to the 18 kDa active subunit. Calcium release is responsible for ATP loss, since BAPTA-AM protected cells from  $\beta$ -lap –mediated ATP loss, as well as lethality.
- Caspases are not activated during NQ01-dependent  $\beta$ -lap-mediated apoptosis, presumably due to the dramatic loss of ATP within the cell.
- The necessary reagents, C- and N-terminal his- and flag-tagged PARP, have been made and transfected into NQ01-containing cells for the isolation of the  $\beta$ -lap-activated apoptotic protease.
- Transfection of cells with calpastatin, a specific endogenous calpain protein inhibitor, protected MCF-7 cells from  $\beta$ -lap-induced apoptosis as well as lethality.

## REPORTABLE OUTCOMES:

### Prior Appendix Items Already Supplied to the DOD In Past Reports:

1. Wuerzberger, S.M., Planchon, S.M., Pink, J.J., Bornmann, W. and Boothman, D.A.  $\beta$ -Lapachone-induced apoptosis in MCF-7 human breast cancer cells. 1998; *Cancer Res.* **58**: 1876-1885.
2. Mendonca, M.S., Howard, K.L., Farrington, D.L., Desmond, L.A., Temples, T.M., Mayhugh, B.M., Pink, J.J. and Boothman, D.A. Delayed apoptotic responses associated with radiation-induced neoplastic transformation of human hybrid cells. 1999; *Cancer Res.* **59**: 3972-3979.
3. Separovic, D., Pink, J.J., Oleinick, N.L., Kester, M., Boothman, D.A., McLoughlin, M., Pena, L.A., and Haimovitz-Friedman, A. Nieman-Pick human lymphoblasts are resistant to phthalocyanine 4-photodynamic therapy-induced apoptosis. 1999; *Biomed Biophys. Res. Commun.*, **258**: 506-512.

## CURRENT LIST OF PUBLICATIONS RESULTING FROM THIS AWARD PAPERS PUBLISHED IN PEER-REVIEWED JOURNALS:

4. Pink, J.J., Planchon, S.M., Tagliarino, C., Wuerzberger-Davis, S.M., Varnes, M.E., Siegel, D., and Boothman, D.A. NAD(P)H:quinone oxidoreductase (NQO1) activity is the principal determinant of  $\beta$ -lapachone cytotoxicity. 2000; *J. Biol. Chem.*, **275** (8): 5416-5422.
5. Pink, J.J., Wuerzberger-Davis, S.M., Tagliarino C., Planchon, S.M., Yang, X-H., Froelich, C.J., and Boothman, D.A. A novel non-caspase-mediated proteolytic pathway activated in breast cancer cells during  $\beta$ -lapachone-mediated apoptosis. 2000; *Exp. Cell. Res.*, **255** (2): 144-155.
6. Huang, T.T., Wuerzberger-Davis, S.M., Seuffer, B.J., Shumway, S.D., Kurama, T., Boothman, D.A., and Miyamoto, S. NF- $\kappa$ B activation by camptothecin: A linkage between nuclear DNA damage and cytoplasmic signaling events. 2000; *J. Biol. Chem.*, **275** (13): 9501-9509.
7. Tagliarino, C., Pink, J.J., Dubyak, G.R., Nieminen, A-L., and Boothman, D.A. Calcium is a key signaling molecule in  $\beta$ -lapachone-mediated cell death. 2001; *J. Biol. Chem.* **276**(22): 19150-19159.
8. Planchon, S.M., Pink, J.J., Tagliarino, C., Bornmann, W.G., Varnes, M.E., and Boothman, D.A.  $\beta$ -Lapachone-induced apoptosis in human prostate cancer cells: involvement of NQO1/xip3. 2001; *Exp. Cell Res.*, **267**: 95-106.
9. Tagliarino, C., Pink, J.J., Wuerzberg-Davis, S., and Boothman, D.A.  $\mu$ -Calpain activation in  $\beta$ -lapachone-mediated apoptosis. *Cancer Biology & Therapy*, **2**(2):141-152, 2003.

## PAPERS PUBLISHED IN NON-PEER-REVIEWED JOURNALS:

9. Pink, J.J., Tagliarino, C. Planchon, S., Varnes, M. Simmers, S., and Boothman, D.A. Cell death pathways triggered by  $\beta$ -lapachone. *Free Radical Biology*, In Press, 2001.
10. Miyamoto, S., Huang, T., Wuerzberger-Davis, S., Bornmann, W.,G., Pink, J.J., Tagliarino, C., Kinsella, T.J., and Boothman, D.A. Cellular and Molecular Responses to Topoisomerase I Poisons: Exploiting Synergy For Improved Radiotherapy. 2000; *Annals of the New York Academy of Sciences*, **922**: 274-292.



Wagner MW/Tagliarino C

11. Tagliarino, C. Pink, J.J. and Boothman, D.A. Calpains and apoptosis. 2002; Korean J. Biol Sci., 5: 267-274.

### Abstracts and Presentations Related to this Grant:

For Colleen Tagliarino:

1. **Invited Speaker with Abstract**, "Exploitation of and IR-inducible protein (xip3) in human cancer cells using  $\beta$ -lapachone" C. Tagliarino, J.J. Pink, S.M. Wuerzberger-Davis, S.M. Planchon, and D.A. Boothman. 11<sup>th</sup> Int Congress of Rad Res., Ireland, July 14-17, 1999. Also paid for by grants from the Radiation Research Society to C.T. and D.A.B.
2. **Invited Speaker**, "Exploiting radiation-inducible proteins for targeted apoptosis" Northern Illinois University, Host: Dr. James B. Mitchel, Feb. 5, 1999.
3. **Poster presentation**, DOD Symposium on Breast Cancer Initiative. Seminar entitled " $\beta$ -Lapachone triggers NQO1-dependent apoptosis in human breast cancer cells by activating a calcium-dependent noncaspase cysteine protease." Atlanta, GA, June 11-12, 2000.
11. **Invited Speaker**, "Exploiting IR-inducible responses for chemo- and/or radiotherapy" Department of Pharmacology, University of Pittsburgh, Host: Dr. Jack Yalowich. November 9-10, 2000.
12. **Invited Speaker with Abstract**, Exploiting IR-inducible gene expression for breast cancer therapy, Department of Pharmacology, University of Wisconsin-Madison, December 4, 2001.
13. **Invited Speaker**, "A novel apoptotic pathway induced by  $\beta$ -lapachone", Medical College of Wisconsin, December 5, 2001.

Patents and licenses applied for and/or issued.

None

Degrees Obtained During This Award.

Tagliarino, Colleen  
Oct., 2001.

Ph.D., Case Western Reserve University, Dept. Pharmacology,

### Development of Cell Lines, Tissue or Serum Repositories:

- MDA-MB-468 NQ1-6, human NQO1-deficient cells stably transfected with CMV-directed NQO1.
- vector-alone MDA0-MB-468 cells.
- Stably transfected MCF-7:WS8 cells expressing caspase 3.
- Stably transfected MCF-7 cell clones expressing calpastatin.
- Tetracycline-inducible MCF-7, as well as LNCaP and MDA-MB-231 and MDA-MB-468 cell clones.

Informatics such as databases and animal models, etc.

None

Funding applied for based on work supported by  
this award.

1a. Source and identifying no. NIH/NCI R01 CA-92250

P.I. Boothman, D. A.

b. Title "Exploiting NQO1 for improved therapy of human breast cancers".

c. Dates and costs of entire project 12/01/01 - 11/30/04 \$ 825,594

d. Dates and costs of first year 12/01/01 - 11/30/02 \$ 200,000

e. Specific aims of project The goal of this project is to test the hypothesis that  $\beta$ -lapachone radiosensitizes cells through the IR

Wagner MW/Tagliarino C

inducible enzyme, NQO1 in human breast cancer cells. Another objective of this grant is to further define and clone the apoptotic protease(s) activated by  $\beta$ -lap in NQO1-expressing human breast cancer cell lines.

f. Describe scientific and budgetary overlap. This grant was funded using the preliminary data developed from a DOD breast cancer grant to D.A.B..

g. Describe adjustments you will make if the present application is funded (budget, % effort, aims, etc.). None.

Employment or research opportunities applied for and/or received on experiences/training supported by this award.

Colleen Tagliarino, Ph.D.      Post-doctoral Fellow, Johnson and Johnson Drug Development Center, Philadelphia, PA.



## CONCLUSIONS:

The goal of this grant was to clone the unknown protease activated by the active anti-breast cancer agent,  $\beta$ -lapachone ( $\beta$ -lap). The research team showed for the first time that  $\beta$ -lap required NQ01, a two-electron reduction enzyme elevated in many human breast cancers, for bioactivation. The team then characterized the unknown apoptotic protease activated in human breast cancer cells by  $\beta$ -lap, defining endpoints that will be essential for the ultimate isolation of this novel apoptotic protease. The unknown protease: (a) is a non-caspase cysteine protease; (b) cleaves p53, lamin B, and PARP (atypically) in an NQ01-dependent manner at a time co-incident with calpain activation (appearance of an 18 kDa active form and its movement into the nucleus by confocal microscopy); (c) is calcium-dependent (e.g., the proteolytic cleavage of PARP or p53 was blocked by co-administration of EGTA or EDTA), and the drug causes massive NQ01-dependent calcium influx within 3 mins posttreatment with 5-8  $\mu$ M  $\beta$ -lap; (d) is suppressed by over-expression of calpastatin, a specific endogenous inhibitor of calpain. Furthermore, significant progress has been made in developing reagents that will be required for the cloning of this novel noncaspase cysteine protease. The new hypothesis being tested is that  $\beta$ -lap activates calpain, which then triggers DNA fragmentation and apoptosis. We have complemented the studies above via the use of MEFs and ES cells from calpain knockout mice, as well as the construction of his-tagged C- and N-terminal PARP reagents that will be useful for novel affinity purification methodology as well as the preparation of a biochemical activity assay, which we have also demonstrated can be used from  $\beta$ -lap-treated cells.

From work of this DOD grant, we hypothesized that NQ01 could be exploited for breast cancer because (1) the enzyme is elevated in many human breast cancers and tumors can be rapidly assayed for overall levels prior to treatment; (2) the enzyme is induced by cytotoxic agents, such as ionizing radiation (e.g., it was isolated by our laboratory in 1993 as XIP3), and this attribute of the enzyme should be exploitable for improved radiotherapeutic strategies using  $\beta$ -lapachone; and (3) the data implicates  $\beta$ -lapachone for chemopreventive therapy against cancer, such as breast cancers, since NQ01 is an early known marker of neoplastic transformation of normal epithelial and other cell types. Based on funding from this DOD award, we were recently able to obtain funding from the National Institutes of Health to explore this hypothesis. We are also currently preparing a grant to be submitted to the NIH for support of the purification of  $\beta$ -lap-activated calpain or the calpain-like protease.

## REFERENCES:

1. Malkinson, A. M. Molecular comparison of human and mouse pulmonary adenocarcinomas. *Exp Lung Res*, 24: 541-555, 1998.
2. Malkinson, A. M., Siegel, D., Forrest, G. L., Gazdar, A. F., Oie, H. K., Chan, D. C., Bunn, P. A., Mabry, M., Dykes, D. J., Harrison, S. D., and et al. Elevated DT-diaphorase activity and messenger RNA content in human non- small cell lung carcinoma: relationship to the response of lung tumor xenografts to mitomycin C. *Cancer Res*, 52: 4752-4757, 1992.
3. Belinsky, M. and Jaiswal, A. K. NAD(P)H:quinone oxidoreductase1 (DT-diaphorase) expression in normal and tumor tissues. *Cancer Metastasis Rev*, 12: 103-117, 1993.
4. Marin, A., Lopez de Cerain, A., Hamilton, E., Lewis, A. D., Martinez-Penuela, J. M., Idoate, M. A., and Bello, J. DT-diaphorase and cytochrome B5 reductase in human lung and breast tumours. *Br J Cancer*, 76: 923-929, 1997.
5. Llopis, J., Ernster, L., and Cadenas, E. Effect of glutathione on the redox transitions of naphthohydroquinone derivatives formed during DT-diaphorase catalysis. *Free Radic Res Commun*, 8: 271-285, 1990.
6. Buettner, G. R. The pecking order of free radicals and antioxidants: lipid peroxidation, alpha-tocopherol, and ascorbate. *Arch Biochem Biophys*, 300: 535-543, 1993.
7. Ross, D., Siegel, D., Beall, H., Prakash, A. S., Mulcahy, R. T., and Gibson, N. W. DT-diaphorase in activation and detoxification of quinones. Bioreductive activation of mitomycin C. *Cancer Metastasis Rev*, 12: 83-101, 1993.
8. Ross, D., Beall, H., Traver, R. D., Siegel, D., Phillips, R. M., and Gibson, N. W. Bioactivation of quinones by DT-diaphorase, molecular, biochemical, and chemical studies. *Oncol Res*, 6: 493-500, 1994.
9. Siegel, D., Beall, H., Kasai, M., Arai, H., Gibson, N. W., and Ross, D. pH-dependent inactivation of DT-diaphorase by mitomycin C and porfiromycin. *Mol Pharmacol*, 44: 1128-1134, 1993.
10. Siegel, D., Beall, H., Senekowitsch, C., Kasai, M., Arai, H., Gibson, N. W., and Ross, D. Bioreductive activation of mitomycin C by DT-diaphorase. *Biochemistry*, 31: 7879-7885, 1992.
11. Cadenas, E. Antioxidant and prooxidant functions of DT-diaphorase in quinone metabolism. *Biochem Pharmacol*, 49: 127-140, 1995.
12. Beall, H. D., Murphy, A. M., Siegel, D., Hargreaves, R. H., Butler, J., and Ross, D. Nicotinamide adenine dinucleotide (phosphate): quinone oxidoreductase (DT-diaphorase) as a target for bioreductive antitumor quinones: quinone cytotoxicity and selectivity in human lung and breast cancer cell lines. *Mol Pharmacol*, 48: 499-504, 1995.
13. Beall, H. D., Liu, Y., Siegel, D., Bolton, E. M., Gibson, N. W., and Ross, D. Role of NAD(P)H:quinone oxidoreductase (DT-diaphorase) in cytotoxicity and induction of DNA damage by streptonigrin. *Biochem Pharmacol*, 51: 645-652, 1996.
14. Radjendirane, V., Joseph, P., Lee, Y. H., Kimura, S., Klein-Szanto, A. J., Gonzalez, F. J., and Jaiswal, A. K. Disruption of the DT diaphorase (NQO1) gene in mice leads to increased menadione toxicity. *J Biol Chem*, 273: 7382-7389, 1998.
15. Rockwell, S., Kemple, B., and Kelley, M. Cytotoxicity of BMS-181174. Effects of hypoxia, dicoumarol, and repair deficits. *Biochem Pharmacol*, 50: 1239-1243, 1995.
16. Prakash, A. S., Beall, H., Ross, D., and Gibson, N. W. Sequence-selective alkylation and cross-linking induced by mitomycin C upon activation by DT-diaphorase. *Biochemistry*, 32: 5518-5525, 1993.
17. Siegel, D., Gibson, N. W., Preusch, P. C., and Ross, D. Metabolism of mitomycin C by DT-diaphorase: role in mitomycin C-induced DNA damage and cytotoxicity in human colon carcinoma cells. *Cancer Res*, 50: 7483-7489, 1990.
18. Siegel, D., Gibson, N. W., Preusch, P. C., and Ross, D. Metabolism of diaziquone by NAD(P)H:(quinone acceptor) oxidoreductase (DT-diaphorase): role in diaziquone-induced DNA damage and cytotoxicity in human colon carcinoma cells. *Cancer Res*, 50: 7293-7300, 1990.
19. Riley, R. J. and Workman, P. DT-diaphorase and cancer chemotherapy. *Biochem Pharmacol*, 43: 1657-1669, 1992.
20. Fitzsimmons, S. A., Workman, P., Grever, M., Paull, K., Camalier, R., and Lewis, A. D. Reductase enzyme expression across the National Cancer Institute Tumor cell line panel: correlation with sensitivity to mitomycin C and EO9 [see comments]. *J Natl Cancer Inst*, 88: 259-269, 1996.

21. Boothman, D. A. and Pardee, A. B. Inhibition of radiation-induced neoplastic transformation by beta-lapachone. *Proc Natl Acad Sci U S A*, 86: 4963-4967., 1989.
22. Ernster, L., Atallah, A. S., and Hochstein, P. DT diaphorase and the cytotoxicity and mutagenicity of quinone-derived oxygen radicals. *Prog Clin Biol Res* 353-363, 1986.
23. Gustafson, D. L. and Pritsos, C. A. Bioactivation of mitomycin C by xanthine dehydrogenase from EMT6 mouse mammary carcinoma tumors [see comments]. *J Natl Cancer Inst*, 84: 1180-1185, 1992.
24. Gustafson, D. L., Beall, H. D., Bolton, E. M., Ross, D., and Waldren, C. A. Expression of human NAD(P)H: quinone oxidoreductase (DT-diaphorase) in Chinese hamster ovary cells: effect on the toxicity of antitumor quinones. *Mol Pharmacol*, 50: 728-735, 1996.
25. Hollander, P. M., Bartfai, T., and Gatt, S. Studies on the reaction mechanism of DT diaphorase. Intermediary plateau and trough regions in the initial velocity vs substrate concentration curves. *Arch Biochem Biophys*, 169: 568-576, 1975.
26. Hollander, P. M. and Ernster, L. Studies on the reaction mechanism of DT diaphorase. Action of dead-end inhibitors and effects of phospholipids. *Arch Biochem Biophys*, 169: 560-567, 1975.
27. Hosoda, S., Nakamura, W., and Hayashi, K. Properties and reaction mechanism of DT diaphorase from rat liver. *J Biol Chem*, 249: 6416-6423, 1974.
28. Ross, D., Siegel, D., Gibson, N. W., Pacheco, D., Thomas, D. J., Reasor, M., and Wierda, D. Activation and deactivation of quinones catalyzed by DT-diaphorase. Evidence for bioreductive activation of diaziquone (AZQ) in human tumor cells and detoxification of benzene metabolites in bone marrow stroma. *Free Radic Res Commun*, 8: 373-381, 1990.
29. Boothman, D. A., Meyers, M., Fukunaga, N., and Lee, S. W. Isolation of x-ray-inducible transcripts from radioresistant human melanoma cells. *Proc Natl Acad Sci U S A*, 90: 7200-7204., 1993.
30. Boothman, D. A., Trask, D. K., and Pardee, A. B. Inhibition of potentially lethal DNA damage repair in human tumor cells by beta-lapachone, an activator of topoisomerase I. *Cancer Res*, 49: 605-612., 1989.
31. Pink, J. J., Planchon, S. M., Tagliarino, C., Varnes, M. E., Siegel, D., and Boothman, D. A. NAD(P)H:Quinone oxidoreductase activity is the principal determinant of beta-lapachone cytotoxicity. *J Biol Chem*, 275: 5416-5424., 2000.
32. Tagliarino, C., Pink, J. J., Reinicke, K. E., Simmers, S. M., Wuerzberger-Davis, S. M., and Boothman, D. A.  $\mu$ -Calpain activation in  $\beta$ -lapachone-mediated apoptosis. *Cancer Biology and Therapy*, 2: In Press., 2003.
33. Tagliarino, C., Pink, J. J., Dubyak, G. R., Nieminen, A. L., and Boothman, D. A. Calcium is a key signaling molecule in beta-lapachone-mediated cell death. *J Biol Chem*, 276: 19150-19159., 2001.
34. Kubbutat, M. H. and Vousden, K. H. Proteolytic cleavage of human p53 by calpain: a potential regulator of protein stability. *Mol Cell Biol*, 17: 460-468, 1997.
35. Shinohara, K., Tomioka, M., Nakano, H., Tone, S., Ito, H., and Kawashima, S. Apoptosis induction resulting from proteasome inhibition. *Biochem J*, 317: 385-388, 1996.
36. Kaufmann, S. H., Desnoyers, S., Ottaviano, Y., Davidson, N. E., and Poirier, G. G. Specific proteolytic cleavage of poly(ADP-ribose) polymerase: an early marker of chemotherapy-induced apoptosis. *Cancer Res*, 53: 3976-3985, 1993.
37. Preusch, P. C., Siegel, D., Gibson, N. W., and Ross, D. A note on the inhibition of DT-diaphorase by dicoumarol. *Free Radic Biol Med*, 11: 77-80, 1991.
38. Planchon, S. M., Pink, J. J., Tagliarino, C., Bornmann, W. G., Varnes, M. E., and Boothman, D. A. beta-Lapachone-induced apoptosis in human prostate cancer cells: involvement of NQO1/xip3. *Exp Cell Res*, 267: 95-106., 2001.
39. Pink, J. J., Planchon, S.M.m Tagliarino, C., Wuerzberger-Davis, S.M., Varnes, M.E., Siegel, D., and Boothman, D.A. NAD(P)H:quinone oxidoreductase (NQO1) activity is the principal determinant of  $\beta$ -lapachone cytotoxicity. *Journal of Biological Chemistry*, 275: 5416-5424, 2000.
40. Wuerzberger, S. M., Pink, J. J., Planchon, S. M., Byers, K. L., Bornmann, W. G., and Boothman, D. A. Induction of apoptosis in MCF-7:WS8 breast cancer cells by beta- lapachone. *Cancer Res*, 58: 1876-1885., 1998.
41. Planchon, S. M., Wuerzberger, S., Frydman, B., Witiak, D. T., Hutson, P., Church, D. R., Wilding, G., and Boothman, D. A. Beta-lapachone-mediated apoptosis in human promyelocytic leukemia (HL- 60) and human prostate cancer cells: a p53-independent response. *Cancer Res*, 55: 3706-3711., 1995.
42. Gonen, H., Shkedy, D., Barnoy, S., Kosower, N. S., and Ciechanover, A. On the involvement of calpains in the degradation of the tumor suppressor protein p53. *FEBS Lett*, 406: 17-22, 1997.
43. Pariat, M., Carillo, S., Molinari, M., Salvat, C., Debussche, L., Bracco, L., Milner, J., and Piechaczyk, M.

- Proteolysis by calpains: a possible contribution to degradation of p53. *Mol Cell Biol*, 17: 2806-2815, 1997.
44. Zhang, X., Wen, J., Bidasee, K. R., Besch, H. R., Jr., and Rubin, R. P. Ryanodine receptor expression is associated with intracellular  $Ca^{2+}$  release in rat parotid acinar cells. *Am J Physiol*, 273: C1306-1314, 1997.
45. Kawasaki, H. and Kawashima, S. Regulation of the calpain-calpastatin system by membranes (review). *Mol Membr Biol*, 13: 217-224, 1996.
46. Janicke, R. U., Ng, P., Sprengart, M. L., and Porter, A. G. Caspase-3 is required for alpha-fodrin cleavage but dispensable for cleavage of other death substrates in apoptosis. *J Biol Chem*, 273: 15540-15545, 1998.
47. McGinnis, K. M., Gnegy, M. E., Park, Y. H., Mukerjee, N., and Wang, K. K. Procaspase-3 and Poly(ADP)ribose polymerase (PARP) are calpain substrates [In Process Citation]. *Biochem Biophys Res Commun*, 263: 94-99, 1999.
48. McGinnis, K. M., Wang, K. K., and Gnegy, M. E. Alterations of extracellular calcium elicit selective modes of cell death and protease activation in SH-SY5Y human neuroblastoma cells. *J Neurochem*, 72: 1853-1863, 1999.
49. Buki, K. G., Bauer, P. I., and Kun, E. Isolation and identification of a proteinase from calf thymus that cleaves poly(ADP-ribose) polymerase and histone H1. *Biochim Biophys Acta*, 1338: 100-106, 1997.
50. Shea, T. B. Restriction of microM-calcium-requiring calpain activation to the plasma membrane in human neuroblastoma cells: evidence for regionalized influence of a calpain activator protein. *J Neurosci Res*, 48: 543-550, 1997.
51. Squier, M. K. and Cohen, J. J. Calpain, an upstream regulator of thymocyte apoptosis. *J Immunol*, 158: 3690-3697, 1997.
52. Nagao, S., Saido, T. C., Akita, Y., Tsuchiya, T., Suzuki, K., and Kawashima, S. Calpain-calpastatin interactions in epidermoid carcinoma KB cells. *J Biochem (Tokyo)*, 115: 1178-1184, 1994.
53. Saido, T. C., Nagao, S., Shiramine, M., Tsukaguchi, M., Yoshizawa, T., Sorimachi, H., Ito, H., Tsuchiya, T., Kawashima, S., and Suzuki, K. Distinct kinetics of subunit autolysis in mammalian m-calpain activation. *FEBS Lett*, 346: 263-267, 1994.
54. Suzuki, K., Imajoh, S., Emori, Y., Kawasaki, H., Minami, Y., and Ohno, S. Calcium-activated neutral protease and its endogenous inhibitor. Activation at the cell membrane and biological function. *FEBS Lett*, 220: 271-277, 1987.
55. Mohan, P. S. and Nixon, R. A. Purification and properties of high molecular weight calpastatin from bovine brain. *J Neurochem*, 64: 859-866, 1995.
56. Maki, M., Takano, E., Mori, H., Kannagi, R., Murachi, T., and Hatanaka, M. Repetitive region of calpastatin is a functional unit of the proteinase inhibitor. *Biochem Biophys Res Commun*, 143: 300-308, 1987.
57. Maki, M., Takano, E., Mori, H., Sato, A., Murachi, T., and Hatanaka, M. All four internally repetitive domains of pig calpastatin possess inhibitory activities against calpains I and II. *FEBS Lett*, 223: 174-180, 1987.
58. Maki, M., Bagci, H., Hamaguchi, K., Ueda, M., Murachi, T., and Hatanaka, M. Inhibition of calpain by a synthetic oligopeptide corresponding to an exon of the human calpastatin gene. *J Biol Chem*, 264: 18866-18869, 1989.
59. Emori, Y. [Proteinaceous inhibitor specific for calcium-dependent protease]. *Seikagaku*, 60: 266-272, 1988.
60. Emori, Y., Kawasaki, H., Imajoh, S., Minami, Y., and Suzuki, K. All four repeating domains of the endogenous inhibitor for calcium-dependent protease independently retain inhibitory activity. Expression of the cDNA fragments in *Escherichia coli*. *J Biol Chem*, 263: 2364-2370, 1988.
61. Takano, J., Watanabe, M., Hitomi, K., and Maki, M. Four types of calpastatin isoforms with distinct amino-terminal sequences are specified by alternative first exons and differentially expressed in mouse tissues. *J Biochem (Tokyo)*, 128: 83-92, 2000.
62. Emori, Y., Kawasaki, H., Imajoh, S., Minami, Y., and Suzuki, K. All four repeating domains of the endogenous inhibitor for calcium-dependent protease independently retain inhibitory activity. Expression of the cDNA fragments in *Escherichia coli*. *J Biol Chem*, 263: 2364-2370, 1988.
63. Sasaki, T., Kishi, M., Saito, M., Tanaka, T., Higuchi, N., Kominami, E., Katunuma, N., and Murachi, T. Inhibitory effect of di- and tripeptidyl aldehydes on calpains and cathepsins. *J Enzyme Inhib*, 3: 195-201, 1990.
64. Sun, D. Y., Jiang, S., Zheng, L. M., Ojcius, D. M., and Young, J. D. Separate metabolic pathways leading to DNA fragmentation and apoptotic chromatin condensation. *J Exp Med*, 179: 559-568, 1994.
65. Schoenwaelder, S. M. and Burridge, K. Evidence for a calpeptin-sensitive protein-tyrosine phosphatase

- upstream of the small GTPase Rho. A novel role for the calpain inhibitor calpeptin in the inhibition of protein-tyrosine phosphatases. *J Biol Chem*, 274: 14359-14367, 1999.
66. Spinedi, A., Oliverio, S., Di Sano, F., and Piacentini, M. Calpain involvement in calphostin C-induced apoptosis. *Biochem Pharmacol*, 56: 1489-1492, 1998.
67. Kapprell, H. P. and Goll, D. E. Effect of  $Ca^{2+}$  on binding of the calpains to calpastatin. *J Biol Chem*, 264: 17888-17896, 1989.
68. Yoshimura, N., Hatanaka, M., Kitahara, A., Kawaguchi, N., and Murachi, T. Intracellular localization of two distinct  $Ca^{2+}$ -proteases (calpain I and calpain II) as demonstrated by using discriminative antibodies. *J Biol Chem*, 259: 9847-9852, 1984.
69. Yoshimura, N., Tsukahara, I., and Murachi, T. Calpain and calpastatin in porcine retina. Identification and action on microtubule-associated proteins. *Biochem J*, 223: 47-51, 1984.
70. Lane, R. D., Allan, D. M., and Mellgren, R. L. A comparison of the intracellular distribution of mu-calpain, m-calpain, and calpastatin in proliferating human A431 cells. *Exp Cell Res*, 203: 5-16, 1992.
71. Yang, Y. L. and Li, X. M. The IAP family: endogenous caspase inhibitors with multiple biological activities [In Process Citation]. *Cell Res*, 10: 169-177, 2000.
72. Tang, T. S., Dong, J. B., Huang, X. Y., and Sun, F. Z.  $Ca^{2+}$  oscillations induced by a cytosolic sperm protein factor are mediated by a maternal machinery that functions only once in mammalian eggs. *Development*, 127: 1141-1150, 2000.
73. Squier, M. K., Miller, A. C., Malkinson, A. M., and Cohen, J. J. Calpain activation in apoptosis. *J Cell Physiol*, 159: 229-237, 1994.
74. Squier, M. K., Sehnert, A. J., Sellins, K. S., Malkinson, A. M., Takano, E., and Cohen, J. J. Calpain and calpastatin regulate neutrophil apoptosis. *J Cell Physiol*, 178: 311-319, 1999.
75. Waterhouse, N. J., Finucane, D. M., Green, D. R., Elce, J. S., Kumar, S., Alnemri, E. S., Litwack, G., Khanna, K., Lavin, M. F., and Watters, D. J. Calpain activation is upstream of caspases in radiation-induced apoptosis. *Cell Death Differ*, 5: 1051-1061, 1998.
76. Patel, Y. M. and Lane, M. D. Role of calpain in adipocyte differentiation. *Proc Natl Acad Sci U S A*, 96: 1279-1284, 1999.
77. Wellington, C. L., Ellerby, L. M., Hackam, A. S., Margolis, R. L., Trifiro, M. A., Singaraja, R., McCutcheon, K., Salvesen, G. S., Propp, S. S., Bromm, M., Rowland, K. J., Zhang, T., Rasper, D., Roy, S., Thornberry, N., Pinsky, L., Kakizuka, A., Ross, C. A., Nicholson, D. W., Bredesen, D. E., and Hayden, M. R. Caspase cleavage of gene products associated with triplet expansion disorders generates truncated fragments containing the polyglutamine tract. *J Biol Chem*, 273: 9158-9167, 1998.
78. Nicholson, D. W. Caspase structure, proteolytic substrates, and function during apoptotic cell death. *Cell Death Differ*, 6: 1028-1042, 1999.
79. Nicholson, K. M., Quinn, D. M., Kellett, G. L., and Warr, J. R. Preferential killing of multidrug-resistant KB cells by inhibitors of glucosylceramide synthase. *Br J Cancer*, 81: 423-430, 1999.
80. Neumar, R. W., Meng, F. H., Mills, A. M., Xu, Y. A., Zhang, C., Welsh, F. A., and Siman, R. Calpain activity in the rat brain after transient forebrain ischemia. *Exp Neurol*, 170: 27-35, 2001.
81. Zheng, J., Thylin, M. R., Ghorpade, A., Xiong, H., Persidsky, Y., Cotter, R., Niemann, D., Che, M., Zeng, Y. C., Gelbard, H. A., Shepard, R. B., Swartz, J. M., and Gendelman, H. E. Intracellular CXCR4 signaling, neuronal apoptosis and neuropathogenic mechanisms of HIV-1-associated dementia. *J Neuroimmunol*, 98: 185-200, 1999.
82. Pink, J. J., Planchon, S. M., Tagliarino, C., Varnes, M. E., Siegel, D., and Boothman, D. A. NAD(P)H:Quinone oxidoreductase activity is the principal determinant of beta-lapachone cytotoxicity. *J Biol Chem*, 275: 5416-5424, 2000.
83. Li, X. and Cai, M. Inactivation of the cyclin-dependent kinase Cdc28 abrogates cell cycle arrest induced by DNA damage and disassembly of mitotic spindles in *Saccharomyces cerevisiae*. *Mol Cell Biol*, 17: 2723-2734, 1997.
84. Eguchi, S., Iwasaki, H., Inagami, T., Numaguchi, K., Yamakawa, T., Motley, E. D., Owada, K. M., Marumo, F., and Hirata, Y. Involvement of PYK2 in angiotensin II signaling of vascular smooth muscle cells. *Hypertension*, 33: 201-206, 1999.
85. Eguchi, S., Iwasaki, H., Ueno, H., Frank, G. D., Motley, E. D., Eguchi, K., Marumo, F., Hirata, Y., and Inagami, T. Intracellular signaling of angiotensin II-induced p70 S6 kinase phosphorylation at Ser(411) in vascular smooth muscle cells. Possible requirement of epidermal growth factor receptor, Ras, extracellular signal-regulated kinase, and Akt. *J Biol Chem*, 274: 36843-36851, 1999.



86. Ortaldo, J. R., Winkler-Pickett, R. T., Nagata, S., and Ware, C. F. Fas involvement in human NK cell apoptosis: lack of a requirement for CD16-mediated events. *J Leukoc Biol*, 61: 209-215, 1997.
87. Ruiz-Vela, A., Gonz#lez de Buitrago, G., and Mart#nez, A. C. Implication of calpain in caspase activation during B cell clonal deletion. *Embo J*, 18: 4988-4998, 1999.
88. Wood, D. E. and Newcomb, E. W. Caspase-dependent activation of calpain during drug-induced apoptosis. *J Biol Chem*, 274: 8309-8315, 1999.
89. Wang, Y. G., Rechenmacher, C. E., and Lipsius, S. L. Nitric oxide signaling mediates stimulation of L-type  $Ca^{2+}$  current elicited by withdrawal of acetylcholine in cat atrial myocytes. *J Gen Physiol*, 111: 113-125, 1998.
90. Belmokhtar, C. A., Torriglia, A., Counis, M. F., Courtois, Y., Jacquemin-Sablon, A., and Segal-Bendirdjian, E. Nuclear translocation of a leukocyte elastase Inhibitor/Elastase complex during staurosporine-induced apoptosis: role in the generation of nuclear L-DNase II activity. *Exp Cell Res*, 254: 99-109, 2000.
91. Liu, P., Hopfner, R. L., Xu, Y. J., and Gopalakrishnan, V. Vasopressin-evoked  $[Ca^{2+}]_i$  responses in neonatal rat cardiomyocytes. *J Cardiovasc Pharmacol*, 34: 540-546, 1999.
92. Nath, R., Raser, K. J., McGinnis, K., Nadimpalli, R., Stafford, D., and Wang, K. K. Effects of ICE-like protease and calpain inhibitors on neuronal apoptosis. *Neuroreport*, 8: 249-255, 1996.
93. Nath, R., Raser, K. J., Stafford, D., Hajimohammadreza, I., Posner, A., Allen, H., Talanian, R. V., Yuen, P., Gilbertsen, R. B., and Wang, K. K. Non-erythroid alpha-spectrin breakdown by calpain and interleukin 1 beta-converting-enzyme-like protease(s) in apoptotic cells: contributory roles of both protease families in neuronal apoptosis. *Biochem J*, 319: 683-690, 1996.
94. McGinnis, K. M., Whitton, M. M., Gnegy, M. E., and Wang, K. K. Calcium/calmodulin-dependent protein kinase IV is cleaved by caspase-3 and calpain in SH-SY5Y human neuroblastoma cells undergoing apoptosis. *J Biol Chem*, 273: 19993-20000, 1998.
95. McGinnis, K. M., Gnegy, M. E., Park, Y. H., Mukerjee, N., and Wang, K. K. Procaspase-3 and poly(ADP)ribose polymerase (PARP) are calpain substrates. *Biochem Biophys Res Commun*, 263: 94-99, 1999.
96. Croall, D. E. and DeMartino, G. N. Calcium-dependent affinity purification of transglutaminase from rat liver cytosol. *Cell Calcium*, 7: 29-39, 1986.
97. Croall, D. E., Morrow, J. S., and DeMartino, G. N. Limited proteolysis of the erythrocyte membrane skeleton by calcium- dependent proteinases. *Biochim Biophys Acta*, 882: 287-296, 1986.
98. Sakai, K., Akanuma, H., Imahori, K., and Kawashima, S. A unique specificity of a calcium activated neutral protease indicated in histone hydrolysis. *J Biochem (Tokyo)*, 101: 911-918, 1987.
99. Wang, K. K., Roufogalis, B. D., and Villalobo, A. Characterization of the fragmented forms of calcineurin produced by calpain I. *Biochem Cell Biol*, 67: 703-711, 1989.
100. Wang, K. K., Roufogalis, B. D., and Villalobo, A. Calpain I activates  $Ca^{2+}$  transport by the human erythrocyte plasma membrane calcium pump. *Adv Exp Med Biol*, 269: 175-180, 1990.
101. Murachi, T., Tanaka, K., Hatanaka, M., and Murakami, T. Intracellular  $Ca^{2+}$ -dependent protease (calpain) and its high-molecular-weight endogenous inhibitor (calpastatin). *Adv Enzyme Regul*, 19: 407-424, 1980.
102. Kleese, W. C., Goll, D. E., Edmunds, T., and Shannon, J. D. Immunofluorescent localization of the  $Ca^{2+}$ -dependent proteinase and its inhibitor in tissues of *Crotalus atrox*. *J Exp Zool*, 241: 277-289, 1987.
103. Murachi, T. Calcium-dependent proteinases and specific inhibitors: calpain and calpastatin. *Biochem Soc Symp*, 49: 149-167, 1984.
104. Schollmeyer, J. E. Calpain II involvement in mitosis [see comments]. *Science*, 240: 911-913, 1988.
105. Beckerle, M. C., Burrige, K., DeMartino, G. N., and Croall, D. E. Colocalization of calcium-dependent protease II and one of its substrates at sites of cell adhesion. *Cell*, 51: 569-577, 1987.
106. Yoshimura, N., Murachi, T., Heath, R., Kay, J., Jasani, B., and Newman, G. R. Immunogold electron-microscopic localisation of calpain I in skeletal muscle of rats. *Cell Tissue Res*, 244: 265-270, 1986.
107. Barnoy, S., Zipser, Y., Glaser, T., Grimberg, Y., and Kosower, N. S. Association of calpain ( $Ca^{2+}$ -dependent thiol protease) with its endogenous inhibitor calpastatin in myoblasts. *J Cell Biochem*, 74: 522-531, 1999.
108. Zhang, Y., Chou, J. H., Bradley, J., Bargmann, C. I., and Zinn, K. The *Caenorhabditis elegans* seven-transmembrane protein ODR-10 functions as an odorant receptor in mammalian cells. *Proc Natl Acad Sci U S A*, 94: 12162-12167, 1997.
109. Mellgren, R. L. and Lu, Q. Selective nuclear transport of mu-calpain. *Biochem Biophys Res Commun*, 204:

Wagner MW/Tagliarino C

544-550, 1994.

110. Mellgren, R. L., Shaw, E., and Mericle, M. T. Inhibition of growth of human TE2 and C-33A cells by the cell-permeant calpain inhibitor benzyloxycarbonyl-Leu-Leu-Tyr diazomethyl ketone. *Exp Cell Res*, 215: 164-171, 1994.
111. Tullio, R. D., Passalacqua, M., Averna, M., Salamino, F., Melloni, E., and Pontremoli, S. Changes in intracellular localization of calpastatin during calpain activation. *Biochem J*, 343 Pt 2: 467-472, 1999.
112. Zhang, L., Kelley, J., Schmeisser, G., Kobayashi, Y. M., and Jones, L. R. Complex formation between junctin, triadin, calsequestrin, and the ryanodine receptor. Proteins of the cardiac junctional sarcoplasmic reticulum membrane. *J Biol Chem*, 272: 23389-23397, 1997.
113. Dutt, P., Arthur, J. S., Grochulski, P., Cygler, M., and Elce, J. S. Roles of individual EF-hands in the activation of m-calpain by calcium. *Biochem J*, 348 Pt 1: 37-43, 2000.
114. Azam, M., Andrabi, S. S., Sahr, K. E., Kamath, L., Kuliopulos, A., and Chishti, A. H. Disruption of the mouse mu-calpain gene reveals an essential role in platelet function. *Mol Cell Biol*, 21: 2213-2220, 2001.

## APPENDICES:

### CURRENT LIST OF PUBLICATIONS RESULTING FROM THIS AWARD PAPERS PUBLISHED IN PEER-REVIEWED JOURNALS (Enclosed):

- Pink, J.J., Planchon, S.M., Tagliarino, C., Wuerzberger-Davis, S.M., Varnes, M.E., Siegel, D., and Boothman, D.A. NAD(P)H:quinone oxidoreductase (NQO1) activity is the principal determinant of  $\beta$ -lapachone cytotoxicity. 2000; *J. Biol. Chem.*, 275 (8): 5416-5422.
- Pink, J.J., Wuerzberger-Davis, S.M., Tagliarino C., Planchon, S.M., Yang, X-H., Froelich, C.J., and Boothman, D.A. Activation of a Cysteine Protease in MCF-7 and T47D Breast Cancer Cells during  $\beta$ -Lapachone-Mediated Apoptosis. 2000; *Exp. Cell. Res.*, 255 (2): 144-155.
- Tagliarino, C., Pink, J.J., Dubyak, G.R., Nieminen, A-L., and Boothman, D.A. Calcium is a key signaling molecule in  $\beta$ -lapachone-mediated cell death. 2001; *J. Biol. Chem.* 276(22): 19150-19159.
- Planchon, S.M., Pink, J.J., Tagliarino, C., Bornmann, W.G., Varnes, M.E., and Boothman, D.A.  $\beta$ -Lapachone-induced apoptosis in human prostate cancer cells: involvement of NQO1/xip3. 2001; *Exp. Cell Res.*, 267: 95-106.
- Tagliarino, C., Pink, J.J., Wuerzberg-Davis, S., and Boothman, D.A.  $\mu$ -Calpain activation in  $\beta$ -lapachone-mediated apoptosis. *Cancer Biology & Therapy*, 2(2):141-152, 2003.

### PAPERS PUBLISHED IN NON-PEER-REVIEWED JOURNALS (Not Enclosed).

- Pink, J.J., Tagliarino, C. Planchon, S., Varnes, M. Simmers, S., and Boothman, D.A. Cell death pathways triggered by  $\beta$ -lapachone. *Free Radical Biology*, In Press, 2001.
- Miyamoto, S., Huang, T., Wuerzberger-Davis, S., Bornmann, W.,G., Pink, J.J., Tagliarino, C., Kinsella, T.J., and Boothman, D.A. Cellular and Molecular Responses to Topoisomerase I Poisons: Exploiting Synergy For Improved Radiotherapy. 2000; *Annals of the New York Academy of Sciences*, 922: 274-292.
- Tagliarino, C. Pink, J.J. and Boothman, D.A. Calpains and apoptosis. 2002; *Korean J. Biol Sci.*, 5: 267-274.



Wagner MW/Tagliarino C

**BINDING:** Because all reports are entered into the Department of Defense Technical Reports Database collection and are microfiched, it is recommended that all reports be bound by stapling the pages together in the upper left hand corner. All reports shall be prepared in camera ready copy (legible print, clear photos/illustrations) for microfiching. Figures should include legends and all figures and tables should be clearly marked.

**FINAL REPORTS:** All final reports must include a bibliography of all publications and meeting abstracts and a list of personnel (not salaries) receiving pay from the research effort.

SEE ABOVE.

**NOTE: IF ALL OF THE ABOVE ELEMENTS ARE NOT MET, THE REPORT WILL BE CONSIDERED UNACCEPTABLE AND WILL BE RETURNED FOR REWRITE.**

**HELPFUL HINTS:**

1. Please proof all reports for errors.
2. Please provide supporting data, i.e. tables, figures, graphs, etc.
3. Ensure all publications published as a result of effort acknowledges the work supported by USAMRMC. Copies of all publications supported by the USAMRMC are to be provided with reports.

.....

**Manuscripts/Reprints, Abstracts**

A copy of manuscripts or subsequent reprints resulting from the research shall be submitted to the USAMRMC. An extended abstract suitable for publication in the Proceedings of the Breast Cancer Research Program is required in relation to a DOD BCRP meeting tentatively planned for 2003. The extended abstract shall (1) identify the accomplishments since award and (2) follow instructions to be prepared by the USAMRMC and promulgated at a later date. The extended abstract style will be dependent on the discipline.

**An Extended Abstract will be Submitted and the PI (Mr. Mark Wagner or Dr. David A. Boothman) will attend the next 2003 Breast Cancer Research Program.**

## Calcium Is a Key Signaling Molecule in $\beta$ -Lapachone-mediated Cell Death\*

Received for publication, January 25, 2001, and in revised form, March 1, 2001  
Published, JBC Papers in Press, March 2, 2001, DOI 10.1074/jbc.M100730200

Colleen Tagliarino<sup>§</sup>, John J. Pink<sup>‡</sup>, George R. Dubyak<sup>¶</sup>, Anna-Liisa Nieminen<sup>||</sup>, and David A. Boothman<sup>‡\*\*</sup>

From the <sup>‡</sup>Departments of Radiation Oncology and Pharmacology, <sup>||</sup>Department of Anatomy, and the <sup>¶</sup>Department of Physiology and Biophysics, Case Western Reserve University, Cleveland, Ohio 44106-4942

$\beta$ -Lapachone ( $\beta$ -Lap) triggers apoptosis in a number of human breast and prostate cancer cell lines through a unique apoptotic pathway that is dependent upon NQO1, a two-electron reductase. Downstream signaling pathway(s) that initiate apoptosis following treatment with  $\beta$ -Lap have not been elucidated. Since calpain activation was suspected in  $\beta$ -Lap-mediated apoptosis, we examined alterations in  $\text{Ca}^{2+}$  homeostasis using NQO1-expressing MCF-7 cells.  $\beta$ -Lap-exposed MCF-7 cells exhibited an early increase in intracellular cytosolic  $\text{Ca}^{2+}$ , from endoplasmic reticulum  $\text{Ca}^{2+}$  stores, comparable to thapsigargin exposures. 1,2-Bis-(2-aminophenoxy)ethane-*N,N,N',N'*-tetraacetic acid-acetoxymethyl ester, an intracellular  $\text{Ca}^{2+}$  chelator, blocked early increases in  $\text{Ca}^{2+}$  levels and inhibited  $\beta$ -Lap-mediated mitochondrial membrane depolarization, intracellular ATP depletion, specific and unique substrate proteolysis, and apoptosis. The extracellular  $\text{Ca}^{2+}$  chelator, EGTA, inhibited later apoptotic end points (observed >8 h, e.g. substrate proteolysis and DNA fragmentation), suggesting that later execution events were triggered by  $\text{Ca}^{2+}$  influxes from the extracellular milieu. Collectively, these data suggest a critical, but not sole, role for  $\text{Ca}^{2+}$  in the NQO1-dependent cell death pathway initiated by  $\beta$ -Lap. Use of  $\beta$ -Lap to trigger an apparently novel, calpain-like-mediated apoptotic cell death could be useful for breast and prostate cancer therapy.

$\beta$ -Lap<sup>1</sup> is a naturally occurring compound present in the bark of the South American Lapacho tree. It has antitumor activity against a variety of human cancers, including colon, prostate, promyelocytic leukemia, and breast (1–3).  $\beta$ -Lap was an effective agent (alone and in combination with taxol) against human ovarian and prostate xenografts in mice, with little host

toxicity (4). We recently demonstrated that  $\beta$ -Lap kills human breast and prostate cancer cells by apoptosis, a cytotoxic response significantly enhanced by NAD(P)H:quinone oxidoreductase (NQO1, E.C. 1.6.99.2) enzymatic activity (5).<sup>2</sup>  $\beta$ -Lap cytotoxicity was prevented by co-treatment with dicumaryl (an NQO1 inhibitor) in NQO1-expressing breast and prostate cancer cells (5).<sup>2</sup> NQO1 is a cytosolic enzyme elevated in breast cancers (6) that catalyzes a two-electron reduction of quinones (e.g.  $\beta$ -Lap, menadione), utilizing either NADH or NADPH as electron donors. Reduction of  $\beta$ -Lap by NQO1 presumably leads to a futile cycling of the compound, wherein the quinone and hydroquinone form a redox cycle with a net concomitant loss of reduced NAD(P)H (5).

Apoptosis is an evolutionarily conserved pathway of biochemical and molecular events that underlie cell death processes involving the stimulation of intracellular zymogens. The process is a genetically programmed form of cell death involved in development, normal turnover of cells, and in cytotoxic responses to cellular insults. Once apoptosis is initiated, biochemical and morphological changes occur in the cell. These changes include: DNA fragmentation, chromatin condensation, cytoplasmic membrane blebbing, cleavage of apoptotic substrates (e.g. PARP, lamin B), and loss of mitochondrial membrane potential with concomitant release of cytochrome *c* into the cytoplasm (7–9). Apoptosis is a highly regulated, active process that requires the participation of endogenous cellular enzymes that systematically dismantle the cell. The most well characterized proteases in apoptosis are caspases, aspartate-specific cysteine proteases, that work through a cascade that can be initiated by mitochondrial membrane depolarization leading to the release of cytochrome *c* and Apaf-1 into the cytoplasm (10), that then activates caspase 9 (11). Non-caspase-mediated pathways are less understood.

We previously showed that apoptosis following  $\beta$ -Lap administration was unique, in that an ~60-kDa PARP cleavage fragment, as well as distinct intracellular proteolytic cleavage of p53, were observed in NQO1-expressing breast or prostate cancer cells (5).<sup>2</sup> These cleavage events were distinct from those observed when caspases were activated by topoisomerase I poisons, staurosporine, or administration of granzyme B (5, 12, 13). Furthermore,  $\beta$ -Lap-mediated cleavage events were blocked by administration of global cysteine protease inhibitors, as well as extracellular  $\text{Ca}^{2+}$  chelators (12). Based on these data, we concluded that  $\beta$ -Lap exposure of NQO1-expressing breast and prostate cancer cells caused the activation of a  $\text{Ca}^{2+}$ -dependent protease with properties similar to calpain; in particular, the p53 cleavage pattern of  $\beta$ -Lap-exposed

\* This work was supported by United States Army Medical Research and Materiel Command Breast Cancer Initiative Grant DAMD17-98-1-8260 (to D. A. B.), Predoctoral Fellowship DAMD17-00-1-0194 (to C. T.), and Postdoctoral Fellowship DAMD-17-97-1-7221 (to J. J. P.). The costs of publication of this article were defrayed in part by the payment of page charges. This article must therefore be hereby marked "advertisement" in accordance with 18 U.S.C. Section 1734 solely to indicate this fact.

<sup>§</sup> Partial fulfillment of the requirements for the Ph.D. degree, Case Western Reserve University, Dept. of Pharmacology.

<sup>\*\*</sup> To whom correspondence should be addressed: Dept. of Radiation Oncology (BRB-326 East), Case Western Reserve University, 10900 Euclid Ave., Cleveland, OH 44106-4942. Tel.: 216-368-0840; Fax: 216-368-1142; E-mail: dab30@po.cwru.edu.

<sup>1</sup> The abbreviations used are:  $\beta$ -Lap,  $\beta$ -lapachone; MCP, MCF-7-WS8; NQO1, NAD(P)H:quinone oxidoreductase, DT-diaphorase (E.C. 1.6.99.2); PARP, poly(ADP-ribose) polymerase; TUNEL, terminal deoxynucleotidyl transferase-mediated dUTP nick end labeling; ER, endoplasmic reticulum; TG, thapsigargin; STS, staurosporine; BAPTA-AM, 1,2-bis-(2-aminophenoxy)ethane-*N,N,N',N'*-tetraacetic acid-acetoxymethyl ester.

<sup>2</sup> S. M. Planchon, C. Tagliarino, J. J. Pink, W. G. Bornmann, M. E. Varnes, and D. A. Boothman. *Exp. Cell Res.*, in press.

cells was remarkably similar to the pattern observed after calpain activation (14, 15).

Ca<sup>2+</sup> is recognized as an important regulator of apoptosis (16–21). The cytoplasmic Ca<sup>2+</sup> concentration is maintained at ~100 nM in resting cells by relatively impermeable cell membranes, active extrusion of Ca<sup>2+</sup> from the cell by plasma membrane Ca<sup>2+</sup>-ATPases, plasma membrane Na<sup>+</sup>/Ca<sup>2+</sup> exchangers, and active uptake of cytosolic Ca<sup>2+</sup> into the endoplasmic reticulum (ER) by distinct Ca<sup>2+</sup>-ATPases. In contrast, the concentration of Ca<sup>2+</sup> in the extracellular milieu and in the ER is much higher (in the millimolar range). Evidence for involvement of Ca<sup>2+</sup> influx into the cytosol as a triggering event for apoptosis has come from studies with specific Ca<sup>2+</sup> channel blockers that abrogate apoptosis in regressing prostate following testosterone withdrawal (22). Other support for the involvement of Ca<sup>2+</sup> in apoptosis comes from the observation that agents that directly mobilize Ca<sup>2+</sup> (e.g. Ca<sup>2+</sup> ionophores or the sarcoplasmic reticulum Ca<sup>2+</sup>-ATPase pump inhibitor, thapsigargin, TG) can trigger apoptosis in diverse cell types (23–27). Inhibition of the sarcoplasmic reticulum Ca<sup>2+</sup>-ATPase pump by TG causes a transient increase in cytoplasmic Ca<sup>2+</sup> from ER Ca<sup>2+</sup> stores, and a later influx of Ca<sup>2+</sup> from the extracellular milieu, leading to the induction of apoptotic cell death (24, 27, 28). Consequently, emptying of intracellular Ca<sup>2+</sup> stores may trigger apoptosis by disrupting the intracellular architecture and allowing key elements of the effector machinery (e.g. Apaf-1) to gain access to their substrates (e.g. caspase 9). Ca<sup>2+</sup> has also been shown to be necessary for apoptotic endonuclease activation, eliciting DNA cleavage after many cellular insults (29–31). Buffering intracellular Ca<sup>2+</sup> released from stored Ca<sup>2+</sup> pools (e.g. ER) with BAPTA-AM, or removal of extracellular Ca<sup>2+</sup> with EGTA, can protect cells against apoptosis (32, 33). Therefore, increases in intracellular Ca<sup>2+</sup> levels appear to be important cell death signals in human cancer cells that might be exploited for anti-tumor therapy. Finally, Ca<sup>2+</sup> may act as a signal for apoptosis by directly activating key proapoptotic enzymes (e.g. calpain); however, these proteolytic responses are poorly understood. The role of Ca<sup>2+</sup> in cell death processes involving caspase activation has been examined in detail (28, 34–36). However, the role of Ca<sup>2+</sup> in non-caspase-dependent cell death responses is relatively unexplored.

Recent studies have suggested that alterations in mitochondrial homeostasis play an essential role in apoptotic signal transduction induced by cytotoxic agents (37, 38). Various apoptotic stimuli have been shown to induce mitochondrial changes, resulting in release of apoptogenic factors, apoptosis-inducing factor (39), and mitochondrial cytochrome *c* (9) into the cytoplasm. These changes are observed during the early phases of apoptosis in human epithelial cells, and were linked to the initial cascade of events, sending the cell to an irreversible suicide pathway. During high, sustained levels of cytosolic Ca<sup>2+</sup>, mitochondrial Ca<sup>2+</sup> uptake is driven by mitochondrial membrane potential to maintain Ca<sup>2+</sup> homeostasis in the cytosol. In de-energized mitochondria, Ca<sup>2+</sup> can be released by a reversal of this uptake pathway (40). These data, therefore, linked changes in Ca<sup>2+</sup> homeostasis and mitochondrial membrane potential to the initiation of apoptosis. Li *et al.* (41) reported that  $\beta$ -Lap caused a decrease in mitochondrial membrane potential with release of cytochrome *c* into the cytoplasm in a number of human carcinoma cell lines, shortly after drug addition. Other alterations in metabolism (e.g. ATP depletion) have not been examined in  $\beta$ -Lap-treated cells.

We previously characterized the activation of a novel cysteine protease in various breast cancer cell lines with properties similar to the Ca<sup>2+</sup>-dependent cysteine protease, calpain, after exposure to  $\beta$ -Lap (12). Using NQO1-expressing breast

cancer cells, we show that  $\beta$ -Lap elicits a rise in intracellular Ca<sup>2+</sup> levels shortly after drug administration that eventually leads to apoptosis. This paper suggests a critical, but not sufficient, role for Ca<sup>2+</sup> in the cell death pathway initiated by NQO1-dependent bioactivation of  $\beta$ -Lap. Possible combinatorial effects (e.g. NAD(P)H depletion as well as intracellular calcium alterations) that initiate  $\beta$ -Lap-mediated apoptosis in NQO1-expressing breast cancer cells will be discussed.

#### EXPERIMENTAL PROCEDURES

**Reagents**— $\beta$ -Lapachone (3,4-dihydro-2,2-dimethyl-2H-naphtho[1,2b]pyran-5,6-dione) was synthesized by Dr. William G. Bornmann (Memorial Sloan Kettering, New York), dissolved in dimethyl sulfoxide at 10 mM, and the concentration verified by spectrophotometric analysis (2, 5). EGTA, Hoechst 33258, and thapsigargin were obtained from Sigma. BAPTA-AM (1,2-bis-(2-aminophenoxy)ethane-*N,N,N',N'*-tetraacetic acid tetra-(acetoxymethyl ester)) was obtained from Calbiochem (La Jolla, CA). JC-1 (5,5',6,6'-tetrachloro-1,1',3,3'-tetraethylbenzimidazolylcarbocyanine iodide) and Fluo-4-AM were obtained from Molecular Probes, Inc. (Eugene, OR).

**Cell Culture**—MCF-7:WS8 (MCF-7) human breast cancer cells were obtained from Dr. V. Craig Jordan, (Northwestern University, Chicago, IL). MDA-MB-468 cells were obtained from the American Type Culture Collection and transfected with NQO1 cDNA in the pcDNA3 constitutive expression vector as described previously (5). Tissue culture components were purchased from Life Technologies, Inc., unless otherwise stated. MCF-7 cells were grown in RPMI 1640 cell culture medium supplemented with 10% fetal bovine serum, in a 37 °C humidified incubator with 5% CO<sub>2</sub>, 95% air atmosphere as previously described (2, 5). For all experiments, log-phase breast cancer cells were exposed to 5  $\mu$ M  $\beta$ -Lap for 4 h (unless otherwise indicated), after which fresh medium was added and cells were harvested at various times post-treatment.

**TUNEL Assay**—Cells were seeded at  $1 \times 10^6$  cells/10-cm Petri dish and allowed to grow for 24 h. Log-phase cells were then pretreated for 30 min with 10  $\mu$ M BAPTA-AM, 3 mM EGTA, or 50  $\mu$ M dicumarol followed by a 4-h pulse of 5  $\mu$ M  $\beta$ -Lap, as described above, or 24 h treatment of 10  $\mu$ M ionomycin or 1  $\mu$ M staurosporine. Medium was collected from experimental as well as control conditions 24 h later, and attached along with floating cells were monitored for apoptosis using TUNEL 3'-biotinylated DNA end labeling via the APO-DIRECT kit (Pharmingen, San Diego, CA) as described (5). Apoptotic cells were analyzed and quantified using an EPICS XL-MCL flow cytometer that contained an air-cooled argon laser at 488 nm, 15 mW (Beckman Coulter Electronics; Miami, FL), and XL-MCL acquisition software provided with the instrument.

**Cell Growth Assays**—MCF-7 cells were seeded at  $5 \times 10^4$  cells per well in a 12-well plate and allowed to attach overnight. The following day, log-phase cells were pretreated for 30 min with 5  $\mu$ M BAPTA-AM, followed by a 4-h pulse of  $\beta$ -Lap (0–5  $\mu$ M). Drugs were removed and fresh medium added. Cells were allowed to grow for an additional 6 days. DNA content (a measure of cell growth) was determined by fluorescence using Hoechst dye 33258 as described (5) and changes in growth were monitored using a PerkinElmer HTS 7000 Plus Bio Assay Plate Reader (Norwalk, CT) with 360 and 465 nm excitation and emission filters, respectively. Data were expressed as relative growth, T/C (treated/control), using experiments performed at least twice.

**Confocal Microscopy**—MCF-7 cells were seeded at  $2-3 \times 10^5$  cells per 35-mm glass bottom Petri dishes (MatTek Corp., Ashland, MA) and allowed to attach overnight. Cells were rinsed twice in a Ca<sup>2+</sup>/Mg<sup>2+</sup> balanced salt solution (BSS, 130 mM NaCl, 5 mM KCl, 1.5 mM CaCl<sub>2</sub>, 1 mM MgCl<sub>2</sub>, 25 mM HEPES, pH 7.5, 5 mM glucose, 1 mg/ml bovine serum albumin) and loaded with the Ca<sup>2+</sup>-sensitive fluorescent indicator, fluo-4-AM (5  $\mu$ M), in BSS for ~20–30 min at 37 °C. Cells were rinsed twice in BSS and incubated for an additional 20 min at 37 °C to allow for hydrolysis of the AM-ester. Cells were imaged with a Zeiss 410 confocal microscope (Thornwood, NY) equipped with a  $\times 63$  N.A. 1.4 oil immersion planapochromat objective at room temperature (the same results were observed at room temperature and 37 °C). Confocal images of fluo-4 fluorescence were collected using a 488-nm excitation light from an argon/krypton laser, a 560-nm dichroic mirror, and a 500–550 nm band-pass barrier filter. Three basal images were collected before drug addition (8  $\mu$ M  $\beta$ -Lap,  $\pm$  50  $\mu$ M dicumarol or 200 nM TG). The mean pixel intensity was set to equal one for analyses of fold-increase in fluo-4 fluorescence intensity. Subsequently, images were collected after the indicated treatments at 90-s intervals. BAPTA-AM (20  $\mu$ M) was co-

loaded with fluo-4-AM where indicated. Mean pixels were determined in regions of interest for individual cells at each time point.

**Mitochondrial Membrane Potential Determinations**—MCF-7 cells were seeded at  $2.5 \times 10^6$  cells per 6-well plate, and allowed to grow for 24 h. Log-phase cells were pretreated for 30 min with 10  $\mu$ M BAPTA-AM, 3 mM EGTA, or 50  $\mu$ M dicumarol followed by a 4-h pulse of 5  $\mu$ M  $\beta$ -Lap, unless otherwise indicated. Cells were trypsinized and resuspended in phenol red-minus RPMI medium for analyses. Cells were maintained at 37 °C for the duration of the experiment, including during analyses. Prior to analyses, cells were loaded with 10  $\mu$ M JC-1 for 9–14 min and samples were analyzed using a Beckman Coulter EPICS Elite ESP (Miami, FL) flow cytometer. JC-1 monomer and aggregate emissions were excited at 488 nm and quantified using Elite acquisition software after signal collection through 525- and 590-nm band pass filters, respectively. Shifts in emission spectra were plotted on bivariate dot plots, on a cell-by-cell basis, to determine relative mitochondrial membrane potential of treated and control cells.

**ATP Measurements**—Cells were seeded at  $2.5 \times 10^6$  cells per well in 6-well dishes and allowed to attach for 24 h. Fresh medium was added to the cells along with Ca<sup>2+</sup> chelators or dicumarol 30 min prior to  $\beta$ -Lap exposure (4 h unless otherwise indicated). Floating cells were collected, pelleted, and lysed in 1.67 M perchloric acid. Attached cells were lysed directly in 1.67 M perchloric acid. Following a 20-min incubation at room temperature, attached cells were scraped and transferred to corresponding microcentrifuge tube, cooled on ice for several minutes, and spun to pellet protein precipitates. Deproteinized samples were neutralized with 3.5 M KOH and HEPES/KOH (25 mM HEPES, 15 mM KOH, pH 8), and incubated on ice for 15 min. Precipitates were removed by centrifugation and samples stored at -20 °C. Cell extracts were analyzed for ATP and ADP levels using a luciferase-based bioluminescent assay and rephosphorylation protocols, as described (42).

**Western Blot Analyses**—Whole cell extracts from control or  $\beta$ -Lap-exposed MCF-7 cells were prepared and analyzed by SDS-polyacrylamide gel electrophoresis/Western blot analyses as previously described (2, 5, 12). Loading equivalence and transfer efficiency were monitored by Western blot analyses of proteins that are known to be unaltered by experimental treatments (2), and using Ponceau S staining of the membrane, respectively. Probed membranes were then exposed to x-ray film for an appropriate time and developed. Dilutions of 1:10,000 for the C-2-10 anti-PARP antibody (Enzyme Systems Products, Livermore, CA), and 1:2000 for anti-p53 DO-1 and anti-lamin B (Santa Cruz Biotechnology, Santa Cruz, CA) antibodies were used as described (2, 12).

## RESULTS

**Ca<sup>2+</sup> Chelators Prevent  $\beta$ -Lap-induced Apoptotic DNA Fragmentation and Protect against Cell Death**—Log-phase MCF-7 cells were treated for 4 h with 5  $\mu$ M  $\beta$ -Lap, fresh medium was then applied, and cells were harvested 24 h later and analyzed for DNA fragmentation (i.e. apoptotic cells staining positive in a TUNEL assay). Treatment of MCF-7 cells with  $\beta$ -Lap resulted in >90% apoptotic cells (Fig. 1, A and B). However, MCF-7 cells exposed to a 30-min pretreatment with 10  $\mu$ M BAPTA-AM or 3 mM EGTA, followed by a 4-h pulse of 5  $\mu$ M  $\beta$ -Lap, exhibited only 20 or 39% apoptotic cells, respectively, in 24 h.

To examine whether BAPTA-AM could affect  $\beta$ -Lap lethality, we measured relative growth of MCF-7 cells with or without exposure to  $\beta$ -Lap, and in the presence or absence of BAPTA-AM. MCF-7 cells were treated for 30 min with 5  $\mu$ M BAPTA-AM, subsequently exposed to a 4-h pulse of  $\beta$ -Lap (1.5–5  $\mu$ M), and relative cell growth was measured 6 days later (Fig. 1C). The LD<sub>50</sub> dose of  $\beta$ -Lap in MCF-7 cells was ~2.5  $\mu$ M in colony forming assays, which correlated well with IC<sub>50</sub> relative growth inhibition, as measured by DNA content (2, 5). At 1.5  $\mu$ M  $\beta$ -Lap, cells exhibited little or no toxicity. At  $\beta$ -Lap doses of 3 or 5  $\mu$ M, cells exhibited considerable toxicity, >90% growth inhibition, as previously reported (2, 5). Toxicity was significantly prevented by 5  $\mu$ M BAPTA-AM pretreatment. BAPTA-AM pretreated cells exhibit only 44 and 73% growth inhibition after 3 or 5  $\mu$ M  $\beta$ -Lap treatments, respectively (Fig. 1C). BAPTA alone did not affect MCF-7 cell growth compared with untreated controls.

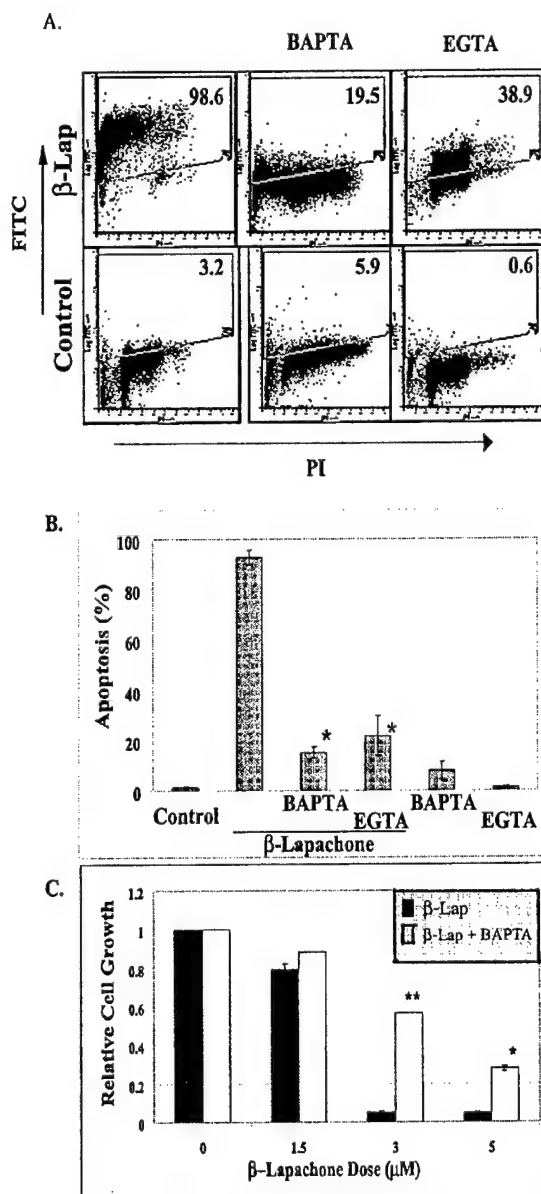


**FIG. 1.  $\beta$ -Lap-mediated apoptosis and relative cell growth is Ca<sup>2+</sup>-dependent.** DNA fragmentation was assessed using the TUNEL assay. Log phase MCF-7 cells were treated with the indicated Ca<sup>2+</sup> chelator for 30 min prior to a 4-h pulse of 5  $\mu$ M  $\beta$ -Lap. TUNEL assays were performed to monitor apoptosis 24 h after  $\beta$ -Lap addition (A and B). A, shown are the results of any one experiment from studies performed at least three times. The number in the upper right corner represents percent cells staining positive in the TUNEL assay. Results are graphically summarized in B as the average of at three independent experiments, mean  $\pm$  S.E. Student's *t* test for paired samples, experimental group compared with MCF-7 cells treated with  $\beta$ -Lap alone are indicated (\**p* < 0.01). C, cells were exposed to a 4-h pulse of various concentrations of  $\beta$ -Lap either alone (closed), or after a 30-min pretreatment with 5  $\mu$ M BAPTA-AM (open). Relative DNA per well was determined by Hoechst 33258 fluorescence, and graphed as relative growth (treated/control DNA); mean relative DNA per well,  $\pm$  S.E. Shown are representative results of experiments performed at least twice. Student's *t* test for paired samples, experimental group compared with MCF-7 cells treated with  $\beta$ -Lap alone are indicated (\*, *p* < 0.05; and \*\*, *p* < 0.005).

**Ca<sup>2+</sup> Chelators Do Not Block Apoptosis Induced by Other Agents**—It was possible based on the data in Fig. 1 that calcium chelators may block  $\beta$ -Lap-mediated apoptosis by sequestering

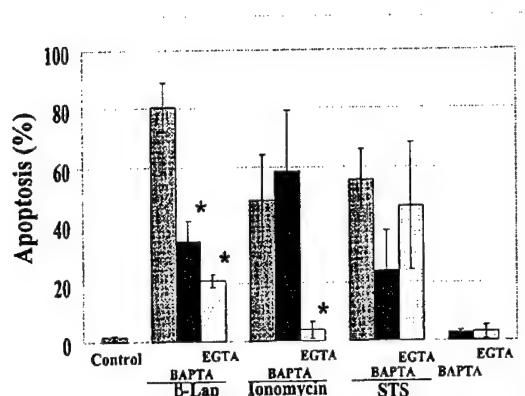


FIG. 2. Ca<sup>2+</sup> chelators did not block Ca<sup>2+</sup>-activated endonuclease activation after  $\beta$ -Lap. NQO1-expressing MDA-468-NQ3 cells (generated from non-expressing human breast cancer cells (5)) were treated with either 3 mM EGTA or 30  $\mu$ M BAPTA-AM for 30 min prior to drug addition; either a 4-h pulse of 8  $\mu$ M  $\beta$ -Lap, or 24 h continuous treatment of 10  $\mu$ M ionomycin or 1  $\mu$ M STS. Cells were then analyzed using the TUNEL assay for DNA fragmentation. Shown are mean  $\pm$  S.E. of at least two independent experiments. Student's *t* test for paired samples, experimental group compared with cells treated with drug alone are indicated (\*, *p* < 0.05).

calcium required for the activation of apoptotic endonucleases. We, therefore, examined both intra- and extracellular Ca<sup>2+</sup> chelators for their ability to prevent apoptosis in NQO1-transfected MDA-468 (MDA-468-NQ3) cells induced by  $\beta$ -Lap, ionomycin (which induces Ca<sup>2+</sup>-mediated cell death (36)), and staurosporine (STS, which inhibits protein kinase C and works via a caspase-mediated cell death pathway (43, 44)). We used MDA-468-NQ3 cells to assay for caspase-mediated endonuclease activation and DNA fragmentation since they express the endonuclease-activating caspase 3, unlike MCF-7 cells (45). We previously demonstrated that MDA-468-NQ3 cells responded similarly to  $\beta$ -Lap as MCF-7 cells (Fig. 2 and Ref. 5). EGTA significantly protected MDA-468-NQ3 cells against ionomycin-induced apoptosis, but not against STS-induced apoptosis (Fig. 2). MDA-468-NQ3 cells treated for 24 h with 10  $\mu$ M ionomycin exhibited 49% apoptotic cells, whereas, MDA-468-NQ3 cells pretreated for 30 min with 3 mM EGTA followed by a 24-h exposure to ionomycin exhibited only 4% apoptotic cells. Cells treated for 24 h with 1  $\mu$ M STS in the absence or presence of 3 mM EGTA exhibited 56 and 46% apoptosis, respectively. BAPTA-AM (10  $\mu$ M) did not significantly block apoptosis induced by ionomycin. BAPTA-AM pretreatment of STS-exposed MDA-468-NQ3 cells did not significantly decrease apoptosis (*p* < 0.4) compared with cells exposed to STS alone; the modest effect of BAPTA-AM on STS-induced apoptosis may reflect the Ca<sup>2+</sup> dependence of the apoptotic endonucleases involved in this response. Neither BAPTA-AM nor EGTA alone elicited apoptotic responses at the doses used in the aforementioned experiments (Figs. 1B and 2). Furthermore, preliminary data suggest that DFF45 (ICAD) was cleaved in NQO1-expressing MCF-7 or MDA-468-NQ3 cells at 8 h after  $\beta$ -Lap treatment, in a temporal manner corresponding to the induction of apoptosis (data not shown). Cleavage of DFF45, an endogenous inhibitor of the magnesium-dependent and Ca<sup>2+</sup>-independent apoptotic endonuclease, DFF40 (CAD), suggests that DFF40 is activated following treatment with  $\beta$ -Lap. Taken together with results in Fig. 1, these data strongly suggest that a rise in intracellular Ca<sup>2+</sup> levels is part of a critical signaling pathway for the induction of apoptosis in NQO1-expressing human breast cancer cells following  $\beta$ -Lap exposure.

**Exposure of NQO1-expressing MCF-7 Cells to  $\beta$ -Lap Results in Increased Intracellular Ca<sup>2+</sup>.**—We next directly examined

whether intracellular Ca<sup>2+</sup> levels were increased in log-phase MCF-7 cells after  $\beta$ -Lap treatment using the cell-permeant intracellular Ca<sup>2+</sup> indicator dye, fluo-4. Cells were loaded with 5  $\mu$ M fluo-4-AM, and where indicated, 20  $\mu$ M BAPTA-AM, incubated for ~25 min to allow for the dye to permeate cells, rinsed, and then incubated for an additional ~20 min for hydrolysis of the AM-ester. Following drug addition, images were collected every 90 s for ~60 min using confocal microscopy. Three basal images were recorded before drug addition and average pixels per cell were determined (indicative of fluo-4 fluorescence and, therefore, basal intracellular Ca<sup>2+</sup> levels) and used for analyses over time. The fluorescence of basal images were averaged and set to equal one; fold increases were determined from changes in fluo-4 fluorescence over control.

After exposure to 8  $\mu$ M  $\beta$ -Lap, MCF-7 cells exhibited an ~2-fold increase in fluo-4 fluorescence from 4 to 9 min, after which time Ca<sup>2+</sup> levels returned to basal levels in a majority of cells examined (43 of 50, 86%) (Fig. 3A). The rise in intracellular Ca<sup>2+</sup> levels in MCF-7 cells following  $\beta$ -Lap exposure was prevented by preloading cells with BAPTA-AM (20  $\mu$ M) (Fig. 3B). Interestingly, not all  $\beta$ -Lap-exposed MCF-7 cells were affected by pretreatment with BAPTA-AM; 3 of 26 cells (12%) exhibited a rise in intracellular Ca<sup>2+</sup> levels after exposure to  $\beta$ -Lap despite the presence of this Ca<sup>2+</sup> chelator. However, BAPTA-AM pretreated MCF-7 cells that did exhibit a rise in intracellular Ca<sup>2+</sup> levels following  $\beta$ -Lap treatment exhibited a similar, but delayed Ca<sup>2+</sup> increase (10–20 min), as compared with  $\beta$ -Lap-exposed MCF-7 cells in the absence of BAPTA-AM (4–9 min). This may be due to a saturation of the chelator or heterogeneity of the tumor cell population. These results are consistent with previous reports that the buffering capacity of BAPTA-AM may be overwhelmed with time (34, 46). Higher doses of BAPTA-AM were not used due to toxicity caused by the drug alone (data not shown).

Since the ER is a major store of Ca<sup>2+</sup> in the cell, we tested if the initial rise in intracellular Ca<sup>2+</sup> levels after exposure of MCF-7 cells to  $\beta$ -Lap was due to release of Ca<sup>2+</sup> from this organelle. If  $\beta$ -Lap exposure led to release of Ca<sup>2+</sup> stored in the ER, then TG (a sarcoplasmic reticulum Ca<sup>2+</sup>-ATPase pump inhibitor) administration should not cause additional Ca<sup>2+</sup> release. Similarly, if the sequence of drug administration were reversed, additional Ca<sup>2+</sup> release would also not be observed. When  $\beta$ -Lap was added after TG-induced depletion of ER Ca<sup>2+</sup> stores, no measurable rise in intracellular Ca<sup>2+</sup> levels occurred in 25 of 27 (93%) cells analyzed (Fig. 3C). Similarly, when TG was added to cells after  $\beta$ -Lap, only 1 of 18 (6%) cells that initially responded to  $\beta$ -Lap exhibited a rise in intracellular Ca<sup>2+</sup> levels following subsequent TG administration (Fig. 3D). At the end of the experiment, all cells analyzed remained responsive to ionomycin. Thus, cells exposed to  $\beta$ -Lap and/or TG were still capable of altering Ca<sup>2+</sup> levels, and the Ca<sup>2+</sup> indicator dye was not saturated. We noted that the increase in fluo-4 fluorescence (2–3-fold over basal levels, Fig. 3A) in MCF-7 cells observed after exposure to  $\beta$ -Lap was comparable to that elicited by TG (1.5–2.5-fold over basal levels, Fig. 3C), further suggesting that the two agents mobilized the same ER pool of Ca<sup>2+</sup>. All cells analyzed started with comparable basal levels of Ca<sup>2+</sup> and appeared to load equal amounts of the indicator dye, as determined by basal fluorescence (measured by pixels per cell) at the beginning of each analysis; relative basal fluo-4 fluorescence for each experiment in Fig. 3 were: A, 56  $\pm$  7; B, 52  $\pm$  7; C, 78  $\pm$  8; D, 79  $\pm$  8 S.E. Untreated or BAPTA-AM-loaded MCF-7 cells did not show any fluctuations in basal Ca<sup>2+</sup> levels during the time course of the experiment, nor did any of the drugs interfere with the Ca<sup>2+</sup> indicator dye (data not shown).



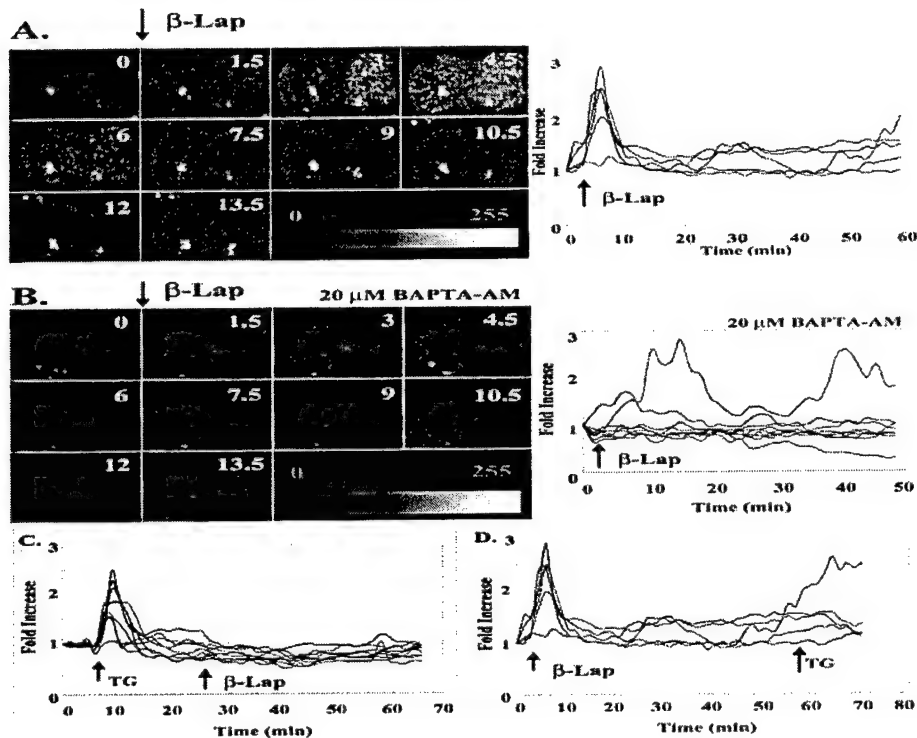


**FIG. 3. Intracellular Ca<sup>2+</sup> changes after  $\beta$ -Lap.** Intracellular Ca<sup>2+</sup> levels were measured in live cells via confocal microscopy using the Ca<sup>2+</sup> indicator dye, fluo-4-AM. MCF-7 cells were loaded with either fluo-4-AM alone (A, C, and D) or fluo-4-AM and 20  $\mu$ M BAPTA-AM (B).  $\beta$ -Lap (8  $\mu$ M) was added to cells after basal images were recorded. Images were collected every 90 s for 45–75 min, as indicated. The number in the upper right corner of each Ca<sup>2+</sup> image represents the time (min) after  $\beta$ -Lap addition. A, representative cells before and after  $\beta$ -Lap treatments are shown as pseudocolored images. These results are also displayed in graph form showing fold change (as compared with basal levels) in fluo-4 fluorescence in cells after  $\beta$ -Lap treatment over time, with or without co-loading of BAPTA-AM (A and B). C, TG (200 nM) was added to MCF-7 cells after basal images were recorded. Once fluo-4 fluorescence returned to basal levels, cells were subsequently exposed to  $\beta$ -Lap. D,  $\beta$ -Lap was added to MCF-7 cells after basal images were recorded. After fluo-4 fluorescence returned to basal levels, TG was subsequently added to the cells. Each line represents the change in fluo-4 fluorescent emission of an individual cell over time; each graph is representative of one of at least three independent experiments.

**Loss of Mitochondrial Membrane Potential After  $\beta$ -Lap Is Attenuated by Intracellular, but Not Extracellular, Ca<sup>2+</sup> Chelation**—Mitochondrial membrane potential was previously shown to drop from a hyperpolarized state to a depolarized state after treatment of various human cancer cells with  $\beta$ -Lap (41). A drop in mitochondrial membrane potential in  $\beta$ -Lap-treated cells was accompanied by a concomitant release of cytochrome *c* into the cytosol (41). To explore whether early changes in intracellular Ca<sup>2+</sup> levels were upstream of mitochondrial changes in NQO1-expressing breast cancer cells, log phase MCF-7 cells were pretreated for 30 min with either 10  $\mu$ M BAPTA-AM or 3 mM EGTA and then exposed to 5  $\mu$ M  $\beta$ -Lap for 4 h. Prior to analyses, cells were loaded with JC-1, a cationic dye commonly used to monitor alterations in mitochondrial membrane potential (47, 48). Mitochondrial depolarization measurements using JC-1 were indicated by a decrease in the red/green fluorescence intensity ratio (a movement of events from upper left to lower right, Fig. 4), as seen following a 10-min treatment with the potassium ionophore, valinomycin (100 nM), which causes a collapse of mitochondrial membrane potential by uncoupling mitochondrial respiration (Fig. 4e) (49); cells in the upper left-hand quadrant exhibited high mitochondrial membrane potential, whereas, cells in the lower right-hand quadrant have low mitochondrial membrane potential and are depolarized. Cells in the upper right-hand quadrant exhibited intermediate membrane potential. Mitochondrial membrane potential decreased in MCF-7 cells in a time- and dose-dependent manner following exposure to  $\beta$ -Lap (Figs. 4, a–d, and data not shown). By 4 h, the majority of  $\beta$ -Lap-treated MCF-7 cells

exhibited low mitochondrial membrane potential (53%), while the majority of control cells maintained high mitochondrial membrane potential (51%) (Fig. 4, b, a and g, f, respectively). This drop in mitochondrial membrane potential observed 4 h after treatment with  $\beta$ -Lap (low, 53%) was abrogated by pretreatment with BAPTA-AM (low, 23%), but not by EGTA (low, 48%) (Fig. 4, g–i, respectively). Pretreatment with 10  $\mu$ M BAPTA-AM prevented the decrease in mitochondrial membrane potential (low, 23%); however, BAPTA-AM did not maintain  $\beta$ -Lap-exposed cells in a high-potential state (high, 28%) as observed in control untreated cells (high, 51%). Approximately half of the BAPTA-AM-exposed cells were in an intermediate membrane potential state (45%) (Fig. 4h). We noted, however, that BAPTA-AM or EGTA exposures alone caused depolarization of the mitochondria, with a majority of the cells residing in the same intermediate energized state as observed following BAPTA-AM and  $\beta$ -Lap (Fig. 4, j–k). Therefore, BAPTA-AM prevented mitochondrial depolarization induced by  $\beta$ -Lap to the same extent as in cells treated with BAPTA-AM alone. Pretreatment with 3 mM EGTA did not affect the loss of mitochondrial membrane potential caused by  $\beta$ -Lap (low 48%), implying that an early rise in intracellular Ca<sup>2+</sup> levels from intracellular stores was sufficient to cause a drop in mitochondrial membrane potential, and that extracellular calcium was not needed for these effects in  $\beta$ -Lap-treated cells (Fig. 4, h–i).

**Loss of ATP After  $\beta$ -Lap Is Attenuated by Intracellular Ca<sup>2+</sup> Chelation**—The bioactivation of  $\beta$ -Lap by NQO1 is thought to lead to a futile cycling between quinone and hydroquinone forms of the compound, presumably due to the instability of the



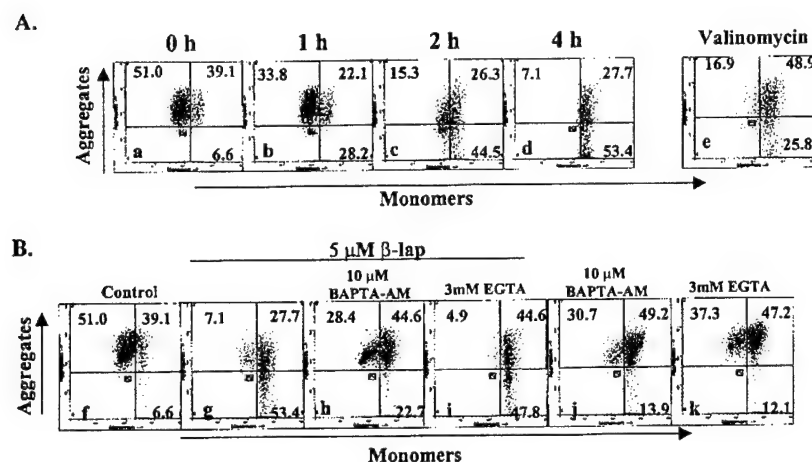


**FIG. 4.  $\beta$ -Lap-induced loss of mitochondrial membrane potential is mediated by alterations in Ca<sup>2+</sup> homeostasis.** Mitochondrial membrane potential was measured in control or drug-treated MCF-7 cells with the JC-1 dye. **A**, cells were treated with 5  $\mu$ M  $\beta$ -Lap and assayed for changes in mitochondrial membrane potential at 1, 2, and 4 h post-treatment. Exposure of MCF-7 cells to 100 nM valinomycin for 15 min served as a positive control as described (49). Cells in the upper left-hand quadrant exhibit high mitochondrial membrane potential, while cells in the lower right-hand quadrant exhibit low mitochondrial membrane potential. **B**, cells were treated for 30 min with either 10  $\mu$ M BAPTA-AM or 3 mM EGTA prior to a 4-h treatment with 5  $\mu$ M  $\beta$ -Lap. At 4 h, cells were harvested for analyses of changes in mitochondrial membrane potential using JC-1 as described above. Shown are representative experiments performed at least three times, and numbers in each quadrant represent the average of cells in that quadrant of at least three independent experiments. S.E. for any single number was not more than 11%.

hydroquinone form of  $\beta$ -Lap (5). This futile cycling led to depletion of NADH and NADPH, electron donors for NQO1 in *in vitro* assays (5). Exhaustion of reduced enzyme co-factors may be a critical event for the activation of the apoptotic pathway in NQO1-expressing cells following  $\beta$ -Lap exposure. We, therefore, measured intracellular ATP and ADP in log-phase MCF-7 cells after various doses and times of  $\beta$ -Lap (using a luciferase-based bioluminescent assay (42)). Intracellular ATP levels were reduced in MCF-7 cells after treatment with  $\beta$ -Lap in a dose- and time-dependent manner (Fig. 5A). At all doses of  $\beta$ -Lap above the LD<sub>50</sub> of the drug ( $\sim$ 2.5  $\mu$ M) in MCF-7 cells (2), intracellular ATP levels were reduced by >85% at 4 h, the time at which drug was removed (Fig. 5A, left); the loss of ATP correlated well with  $\beta$ -Lap-induced cell death in MCF-7 cells (Fig. 1C). ADP levels remained relatively unchanged after various doses of  $\beta$ -Lap, however, the [ATP]/[ADP][P<sub>i</sub>] ratio decreased dramatically. Intracellular ATP levels began to drop to 70% of control levels 2 h after 5  $\mu$ M  $\beta$ -Lap exposure, the time at which  $\beta$ -Lap began to elicit mitochondrial membrane depolarization (Figs. 5, A, right, and 4, c). ATP levels continued to drop to 8% of control levels by 4 h after drug exposure (Fig. 5A, right). In contrast, ADP levels remained relatively unchanged during the course of the experiment, with an increase at 30 min (172% control levels) that returned to control levels by 1 h post-treatment. Cellular ATP levels in  $\beta$ -Lap-treated cells did not appear to recover to normal levels within the 6–24-h interval after drug removal (data not shown).

Loss of ATP following  $\beta$ -Lap was prevented by a 30-min pretreatment with an intracellular Ca<sup>2+</sup> chelator, but not an extracellular Ca<sup>2+</sup> chelator (Fig. 5B). At 4 h, pretreatment with 10 or 30  $\mu$ M BAPTA-AM elicited only 58 and 43% ATP loss, respectively, compared with  $\beta$ -Lap alone (92% loss). The extracellular Ca<sup>2+</sup> chelator, EGTA, did not significantly affect the loss of ATP, nor [ATP]/[ADP][P<sub>i</sub>] ratio observed in MCF-7 cells after  $\beta$ -Lap treatment (Fig. 5B). Exposure of MCF-7 cells to TG (200 nM) did not elicit decreases in ATP or ADP levels 4 h after drug exposure, compared with untreated control cells.

**Ca<sup>2+</sup> Chelators Prevent  $\beta$ -Lap-induced Proteolysis**—We previously showed that apoptosis in various breast cancer cell lines induced by  $\beta$ -Lap was unique, causing a pattern of PARP and p53 intracellular cleavage events distinct from those in-

duced by caspase activating agents (12). After  $\beta$ -Lap treatment, we observed an  $\sim$ 60-kDa PARP cleavage fragment and specific cleavage of p53 in NQO1-expressing breast cancer cells. Furthermore, we showed that this proteolysis in  $\beta$ -Lap-treated cells was the result of activation of a Ca<sup>2+</sup>-dependent protease with properties similar to  $\mu$ -calpain (12). PARP and p53 proteolysis in  $\beta$ -Lap-exposed, NQO1-expressing cells was prevented by pretreatment with the extracellular Ca<sup>2+</sup> chelators, EGTA and EDTA, in a dose-dependent manner (at 8 and 24 h) (Ref. 12, and data not shown). Additionally, PARP, p53, and lamin B proteolysis induced at 24 h in MCF-7 cells following  $\beta$ -Lap treatment were abrogated by pretreatment with 10 or 30  $\mu$ M BAPTA-AM (Fig. 6). These data strongly suggest that a Ca<sup>2+</sup>-dependent pathway and potentially a Ca<sup>2+</sup>-dependent protease are operative in  $\beta$ -Lap-mediated apoptosis.

A simple explanation for the aforementioned results could be that BAPTA blocks bioactivation of  $\beta$ -Lap by NQO1 in a manner similar to that of dicumarol (5). However, BAPTA (free acid) did not affect the enzymatic activities of NQO1 using standard enzymatic assays (data not shown) (5). The free acid (active) form of BAPTA, instead of its -AM ester form, was used in these assays since intracellular accumulation of this Ca<sup>2+</sup> chelator was not necessary and was physiologically relevant in the *in vitro* enzyme assay. Using  $\beta$ -Lap as a substrate, NQO1 enzymatic activity in the presence of 10 mM BAPTA (a dose of the free acid form of BAPTA that was >1000-fold higher than that used in the experiments of Figs. 1–6) was reduced by <20%. Thus, BAPTA-AM did not affect the activity of NQO1, a two-electron reductase required for  $\beta$ -Lap cytotoxicity (5). We conclude that BAPTA-AM prevents  $\beta$ -Lap-induced apoptosis by blocking Ca<sup>2+</sup>-mediated signaling events via chelating intracellular Ca<sup>2+</sup>.

**$\beta$ -Lap Bioactivation by NQO1 Is Critical for Ca<sup>2+</sup>-mediated Signaling**—We previously reported that cells expressing NQO1 are more sensitive to the cytotoxic effects of  $\beta$ -Lap (5).<sup>2</sup> NQO1 is inhibited by dicumarol, which competes with NADH or NADPH for binding to the oxidized form of the enzyme. Dicumarol thereby prevents reduction of quinones (50, 51). We demonstrated that dicumarol attenuates  $\beta$ -Lap-mediated proteolysis of apoptotic substrates (e.g. PARP and p53), apoptosis, and survival in NQO1-expressing cells (5).<sup>2</sup> As expected, increases

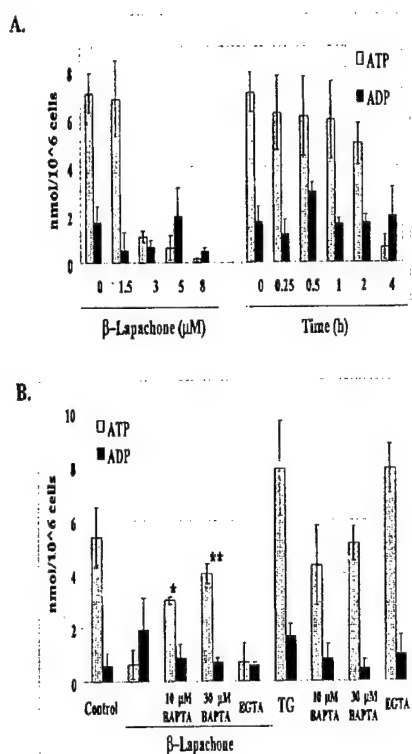


**FIG. 5. ATP depletion after  $\beta$ -Lap treatment is Ca<sup>2+</sup> dependent.** Intracellular ATP and ADP levels were measured using a luciferase-based bioluminescent assay. **A**, cells were treated with the indicated dose of  $\beta$ -Lap for 4 h or were treated with 5  $\mu$ M  $\beta$ -Lap for the time indicated, and harvested for ATP analyses. ATP levels were expressed as nanomoles of ATP per 10<sup>6</sup> cells. Purified ATP was used as a standard to determine intracellular ATP concentrations. **B**, cells were either pretreated or untreated with the indicated Ca<sup>2+</sup> chelators for 30 min prior to drug addition, and  $\beta$ -Lap (5  $\mu$ M) was then added for 4 h. Cells were harvested for analyses following  $\beta$ -Lap exposure. Results represent the average of at least three independent experiments,  $\pm$  S.E. Student's *t* test for paired samples, experimental group compared with drug alone are indicated (\*,  $p < 0.05$ ; \*\*,  $p < 0.01$ ).

in intracellular Ca<sup>2+</sup> levels in NQO1-expressing human cancer cells elicited by  $\beta$ -Lap were abrogated by co-treatment with 50  $\mu$ M dicumarol in 26 of 27 cells (96%) examined (Fig. 7A, lower panel). The ability of dicumarol to inhibit increases in intracellular Ca<sup>2+</sup> levels was greater than that observed with BAPTA-AM, where intracellular Ca<sup>2+</sup> level increases were prevented in only 89% of cells examined (Fig. 3B). Thus, NQO1 was critical for the rise in intracellular Ca<sup>2+</sup> levels observed in MCF-7 cells after  $\beta$ -Lap exposure.

Mitochondrial membrane depolarization induced by  $\beta$ -Lap was also abrogated by pretreatment with dicumarol (Fig. 7B). By 4 h, the majority of  $\beta$ -Lap-treated cells exhibited low mitochondrial membrane potential (58%), while very few control cells were depolarized (9%) (Fig. 7B). Pretreatment with dicumarol attenuated this response to  $\beta$ -Lap, with only 34% being depolarized. The inability of dicumarol to prevent mitochondrial depolarization in 34% of  $\beta$ -Lap-treated cells was probably due to the high background of control cells (20%) that were depolarized after exposure to dicumarol alone. In comparison with intracellular Ca<sup>2+</sup> buffering, BAPTA-AM elicited only a minor depolarization of the mitochondria on its own (low, 14%) and thus was able to elicit a greater protective effect (Fig. 4B); only 23% of cells exposed to BAPTA-AM and  $\beta$ -Lap exhibited low mitochondrial membrane potential as compared with  $\beta$ -Lap exposed cells in the presence of dicumarol (34%).

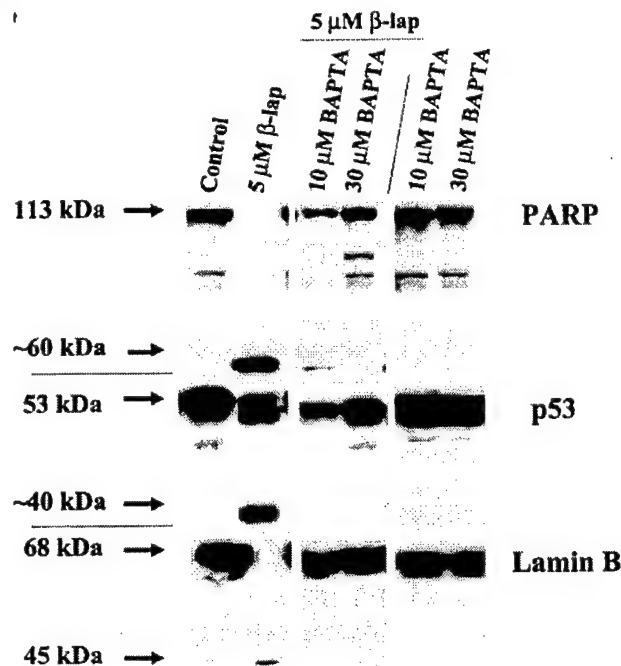


**FIG. 6. Intracellular Ca<sup>2+</sup> chelators prevent apoptotic proteolysis after  $\beta$ -Lap treatment.** Apoptotic proteolysis was measured in MCF-7 cells exposed to a 4-h pulse of 5  $\mu$ M  $\beta$ -Lap, with or without a 30-min pretreatment of the indicated dose of BAPTA-AM. Whole cell extracts were prepared 24 h after drug addition, and analyzed using standard Western blotting techniques with antibodies to PARP, p53, and lamin B. Shown is a representative Western blot of whole cell extracts from experiments performed at least three times.

The dramatic loss of intracellular ATP in MCF-7 cells following  $\beta$ -Lap exposure was inhibited by a 30-min pretreatment with 50  $\mu$ M dicumarol (Fig. 7C).  $\beta$ -Lap-treated MCF-7 cells pretreated with dicumarol exhibited only 34% loss of intracellular ATP, compared with 92% loss after  $\beta$ -Lap treatment alone (Fig. 7C). ADP levels were not altered by any of the treatments used, however, the [ATP]/[ADP] ratio decreased dramatically in  $\beta$ -Lap-treated cells, and was only partially decreased with dicumarol pretreatment alone, as compared with control untreated cells.

Dicumarol also abrogated DNA fragmentation induced by  $\beta$ -Lap in MCF-7 cells. MCF-7 cells exhibited 94% apoptosis following  $\beta$ -Lap exposure that was prevented by a 30-min pretreatment with 50  $\mu$ M dicumarol; only 6% of the cells staining positive in a TUNEL assay at 24 h post-treatment (Fig. 7D). These data are consistent with prior results (5), and correlate well with the survival protection afforded by dicumarol to  $\beta$ -Lap-treated cells. Dicumarol did not induce DNA fragmentation on its own. These data are consistent with the protection from apoptosis observed with either intra- and extracellular Ca<sup>2+</sup> chelators. BAPTA-AM or EGTA protected  $\beta$ -Lap exposed MCF-7 cells from apoptosis (Fig. 1, A and B). Collectively, these data implicate the bioactivation of  $\beta$ -Lap by NQO1 as a critical step in the rise of intracellular Ca<sup>2+</sup> levels following  $\beta$ -Lap exposure, and thus  $\beta$ -Lap-mediated downstream apoptotic events.

#### DISCUSSION

When homeostatic mechanisms for regulating cellular Ca<sup>2+</sup> are compromised, cells may die, either by necrosis or apoptosis (20, 21, 36). We demonstrated that bioactivation of  $\beta$ -Lap by NQO1 induced cell death in a manner that was dependent upon Ca<sup>2+</sup> signaling (Figs. 1–6).  $\beta$ -Lap can be reduced by NQO1 and

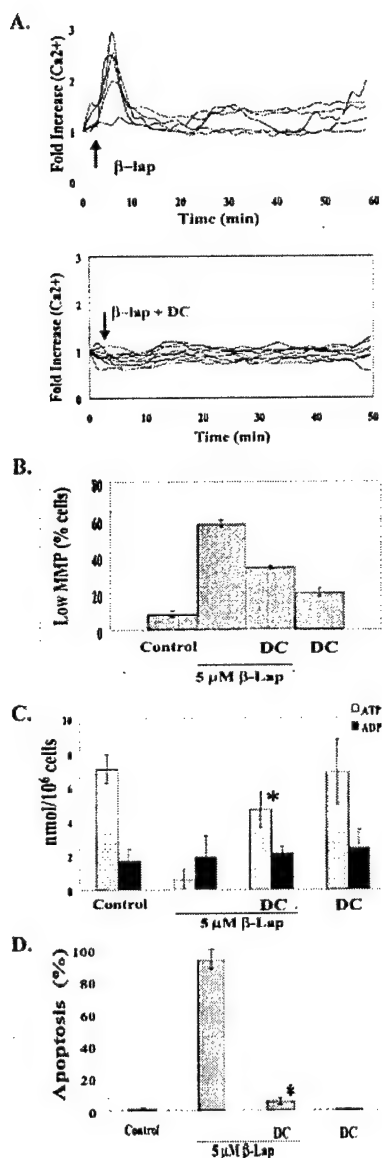


**FIG. 7. NQO1-dependent activation of  $\beta$ -Lap is critical for  $Ca^{2+}$  signaling.** A, intracellular  $Ca^{2+}$  was measured on live cells using the  $Ca^{2+}$  indicator dye, fluo-4-AM, and confocal microscopy as described in the legend to Fig. 3. Three basal images were recorded before drug treatments.  $\beta$ -Lap (8  $\mu$ M) was then added to MCF-7 cells, either alone (upper panel) or in combination with 50  $\mu$ M dicumarol (lower panel). Images were collected every 90 s for 50–60 min. Shown are representative graphs displaying changes in fluo-4 fluorescence for the duration of the experiment. Each line represents the fold change in fluo-4 fluorescent emission (as compared with basal levels) of an individual cell from one experiment, and the graph is representative of experiments performed at least three times. B, mitochondrial membrane potential was measured using the JC-1 dye as described in the legend to Fig. 4. MCF-7 cells were treated with 50  $\mu$ M dicumarol 30 min prior to  $\beta$ -Lap exposure. Four hours later, cells were harvested for analyses of mitochondrial membrane potential. Shown are mean  $\pm$  S.E. of the percentage of cells with low mitochondrial membrane potential of at least two independent experiments. C, ATP and ADP levels were assayed as described in the legend to Fig. 5. Cells were pretreated with dicumarol for 30 min prior to drug addition, 5  $\mu$ M  $\beta$ -Lap was added for 4 h, and cells were harvested immediately thereafter for analyses. Results represent the mean of at least three independent experiments  $\pm$  S.E. Student's *t* test for paired samples, experimental groups compared with drug alone are indicated (\**p* < 0.05). D, apoptosis, using the TUNEL assay, was assessed as per Fig. 1. MCF-7 cells were treated with 50  $\mu$ M dicumarol 30 min prior to a 4-h exposure of 5  $\mu$ M  $\beta$ -Lap. Cells were then harvested for TUNEL analyses at 24 h post-treatment. Shown are

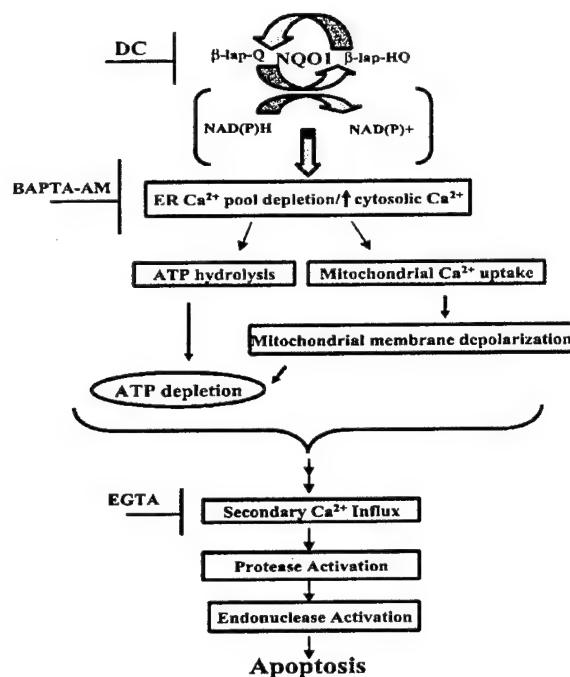


**FIG. 8. Proposed model for  $\beta$ -lapachone-mediated apoptosis in NQO1-expressing cells.** In cells that express NQO1,  $\beta$ -Lap is reduced from the quinone ( $\beta$ -lap-Q) to the hydroquinone ( $\beta$ -lap-HQ) form in a futile cycle that results in dramatic losses of NAD(P)H (5). During the metabolism of  $\beta$ -Lap by NQO1,  $Ca^{2+}$  is subsequently released from the ER causing a rise in cytosolic  $Ca^{2+}$  levels by an as yet unknown mechanism. To maintain low cytoplasmic  $Ca^{2+}$  levels, we theorize that mitochondria sequester  $Ca^{2+}$  and numerous cellular ATPases probably function to pump  $Ca^{2+}$  out of the cytosol. This leads to mitochondrial membrane depolarization and ATP hydrolysis, respectively (Figs. 4 and 5). Sustained depolarization of the mitochondrial membrane leads to further loss of ATP and prevents ATP synthesis by inhibiting respiration. The loss of ATP disrupts ionic homeostasis within the cell and thereby allows extracellular  $Ca^{2+}$  to enter the cell down its concentration gradient (see "Discussion"). The secondary rise in cytosolic  $Ca^{2+}$  levels leads to protease (presumably of calpain or a calpain-like protease) and, thus, endonuclease (DFF40) activation, ultimately resulting in apoptosis.

may undergo futile cycling between quinone and hydroquinone forms ( $\beta$ -Lap-Q and  $\beta$ -Lap-HQ, Fig. 8), presumably depleting NADH and/or NADPH in the cell (5). We theorize that depletion of NAD(P)H, along with a rise in intracellular  $Ca^{2+}$  levels in response to  $\beta$ -Lap, activate a novel caspase-independent apoptotic pathway, as described in this paper and previously (2, 5, 12). The rise in intracellular  $Ca^{2+}$  appears to be dependent upon the bioactivation of  $\beta$ -Lap by NQO1, suggesting a critical and necessary signaling role for  $Ca^{2+}$  in the downstream apoptotic pathway induced by this drug. Dicumarol completely abrogated intracellular  $Ca^{2+}$  changes (Fig. 7), as well as apoptosis and survival, following  $\beta$ -Lap exposure of NQO1-expressing cells (5).<sup>2</sup> When increases in intracellular  $Ca^{2+}$  levels were directly prevented by pretreatment with BAPTA-AM, downstream apoptotic responses, as well as lethality, caused by  $\beta$ -Lap were prevented; when corrected for BAPTA-AM affects alone,  $\beta$ -Lap-induced apoptosis, proteolysis, and lethality were essentially blocked by preventing early  $Ca^{2+}$  release from ER stores. Thus, correcting for the BAPTA-AM affects alone, the role of  $Ca^{2+}$  in  $\beta$ -Lap-mediated apoptosis may be more significant than that revealed by the data shown. These data strongly

mean  $\pm$  S.E. of at least three independent experiments. Student's *t* test for paired samples, experimental groups compared with  $\beta$ -Lap exposure alone are indicated (\*, *p* < 0.005). DC, 50  $\mu$ M dicumarol.

suggest that DNA fragmentation, mitochondrial membrane depolarization, ATP loss, and apoptotic proteolysis were a consequence of the increase in intracellular Ca<sup>2+</sup> levels (Figs. 1–6 and 8). Interestingly, the cell death pathway induced by  $\beta$ -Lap was quite distinct from that observed after exposure to TG, an agent known to specifically cause release of Ca<sup>2+</sup> from ER stores and mediate caspase-dependent apoptosis (24, 28, 33, 52). Thus, Ca<sup>2+</sup> release was necessary for  $\beta$ -Lap-induced cytotoxicity, but apparently not sufficient for the unique apoptotic responses induced by  $\beta$ -Lap.

**$\beta$ -Lap and TG-induced Similar Ca<sup>2+</sup> Responses, but Different Patterns of Apoptosis**— $\beta$ -Lap elicited an early rise in intracellular Ca<sup>2+</sup> levels from the same ER store as released by TG, however, subsequent cell death processes were remarkably different between the two compounds. TG is known to cause transient increases in intracellular Ca<sup>2+</sup> levels, however, these were insufficient to induce apoptosis. Much like  $\beta$ -Lap, Ca<sup>2+</sup> was needed from the extracellular milieu, along with a sustained increase in intracellular Ca<sup>2+</sup> levels, for TG-induced apoptosis (23) in MCF-7 cells (27). Depolarization of the mitochondrial membrane potential and loss of intracellular ATP in cells exposed to  $\beta$ -Lap, may have prevented plasma membrane Ca<sup>2+</sup> pumps and ER Ca<sup>2+</sup> pumps from functioning and maintaining Ca<sup>2+</sup> homeostasis. This, in turn, may have facilitated Ca<sup>2+</sup> leakage down its concentration gradient into the cytosol, providing a secondary and sustained elevation of Ca<sup>2+</sup> that initiated a protease cascade(s) and ultimately caused apoptosis after exposure to  $\beta$ -Lap. This is consistent with what we observed in NQO1-expressing cells after  $\beta$ -Lap treatment and co-administration of Ca<sup>2+</sup> chelators. Buffering intracellular Ca<sup>2+</sup> with BAPTA-AM partially abrogated all of the downstream events induced in MCF-7 cells by  $\beta$ -Lap (and thus prevented secondary Ca<sup>2+</sup> entry by buffering the initial rise in cytosolic Ca<sup>2+</sup>). In contrast, extracellular chelation by EGTA only prevented those events initiated by secondary Ca<sup>2+</sup> entry (e.g. protease activation and DNA fragmentation). Thus, a secondary rise in intracellular Ca<sup>2+</sup> levels after exposure to  $\beta$ -Lap seems probable, and necessary, for protease activation and DNA fragmentation as was observed for TG-induced caspase-mediated apoptosis (23, 27). However, a secondary influx of Ca<sup>2+</sup> does not appear to be necessary for reduction in mitochondrial membrane potential or loss of intracellular ATP after  $\beta$ -Lap exposure, since EGTA did not prevent these responses.

Although MCF-7 cells treated with  $\beta$ -Lap had similar calcium responses, as do TG-exposed cells,  $\beta$ -Lap-exposed cells exhibited a very different pattern of apoptosis than TG-treated cells.  $\beta$ -Lap-exposed cells exhibit loss of intracellular ATP and a decrease in the [ATP]/[ADP][P<sub>i</sub>] ratio. In contrast, TG-exposed cells did not exhibit loss of ATP (Fig. 5, and as reported by Ref. 53). Our data suggest that in contrast to TG where ATP-dependent caspase activation results in cell death (28, 33, 34, 54), an ATP-independent protease is activated after exposure to  $\beta$ -Lap. Ca<sup>2+</sup> may regulate apoptosis by activating Ca<sup>2+</sup>-dependent protein kinases and/or phosphatases leading to alterations in gene transcription. However, with the rapid loss of intracellular ATP after exposure to  $\beta$ -Lap (2–4 h, Fig. 5),  $\beta$ -Lap-mediated cell death unlikely involves stimulated kinases or phosphatases or new protein synthesis. Instead, indirect kinase inhibition, due to ATP depletion, along with continued phosphatase activity is likely. Consistent with this notion, we found dramatic de-phosphorylation of pRb in cells exposed to  $\beta$ -Lap at 3 h (2), a time consistent with loss of ATP following exposure to this drug. Furthermore, loss of ATP at 2 h may also be responsible for inhibition of NF- $\kappa$ B activation induced by tumor necrosis factor- $\alpha$  in  $\beta$ -Lap pre-exposed cells (55), since significant loss of ATP would prevent proteosome-

mediated I $\kappa$ B degradation. Thus, Ca<sup>2+</sup>-dependent loss of ATP in NQO1-expressing cells following  $\beta$ -Lap treatment may explain the reported pleiotropic effects of this agent.

$\beta$ -Lap-exposed cells also exhibited a very different pattern of substrate proteolysis compared with that observed after TG (2, 12, 28). We previously showed that  $\beta$ -Lap elicited a unique cleavage of PARP (~60-kDa fragment), compared with the classical caspase-3-mediated fragmentation of the protein (~89 kDa) observed after TG exposure (data not shown and Ref. 28). In a variety of NQO1-expressing cells exposed to  $\beta$ -Lap, atypical PARP cleavage was inhibited by the global cysteine protease inhibitors, iodoacetamide and *N*-ethylmaleimide, as well as the extracellular Ca<sup>2+</sup> chelators, EGTA and EDTA (12). In addition,  $\beta$ -Lap-mediated apoptotic responses were insensitive to inhibitors of caspases, granzyme B, cathepsins B and L, trypsin, and chymotrypsin-like proteases (12). In contrast, classic caspase inhibitors blocked TG-induced caspase activation and apoptosis (28). Caspase activation, as measured by procaspase cleavage via Western blot analyses, does not occur following  $\beta$ -Lap exposures.<sup>3</sup> Thus, protease activation after  $\beta$ -Lap treatment appears to be Ca<sup>2+</sup>-dependent, or alternatively, is activated by another protease or event that is Ca<sup>2+</sup>-dependent (Figs. 1–6 and Ref. 12).

**Loss of Reducing Equivalents Is Also Necessary for  $\beta$ -Lap-mediated Apoptosis, Similar to Menadione-mediated Apoptosis**—Menadione is a quinone that can be detoxified by NQO1 two-electron reduction. However, menadione can also be reduced through two, one-electron reductions via other cellular reductases (56), thus eliciting menadione's toxic effects. Menadione toxicity, elicited via two, one-electron reductions, exhibited many similarities to  $\beta$ -Lap-mediated, NQO1-dependent, toxicity (5). These included: (a) elevations in cytosolic Ca<sup>2+</sup> (57, 58); (b) NAD(P)H depletion (5, 59, 60); (c) ATP depletion (<0.1% control)<sup>3</sup> (61–63); and (d) mitochondrial membrane potential depolarization<sup>3</sup> (64). We previously demonstrated that menadione caused similar substrate proteolysis (p53 and atypical PARP cleavage) in NQO1-deficient cells, or at high doses in cells that express NQO1 where detoxification processes were over-ridden (5).<sup>3</sup> The semiquinone form of menadione can undergo spontaneous oxidation to the parent quinone (59, 63, 65, 66); a pattern similar to the futile cycling observed after  $\beta$ -Lap bioactivation by NQO1 (5). Loss of reducing equivalents, such as NADH, due to the futile cycling of menadione may cause inactivation of the electron transport chain with the concomitant loss of mitochondrial membrane potential, and thus, loss of ATP (67, 68). These responses were also observed in MCF-7 cells exposed to  $\beta$ -Lap (Figs. 4 and 5). Extensive mitochondrial Ca<sup>2+</sup> accumulation can also mediate mitochondrial depolarization (69, 70). Thus, Ca<sup>2+</sup> sequestration may elicit mitochondrial membrane depolarization and consequent ATP depletion in cells exposed to  $\beta$ -lap. These data further suggest that Ca<sup>2+</sup> is necessary for  $\beta$ -Lap-mediated cell death, but other factors are apparently needed for the initiation of the novel execution apoptotic pathway observed in cells treated with this compound.

The rise in intracellular Ca<sup>2+</sup> appears to be dependent on the bioactivation of  $\beta$ -Lap by NQO1, suggesting a critical and necessary signaling role for Ca<sup>2+</sup> in the downstream apoptotic pathway induced by this drug. These data suggest that DNA fragmentation, mitochondrial membrane depolarization, ATP loss, and apoptotic proteolysis were a consequence of the increase in intracellular Ca<sup>2+</sup> levels. Work in our laboratory is focused on elucidating the signaling response(s) that elicits ER Ca<sup>2+</sup> release following  $\beta$ -Lap bioactivation by NQO1. The cell

<sup>3</sup> C. Tagliarino, J. J. Pink, and D. A. Boothman, unpublished results.

death pathway induced by  $\beta$ -Lap is quite distinct from that observed after exposure to TG, and  $\beta$ -Lap-mediated apoptosis exhibited many similarities to menadione-mediated apoptosis. These observations further suggest that early release of Ca<sup>2+</sup> from ER stores, as well as influx of Ca<sup>2+</sup> from the extracellular milieu are necessary, but not sufficient for the novel apoptotic execution pathway induced by  $\beta$ -Lap. Thus, changes in Ca<sup>2+</sup> homeostasis in conjunction with the presumed loss of reducing equivalents are both necessary and sufficient for  $\beta$ -Lap-mediated apoptosis. We propose that development of  $\beta$ -Lap for treatment of human cancers that have elevated NQO1 levels (e.g. breast and lung) is warranted (6). Since most clinical agents used to date kill cells by caspase-dependent and p53-dependent pathways, and many cancers evade death by altering these pathways, development of agents that kill by specific targets (NQO1-mediated) and in p53- and caspase-independent manners are needed.

**Acknowledgments**—We thank Sara Simmers and Rich Tarin for all their technical help, as well as R. Michael Sramkoski, MT-(ASCP)H. We are grateful to Dr. William G. Bornmann for synthesizing  $\beta$ -lapachone, and Edmunds Z. Reineks and Philip A. Verhoef for critical review of this manuscript. We are also indebted to Sarah Hildebrand for her enduring support of our research.

## REFERENCES

- Planchon, S. M., Wuerzberger, S., Frydman, B., Witiak, D. T., Hutson, P., Church, D. R., Wilding, G., and Boothman, D. A. (1995) *Cancer Res.* **55**, 3706–3711
- Wuerzberger, S. M., Pink, J. J., Planchon, S. M., Byers, K. L., Bornmann, W. G., and Boothman, D. A. (1998) *Cancer Res.* **58**, 1876–1885
- Li, C. J., Wang, C., and Pardee, A. B. (1995) *Cancer Res.* **55**, 3712–3715
- Li, C. J., Li, Y. Z., Pinto, A. V., and Pardee, A. B. (1999) *Proc. Natl. Acad. Sci. U. S. A.* **96**, 13369–13374
- Pink, J. J., Planchon, S. M., Tagliarino, C., Varnes, M. E., Siegel, D., and Boothman, D. A. (2000) *J. Biol. Chem.* **275**, 5416–5424
- Marin, A., Lopez de Cerain, A., Hamilton, E., Lewis, A. D., Martinez-Penuela, J. M., Idoate, M. A., and Bello, J. (1997) *Br. J. Cancer* **76**, 923–929
- Patel, T., Gores, G. J., and Kaufmann, S. H. (1996) *FASEB J.* **10**, 587–597
- Gerschenson, L. E., and Rotello, R. J. (1992) *FASEB J.* **6**, 2450–2455
- Kluck, R. M., Bossy-Wetzel, E., Green, D. R., and Newmeyer, D. D. (1997) *Science* **275**, 1132–1136
- Li, P., Nijhawan, D., Budihardjo, I., Srinivasula, S. M., Ahmad, M., Alnemri, E. S., and Wang, X. (1997) *Cell* **91**, 479–489
- Eguchi, Y., Srinivasan, A., Tomaselli, K. J., Shimizu, S., and Tsujimoto, Y. (1999) *Cancer Res.* **59**, 2174–2181
- Pink, J. J., Wuerzberger-Davis, S., Tagliarino, C., Planchon, S. M., Yang, X., Froelich, C. J., and Boothman, D. A. (2000) *Exp. Cell Res.* **255**, 144–155
- Froelich, C. J., Hanna, W. L., Poirier, G. G., Duriez, P. J., D'Amours, D., Salvesen, G. S., Alnemri, E. S., Earnshaw, W. C., and Shah, G. M. (1996) *Biochem. Biophys. Res. Commun.* **227**, 658–665
- Pariat, M., Carillo, S., Molinari, M., Salvat, C., Debussche, L., Bracco, L., Milner, J., and Piechaczyk, M. (1997) *Mol. Cell. Biol.* **17**, 2806–2815
- Kubbutat, M. H., and Vousden, K. H. (1997) *Mol. Cell. Biol.* **17**, 460–468
- Distelhorst, C. W., and Dubyak, G. (1998) *Blood* **91**, 731–734
- Fang, M., Zhang, H., Xue, S., Li, N., and Wang, L. (1998) *Cancer Lett.* **127**, 113–121
- Marks, A. R. (1997) *Am. J. Physiol.* **272**, H597–605
- McConkey, D. J., Hartzell, P., Amador-Perez, J. F., Orrenius, S., and Jondal, M. (1989) *J. Immunol.* **143**, 1801–1806
- McConkey, D. J., and Orrenius, S. (1997) *Biochem. Biophys. Res. Commun.* **239**, 357–366
- McConkey, D. J. (1996) *Scanning Microsc.* **10**, 777–793
- Martikainen, P., and Isaacs, J. (1990) *Prostate* **17**, 175–187
- Jiang, S., Chow, S. C., Nicotera, P., and Orrenius, S. (1994) *Exp. Cell Res.* **212**, 84–92
- Kaneko, Y., and Tsukamoto, A. (1994) *Cancer Lett.* **79**, 147–155
- Levick, V., Coffey, H., and D'Mello, S. R. (1995) *Brain Res.* **676**, 325–335
- Choi, M. S., Boise, L. H., Gottschalk, A. R., Quintans, J., Thompson, C. B., and Klaus, G. G. (1995) *Eur. J. Immunol.* **25**, 1352–1357
- Jackisch, C., Hahm, H. A., Tombal, B., McCloskey, D., Butash, K., Davidson, N. E., and Denmeade, S. R. (2000) *Clin. Cancer Res.* **6**, 2844–2850
- McColl, K. S., He, H., Zhong, H., Whitacre, C. M., Berger, N. A., and Distelhorst, C. W. (1998) *Mol. Cell. Endocrinol.* **139**, 229–238
- Yakovlev, A. G., Wang, G., Stoica, B. A., Boulares, H. A., Spoonde, A. Y., Yoshihara, K., and Smulson, M. E. (2000) *J. Biol. Chem.* **275**, 21302–21308
- Gaido, M. L., and Cidlowski, J. A. (1991) *J. Biol. Chem.* **266**, 18580–18585
- Urbano, A., McCaffrey, R., and Foss, F. (1998) *J. Biol. Chem.* **273**, 34820–34827
- McConkey, D. J., Nicotera, P., Hartzell, P., Bellomo, G., Wyllie, A. H., and Orrenius, S. (1989) *Arch. Biochem. Biophys.* **269**, 365–370
- Srivastava, R. K., Sollott, S. J., Khan, L., Hansford, R., Lakatta, E. G., and Longo, D. L. (1999) *Mol. Cell. Biol.* **19**, 5659–5674
- Wertz, I. E., and Dixit, V. M. (2000) *J. Biol. Chem.* **275**, 11470–11477
- Lotem, J., and Sachs, L. (1998) *Proc. Natl. Acad. Sci. U. S. A.* **95**, 4601–4606
- Petersen, A., Castilho, R. F., Hansson, O., Wieloch, T., and Brundin, P. (2000) *Brain Res.* **857**, 20–29
- Green, D. R., and Reed, J. C. (1998) *Science* **281**, 1309–1312
- Kroemer, G., Dallaporta, B., and Resche-Rigon, M. (1998) *Annu. Rev. Physiol.* **60**, 619–642
- Susin, S. A., Lorenzo, H. K., Zamzami, N., Marzo, I., Snow, B. E., Brothers, G. M., Mangion, J., Jacotot, E., Costantini, P., Loeffler, M., Larochette, N., Goodlett, D. R., Aebersold, R., Siderovski, D. P., Penninger, J. M., and Kroemer, G. (1999) *Nature* **397**, 441–446
- Richter, C. (1993) *FEBS Lett.* **325**, 104–107
- Li, Y. Z., Li, C. J., Pinto, A. V., and Pardee, A. B. (1999) *Mol. Med.* **5**, 232–239
- Beigi, R. D., and Dubyak, G. R. (2000) *J. Immunol.* **165**, 7189–7198
- Tang, D., Lahti, J. M., and Kidd, V. J. (2000) *J. Biol. Chem.* **275**, 9303–9307
- Kim, J. E., Oh, J. H., Choi, W. S., Chang, I. I., Sohn, S., Krajewski, S., Reed, J. C., O'Malley, K. L., and Oh, Y. J. (1999) *J. Neurochem.* **72**, 2456–2463
- Kurokawa, H., Nishio, K., Fukumoto, H., Tomonari, A., Suzuki, T., and Saijo, N. (1999) *Oncol. Rep.* **6**, 33–37
- Yao, Y., and Tsien, R. Y. (1997) *J. Gen. Physiol.* **109**, 703–715
- Cossarizza, A., Baccarani-Conti, M., Kalashnikova, G., and Franceschi, C. (1993) *Biochem. Biophys. Res. Commun.* **197**, 40–45
- Salvioli, S., Ardizzone, A., Franceschi, C., and Cossarizza, A. (1997) *FEBS Lett.* **411**, 77–82
- Inai, Y., Yabuki, M., Kanno, T., Akiyama, J., Yasuda, T., and Utsumi, K. (1997) *Cell Struct. Funct.* **22**, 555–563
- Hollander, P. M., and Ernster, L. (1975) *Arch. Biochem. Biophys.* **169**, 560–567
- Hosoda, S., Nakamura, W., and Hayashi, K. (1974) *J. Biol. Chem.* **249**, 6416–6423
- Distelhorst, C. W., and McCormick, T. S. (1996) *Cell Calcium* **19**, 473–483
- Waring, P., and Beaver, J. (1996) *Exp. Cell Res.* **227**, 264–276
- Qi, X. M., He, H., Zhong, H., and Distelhorst, C. W. (1997) *Oncogene* **15**, 1207–1212
- Manna, S. K., Gad, Y. P., Mukhopadhyay, A., and Aggarwal, B. B. (1999) *Biochem. Pharmacol.* **57**, 763–774
- Iyanagi, T., and Yamazaki, I. (1970) *Biochim. Biophys. Acta* **216**, 282–294
- Jewell, S. A., Bellomo, G., Thor, H., Orrenius, S., and Smith, M. (1982) *Science* **217**, 1257–1259
- Nicotera, P., McConkey, D., Svensson, S. A., Bellomo, G., and Orrenius, S. (1988) *Toxicology* **52**, 55–63
- Di Monte, D., Bellomo, G., Thor, H., Nicotera, P., and Orrenius, S. (1984) *Arch. Biochem. Biophys.* **235**, 343–350
- Smith, P. F., Alberts, D. W., and Rush, G. F. (1987) *Toxicol. Appl. Pharmacol.* **89**, 190–201
- Akman, S. A., Doroshov, J. H., Dietrich, M. F., Chlebowsky, R. T., and Block, J. S. (1987) *J. Pharmacol. Exp. Ther.* **240**, 486–491
- Mehendale, H. M., Svensson, S. A., Baldi, C., and Orrenius, S. (1985) *Eur. J. Biochem.* **149**, 201–206
- Redegeld, F. A., Moison, R. M., Koster, A. S., and Noordhoek, J. (1989) *Arch. Biochem. Biophys.* **273**, 215–222
- Saxena, K., Henry, T. R., Solem, L. E., and Wallace, K. B. (1995) *Arch. Biochem. Biophys.* **317**, 79–84
- Mirabelli, F., Salis, A., Marinoni, V., Finardi, G., Bellomo, G., Thor, H., and Orrenius, S. (1988) *Arch. Biochem. Biophys.* **264**, 261–269
- Frei, B., Winterhalter, K. H., and Richter, C. (1986) *Biochemistry* **25**, 4438–4443
- Redegeld, F. A., Moison, R. M., Barentsen, H. M., Koster, A. S., and Noordhoek, J. (1990) *Arch. Biochem. Biophys.* **280**, 130–136
- Bellomo, G., Jewell, S. A., and Orrenius, S. (1982) *J. Biol. Chem.* **257**, 11558–11562
- Akerman, K. E. (1978) *Biochim. Biophys. Acta* **502**, 359–366
- Budd, S. L., Tenneti, L., Lishnak, T., and Lipton, S. A. (2000) *Proc. Natl. Acad. Sci. U. S. A.* **97**, 6161–6166



## β-Lapachone-Induced Apoptosis in Human Prostate Cancer Cells: Involvement of NQO1/xip3

Sarah M. Planchon,\* John J. Pink,\* Colleen Tagliarino,\* William G. Bornmann,† Marie E. Varnes,\* and David A. Boothman\*<sup>1</sup>

\*Department of Radiation Oncology and Department of Pharmacology, Ireland Comprehensive Cancer Center, Laboratory of Molecular Stress Responses, Case Western Reserve University, 10900 Euclid Avenue, Cleveland, Ohio 44106-4942; and †Preparative Synthesis Core Facility, Memorial Sloan-Kettering Cancer Center, New York, New York 10021

β-Lapachone (β-lap) induces apoptosis in various cancer cells, and its intracellular target has recently been elucidated in breast cancer cells. Here we show that NAD(P)H:quinone oxidoreductase (NQO1/xip3) expression in human prostate cancer cells is a key determinant for apoptosis and lethality after β-lap exposures. β-Lap-treated, NQO1-deficient LNCaP cells were significantly more resistant to apoptosis than NQO1-expressing DU-145 or PC-3 cells after drug exposures. Formation of an atypical 60-kDa PARP cleavage fragment in DU-145 or PC-3 cells was observed after 10 μM β-lap treatment and correlated with apoptosis. In contrast, LNCaP cells required 25 μM β-lap to induce similar responses. Atypical PARP cleavage in β-lap-treated cells was not affected by 100 μM zVAD-fmk; however, coadministration of dicoumarol, a specific inhibitor of NQO1, reduced β-lap-mediated cytotoxicity, apoptosis, and atypical PARP cleavage in NQO1-expressing cells. Dicoumarol did not affect the more β-lap-resistant LNCaP cells. Stable transfection of LNCaP cells with NQO1 increased their sensitivity to β-lap, enhancing apoptosis compared to parental LNCaP cells or vector-alone transfectants. Dicoumarol increased survival of β-lap-treated NQO1-expressing LNCaP transfectants. NQO1 activity, therefore, is a key determinant of β-lap-mediated apoptosis and cytotoxicity in prostate cancer cells. © 2001

Academic Press

**Key Words:** β-lapachone; apoptosis; NQO1; X-ray-inducible protein 3 (xip3); prostate cancer; atypical PARP cleavage; p53 cleavage.

### INTRODUCTION

β-Lapachone (β-lap, 3,4-dihydro-2,2-dimethyl-2H-naphtho[1,2-b]pyran-5,6-dione)<sup>2</sup> is a naturally occur-

ring *o*-naphthoquinone present in the bark of the Lapacho tree (*Tabebuia avellanedae*) native to South America. The purified drug has anti-trypanosomal, -fungal, -tumor, and -HIV properties and induces apoptosis in a variety of cell types [1]. The mechanism of action and intracellular target(s) of the compound have, however, remained elusive and prevented the preclinical development of this drug for use as an antitumor or antiviral agent. Using a series of *in vitro* assays, proposed mechanisms of action for this drug have included: (a) activation of topoisomerase (Topo) I [2]; (b) induction of apoptosis [3]; (c) inhibition of Topo I [1, 4, 5]; (d) inhibition of Topo II-α [6]; and (e) suppression of NF-κB activation [7]. β-lap can induce apoptosis in several cell systems, including leukemic (HL-60), prostate, and breast cancer cell lines [1, 3, 5]. The apoptotic response caused by β-lap was independent of both p53 status and androgen dependence in human prostate cancer cell lines [1]. Camptothecin (CPT), a Topo I poison, induces classical caspase-mediated apoptotic responses [3].

We recently showed that the enzymatic activity of NQO1 in breast cancer cell lines is a key determinant for β-lap-mediated cytotoxicity [8]. NAD(P)H:quinone reductase (NQO1, DT diaphorase, xip3; EC 1.6.99.2) is a flavoenzyme that catalyzes the two-electron reduction of quinones into their hydroquinone form, bypassing the often mutagenic semiquinone intermediate and the formation of free radicals [9, 10]. NQO1 detoxifies many quinones [e.g., menadione] [11, 12] and bioactivates other compounds, such as mitomycin C, streptozotocin, or E09 [13–16]. NQO1 gene expression is widespread, with detectable levels in human heart, brain, placenta, lung, skeletal muscle, kidney, and pancreatic tissue, and low or absent in human liver [17]. More

NQO1, NAD(P)H:quinone oxidoreductase 1; PARP, poly(ADP-ribose) polymerase; P450r, NADH:cytochrome P-450 reductase; SD, standard deviation; TUNEL, terminal dUTP nick-end labeling; zVAD-fmk, benzyloxycarbonyl-val-ala-aspartate (OMe) fluoromethylketone.

<sup>1</sup> To whom correspondence and reprint requests should be addressed. Fax: (216) 368-1142. E-mail: [dab30@po.cwru.edu](mailto:dab30@po.cwru.edu).

<sup>2</sup> Abbreviations used: β-lap, β-lapachone; b5R, NADH:cytochrome b5 reductase; CFA, colony-forming ability; CPT, camptothecin;





importantly, NQO1 levels have been shown to be significantly up-regulated (5- to 20-fold above adjacent normal tissue) in several forms of cancer, including breast and non-small-cell lung tumors [17-19]. Such elevations in certain cancers make NQO1 a potential target for the development of tumor-directed therapies involving  $\beta$ -lap or its derivatives [8, 20].

Apoptosis is a genetically programmed form of cell death, the initiation and execution of which are thought to be the basis of lethality caused by many chemotherapeutic agents [21-23]. Cells undergoing apoptosis exhibit characteristic changes, including cell shrinkage, membrane blebbing, chromatin condensation, internucleosomal DNA cleavage, and cleavage of specific intracellular substrates involved in cell structure, DNA repair [e.g., poly(ADP-ribosyl) polymerase (PARP)], and general homeostasis. These intracellular alterations are often the result of activation of a family of apoptotic proteases, including caspases [24-28] and/or calpains [29-32].

Caspases are activated by multiple signaling pathways during apoptosis and typically result in the cleavage of PARP; the full-length 113-kDa polypeptide is cleaved to diagnostic 89-kDa and 24-kDa proteins [33]. In HL-60 cells, CPT induced an apoptotic pathway that included activation of the caspases, leading to classical PARP cleavage [20, 34]. HL-60 cells treated with  $\beta$ -lap also activated the caspases [20]. However, a different cell death response appeared to be stimulated by the drug in various human breast cancer cells [3, 35]. In many breast cancer (especially MCF-7:WS8) cells, an atypical PARP fragmentation *in vivo* was noted at times and doses correlating with apoptosis. Apoptotic responses induced by  $\beta$ -lap were monitored by DNA fragmentation (cells staining positive in a TUNEL assay), dephosphorylation of pRb, lamin B cleavage, cleavage of p53, and an atypical cleavage of PARP, leading to an ~60-kDa fragment.  $\beta$ -Lap-mediated apoptosis was thought to involve the activation of a calpain-like protease due to the specific calcium-dependent cleavage of both p53 and PARP [8]. Recently, our laboratory discovered that NQO1 was the key determinant of  $\beta$ -lap cytotoxicity in human breast cancer cell lines [8].

In this report, we demonstrate that NQO1 is also a key determinant of  $\beta$ -lap-induced apoptosis and lethality in human prostate cancer cell lines, suggesting a general mechanism of activation for the compound. Variations in NQO1 activity dramatically affected the sensitivity of human prostate cancer cell lines to  $\beta$ -lap, as determined by comparing various cell lines expressing different levels of the enzyme, by transfection of NQO1 expression vectors into enzyme-deficient cells, and/or by the use of the NQO1 inhibitor, dicoumarol. Coadministration of dicoumarol abrogated  $\beta$ -lap-mediated cytotoxicity and downstream apoptotic end points

in NQO1-expressing, but not in NQO1-deficient, human prostate cancer cell lines. Transfection of NQO1-deficient LNCaP cells with NQO1 significantly enhanced sensitivity (apoptosis, substrate proteolysis, and lethality) to  $\beta$ -lap, which was subsequently blocked by dicoumarol coadministration.

## MATERIALS AND METHODS

**Compounds and drug preparations.**  $\beta$ -Lap was synthesized and dissolved in DMSO as described [1]. CPT and dicoumarol were obtained from Sigma Chemical Co. (St. Louis, MO) and prepared in DMSO or water, respectively [3]. zVAD-fmk and zDEVD-fmk were obtained from Enzyme Systems Products (Dublin, CA). Control treatments containing an equivalent percentage of DMSO were included as described [1-3]. The highest DMSO concentration used was 0.2%, which did not affect survival, cell growth, or apoptosis in various human breast or prostate cancer cells examined [1-3].

**Cell culture conditions.** PC-3, DU-145, and LNCaP human prostate cancer cells were obtained from Dr. George Wilding (University of Wisconsin-Madison) and grown in Dulbecco's minimal essential medium (DMEM) with 5% FBS at 37°C in a humidified 5% CO<sub>2</sub>-95% air atmosphere as described [36-38]. Tests for mycoplasma infection, using the Gen-Probe Rapid Detection Kit (Fisher Scientific, Pittsburgh, PA), were performed quarterly and all cell lines were negative.

**Drug treatments.** For all experiments, cells were plated, allowed at least 24 h to initiate log-phase growth, and then exposed to  $\beta$ -lap or CPT at indicated doses for 4 h. After exposure, drug-containing media were removed and replaced with complete media. Dicoumarol was administered (50  $\mu$ M) concomitantly with  $\beta$ -lap or CPT for 4 h as described above. For zVAD-fmk exposures, cells were pretreated with 100  $\mu$ M zVAD-fmk for 30 min or treated with media alone.  $\beta$ -Lap or CPT was then coadministered in the presence or absence of zVAD-fmk for 4 h. All drug-containing media were then removed and replaced with media containing 100  $\mu$ M zVAD-fmk alone or with fresh, non-drug-containing media.

**Stable transfection of LNCaP cells with NQO1.** Log-phase LNCaP cells were seeded onto 6-well dishes at  $2 \times 10^5$  cells/well and allowed to attach overnight. The following day, 1.0  $\mu$ g of BE8 plasmid DNA, containing human NQO1 cDNA under the control of the CMV promoter in the pcDNA3 constitutive expression vector [39], was added into each of three wells using standard calcium phosphate transfection methodology [40]. After 2 days of growth without selection, cells were exposed to 350  $\mu$ g/ml geneticin (G418, GIBCO BRL, Gaithersburg, MD). A stable, pooled population was established after approximately 3 weeks of growth in media containing 350  $\mu$ g/ml G418. Clonal transfectants were finally derived from the pooled population by limiting dilution cloning. Isolated transfectants were then analyzed for NQO1 expression and enzymatic activity as described below and under Results (Table 1).

**Colony-forming ability assays.** Anchorage-dependent colony-forming ability (CFA) assays were performed [1, 41]. For CFA assays, cells were seeded at 1-2000 viable cells per dish in 35 mm<sup>2</sup>-tissue culture plates (with grids) and incubated overnight. Plated cells were then treated with equal volumes of media containing  $\beta$ -lap at various concentrations for 4 h. Control cells were treated with DMSO equivalent to the highest dose of  $\beta$ -lap used.  $\beta$ -Lap exposures in the presence or absence of 50  $\mu$ M dicoumarol were performed as indicated above and under Results. Colonies were allowed to grow for 10-14 days, with one change of medium at day seven. Plates were stained with 1.0% crystal violet in 20% EtOH and destained with water, and colonies of >50 normal-appearing cells were counted [1, 41].

**TUNEL assays.** Flow cytometric TUNEL analyses were performed to measure DNA fragmentation, sub-G<sub>0</sub>/G<sub>1</sub> cell populations, and changes in cell cycle distribution following various drug treatments [1, 35]. TUNEL assays were performed using APO-DIRECT as described by the manufacturer (Pharmingen, San Diego, CA). Samples were analyzed in an EPICS Elite ESP flow cytometer using an air-cooled argon laser at 488 nm, 15 mW (Beckman Coulter Electronics, Miami, FL). Propidium iodide was read with a 640-nm long-pass optical filter. FITC was read with a 525-nm band-pass filter. TUNEL analyses were performed using the Elite acquisition software provided with the instrument. Sub-G<sub>0</sub>/G<sub>1</sub> data were analyzed using ModFit (Verity Software House, Inc., Topsham, ME) [1, 3, 35]. Results presented are means  $\pm$  SD for at least three separate experiments, repeated in duplicate.

**Western immunoblot analyses.** Control or treated human prostate cancer cells were examined for changes in PARP, p53, and lamin B and for levels of NQO1. Actin was used as a loading control. Briefly, control or treated cells were washed in ice-cold PBS and lysed in loading buffer [62.5 mM Tris, pH 6.8, 6M urea, 10% glycerol, 2% SDS, 0.003% bromophenol blue, 5% 2-mercaptoethanol (freshly added)]. Samples were sonicated with a Fisher Scientific Sonic Dismembrator (model 550) fitted with a microtip probe and stored at  $-20^{\circ}\text{C}$  for later analyses as described [35]. Equivalent amounts of protein were incubated at  $65^{\circ}\text{C}$  for 15 min and polypeptides were separated by SDS-PAGE. Separated proteins were then transferred to Immobilon-P membranes (Millipore, Danvers, MA), and equivalent protein loading was confirmed by Ponceau S staining [0.2% Ponceau S (w/v) in 3% trichloroacetic acid (w/v) and 3% sulfosalicylic acid (w/v)] (Sigma) using standard techniques. Western immunoblots were incubated with PBS containing 0.2% Tween 20 and 10% FBS for 1 h to prevent nonspecific binding. Membranes were then incubated overnight with primary antibodies diluted in the same blocking buffer at  $4^{\circ}\text{C}$ . Primary antibodies included separate, and sometimes in combination, exposures to anti-PARP C2-10 (Enzyme Systems Products), anti-p53 DO-1 (Santa Cruz Biotechnology, Santa Cruz, CA), anti-lamin B (Calbiochem, San Diego, CA), and anti-actin (Amersham Pharmacia Biotech, Piscataway, NJ). An NQO1 antibody was contained in medium from a mouse hybridoma, clone A180, and used according to previously published procedures [42]. Membranes were washed in PBS containing 0.2% Tween and then incubated with horseradish peroxidase-conjugated secondary antibody (Santa Cruz Biotechnology) for 1 h. Western immunoblots were then washed in PBS containing 0.2% Tween, developed with enhanced chemiluminescence (ECL) substrate (Amersham, Arlington Heights, IL), and exposed to Fuji X-ray film. All Western immunoblots shown below are representative of experiments repeated at least three times.

**Preparation of S9 supernatants.** Cellular extracts for enzyme assays were prepared from cells in mid- to late-log-phase growth. Cells were harvested by trypsinization (0.25% trypsin and 1 mM EDTA), washed twice in ice-cold, phenol red-free Hank's balanced salt solution, and resuspended in a small volume of PBS, pH 7.2, containing 10  $\mu\text{g}/\mu\text{l}$  aprotinin. Cell suspensions were sonicated four times on ice using 10-s pulses, then centrifuged at 14,000g for 20 min. S9 supernatants were aliquoted into microfuge tubes and stored at  $-80^{\circ}\text{C}$  for later use as described below.

**NQO1, cytochrome b5 reductase, and cytochrome P450 reductase enzyme assays.** Three general reductase enzyme assays were completed as described [43–46]. Enzyme reactions contained 77  $\mu\text{M}$  cytochrome *c* (practical grade, Sigma) and 0.14% bovine serum albumin in Tris-HCl buffer (50 mM, pH 7.5). NQO1 activity was measured using NADH (200  $\mu\text{M}$ ) as the immediate electron donor and menadione (10  $\mu\text{M}$ ) as the intermediate electron acceptor. Each assay was repeated in the presence of 10  $\mu\text{M}$  dicoumarol, and the activity attributed to NQO1 was that inhibited by dicoumarol [44, 47]. NADH:cytochrome b5 reductase (b5R) was measured using NADH (200  $\mu\text{M}$ ) as the electron donor, and NADH:cytochrome P-450

TABLE 1

NQO1, Cytochrome b5R, and Cytochrome P450 Reductase Enzyme Activity Levels in Prostate Cancer Cell Lines

Cell line	NQO1	b5R	P450
LNCaP	9.0 $\pm$ 2.4	17 $\pm$ 3.2	7.0 $\pm$ 2.3
DU-145	500 $\pm$ 48	39 $\pm$ 3.3	6.8 $\pm$ 0.6
PC-3	740 $\pm$ 100	38 $\pm$ 5.1	7.9 $\pm$ 1.1
LN-pcDNA3 Clone 5	3.9 $\pm$ 0.5	22 $\pm$ 1.8	10 $\pm$ 2.8
LN-NQ Clone 1	140 $\pm$ 22	15 $\pm$ 1.9	9.5 $\pm$ 0.5
LN-NQ Clone 2	250 $\pm$ 61	34 $\pm$ 5.4	9.3 $\pm$ 4.5
LN-NQ Clone 3	290 $\pm$ 30	26 $\pm$ 1.5	9.8 $\pm$ 1.9
LN-NQ Clone 4	270 $\pm$ 30	22 $\pm$ 6.3	5.0 $\pm$ 1.0
LN-NQ Clone 10	210 $\pm$ 24	31 $\pm$ 3.3	9.7 $\pm$ 2.8

*Note.* Enzyme levels were measured in S9 supernatant whole cell lysates as described under Materials and Methods. Activities are reported as nmol cytochrome *c* reduced/min/mg protein.

reductase (P450r) was measured using NADPH (200  $\mu\text{M}$ ) as the electron donor [54] in a Beckman DU 640 spectrophotometer (Beckman Instruments, Fullerton, CA). Reactions were performed at  $37^{\circ}\text{C}$  and were initiated by addition of S9 supernatants. Varying amounts (10 to 40  $\mu\text{l}$ ) of S9 supernatants were used to ensure linearity of enzyme rates with protein concentration. Enzyme activities were calculated as nmol cytochrome *c* reduced/min/mg protein, based on the initial rate of change in OD at 550 nm. An extinction coefficient of 21.1 mM/cm was used for cytochrome *c*.

## RESULTS

**Expression of NQO1 and p53 in human prostate cancer cells.** In examining the apoptotic responses of human prostate cancer cells to  $\beta$ -lap, we noted that LNCaP was resistant to this drug. Since we previously published data that suggested NQO1 expression/activity was a critical determinant in the cytotoxicity of this drug [8], we examined LNCaP, PC-3, and DU-145 cells for expression of this two-electron reductase. DU-145 and PC-3 cells expressed NQO1 protein (Fig. 1) and demonstrated dicoumarol-sensitive enzyme activity (Table 1); enzymatic activity was measured by menadione-mediated, NQO1 reduction of cytochrome *c* as described under Materials and Methods [43]. In contrast, LNCaP cells did not express NQO1 protein or enzyme activity (Fig. 1 and Table 1).

**Dicoumarol enhanced the survival of DU-145 or PC-3, but not LNCaP, cells following  $\beta$ -lap exposure.** Since dicoumarol is a relatively specific inhibitor of NQO1, its effects on the survival of  $\beta$ -lap-treated prostate cancer cells were determined. Dicoumarol significantly enhanced the survival of  $\beta$ -lap-treated DU-145 or PC-3 cells (Fig. 2). The LD<sub>50</sub> values for DU-145 and PC-3 cells were increased (i.e., the drug was less toxic) by three- and two-fold, respectively, compared to  $\beta$ -lap alone. For example, over 95% lethality was noted in DU-145 cells treated with 4.0  $\mu\text{M}$   $\beta$ -lap, whereas the same  $\beta$ -lap exposure was ineffective (>95% survival)

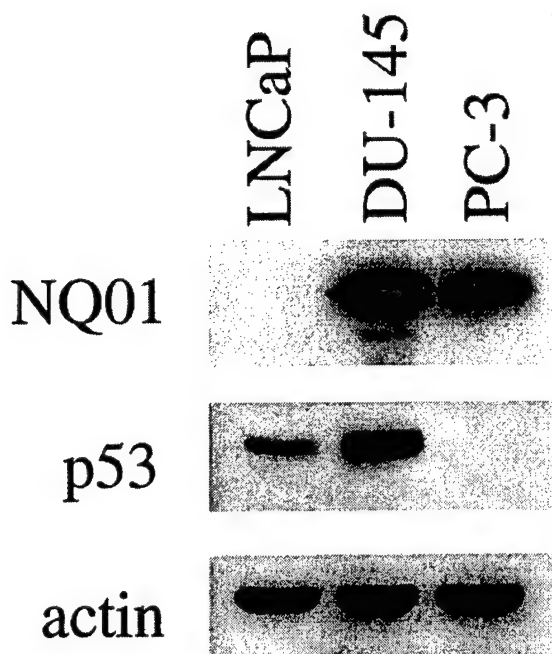


FIG. 1. NQ01 and p53 status of three human prostate cancer cell lines. Western immunoblot analyses of untreated lysates from three human prostate cancer cell lines, DU-145, PC-3, and LNCaP, were performed as described under Materials and Methods. Accurate loading was determined by monitoring actin levels.

when 50  $\mu$ M dicoumarol was coadministered. In contrast, dicoumarol had no influence on the survival of  $\beta$ -lap-treated LNCaP cells, which also exhibited more intrinsic resistance to  $\beta$ -lap-mediated lethality ( $LD_{90}$ , 8.0  $\mu$ M;  $LD_{99}$ , 12  $\mu$ M) compared to DU-145 ( $LD_{90}$ , 3.5  $\mu$ M;  $LD_{99}$ , 5.0  $\mu$ M) or PC-3 ( $LD_{90}$ , 5.0  $\mu$ M;  $LD_{99}$ , 7.5  $\mu$ M) cells.  $\beta$ -Lap-treated LNCaP cells also exhibited three-fold less apoptosis than either DU-145 or PC-3 cells when exposed to equitoxic concentrations [1]. In contrast, dicoumarol coadministration did not significantly affect the survival of LNCaP, DU-145, or PC-3 cells following CPT exposures (Fig. 2).

*Dicoumarol blocked morphologic changes and apoptosis of DU-145 cells after  $\beta$ -lap treatment.* In human breast cancer cells,  $\beta$ -lap induced morphologic changes indicative of apoptosis [3]. Similar alterations in morphology, such as chromatin condensation, cell shrinkage, and detachment occurred in DU-145 or PC-3 cells following 4-h  $\beta$ -lap exposures (shown are DU-145 cells, Fig. 3A). Addition of 50  $\mu$ M dicoumarol significantly blocked  $\beta$ -lap-induced morphologic changes (Fig. 3A), and cells grew normally, consistent with enhanced survival as measured using CFA assays (Fig. 2).

We previously demonstrated the formation of an apoptotic sub- $G_0/G_1$  peak, representing apoptotic cells

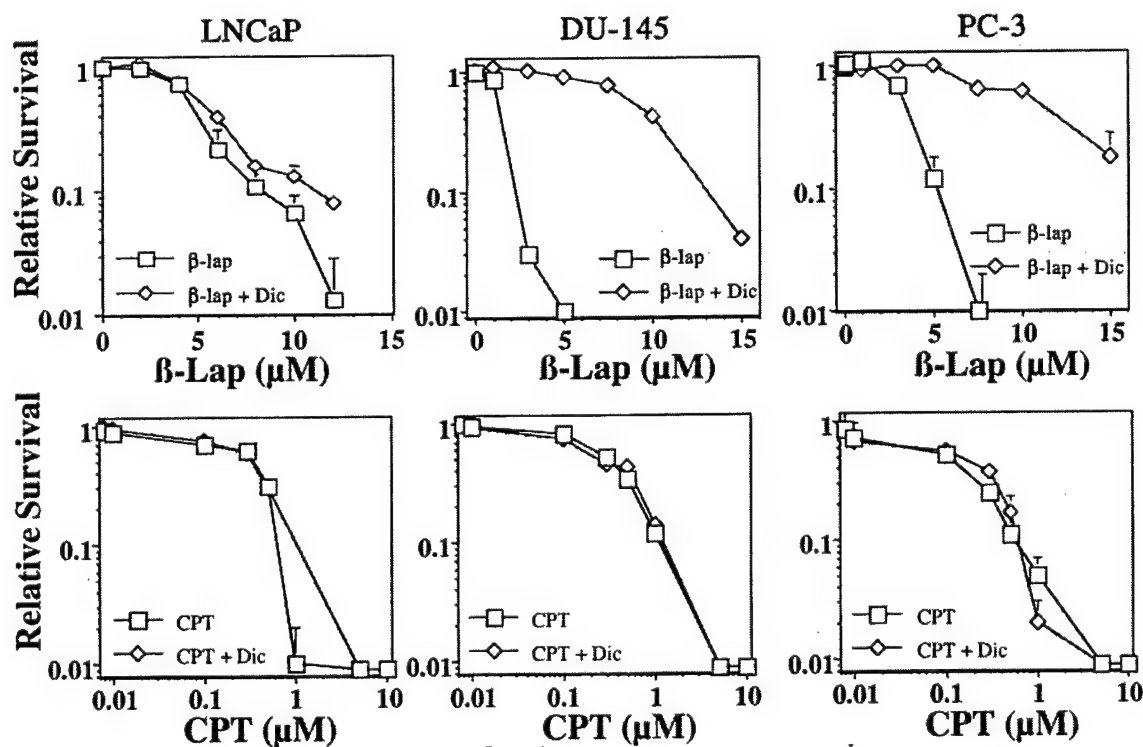
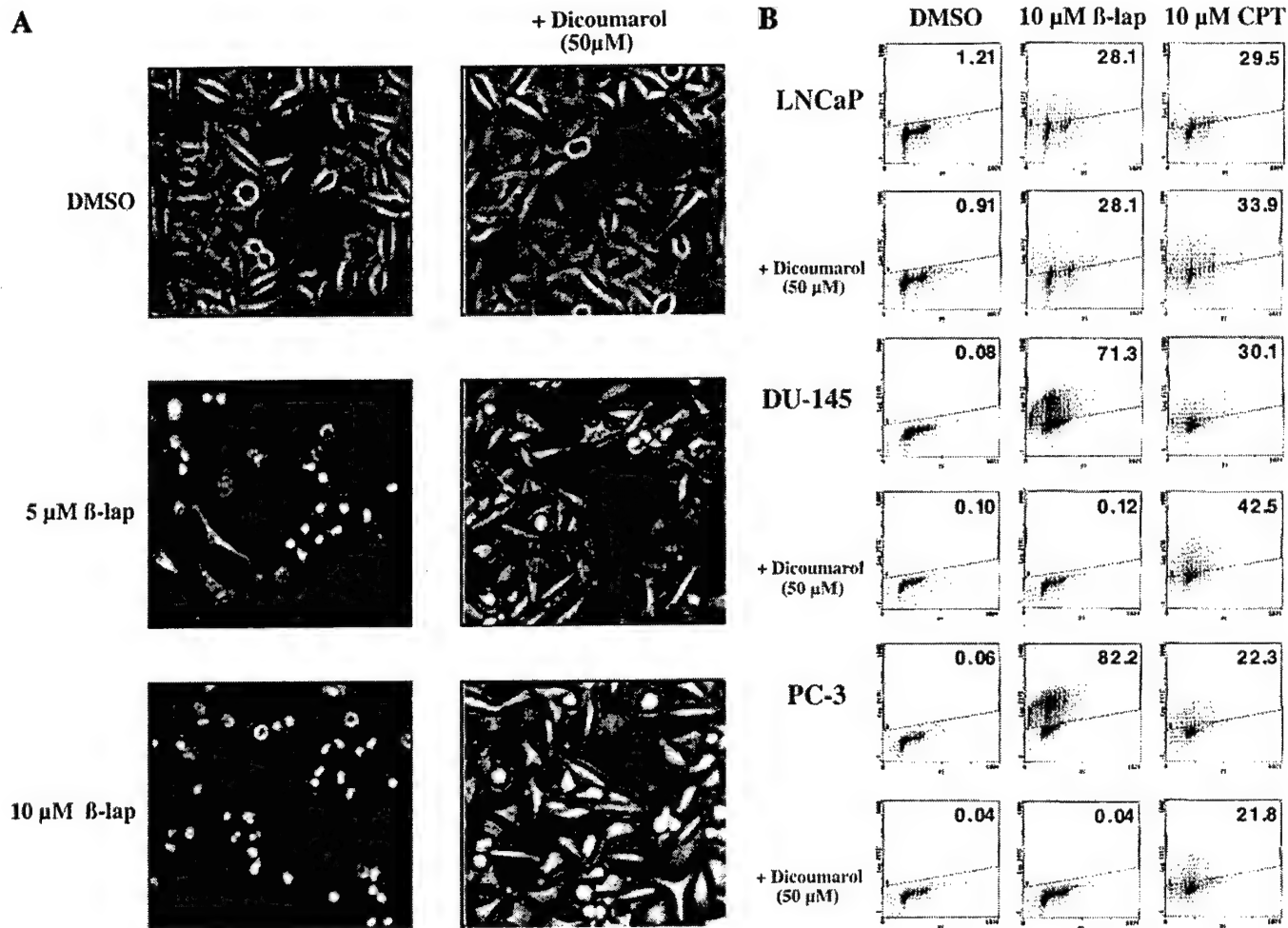


FIG. 2. Dicoumarol protects DU-145 and PC-3, but not LNCaP, human prostate cancer epithelial cell lines from  $\beta$ -lap-induced cytotoxicity. The survival of DU-145, PC-3, and LNCaP human prostate cancer cell lines following  $\beta$ -lap treatment, with or without dicoumarol coadministration, was determined by colony-forming-ability assays as described under Materials and Methods.  $\beta$ -Lap or CPT, with or without 50  $\mu$ M dicoumarol cotreatments, was given as 4-h pulse treatments as described under Materials and Methods. Shown are the results (means  $\pm$  SD) of three experiments repeated in duplicate.



**FIG. 3.** (A) Dicoumarol blocks morphologic changes in DU-145 cells after  $\beta$ -lap treatment. DU-145 cells were treated with 5  $\mu$ M or 10  $\mu$ M  $\beta$ -lap, with or without 50  $\mu$ M dicoumarol, for 4 h. At 24 h posttreatment, phase-contrast photomicrographs were taken of treated or control cells. Shown are representative photos of experiments repeated three or more times. Magnification, 100 $\times$ . (B) Dicoumarol prevents apoptosis induced in human prostate cancer cells following  $\beta$ -lap, but not CPT. TUNEL assays to monitor apoptosis in  $\beta$ -lap- or CPT-treated human prostate cancer cells, with or without 50  $\mu$ M dicoumarol coadministration, were performed 48 h following 4-h drug treatments. The percentage of cells that stained positive by TUNEL assay appears in the top right corner of each panel.

with fractional DNA content, in human prostate or breast cancer cell lines following  $\beta$ -lap treatment. DU-145 or PC-3 cells showed a prominent sub- $G_0/G_1$  population of cells. In contrast, NQO1-deficient LNCaP cells showed significantly lower levels of sub- $G_0/G_1$  cells [1]. To further characterize cell death responses in human prostate cancer cell lines after exposure to  $\beta$ -lap or CPT, TUNEL assays were performed to monitor apoptotic-related DNA fragmentation, with or without dicoumarol (Fig. 3B). DU-145 or PC-3 cells were positively stained by TUNEL (71.3 and 82.2%, respectively) after  $\beta$ -lap treatment, and these responses were abrogated by dicoumarol cotreatments. In contrast,  $\beta$ -lap-treated LNCaP cells exhibited a much lower percentage of apoptotic cells (28.1%), consistent with prior data [1]. Coadministration of dicoumarol did not affect  $\beta$ -lap-mediated responses in these

cells. Treatment of each cell line with CPT resulted in only modest apoptosis (i.e., 22–43% apoptotic cells), as previously described [3]. Predictably, CPT-induced apoptosis was not affected by dicoumarol cotreatments (Fig. 3B).

*Apoptotic substrate cleavage events in human prostate cancer cells after  $\beta$ -lap exposure.* Human prostate cancer cell lines treated with  $\beta$ -lap exhibited the formation of an atypical  $\sim$ 60-kDa PARP polypeptide (Fig. 4A, open arrow), in contrast to classical, CPT-induced, caspase-mediated, 89-kDa PARP cleavage (Fig. 4A, closed arrow). Atypical 60-kDa PARP fragmentation was apparent in DU-145 and PC-3 cells treated with 10  $\mu$ M  $\beta$ -lap and correlated well with apoptosis (Fig. 3B) [8, 35]. Furthermore, formation of  $\beta$ -lap-induced PARP cleavage was completely blocked by coadministration



of 50  $\mu$ M dicoumarol (Fig. 4A), consistent with this NQO1 inhibitor's ability to prevent  $\beta$ -lap-mediated apoptosis (Fig. 3B) and lethality (Fig. 2).  $\beta$ -Lap-resistant LNCaP cells required a greater concentration of  $\beta$ -lap (25  $\mu$ M) to induce an identical atypical PARP cleavage fragment. As with survival responses, coadministration of dicoumarol with  $\beta$ -lap did not affect the formation of the 60-kDa PARP cleavage fragment in  $\beta$ -lap-treated LNCaP cells (Fig. 4A). In contrast, all three human prostate cancer cell lines exhibited the formation of an 89-kDa PARP cleavage fragment (Fig. 4A, closed arrow) after 10  $\mu$ M CPT exposures, correlating with the level of apoptosis observed (Fig. 3B). Dicoumarol coadministration had no effect on classical, caspase-mediated PARP cleavage after CPT exposures.

Global caspase inhibitors, such as zVAD-fmk, can inhibit the activation of many of the caspases and their downstream events (i.e., substrate proteolysis) [5, 26]. Addition of 100  $\mu$ M zVAD-fmk completely abrogated the formation of CPT-induced PARP cleavage (89 kDa), (Fig. 4B). In contrast, atypical PARP cleavage noted in  $\beta$ -lap-treated DU-145 cells (open arrow) was not affected by 100  $\mu$ M zVAD-fmk, suggesting either that  $\beta$ -lap induces a non-caspase-mediated pathway or that zVAD-fmk cannot inhibit this particular caspase-mediated pathway (Fig. 4B).

Cleavage of lamin B (60-kDa full-length protein) to a characteristic 46-kDa polypeptide, typically by caspase 6, is believed to aid in the breakdown of the architecture necessary for apoptosis-related nuclear condensation and membrane blebbing [48–50]. Cleavage of lamin B in  $\beta$ -lap-treated MCF-7:WS8 cells was noted [3]. In DU-145 cells,  $\beta$ -lap but not CPT treatment resulted in lamin B cleavage, possibly due to the relatively poor apoptotic responses induced by CPT compared to those induced by  $\beta$ -lap. Interestingly, 100  $\mu$ M zVAD-fmk, the pan-caspase inhibitor, did not inhibit  $\beta$ -lap-mediated cleavage of lamin B (Fig. 4B). These data are consistent with prior data from our laboratory that  $\beta$ -lap can stimulate a non-caspase-mediated, cysteine protease-directed apoptotic pathway in certain human cancer cells [35].

We previously showed that p53 was not necessary for  $\beta$ -lap-induced apoptosis [1]. In fact, we reported that the level of p53 decreased following treatment of wild-type p53-expressing MCF-7 breast cancer cells following 4–10  $\mu$ M  $\beta$ -lap [3]. In mutant p53-expressing DU-145 cells,  $\beta$ -lap treatment resulted in the formation of two cleavage fragments (40 kDa and ~20 kDa) that were not inhibited by 100  $\mu$ M zVAD-fmk coadministration (Fig. 4B). A similar cleavage of p53 was described during calpain-mediated apoptosis, and this protease may be involved in  $\beta$ -lap-mediated cell death responses [35]. Treatment of DU-145 cells with CPT did not result in any changes in the level or cleavage of p53, even

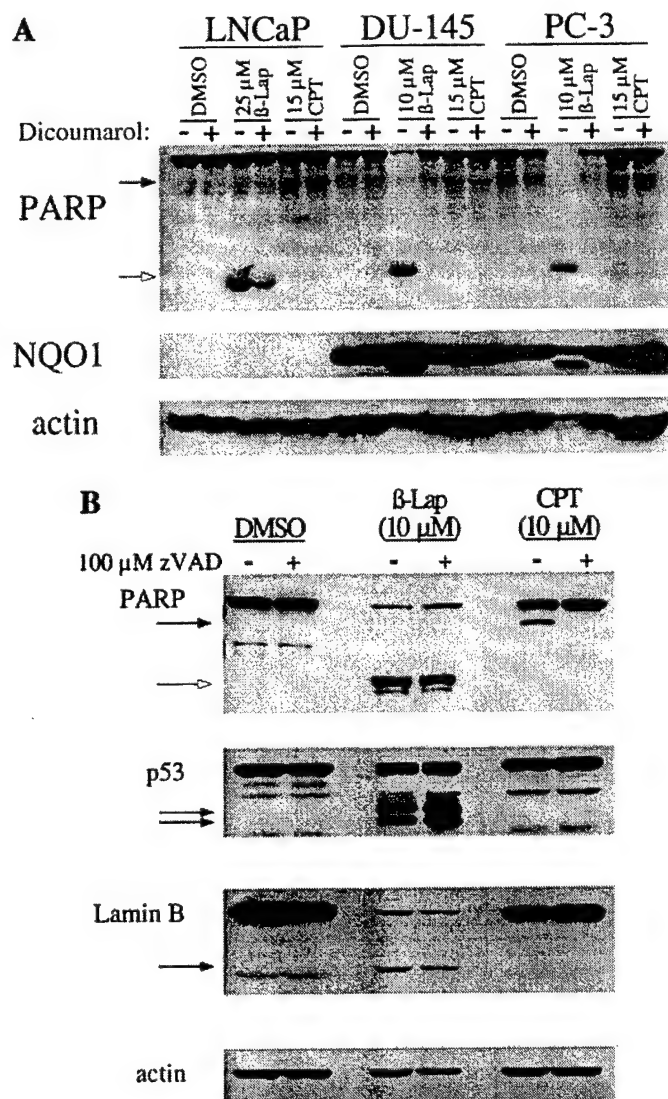


**FIG. 4.** (A) PARP cleavage in human prostate cancer cells following  $\beta$ -lap or CPT exposure. Human prostate cancer cell lines were treated for 4 h with  $\beta$ -lap (10 or 25  $\mu$ M) or CPT (15  $\mu$ M), with or without 50  $\mu$ M dicoumarol. Cells were harvested for analyses 24 h posttreatment and analyzed for specific changes in protein cleavage events by Western blot analyses. Closed arrow; typical 89-kDa PARP cleavage fragment. Open arrow, atypical 60-kDa PARP cleavage fragment. (B) zVAD-fmk blocks CPT-, but not  $\beta$ -lap-, induced apoptotic proteolytic substrate cleavage in DU-145 cells. DU-145 human prostate cancer cells were treated with either 10  $\mu$ M  $\beta$ -lap or 10  $\mu$ M CPT, with or without 100  $\mu$ M zVAD-fmk, for 4 h and specific protein cleavage events were monitored by Western immunoblot analyses. zVAD-fmk treatment began 1 h prior to  $\beta$ -lap addition; treatment was continued throughout the  $\beta$ -lap treatment, and cells were harvest as described under Materials and Methods. PARP: full-length polypeptide, 113 kDa; typical PARP cleavage fragment (closed arrow), 89 kDa; atypical PARP cleavage fragment (open arrow), ~60 kDa. p53: full-length polypeptide, 53 kDa; p53 cleavage fragment, ~40 kDa. Lamin B: full-length polypeptide, 68 kDa; lamin B cleavage fragment, 45 kDa.

though 20% of the cells were apoptotic; DU-145 cells express stable, high levels of mutant p53 protein that are not stabilized by CPT-mediated damage.

**Stable transfection of LNCaP cells with NQO1.** In order to further characterize the role of NQO1 in  $\beta$ -lap-mediated apoptosis, LNCaP cells were transfected with either pcDNA3 empty vector or pcDNA3 containing full-length NQO1 cDNA, in which expression of this two-electron reductase was controlled by the CMV promoter. Five clonal cell lines containing NQO1 (LN-NQ Clones 1–4, 10) and one vector-alone control (LN-pcDNA3) were isolated. All five NQO1-containing cell lines demonstrated both enzyme activity (15- to 30-fold above nontransfected levels, Table 1) and protein expression (Fig. 7). LNCaP transfectants containing pcDNA3 vector alone exhibited neither NQO1 enzyme activity nor protein expression, similar to nontransfected LNCaP parental cells (Table 1, Fig. 7).

**Transfection of NQO1 sensitized human LNCaP prostate cancer cells to  $\beta$ -lap.** In clonogenic assays, NQO1-deficient parental LNCaP cells showed moderate resistance to  $\beta$ -lap, relative to DU-145 and PC-3 cells, which express high levels of the enzyme (Fig. 2). Similarly, NQO1-containing LNCaP clones demonstrated significantly increased sensitivity to  $\beta$ -lap relative to NQO1-deficient LNCaP cells containing pcDNA3 vector alone (Fig. 5A). As previously observed with NQO1-expressing DU-145 or PC-3 cells, coadministration of dicoumarol blocked  $\beta$ -lap-mediated cytotoxicity. This resulted in a relatively resistant phenotype, similar to that of NQO1-deficient, pcDNA3 vector-alone, control LNCaP cells. Dicoumarol coadministration had no effect on the sensitivity of NQO1-deficient, LNCaP cells (containing pcDNA3 vector alone) to  $\beta$ -lap treatment (Fig. 5A).

Menadione is detoxified by NQO1 and is thus toxic to cells in the absence of NQO1 activity. In contrast to  $\beta$ -lap-mediated toxicity, NQO1-deficient LNCaP parental or vector-alone transfectants were more sensitive to menadione on an equimolar basis. NQO1-containing LN-NQ clone 10 cells were more resistant to menadione toxicity than NQO1-deficient LN-pcDNA3 cells (Fig. 5B). Thus, the toxicities of menadione and  $\beta$ -lap were reversed. Similar results were found with human NQO1-transfected (or vector-alone-transfected) MDA-MB-468 breast cancer cells treated with  $\beta$ -lap or menadione [8].

To determine whether LNCaP cells compensated for their NQO1 deficiency by increasing the activities of one-electron enzymes, levels of P450 reductase and cytochrome b5R were determined in the three parental cell lines, as well as in the six NQO1-expressing LNCaP clones. No significant differences in P450 reductase or b5R activities were noted (Table 1).

**Transfection of LNCaP cells with NQO1 enhanced  $\beta$ -lap-induced apoptosis.** Exposure of each NQO1-expressing LNCaP transfectant (LN-NQ Clones 1–4, 10) to 10  $\mu$ M  $\beta$ -lap resulted in significantly increased apo-

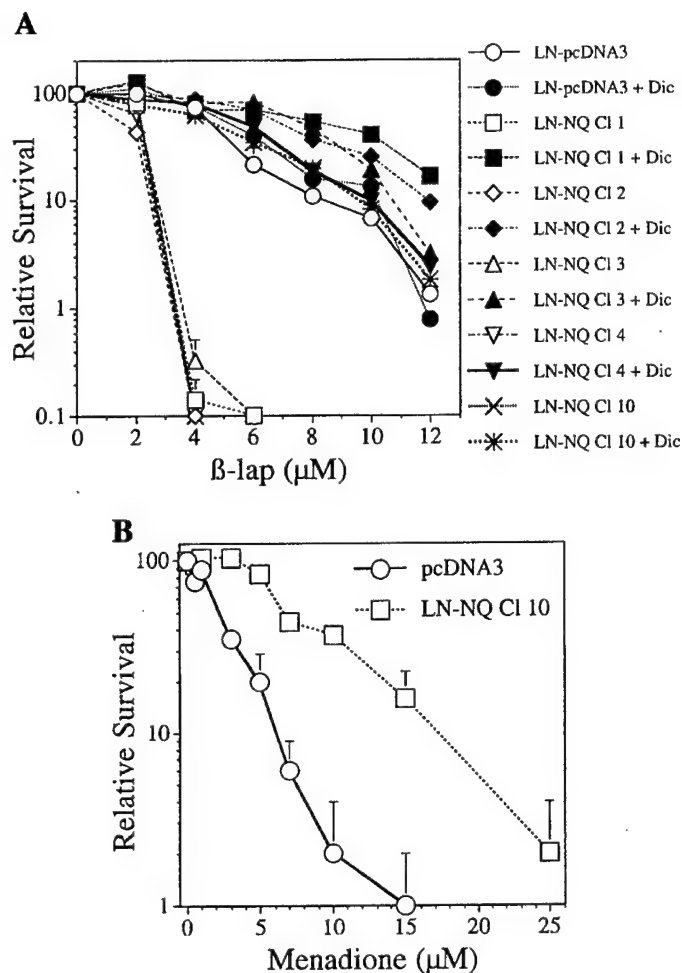


**FIG. 5.** (A) Transfection of LNCaP cells with NQO1 enhances  $\beta$ -lap-induced lethality. NQO1-containing (LN-NQ Clones 1–4, 10) and -deficient (LN-pcDNA3) LNCaP clonal cell lines were treated with 4-h pulses of various doses of  $\beta$ -lap, with or without concomitant 50  $\mu$ M dicoumarol coadministration. Survival was then determined by colony-forming-ability assays as described under Materials and Methods. Experiments were performed three times, each in triplicate. Symbols represent means  $\pm$  SD. Open symbols,  $\beta$ -lap alone. Closed symbols,  $\beta$ -lap with 50  $\mu$ M dicoumarol coadministration. (B) Transfection of LNCaP cells with NQO1 decreases menadione-induced lethality. One NQO1-transfected LNCaP clonal cell line (LN-NQ Cl 10) and the LNCaP vector-alone clonal isolate (LN-pcDNA3) were treated with 4-h pulses of various doses of menadione, and survival was determined by CFA assays as described under Materials and Methods. Experiments were performed three times, each in triplicate. Symbols represent means  $\pm$  SD.

ptosis (i.e., 80–90%) compared to that of control LN-CaP transfectants containing pcDNA3 vector alone (5%) (Fig. 6). As expected, NQO1-mediated,  $\beta$ -lap-stimulated apoptosis in LN-NQ Clone 1–4 and 10 cell lines were prevented by 50  $\mu$ M dicoumarol.

**Expression of NQO1 in LNCaP cells enhanced atypical PARP cleavage in response to  $\beta$ -lap exposure.** Parental LNCaP cells produced an apoptosis-related, atypical cleavage of PARP (formation of a 60-kDa



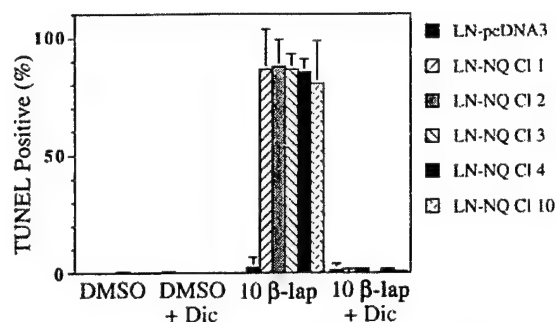


**FIG. 6.** Stable transfection of LNCaP cells with NQO1 enhances  $\beta$ -lap-induced apoptosis. Stably transfected LNCaP clonal cell lines containing NQO1 or vector alone (from Fig. 5A) were treated for 4 h with various concentrations of  $\beta$ -lap, with or without 50  $\mu$ M dicoumarol, as described under Materials and Methods. Forty-eight hours posttreatment, cells were monitored for apoptosis-related DNA fragmentation using TUNEL assays. Symbols represent means  $\pm$  SD of experiments performed three or more times, each in triplicate. LNCaP isolated clonal cell lines examined were pcDNA3, LNCaP stably transfected with vector alone; LN-NQ CI 1–4 and 10, five separate LNCaP cell lines stably transfected with CMV-controlled NQO1 cDNA, Clones 1–4 and 10.

PARP polypeptide) following 25  $\mu$ M  $\beta$ -lap, a concentration nearly five times higher than the LD<sub>50</sub> for the drug (see Figs. 2 and 4A). In contrast, atypical PARP cleavage was apparent in PC-3 or DU-145 cells after 10  $\mu$ M  $\beta$ -lap, at or near the drug's LD<sub>90</sub> for these cells. In general, atypical PARP cleavage correlated well with the sensitivities (apoptosis) of each prostate cancer cell line to  $\beta$ -lap exposure (Figs. 2 and 4A), similar to that observed in human breast carcinoma epithelial cells [35]. Empty vector (LN-pcDNA3)- or NQO1-transfected LNCaP (LN-NQ Clones 1–4 and 10) cells were also examined for PARP cleavage following  $\beta$ -lap treatments. Atypical 60-kDa PARP fragmentation was observed in each NQO1-expressing clone following 10  $\mu$ M  $\beta$ -lap, whereas the parental and vector-alone clones needed significantly greater doses of the compound ( $\geq 25$   $\mu$ M) to initiate detectable levels of PARP cleavage (Fig. 7). Thus, PARP fragmentation in NQO1-contain-

ing LNCaP cells, but not in LNCaP parental or empty vector transfectants, following  $\beta$ -lap treatment strongly correlated with overall apoptosis (Fig. 6) and lethality (Fig. 5A). In contrast, altered expression of NQO1 did not influence apoptotic reactions induced by CPT in any of the LNCaP cell lines examined above.

## DISCUSSION

NQO1 may be a clinically exploitable target for therapy against certain tumors using  $\beta$ -lap or its derivatives. Our results demonstrate that NQO1 is a key intracellular determinant for  $\beta$ -lap toxicity in human prostate epithelial cancer cells, since dicoumarol prevented  $\beta$ -lap-mediated apoptosis and lethality in DU-145 and PC-3. In contrast, dicoumarol did not affect  $\beta$ -lap-induced apoptosis in NQO1-deficient LNCaP cells. Furthermore, reexpression of NQO1 in deficient LNCaP cells increased their sensitivity to  $\beta$ -lap-mediated apoptosis and lethality. These data suggest that NQO1 activity is a key determinant in  $\beta$ -lap-mediated cytotoxicity, a conclusion also made using human breast cancer cells [8]. Although many laboratories (including our own) have published data supporting other potential targets *in vitro*, including Topo I and Topo II- $\alpha$ , none of these previous studies demonstrated convincing data for an intracellular target for this drug.

We previously showed that  $\beta$ -lap induced a p53-independent apoptotic response in human prostate cancer cells [37]. We now demonstrate that these p53-independent apoptotic responses initiated by this drug are greatly enhanced by NQO1 expression (Fig. 7). Furthermore, we demonstrate that lethality caused by  $\beta$ -lap is opposite to that induced by menadione, wherein NQO1 overexpression increases  $\beta$ -lap lethality but decreases the cytotoxicity of menadione. Similar results were found in human breast cancer cells [8]. Collectively, our data strongly suggest that  $\beta$ -lap is bioactivated in cells expressing NQO1. The possibility of a bioactivated form of  $\beta$ -lap interacting with previ-

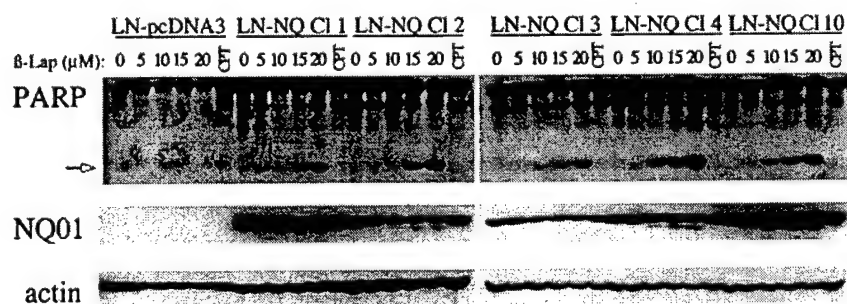


**FIG. 7.**  $\beta$ -Lap-induced atypical PARP cleavage is enhanced by NQO1 overexpression. NQO1-containing and -deficient LNCaP clonal cell lines (described in the legends to Figs. 5A and 6), were exposed to 4-h treatments with various doses of  $\beta$ -lap or 10  $\mu$ M CPT. Cells were harvested for Western immunoblot analyses 24 h following drug removal, as previously described. Open arrow, atypical PARP cleavage fragment of ~60-kDa molecular weight by SDS-PAGE.

ously suggested *in vitro* targets, such as Topo I [2], is being explored.

$\beta$ -Lap induces a unique apoptotic response in epithelial cancer cell lines, such as those of breast or prostate origin.  $\beta$ -Lap stimulates a novel cell death pathway that appears to be caspase-independent (Fig. 4B), calcium-dependent, and NQO1-mediated (Fig. 7) [8, 35]; dicoumarol prevents its activation and cells lacking NQO1 do not demonstrate p53 or PARP proteolytic cleavage events after physiological  $\beta$ -lap exposures (non-supra-lethal doses) (Fig. 4A) [8]. Treatment of human prostate cancer cells with  $\beta$ -lap induced the formation of an atypical PARP cleavage fragment, different from the classical 89-kDa fragment formed during caspase-mediated (via caspases 3, 6, and 7) apoptosis [34]. Production of this atypical 60-kDa PARP fragment correlated well with apoptosis and overall sensitivity of human prostate or breast epithelial cancer cells to  $\beta$ -lap (compare Figs. 5A and 7) [8]. As with  $\beta$ -lap-treated human breast cancer cells, although the overall number of adherent cells was markedly reduced, no evidence of cell lysis during  $\beta$ -lap-mediated apoptosis in DU-145 or PC-3 cells was noted, suggesting that cell death was not necrotic in nature. Addition of 100  $\mu$ M zVAD-fmk, a widely used pancaspase inhibitor, blocked caspase-induced typical PARP cleavage initiated in DU-145 cells by treatment with 10  $\mu$ M CPT (Fig. 3B). However, the same concentration of zVAD-fmk had no effect on atypical PARP cleavage or cleavage of other  $\beta$ -lap-induced apoptotic substrates, such as lamin B or p53, in NQO1-expressing human prostate cancer cell lines. Thus,  $\beta$ -lap predominantly stimulates a non-caspase-mediated apoptotic response, which we theorize is directed by the activation of a calcium-dependent cysteine protease with properties similar to calpain [35].

LNCaP cells did exhibit toxicity following nonphysiologically high doses of  $\beta$ -lap, despite their deficiency in NQO1 expression. The observed apoptotic responses in LNCaP parental cells following supra-lethal doses of  $\beta$ -lap are probably attributed to the lower affinity reduction of this compound by one-electron reducing enzymes, such as p450 reductase, as well as other non-related enzymes (e.g., cytochrome b5 reductase). These enzymes may catalyze two-step, one-electron reductions of quinones (i.e.,  $\beta$ -lap) in order to form the hydroquinone, whereas NQO1 mediates one higher affinity, two-electron reduction forming the same byproduct. As a result, a higher dose of  $\beta$ -lap was required (compared to NQO1-containing PC-3, DU-145, or LNCaP transfectants) for a similar apoptotic reaction. Expression of NQO1 in LNCaP cells, via stable transfection with CMV-controlled mammalian NQO1 expression vectors, significantly increased their sensitivity to  $\beta$ -lap, a sensitivity ablated by dicoumarol coadministration. These data indicate that while

NQO1 is not the only enzyme capable of activating or metabolizing  $\beta$ -lap, its ability far surpasses the efficiency of other reductases (or other as yet unidentified enzymes) in the cell to bioactivate the drug.

Current dogma states that all apoptotic pathways include caspase activation and that all caspase-independent mechanisms lead exclusively to necrosis. Our data strongly suggest that other non-caspase-mediated apoptotic pathways (e.g., mediated by calpain) are activated after certain drug treatments. Non-caspase-mediated apoptotic pathways have been described in several other cell systems [51–56]. Furthermore, we suggest that there is a spectrum of cell death responses, ranging from caspase-mediated apoptosis to cell lysis during necrosis (i.e., cell plasma membrane rupture and lysis, as observed after sodium azide exposure). Cells treated with  $\beta$ -lap exhibit many characteristics of cells undergoing apoptosis, including morphologic changes (Fig. 3A); chromatin condensation [63]; DNA ladder formation [14, 20]; generation of sub-G<sub>0</sub>/G<sub>1</sub> apoptotic cells [1]; cells staining positive with the TUNEL assay, which monitors for endonuclease-specific DNA double-strand breaks (Fig. 3B, 6); specific dephosphorylation of pRb [3]; and specific intracellular cleavage of unique substrates (e.g., Topo I, Topo II, lamin B, and p53), while most other proteins (e.g., cyclins A, B, E and bcl-2) remained intact (Figs. 4A, 4B, and 7) [3, 35]. Yet, concrete evidence of caspase activation is lacking. It was previously reported that  $\beta$ -lap induced apoptosis in some cell systems and necrosis in others, although specific end points for necrosis were not examined [57].  $\beta$ -Lap-treated breast or prostate cancer cells demonstrated extensive formation of apoptotic cells, as monitored by TUNEL assays, formation of sub-G<sub>0</sub>/G<sub>1</sub> cells, morphology changes (i.e., condensed nuclei and rounded cells), and lamin B cleavage (Fig. 4B), as early as 4–8 h following  $\beta$ -lap treatment [8, 35]. Since DNA fragmentation may occur during late-stage necrosis [58], the early (4–8 h) appearance of cells staining positive using a TUNEL assay, concomitant with specific protein cleavage events (e.g., PARP and p53) following  $\beta$ -lap treatment, strongly suggests that an apoptotic, rather than necrotic, cell death mechanism was triggered by  $\beta$ -lap.  $\beta$ -Lap-treated NQO1-expressing cells demonstrate extensive nuclear condensation and unique intracellular substrate cleavages, and the cells detached in a rounded form (Fig. 3). Most importantly,  $\beta$ -lap-treated cells show no visible morphologic hallmarks of necrosis, such as extensive cell debris (Fig. 3). Few cells survive the treatment and the cytotoxic responses have a sharp dose-response curve in which apoptosis and loss of survival are directly correlated in NQO1-expressing cells. All NQO1-containing breast and prostate cancer cells examined thus far respond with identical apoptotic mechanisms to the drug. In contrast, all NQO1-deficient breast or prostate

cancer cells appear to be more resistant to  $\beta$ -lap, showing significantly less apoptosis [8].

We have previously shown that  $\beta$ -lap was a radiosensitizer (after IR exposure) of human cancer cells compared to normal cells [2]. Furthermore, those normal cells that did survive the IR exposures plus  $\beta$ -lap posttreatments demonstrated lower than basal levels of neoplastic transformants [59]. Our laboratory also demonstrated that NQO1 was an X-ray-inducible transcript (i.e., xip3) [10]. The discovery that NQO1 is a major determinant in the sensitivity of human prostate and breast epithelial cancer cells to  $\beta$ -lap [8] may explain the compound's ability to radiosensitize certain cancer cells that express low basal levels of NQO1, but in which the cell's enzyme levels can be dramatically induced by IR pretreatment. We previously found that posttreatments, and not pretreatments, of  $\beta$ -lap sensitized cells to IR [2, 59–61]. A 5-h posttreatment of 4–5  $\mu$ M  $\beta$ -lap was required, in which IR-treated cells were killed and non-IR-treated cells were spared (<20% lethality). Since NQO1 levels were induced 5- to 20-fold in 3 to 4 h in the same cell line [59], we speculate that the compound's radiosensitizing capacity was due to the exploitation of this damage-inducible, bioactivating (for  $\beta$ -lap) enzyme. Since NQO1 is commonly elevated during early stages of carcinogenesis [62, 63], normal cells that become genetically unstable following IR exposure and later induce stable expression of NQO1 would be rather sensitive to cell death by  $\beta$ -lap posttreatments. We previously demonstrated that post-IR-exposure to 4–5  $\mu$ M  $\beta$ -lap could dramatically reduce IR-mediated neoplastic transformants [59]. We speculate, therefore, that this compound not only may be useful against NQO1-overexpressing cancer cells (e.g., breast, lung, and possibly prostate cancers), but also could possess great potential as an anti-carcinogenic agent by eliminating genetically unstable, NQO1-overexpressing transformed cells within a normal cell population.

Support for this research was provided by grants from the United States Army Medical Research and Materiel Command Breast Cancer Initiative: Idea Award No. DAMD17-98-1-8260 to D.A.B. and Postdoctoral Fellowship No. DAMD17-97-1-7221 to J.J.P. We are also grateful for support for S.M.P. from the Human Oncology Training Grant, Department of Human Oncology, University of Wisconsin–Madison. We would like to thank Shelly Wuerzberger-Davis for her outstanding assistance in the early stages of this study, as well as Drs. Tom Davis, Nancy Oleinick, and Timothy Kinsella for their helpful discussions. We are grateful to Sara Hildebrand for her moral and financial support. This paper is dedicated to her and her family.

## REFERENCES

1. Planchon, S. M., Wuerzberger, S., Frydman, B., Witlak, D. T., Hutson, P., Church, D. R., Wilding, G., and Boothman, D. A. (1995). Beta-lapachone-mediated apoptosis in human promyelocytic leukemia (HL-60) and human prostate cancer cells: A p53-independent response. *Cancer Res.* **55**, 3706–3711.
2. Boothman, D. A., Trask, D. K., and Pardee, A. B. (1989). Inhibition of potentially lethal DNA damage repair in human tumor cells by beta-lapachone, an activator of topoisomerase I. *Cancer Res.* **49**, 605–612.
3. Wuerzberger, S. M., Pink, J. J., Planchon, S. M., Byers, K. L., Bornmann, W. G., and Boothman, D. A. (1998). Induction of apoptosis in MCF-7-WS8 breast cancer cells by beta-lapachone. *Cancer Res.* **58**, 1876–1885.
4. Li, C. J., Wang, C., and Pardee, A. B. (1995). Induction of apoptosis by beta-lapachone in human prostate cancer cells. *Cancer Res.* **55**, 3712–3715.
5. Li, C. J., Averboukh, L., and Pardee, A. B. (1993). beta-Lapachone, a novel DNA topoisomerase I inhibitor with a mode of action different from camptothecin. *J. Biol. Chem.* **268**, 22463–22468.
6. Frydman, B., Marton, L. J., Sun, J. S., Neder, K., Witlak, D. T., Liu, A. A., Wang, H. M., Mao, Y., Wu, H. Y., Sanders, M. M., and Liu, L. F. (1997). Induction of DNA topoisomerase II-mediated DNA cleavage by beta-lapachone and related naphthoquinones. *Cancer Res.* **57**, 620–627.
7. Manna, S. K., Cad, Y. P., Mukhopadhyay, A., and Aggarwal, B. B. (1999). Suppression of tumor necrosis factor-activated nuclear transcription factor-kappaB, activator protein-1, c-Jun N-terminal kinase, and apoptosis by beta-lapachone. *Biochem. Pharmacol.* **57**, 763–774.
8. Pink, J. J., Planchon, S. M., Tagliarino, C., Varnes, M. E., Siegel, D., and Boothman, D. A. (2000). NAD(P)H:quinone oxidoreductase activity is the principal determinant of beta-lapachone cytotoxicity. *J. Biol. Chem.* **275**, 5416–5424.
9. Joseph, P., Xie, T., Xu, Y., and Jaiswal, A. K. (1994). NAD(P)H:quinone oxidoreductase1 (DT-diaphorase): Expression, regulation, and role in cancer. *Oncol. Res.* **6**, 525–532.
10. Boothman, D. A., Meyers, M., Fukunaga, N., and Lee, S. W. (1993). Isolation of X-ray-inducible transcripts from radioresistant human melanoma cells. *Proc. Natl. Acad. Sci. USA* **90**, 7200–7204.
11. Tampo, Y., and Yonaha, M. (1996). Enzymatic and molecular aspects of the antioxidant effect of menadione in hepatic microsomes. *Arch. Biochem. Biophys.* **334**, 163–174.
12. Joseph, P., and Jaiswal, A. K. (1994). NAD(P)H:quinone oxidoreductase1 (DT-diaphorase) specifically prevents the formation of benzo[a]pyrene quinone–DNA adducts generated by cytochrome P4501A1 and P450 reductase. *Proc. Natl. Acad. Sci. USA* **91**, 8413–8417.
13. Ross, D., Siegel, D., Beall, H., Prakash, A. S., Mulcahy, R. T., and Gibson, N. W. (1993). DT-diaphorase in activation and detoxification of quinones: Bioreductive activation of mitomycin C. *Cancer Metastasis Rev.* **12**, 83–101.
14. Tedeschi, G., Chen, S., and Massey, V. (1995). DT-diaphorase: Redox potential, steady-state, and rapid reaction studies. *J. Biol. Chem.* **270**, 1198–1204.
15. Smitskamp-Wilms, E., Hendriks, H. R., and Peters, G. J. (1996). Development, pharmacology, role of DT-diaphorase and prospects of the indoloquinone EO9. *Gen. Pharmacol.* **27**, 421–429.
16. Ross, D., Beall, H., Traver, R. D., Siegel, D., Phillips, R. M., and Gibson, N. W. (1994). Bioactivation of quinones by DT-diaphorase, molecular, biochemical, and chemical studies. *Oncol. Res.* **6**, 493–500.
17. Belinsky, M., and Jaiswal, A. K. (1993). NAD(P)H:quinone oxidoreductase1 (DT-diaphorase) expression in normal and tumor tissues. *Cancer Metastasis Rev.* **12**, 103–117.
18. Marin, A., Lopez de Cerain, A., Hamilton, E., Lewis, A. D., Martinez-Penuela, J. M., Idoate, M. A., and Bello, J. (1997).

- DT-diaphorase and cytochrome B5 reductase in human lung and breast tumours. *Br. J. Cancer* **76**, 923-929.
19. Rauth, A. M., Goldberg, Z., and Misra, V. (1997). DT-diaphorase: Possible roles in cancer chemotherapy and carcinogenesis. *Oncol. Res.* **9**, 339-349.
20. Planchon, S. M., Wuerzberger-Davis, S. M., Pink, J. J., Robertson, K. A., Bornmann, W. G., and Boothman, D. A. (1999). Bcl-2 protects against beta-lapachone-mediated caspase 3 activation and apoptosis in human myeloid leukemia (HL-60) cells. *Oncol. Rep.* **6**, 485-492.
21. da Silva, C. P., de Oliveira, C. R., da Conceicao, M., and de Lima, P. (1996). Apoptosis as a mechanism of cell death induced by different chemotherapeutic drugs in human leukemic T-lymphocytes. *Biochem. Pharmacol.* **51**, 1331-1340.
22. Decaudin, D., Geley, S., Hirsch, T., Castedo, M., Marchetti, P., Macho, A., Kofler, R., and Kroemer, G. (1997). Bcl-2 and Bcl-XL antagonize the mitochondrial dysfunction preceding nuclear apoptosis induced by chemotherapeutic agents. *Cancer Res.* **57**, 62-67.
23. Cotter, T. G., Glynn, J. M., Echeverri, F., and Green, D. R. (1992). The induction of apoptosis by chemotherapeutic agents occurs in all phases of the cell cycle. *Anticancer Res.* **12**, 773-779.
24. Casiano, C. A., Martin, S. J., Green, D. R., and Eng, M. T. (1996). Selective cleavage of nuclear autoantigens during Cd95 (Fas/Apo-1)-mediated T cell apoptosis. *J. Exp. Med.* **184**, 765-770.
25. Yuan, J. (1997). Transducing signals of life and death. *Curr. Opin. Cell Biol.* **9**, 247-251.
26. Talanian, R. V., Quinlan, C., Trautz, S., Hackett, M. C., Manovich, J. A., Banach, D., Ghayur, T., Brady, K. D., and Wong, W. W. (1997). Substrate specificities of caspase family proteases. *J. Biol. Chem.* **272**, 9677-9682.
27. Miller, D. K. (1997). The role of the caspase family of cysteine proteases in apoptosis. *Semin. Immunol.* **9**, 35-49.
28. Porter, A. G., Ng, P., and Janicke, R. U. (1997). Death substrates come alive. *Bioessays* **19**, 501-507.
29. Wolf, B. B., Goldstein, J. C., Stennicke, H. R., Beere, H., Amarante-Mendes, G. P., Salvesen, G. S., and Green, D. R. (1999). Calpain functions in a caspase-independent manner to promote apoptosis-like events during platelet activation. *Blood* **94**, 1683-1692.
30. Wood, D. E., and Newcomb, E. W. (1999). Caspase-dependent activation of calpain during drug-induced apoptosis. *J. Biol. Chem.* **274**, 8309-8315.
31. Squier, M. K., Sehnert, A. J., Sellins, K. S., Malkinson, A. M., Takano, E., and Cohen, J. J. (1999). Calpain and calpastatin regulate neutrophil apoptosis. *J. Cell. Physiol.* **178**, 311-319.
32. Squier, M. K., Miller, A. C., Malkinson, A. M., and Cohen, J. J. (1994). Calpain activation in apoptosis. *J. Cell. Physiol.* **159**, 229-237.
33. Lazebnik, Y. A., Kaufmann, S. H., Desnoyers, S., Poirier, G. G., and Earnshaw, W. C. (1994). Cleavage of poly(ADP-ribose) polymerase by a proteinase with properties like ICE. *Nature* **371**, 346-347.
34. Datta, R., Banach, D., Kojima, H., Talanian, R. V., Alnemri, E. S., Wong, W. W., and Kufe, D. W. (1996). Activation of the Cpp32 protease in apoptosis induced by 1-beta-D-arabino-furanosylcytosine and other DNA-damaging agents. *Blood* **88**, 1936-1943.
35. Pink, J. J., Wuerzberger-Davis, S., Tagliarino, C., Planchon, S. M., Yang, X., Froelich, C. J., and Boothman, D. A. (2000). Activation of a cysteine protease in MCF-7 and T47D breast cancer cells during beta-lapachone-mediated apoptosis. *Exp. Cell Res.* **255**, 144-155.
36. Stone, K. R., Mickey, D. D., Wunderli, H., Mickey, G. H., and Paulson, D. F. (1978). Isolation of a human prostate carcinoma cell line (DU 145). *Int. J. Cancer* **21**, 274-281.
37. Mickey, D. D., Stone, K. R., Wunderli, H., Mickey, G. H., and Paulson, D. F. (1980). Characterization of a human prostate adenocarcinoma cell line (DU 145) as a monolayer culture and as a solid tumor in athymic mice. *Prog. Clin. Biol. Res.* **37**, 67-84.
38. Horoszewicz, J. S., Leong, S. S., Kawinski, E., Karr, J. P., Rosenthal, H., Chu, T. M., Mirand, E. A., and Murphy, G. P. (1983). LNCaP model of human prostatic carcinoma. *Cancer Res.* **43**, 1809-1818.
39. Gustafson, D. L., Beall, H. D., Bolton, E. M., Ross, D., and Waldren, C. A. (1996). Expression of human NAD(P)H:quinone oxidoreductase (DT-diaphorase) in Chinese hamster ovary cells: Effect on the toxicity of antitumor quinones. *Mol. Pharmacol.* **50**, 728-735.
40. Sambrook, J., Fritsch, E. F., and Maniatis, T. (1989). "Molecular Cloning—A Laboratory Manual," Cold Spring Harbor Laboratory Press, Cold Spring Harbor, NY.
41. Rago, R., Mitchen, J., and Wilding, G. (1990). DNA fluorometric assay in 96-well tissue culture plates using Hoechst 33258 after cell lysis by freezing in distilled water. *Anal. Biochem.* **191**, 31-34.
42. Siegel, D., Franklin, W. A., and Ross, D. (1998). Immunohistochemical detection of NAD(P)H:quinone oxidoreductase in human lung and lung tumors. *Clin. Cancer Res.* **4**, 2065-2070.
43. Fitzsimmons, S. A., Workman, P., Grever, M., Paull, K., Camalleri, R., and Lewis, A. D. (1996). Reductase enzyme expression across the National Cancer Institute tumor cell line panel: Correlation with sensitivity to mitomycin C and EO9 [see comments]. *J. Natl. Cancer Inst.* **88**, 259-269.
44. Thor, H., Smith, M. T., Hartzell, P., Bellomo, G., Jewell, S. A., and Orrenius, S. (1982). The metabolism of menadione (2-methyl-1,4-naphthoquinone) by isolated hepatocytes: A study of the implications of oxidative stress in intact cells. *J. Biol. Chem.* **257**, 12419-12425.
45. Hollander, P. M., Bartfai, T., and Gatt, S. (1975). Studies on the reaction mechanism of DT diaphorase: Intermediary plateau and trough regions in the initial velocity vs substrate concentration curves. *Arch. Biochem. Biophys.* **169**, 568-576.
46. Strobel, H. W., and Dignam, J. D. (1978). Purification and properties of NADPH-cytochrome P-450 reductase. *Methods Enzymol.* **52**, 89-96.
47. Preusch, P. C., Siegel, D., Gibson, N. W., and Ross, D. (1991). A note on the inhibition of DT-diaphorase by dicoumarol. *Free Radical Biol. Med.* **11**, 77-80.
48. Lotem, J., and Sachs, L. (1996). Differential suppression by protease inhibitors and cytokines of apoptosis induced by wild-type p53 and cytotoxic agents [published erratum appears in (1997) *Proc. Natl. Acad. Sci. USA* **94**, 1603]. *Proc. Natl. Acad. Sci. USA* **93**, 12507-12512.
49. Rao, L., Perez, D., and White, E. (1996). Lamin proteolysis facilitates nuclear events during apoptosis. *J. Cell Biol.* **135**, 1441-1455.
50. Zhivotovsky, B., Gahm, A., and Orrenius, S. (1997). Two different proteases are involved in the proteolysis of lamin during apoptosis. *Biochem. Biophys. Res. Commun.* **233**, 96-101.
51. Margolin, N., Raybuck, S. A., Wilson, K. P., Chen, W., Fox, T., Gu, Y., and Livingston, D. J. (1997). Substrate and inhibitor specificity of interleukin-1 beta-converting enzyme and related caspases. *J. Biol. Chem.* **272**, 7223-7228.

52. Kaiser, N., and Edelman, I. S. (1977). Calcium dependence of glucocorticoid-induced lymphocytolysis. *Proc. Natl. Acad. Sci. USA* **74**, 638–642.
53. Lam, M., Dubyak, G., and Distelhorst, C. W. (1993). Effect of glucocorticosteroid treatment on intracellular calcium homeostasis in mouse lymphoma cells. *Mol. Endocrinol.* **7**, 686–693.
54. Squier, M. K., and Cohen, J. J. (1997). Calpain, an upstream regulator of thymocyte apoptosis. *J. Immunol.* **158**, 3690–3697.
55. Nath, R., Raser, K. J., Stafford, D., Hajimohammadreza, I., Posner, A., Allen, H., Talanian, R. V., Yuen, P., Gilbertsen, R. B., and Wang, K. K. (1996). Non-erythroid alpha-spectrin breakdown by calpain and interleukin 1 beta-converting-enzyme-like protease(s) in apoptotic cells: Contributory roles of both protease families in neuronal apoptosis. *Biochem. J.* **319**, 683–690.
56. Vanags, D. M., Porn-Ares, M. I., Coppola, S., Burgess, D. H., and Orrenius, S. (1996). Protease involvement in fodrin cleavage and phosphatidylserine exposure in apoptosis. *J. Biol. Chem.* **271**, 31075–31085.
57. Li, Y. Z., Li, C. J., Pinto, A. V., and Pardee, A. B. (1999). Release of mitochondrial cytochrome C in both apoptosis and necrosis induced by beta-lapachone in human carcinoma cells. *Mol. Med.* **5**, 232–239.
58. Nishizaki, K., Yoshino, T., Orita, Y., Nomiya, S., and Masuda, Y. (1999). TUNEL staining of inner ear structures may reflect autolysis, not apoptosis. *Hear. Res.* **130**, 131–136.
59. Boothman, D. A., and Pardee, A. B. (1989). Inhibition of radiation-induced neoplastic transformation by beta-lapachone. *Proc. Natl. Acad. Sci. USA* **86**, 4963–4967.
60. Boothman, D. A., Greer, S., and Pardee, A. B. (1987). Potentiation of halogenated pyrimidine radiosensitizers in human carcinoma cells by beta-lapachone (3,4-dihydro-2,2-dimethyl-4H-naphtho[1,2-b]pyran-5,6-dione), a novel DNA repair inhibitor. *Cancer Res.* **47**, 5361–5366.
61. Boothman, D. A., and Pardee, A. B. (1989). Inhibition of radiation-induced neoplastic transformation by beta-lapachone. *Proc. Natl. Acad. Sci. USA* **86**, 4963–4967.
62. Segura-Aguilar, J., Cortes-Vizcaino, V., Llombart-Bosch, A., Ernster, L., Monsalve, E., and Romero, F. J. (1990). The levels of quinone reductases, superoxide dismutase and glutathione-related enzymatic activities in diethylstilbestrol-induced carcinogenesis in the kidney of male Syrian golden hamsters. *Carcinogenesis* **11**, 1727–1732.
63. Leonard, T. B., Dent, J. G., Graichen, M. E., Lyght, O., and Popp, J. A. (1982). Comparison of hepatic carcinogen initiation-promotion systems. *Carcinogenesis* **3**, 851–856.

Received January 3, 2001

Revised version received March 16, 2001



## Activation of a Cysteine Protease in MCF-7 and T47D Breast Cancer Cells during $\beta$ -Lapachone-Mediated Apoptosis

John J. Pink,\* Shelly Wuerzberger-Davis,\*<sup>1</sup> Colleen Tagliarino,\* Sarah M. Planchon,\* XiaoHe Yang,† Christopher J. Froelich,† and David A. Boothman\*<sup>2</sup>

\*Laboratory of Molecular Stress Responses, Department of Radiation Oncology, Case Western Reserve University, Cleveland, Ohio 44106; and †Evanston Northwestern Healthcare Research Institute, Evanston, Illinois 60201

$\beta$ -Lapachone ( $\beta$ -lap) effectively killed MCF-7 and T47D cell lines via apoptosis in a cell-cycle-independent manner. However, the mechanism by which this compound activated downstream proteolytic execution processes were studied. At low concentrations,  $\beta$ -lap activated the caspase-mediated pathway, similar to the topoisomerase I poison, topotecan; apoptotic reactions caused by both agents at these doses were inhibited by zVAD-fmk. However at higher doses of  $\beta$ -lap, a novel non-caspase-mediated "atypical" cleavage of PARP (i.e., an ~60-kDa cleavage fragment) was observed. Atypical PARP cleavage directly correlated with apoptosis in MCF-7 cells and was inhibited by the global cysteine protease inhibitors iodoacetamide and *N*-ethylmaleimide. This cleavage was insensitive to inhibitors of caspases, granzyme B, cathepsins B and L, trypsin, and chymotrypsin-like proteases. The protease responsible appears to be calcium-dependent and the concomitant cleavage of PARP and p53 was consistent with a  $\beta$ -lap-mediated activation of calpain.  $\beta$ -Lap exposure also stimulated the cleavage of lamin B, a putative caspase 6 substrate. Reexpression of procaspase-3 into caspase-3-null MCF-7 cells did not affect this atypical PARP proteolytic pathway. These findings demonstrate that  $\beta$ -lap kills cells through the cell-cycle-independent activation of a noncaspase proteolytic pathway. © 2000 Academic Press

**Key Words:** apoptosis;  $\beta$ -lapachone; caspase; breast cancer; poly(ADP)-ribose polymerase; PARP; calpain; topotecan.

### INTRODUCTION

The execution phase of apoptosis culminates in the activation of a cascade of specific cysteine proteases

<sup>1</sup> Current address: Department of Human Oncology, University of Wisconsin Comprehensive Cancer Center, Madison, WI 53792.

<sup>2</sup> To whom reprint requests should be directed at the Department of Radiation Oncology, Laboratory of Molecular Stress Responses, BRB-3 East, Case Western Reserve University School of Medicine, 10900 Euclid Avenue, Cleveland, OH 44106-4942. Fax: (216) 368-1142. E-mail: [dab30@po.cwru.edu](mailto:dab30@po.cwru.edu).

which cleave following aspartate residues in target proteins. These proteases, named caspases [1], comprise a family of zymogens that are converted to activated proteases by specific cleavage reactions. Substrate cleavage products include the 89-kDa fragment of poly(ADP-ribose) polymerase (PARP), the 46-kDa polypeptide of lamin B, the ~100-kDa C-terminally or ~68-kDa internally cleaved polypeptides of retinoblastoma protein (pRb), and the ~68-kDa fragment derived from Sp1 [2–5]. The cleavage sites within some apoptotic death substrates have been precisely mapped and used to design inhibitors of the caspases, such as zVAD-fmk and DEVD-fmk, which were developed using the recognition sites for caspases-1 and -3, respectively [6]. In contrast, the global cysteine protease inhibitors iodoacetamide and *N*-ethylmaleimide react directly with active site cysteines and thereby inhibit all cysteine proteases, as well as other enzymes that contain accessible -SH groups [7, 8].

While a great deal of information regarding the action of caspases during apoptosis has been generated, less is known about alternate apoptotic proteolytic pathways that are activated after treatment with various cytotoxic agents. A number of reports have shown that the neutral calcium-dependent protease calpain can be activated during apoptosis [9–11]; a key *in vivo* target of calpain appears to be p53. Other reports have demonstrated the activation of noncaspase proteases, such as the nuclear scaffold protease [12, 13] and unknown serine proteases during apoptosis [14, 15]. The serine protease(s) described in these studies appeared to be distinct from granzyme B, which induces apoptosis through caspase activation [16].

$\beta$ -Lapachone ( $\beta$ -lap) is a naturally occurring 1,2-naphthoquinone initially isolated from the bark of the lapacho tree, native to South America. We previously demonstrated that this drug is a radiosensitizing agent against human laryngeal carcinoma and melanoma cell lines [17]. Using cell-free assays,  $\beta$ -lap inhibited topoisomerase I (Topo I) by a mechanism quite different from that of camptothecin (CPT) or the related compounds topotecan (TPT), 9-aminocamptothecin, or



irinotecan [18]. For example,  $\beta$ -lap administration did not stabilize Topo I-DNA cleavable complexes *in vivo* [19] or *in vitro* [20]. In contrast, the CPT family members stabilized cleavable complexes [19], resulting in the formation of DNA single-strand nicks [21] and induction of wild-type p53 [22]. The fact that  $\beta$ -lap did not produce DNA single-strand nicks in human or hamster cancer cells [21, 23] was indirectly confirmed by the absence of wild-type p53 induction in breast or prostate cancer cells [18, 24]. While *in vitro* assays indirectly suggested that Topo I may be an intracellular target of  $\beta$ -lap, it seemed likely that it was not the only mechanism through which this compound acted [24, 25]. We recently reported that the cytotoxicity caused by  $\beta$ -lap in MCF-7 breast cancer cells could be solely accounted for by apoptotic responses [24].

Recent results have suggested that  $\beta$ -lap can lead to Topo II $\alpha$ -mediated DNA breaks [25]. In contrast to Topo I, topoisomerase II $\alpha$  causes ATP-dependent, double-strand DNA unwinding [26]. Topo II $\alpha$  also shares another important distinction from Topo I, in its cell cycle regulation. Topo I is consistently expressed throughout the cell cycle while Topo II $\alpha$  is poorly expressed during G<sub>0</sub>/G<sub>1</sub> and expression increases during S phase, reaching a peak during late S and G<sub>2</sub> [27]. Drugs which primarily target Topo II $\alpha$  are, therefore, cell cycle specific [28], while Topo I-specific drugs can kill cells in all phases of the cell cycle [29]. Variation in sensitivity to either  $\beta$ -lap or TPT during different cell-cycle stages was measured to address the relative importance of Topo I and Topo II $\alpha$  activity for the cytotoxicity of these drugs.

Interestingly,  $\beta$ -lap-mediated apoptosis in MCF-7 cells was accompanied by a dramatic decrease in p53 steady-state levels, prior to the appearance of apoptotic morphologic changes [24]. We were, therefore, interested to see if this relationship between loss of survival and apoptosis held true for other breast cancer cells. We describe the activation of a noncaspase, cysteine protease, which shares some characteristics with the neutral calcium-dependent protease, calpain, during  $\beta$ -lap-mediated apoptosis.  $\beta$ -Lap-mediated cell death and proteolysis are induced in all phases of the cell cycle, suggesting that topoisomerase II $\alpha$  was not the critical target for this death pathway.

## MATERIALS AND METHODS

**Chemicals and tissue culture reagents.** Estradiol (E<sub>2</sub>), 4-hydroxytamoxifen (4-OHT) (Sigma Chemical Co., St. Louis, MO), or ICI 182,780 (a generous gift from Dr. V. Craig Jordan, Northwestern University) were dissolved in 100% ethanol as 1000 $\times$  stocks and maintained at -20°C.  $\beta$ -Lap (MW 242,  $\epsilon$  = 25790), generously supplied by Dr. William G. Bornmann (Memorial Sloan Kettering, New York, NY), and TPT (Smith Kline Beecham, Philadelphia, PA) were dissolved in DMSO and concentrations confirmed by spectrophotometric analyses [24, 30]. Nocodazole was purchased from Sigma Chemical Co., and a 2 mg/ml stock solution was made in DMSO immediately before use. All tissue culture reagents were purchased

TABLE 1  
Characteristics of Breast Cancer Cell Lines

Cell line	ER	p53	pRb
MCF-7:WS8	++++	WT	+
T47D:A18	++	Mutant	+

from GIBCO Laboratories (Grand Island, NY), unless otherwise stated. Charcoal-stripped serum was prepared by treating fetal bovine serum (FBS) three times with dextran-coated charcoal as described [31].

**Antibodies and protease inhibitors.** The C-2-10 PARP monoclonal antibody was purchased from Enzyme Systems Products (Dublin, CA). An N-terminal PARP (clone N-20), an Sp1 polyclonal, a p53 monoclonal (clone DO-1), and all horseradish peroxidase-conjugated secondary antibodies were obtained from Santa Cruz Biotechnologies (Santa Cruz, CA). Monoclonal antibodies to pRb (clone G3-245) and underphosphorylated pRb (clone G99-549) were obtained from PharMingen (San Diego, CA). A polyclonal antibody specific to phosphorylated serine 780 of the pRb protein was obtained from Medical and Biological Laboratories Co. Ltd. (Boston, MA). Antibody to caspase-3 was obtained from Transduction Laboratories (Lexington, KY). Antibody to lamin B was obtained from Matritech, Inc. (Cambridge, MA). zVAD-fmk, DEVD-fmk, zFA-fmk, and zAAD-fmk were obtained from Enzyme Systems Products (Dublin, CA), diluted in DMSO, and used at 25  $\mu$ M unless otherwise stated. TPCK, TLCK, iodoacetamide, and N-ethylmaleimide were purchased from Sigma Chemical Co. and diluted in DMSO (TPCK and TLCK), ethanol (N-ethylmaleimide), or water (iodoacetamide). The pBabe/puro vector was a generous gift from Dr. Todd Sladek.

**Tissue culture and growth conditions.** MCF-7:WS8, T47D:A18 (clones of the standard MCF-7 and T47D cell lines, selected by limiting dilution cloning of the parental cell lines in whole serum [31-33], referred to as MCF-7 and T47D in the text) were obtained from Dr. V. Craig Jordan (Northwestern University, Chicago, IL). The ER, p53, and pRb statuses of these cell lines are outlined in Table 1. Cells were grown in RPMI 1640 medium supplemented with 10% FBS, 6 ng/ml bovine insulin, 2 mM L-glutamine, 100 U/ml penicillin, and 100 mg/ml streptomycin. For estrogen-free tissue culture medium, phenol red-free RPMI and charcoal-stripped FBS were used as previously described [31]. Cells were routinely passed at 1:5 to 1:20 dilutions once per week using 0.1% trypsin. All cells were mycoplasma free and grown at 37°C in a humidified incubator with 5% CO<sub>2</sub>-95% air atmosphere.

**Growth assays and estrogen-deprivation studies.** Forty-eight-hour or 6-day growth assays were used to assess the relative sensitivities of breast cancer cells to various drug treatments as previously described [31-33]. For estrogen-deprivation studies, cells were grown in estrogen-free medium for at least 4 days prior to the start of experiments. Cells were seeded into 96-well plates (1.5  $\times$  10<sup>3</sup> or 1  $\times$  10<sup>4</sup> cells/well) in 0.2 ml of medium on day 0 and allowed to attach for 24 h. On day 1, fresh medium containing the indicated drug(s) was added to the appropriate wells. E<sub>2</sub>, 4-OHT, or ICI 182,780 (ICI) were added to cells at 1:1000 dilutions from appropriate stock solutions. Estrogen-deprivation significantly retarded cell growth and dramatically increased the proportion of MCF-7 and T47D cells in G<sub>1</sub>. For MCF-7, 83% G<sub>1</sub> cells were observed after 6 days of growth in estrogen-free medium compared to 53% in log-phase cultures. Changes in cell number, measured as DNA content, were then determined in untreated or drug-treated cells by an adaptation of the method of Labarca and Paigen [34] and analyzed using a Molecular Dynamics Biolumin 960 plate reader with an excitation wavelength of 360 and emission wavelength of 450 nm. Data were expressed as relative growth (*T/C*) by dividing the DNA content of treated cells

(7) by that of untreated cells (C) at identical times. Data points represent the means  $\pm$  SEM of at least four replicate wells. All experiments were performed at least three times.

**Western immunoblot analyses.** Whole-cell extracts were prepared by direct lysis of PBS-washed cells (both floating and attached cells were pooled) in PARP extraction buffer [6 M urea, 2% SDS, 10% glycerol, 62.5 mM Tris-HCl (pH 6.8), 5%  $\beta$ -mercaptoethanol, and 5 mg/ml bromophenol blue]. Samples were then sonicated with a 15-s burst using a Fisher 550 sonic dismembrator. Equal amounts of protein were heated at 65°C for 10 min and separated by 10% SDS-PAGE. Separated proteins were transferred to Immobilon-P (Millipore Corp., Bedford, MA) membranes using a Multiphor II semidry electroblotting device (Pharmacia Biotech Inc., Piscataway, NJ) according to the manufacturer's instructions. Loading equivalence and transfer efficiency were monitored by Ponceau S staining of transferred membranes. Standard Western immunoblotting techniques were used to probe for various steady-state protein levels as indicated and previously described [18, 24]. Proteins of interest were visualized with ECL using the Super Signal chemiluminescence reagent (Pierce Chemical Co., Rockford, IL) at 20°C for 5 min. Membranes were exposed to X-ray film and developed. Gels shown represent results of experiments repeated at least three times.

**Flow cytometry.** Flow cytometric analyses of breast cancer cell lines before and after  $\beta$ -lap or TPT treatments were performed as previously described [18, 24]. TUNEL assays were performed using the APO-DIRECT kit (Phoenix Flow Systems, Inc., San Diego, CA). The samples were read in a EPICS Elite ESP flow cytometer using an air-cooled argon laser at 488 nm, 15 mW (Beckman Coulter Electronics, Miami, FL). Propidium iodide was read at 640 nm using a long-pass optical filter and FITC was read at 525 nm using a band-pass filter. Analyses were performed using the Elite acquisition software provided with the instrument.

**Retroviral-mediated stable expression of caspase 3 in MCF-7 cells.** The pBabe/puro/cpp32 plasmid was constructed by treating the *Bam*HI/*Pst*II cpp32 cDNA insert from the pBS/cpp32 plasmid (a generous gift from Dr. Vishva Dixit, Genentech, Inc.) with T4 DNA polymerase and then subcloning into the blunt-ended pBabe/puro vector.

MCF-7 cells ( $3 \times 10^5$  cells/plate) were seeded and allowed to grow overnight. The pBabe/puro retroviral vector (a generous gift from Dr. T. Sladek, Chicago Medical School) (2  $\mu$ g/plate) encoding cpp32 (caspase-3) cDNA or empty vector was mixed with 10  $\mu$ l of LipofectAMINE (Life Technologies, Gaithersburg, MD) and transfected into cells according to the manufacturer's instructions. After transfection (24 h), cells were split, diluted, and inoculated into 96-well plates. Transfected cells were selected with 2  $\mu$ g/ml puromycin. Individual clones were screened by immunoblot analysis of caspase-3 expression and positive clones (5 of 12) were pooled for further characterization. A single caspase-3-expressing clone was selected for investigation.

## RESULTS

**Relative drug sensitivities.** Log-phase MCF-7 and T47D breast cancer cells were exposed to a range of  $\beta$ -lap or TPT doses for 48 h and cell numbers were compared (using DNA content measurements) to untreated, log-phase growing control cells as described under Materials and Methods (Fig. 1). At higher doses, MCF-7 cells were more sensitive to  $\beta$ -lap ( $IC_{75} = 3.5 \mu$ M) than were T47D cells ( $IC_{75} = 7.0 \mu$ M); however, the  $IC_{50}$  dose was very similar in both cell lines. In contrast, T47D cells were more sensitive to TPT at all doses tested, with  $IC_{50}$  and  $IC_{75}$  values of 20 and 500

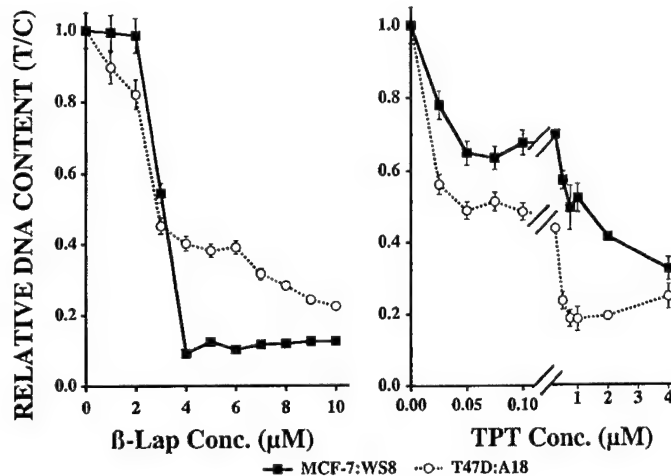


**FIG. 1.** Sensitivities of breast cancer cells to  $\beta$ -lap or TPT. Cells were seeded into 96-well tissue culture plates ( $1.5 \times 10^3$  cells/well) and allowed to attach overnight. Drugs were then added and cells were allowed to grow for an additional 48 h, as described under Materials and Methods. Cell number was assessed using Hoechst 33258 fluorescence, and relative growth inhibition (Relative DNA Content T/C) was calculated. Shown are toxicities for MCF-7 (■) and T47D (○) cell lines exposed to various concentrations of  $\beta$ -lap or TPT. Data shown are representative of at least two experiments expressed as means  $\pm$  SEM of at least four replicate wells.

nM, respectively, compared with MCF-7 cells  $IC_{50}$  and  $IC_{75}$  values of 350 nM and 4.0  $\mu$ M, respectively. Differences in relative sensitivities to TPT compared to  $\beta$ -lap suggested a disparate mechanism(s) of growth inhibition or cell death (possibly due to apoptosis).

**Cell cycle-independent cytotoxicity.** Since Topo I poisons are thought to kill cycling, but not arrested, cells (presumably due to DNA synthesis past Topo I-DNA "cleavable complexes"), we assessed the influence of cell cycle progression on  $\beta$ -lap compared to TPT cytotoxicity using DNA content assays. In addition, these studies would address the relative role of topoisomerase II $\alpha$  inhibition in  $\beta$ -lap-mediated cytotoxicity, due to the cell-cycle-dependent expression of this protein. These studies utilized the estrogen-dependent MCF-7 and T47D breast cancer cell lines, since their growth in estrogen-deprived, phenol red-free culture medium has been well defined [33]. Cells were deprived of estrogen for 6 days, which caused a significant G<sub>1</sub> delay at a predetermined point in the cell cycle [33, 35, 36], prior to addition of either  $\beta$ -lap or TPT. Cells were then exposed to various concentrations of  $\beta$ -lap or TPT in estrogen-deprived (control) medium, control medium containing E<sub>2</sub> (10 nM), or medium containing whole serum alone or in the presence of inhibitory concentrations of the anti-estrogens 4-OHT or ICI for 48 h (Fig. 2). Both cell lines were stimulated to enter the cell cycle and begin log-phase growth after addition of medium containing 17 $\beta$ -estradiol or whole serum. Addition of anti-estrogens specifically inhibited

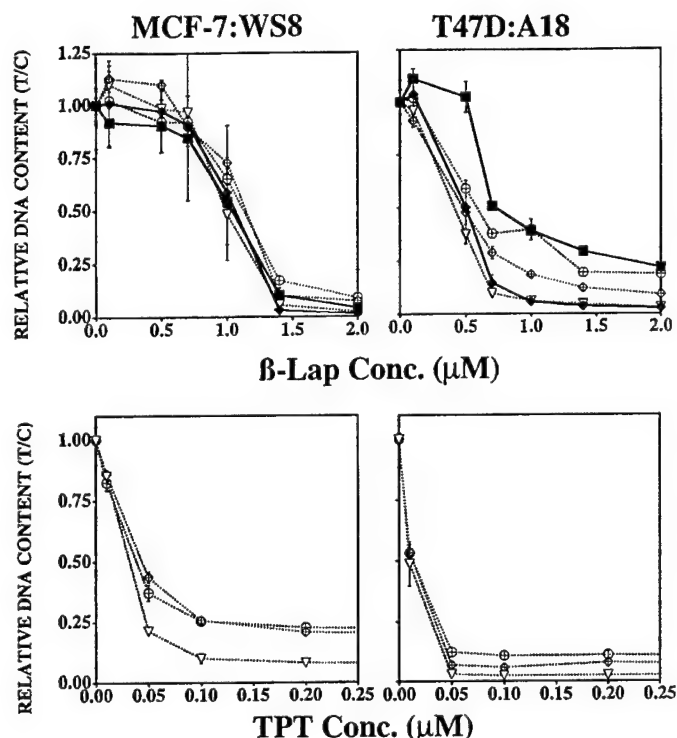


**FIG. 2.**  $\beta$ -Lap- or TPT-mediated cytotoxicity of  $G_1$ -arrested cells. MCF-7 and T47D estrogen-dependent cell lines were grown for 6 days in estrogen-depleted, phenol red-free medium and exposed to varying concentrations of  $\beta$ -lap or TPT for 6 days, as indicated. Drugs were included in RPMI 1640 medium containing estrogen-depleted calf serum (control, ■), estrogen-replenished, stripped calf serum (10 nM  $E_2$ , ◆), whole serum alone (▽), or whole serum treated with the anti-estrogens 4-hydroxytamoxifen (100 nM, ◇) or ICI 182,780 (100 nM, ○). Cell number was then assessed after 6 days using DNA content as in Fig. 1. Relative cell growth of treatment was determined using the DNA content of cells grown in comparable medium without  $\beta$ -lap or TPT. Data shown are representative of at least two experiments expressed as means  $\pm$  SEM of at least four replicate wells.

estrogen-mediated cell growth. Estrogen deprivation and/or anti-estrogen administration led to a cytostatic growth inhibition of 75–85% compared with cells grown in medium containing  $E_2$  or whole serum (data not shown and [32, 37]). Additional  $\beta$ -lap or TPT treatments led to a complete loss of cells, demonstrating a similar cytotoxic response in both log-phase (+ $E_2$ ) and arrested (– $E_2$  or plus antiestrogens) cells (Fig. 2).

**Apoptotic protease activation after  $\beta$ -lap or TPT treatment.** To investigate caspase activation in MCF-7 and T47D breast cancer cells following TPT or  $\beta$ -lap exposures, we examined PARP cleavage using Western immunoblot analyses as described under Materials and Methods. Cells were treated continuously with 5 to 10  $\mu$ M  $\beta$ -lap and PARP cleavage was assessed 48 h later. Treatment with 5  $\mu$ M  $\beta$ -lap induced classic PARP cleavage, resulting in the appearance of an 89-kDa fragment in both cell lines (Fig. 3). In MCF-7 cells,

a cross-reacting protein of ~80 kDa (indicated by an asterisk in Figs. 3, 4, and 5) was present even in untreated cells. The identity of this protein is unknown; however, it does appear to be degraded during apoptosis.

At higher doses of  $\beta$ -lap we observed an atypical ~60-kDa PARP fragment. This atypical cleavage of PARP was most apparent in MCF-7 cells (Fig. 3, lanes 4–6), which were more sensitive to  $\beta$ -lap (Figs. 1 and 2). In general, PARP cleavage reflected the relative sensitivity of each cell line to  $\beta$ -lap, by which MCF-7 cells demonstrated primarily the atypical cleavage pattern and T47D predominantly showed typical caspase-mediated PARP cleavage at lower doses and atypical PARP cleavage following treatment with 10  $\mu$ M  $\beta$ -lap (see lane 12, Fig. 3). A minor PARP cleavage fragment of ~40 kDa was also observed in MCF-7 cells, which display maximal amounts of the 60-kDa PARP fragment (Fig. 3). It is currently unclear whether this is a unique fragment or the result of further cleavage of the original 60-kDa fragment. Interestingly, the apparent amount of the 60-kDa fragment was much greater than that of full-length PARP protein. Loading equivalence, as assessed by Ponceau S staining, showed that all lanes contained equal amounts of protein. This apparent incongruity may be the result of either more efficient extraction of the fragment from the nuclear matrix or increased accessibility of the epitope to the antibody, after  $\beta$ -lap-induced cleavage (Fig. 3).

MCF-7 and T47D cells were treated with a range of TPT doses (10 nM to 10  $\mu$ M) for 48 h. We coadministered 25  $\mu$ M zVAD-fmk, a caspase inhibitor, to deter-

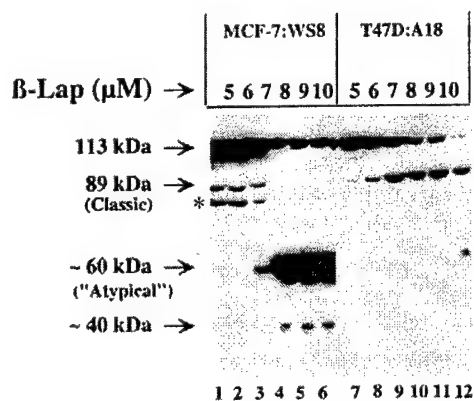


**FIG. 3.** Atypical and classic PARP cleavage in breast cancer cells following  $\beta$ -lap exposure. Breast cancer cell lines were treated with  $\beta$ -lap (5–10  $\mu$ M) for 48 h and whole-cell lysates prepared at various times posttreatment from pooled (attached and floating) cells and assessed for cleavage of PARP using standard Western immunoblot procedures and the C-2-10 monoclonal PARP antibody, described under Materials and Methods. An unknown ~80-kDa cross-reacting protein was present in MCF-7 lysates as indicated by an asterisk. The Western blot shown is representative of at least three separate experiments.

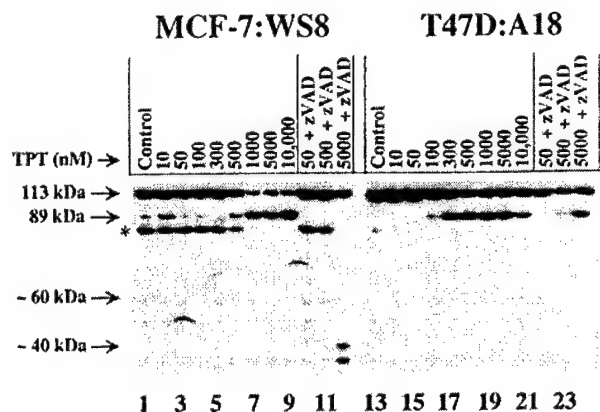


**FIG. 4.** Caspase-mediated, classical PARP cleavage in breast cancer cells following TPT treatment. Log-phase MCF-7 and T47D cells were treated with 10 nM to 10 μM TPT for 48 h. Three doses of TPT (50, 500, and 5000 nM, lanes 10–12 and 22–24, top and bottom) also included the caspase inhibitor zVAD-fmk (25 μM). An unknown ~80-kDa cross-reacting protein is present in MCF-7 lysates as indicated by an asterisk. Cells were then harvested and analyzed by Western immunoblotting using the C-2-10 monoclonal PARP antibody as described for Fig. 3.

mine if PARP cleavage was caused by caspase activation after three doses of TPT (50, 500, and 5000 nM) (Fig. 4). As observed following  $\beta$ -lap exposures, the relative sensitivity of MCF-7 and T47D cells to the growth inhibitory effects of TPT was reflected to some degree in PARP cleavage (Fig. 4). However, the doses of TPT required to elicit PARP cleavage *in vivo* were significantly above the apparent  $IC_{50}$  values for each cell line (see Fig. 1); this was not the case for cells exposed to  $\beta$ -lap. These data are consistent with previous data demonstrating that  $\beta$ -lap is a much more effective inducer of apoptosis than CPT or its derivatives [20]. Coadministration of zVAD-fmk inhibited TPT-mediated PARP cleavage in both MCF-7 (lanes 10–12) and T47D cells (lanes 22 and 23 with 50 and 500 nM, but not 5000 nM, TPT). These data suggested that TPT exposure led to the activation of the classic caspase pathway. Importantly, no dose of TPT gave rise to the atypical PARP cleavage fragment, even when 10 μM TPT was used (lanes 9 and 21, Fig. 4).

**Evidence for two apoptotic proteolytic pathways activated by  $\beta$ -lap.** In order to determine whether atypical PARP cleavage observed after  $\beta$ -lap treatment was the result of an activated caspase family member, or another class of cysteine proteases, cells were exposed for 48 h to 8 μM  $\beta$ -lap in the presence of a battery of known protease inhibitors (Fig. 5). Included were general chemical inhibitors and more specific cleavage site inhibitors [38]. Exposure of MCF-7 cells to 8 μM  $\beta$ -lap caused apoptotic responses (measured by PARP, pRb, and Sp1 cleavage) that were insensitive to any of the inhibitors, simultaneously administered at previously determined efficacious doses [38]. The modest level of

89-kDa PARP cleavage fragment observed in untreated MCF-7 cells was due to slight overgrowth of control cells, which activated a basal level of apoptosis and classic PARP cleavage. This basal, caspase-mediated PARP cleavage was completely inhibited by zVAD-fmk in both cell lines (compare the minor 89-kDa PARP cleavage fragment in lane 1 to the absence of this fragment in lane 2 for MCF-7 in Fig. 5).

As shown in Fig. 3, T47D cells exposed to 8 μM  $\beta$ -lap for 48 h showed classic PARP cleavage. As expected, this apoptotic cleavage reaction was completely blocked by coadministration of zVAD-fmk at 25 μM.  $\beta$ -Lap-treated T47D cells also showed cleavage of Sp1, giving rise to the previously described 68-kDa fragment [2]. In addition, T47D cells treated with  $\beta$ -lap showed a loss of phosphorylated pRb and appearance of an ~100-kDa cleavage fragment, previously described by Janicke *et al.* [4] (compare lanes 13 and 19, Fig. 5). All cleavage reactions observed in T47D cells after  $\beta$ -lap treatment were completely prevented by 25 μM zVAD-fmk. However, accumulation of hypophosphory-

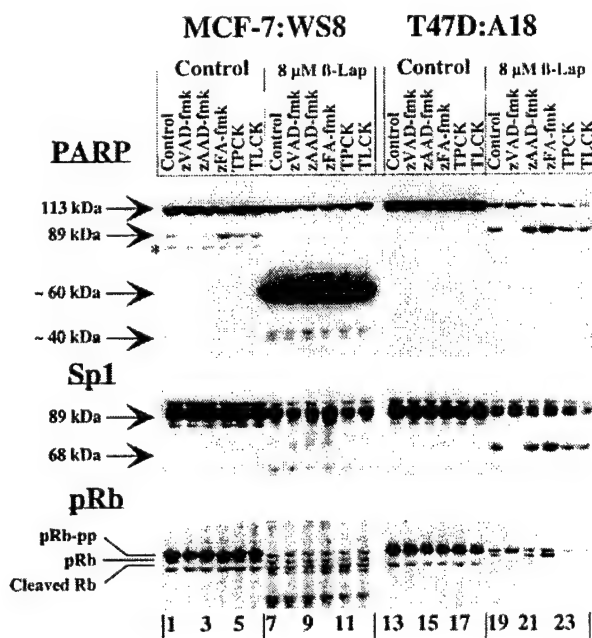


**FIG. 5.** Effect of global or specific cleavage site protease inhibitors on  $\beta$ -lap-mediated atypical PARP cleavage. Log-phase MCF-7 and T47D cells were grown for 48 h in RPMI medium alone or in medium containing 8 μM  $\beta$ -lap. Protease inhibitors were coadministered with  $\beta$ -lap. The protease inhibitors used were 25 μM zVAD-fmk (a caspase family inhibitor), 25 μM zAAD-fmk (an inhibitor of granzyme B), 25 μM zFA-fmk (an inhibitor of cathepsins B and L), 1.0 μM TPCK (a trypsin inhibitor), or 10 μM TLCK (a chymotrypsin inhibitor). Control cells received RPMI medium alone (lanes 1 and 13) or RPMI medium containing 8 μM  $\beta$ -lap (lanes 7 and 19). Whole-cell extracts were then analyzed by Western immunoblotting as described under Materials and Methods for PARP cleavage, pRb dephosphorylation and cleavage, and cleavage of the Sp1 transcription factor by repeated probing of the same blots. The Western blot shown is representative of at least three separate experiments.



lated pRb in T47D cells following  $\beta$ -lap treatment was unaffected by the administration of 25  $\mu$ M zVAD (lanes 19 to 20, Fig. 5). These data are consistent with the activation of a caspase-mediated apoptotic pathway in T47D cells after  $\beta$ -lap treatment, which may be downstream of changes in pRb phosphorylation state.

MCF-7 cells, which showed only atypical PARP cleavage after 8  $\mu$ M  $\beta$ -lap exposure, also demonstrated an overall decline in Sp1 steady-state levels. However, apoptotic cleavage fragments (as observed in T47D cells) were not observed after extended exposures of the Western blots in Fig. 5 (not shown). MCF-7 cells treated with  $\beta$ -lap showed an overall loss of pRb, with the presence of a modest amount of a 60-kDa pRb fragment (visible after extended exposure, data not shown), similar to that described by An and Dou [5]. pRb cleavage in MCF-7 cells caused by  $\beta$ -lap exposure was not affected by coadministered protease inhibitors (Fig. 5, lanes 8–12).

To confirm that  $\beta$ -lap cytotoxicity was primarily mediated by the induction of apoptosis and not necrosis, we utilized the TUNEL assay, which measures DNA breaks created by apoptotic endonucleases [39]. MCF-7 cells were exposed to a 4-h pulse of 8  $\mu$ M  $\beta$ -lap and analyzed for terminal deoxynucleotidyl transferase-mediated incorporation of FITC-labeled dUTP, 20 h later. Greater than 90% of the  $\beta$ -lap-treated MCF-7 cells were TUNEL positive (Fig. 6). This finding, in addition to the dramatic nuclear condensation reported previously [24], confirms that cytotoxicity caused by  $\beta$ -lap is primarily apoptotic and not due to necrosis.

The global cysteine protease inhibitors iodoacetamide and *N*-ethylmaleimide [7, 40, 41] were used to determine if a cysteine protease was responsible for the formation of atypical PARP cleavage fragments in MCF-7 cells (Figs. 3 and 5). MCF-7 cells were treated with 5  $\mu$ M  $\beta$ -lap in medium with or without 10 mM iodoacetamide or 10 mM *N*-ethylmaleimide (data not shown). Cleavage of PARP was prevented by both inhibitors, but was not inhibited by the caspase inhibitors zVAD-fmk or DEVD-fmk (Fig. 5 and data not shown), suggesting that a noncaspase, cysteine protease was primarily responsible for the atypical PARP cleavage observed after  $\beta$ -lap treatment. Administration of *N*-ethylmaleimide caused a mobility shift of the full-length PARP band, possibly due to methylation of cysteine and methionine groups in the protein [40]. Neither iodoacetamide nor *N*-ethylmaleimide prevented  $\beta$ -lap-mediated apoptosis in MCF-7 cells.

**Simultaneous cleavage of PARP and p53.** The inhibition of PARP cleavage by cysteine-alkylating agents suggested that a noncaspase cysteine protease may be responsible for the atypical PARP cleavage observed in cells after treatment with  $\beta$ -lap. One protease which may fit these data would be the neutral calcium-depen-

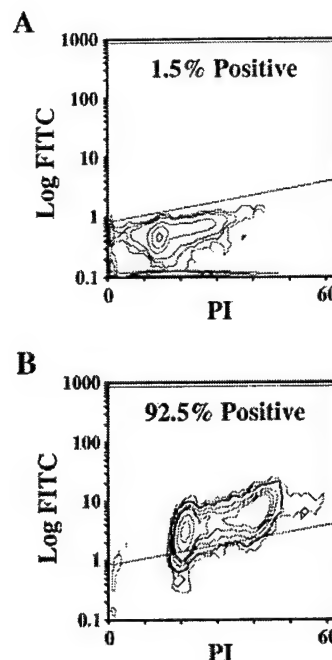


**FIG. 6.**  $\beta$ -Lapachone induced DNA fragmentation. MCF-7 cells were treated with 8  $\mu$ M  $\beta$ -lap for 4 h and harvested 20 h later. Cells were analyzed for DNA fragmentation using the TUNEL assay. Cells which have significant DNA fragmentation incorporate FITC-dUTP and are shown above the line in both graphs. Shown are representative examples of experiments repeated at least three times.

dent protease calpain [9]. Calpain has a wide substrate specificity and has been shown to specifically cleave p53 during apoptosis [42, 43]. We treated MCF-7 cells with a 4-h pulse of 5  $\mu$ M  $\beta$ -lap and isolated whole-cell extracts at various times, up to 28 h after drug exposure. Extracts were probed for PARP and subsequently stripped and reprobed for p53 steady-state expression (Fig. 7A). As expected, PARP cleavage was observed by 8 h after drug administration. Importantly, cleavage of p53, giving rise to an  $\sim$ 40-kDa fragment, accompanied this PARP cleavage. The p53 cleavage pattern resembled that observed by Pariat *et al.* [43] and Kubbutat *et al.* [42], which was the result of calpain activation.

Since calpain activity is dependent upon changes in  $\text{Ca}^{+2}$  homeostasis, we utilized the calcium chelators EDTA and EGTA to determine if removal of extracellular calcium influenced the appearance of atypical PARP cleavage in MCF-7 cells after  $\beta$ -lap treatment. MCF-7 cells were pretreated with 0.25, 1.0, or 3.0 mM EGTA or EDTA in complete medium for 30 min. After treatment, medium containing 5  $\mu$ M  $\beta$ -lap or DMSO (control medium), including the corresponding concentration of EDTA or EGTA used in the pretreatment, was added for an additional 4 h. All cells were then treated with medium alone containing EGTA or EDTA for an additional 20 h. Whole-cell extracts were then prepared and analyzed for PARP and p53 cleavage

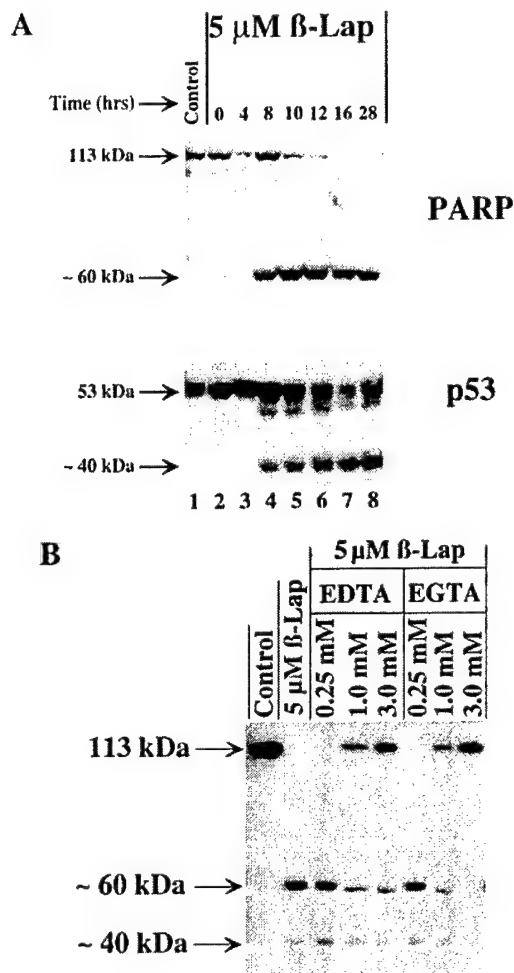


**FIG. 7.** Implication of calpain in atypical PARP cleavage. (A) MCF-7 cells were treated with 5  $\mu$ M  $\beta$ -lap for 4 h and whole-cell extracts were prepared 20 h later. Western blots were probed with anti-PARP antibody, then stripped and reprobed with anti-p53 antibody. (B) MCF-7 cells were pretreated for 30 min with the designated concentrations of EDTA or EGTA in complete medium. Medium containing 5  $\mu$ M  $\beta$ -lap was then added for 4 h in the continued presence of EDTA or EGTA. After  $\beta$ -lap exposure cells were treated with medium containing only the designated concentrations of EDTA or EGTA for an additional 20 h. Whole-cell extracts were prepared and probed for PARP as described above. The blots shown are representative of at least two independent experiments.

fragments. Both EDTA and EGTA showed a dose-dependent inhibition of  $\beta$ -lap-mediated atypical PARP cleavage and p53 cleavage in MCF-7 cells (Fig. 7B and data not shown). These data suggest that extracellular calcium is a necessary component for  $\beta$ -lap-mediated atypical PARP and p53 cleavage, an attribute consistent with activation of a calcium-dependent, non-caspase cysteine protease, such as calpain.

*Loss of hypophosphorylated pRb and apoptosis induced by  $\beta$ -lap is independent of cell cycle status.* To investigate the effects of cell cycle position on  $\beta$ -lap-induced accumulation of hypophosphorylated pRb and

apoptosis, estrogen-dependent MCF-7 cells were cultured in estrogen-free medium for 6 days as described under Materials and Methods. To ensure a complete estrogen block, the pure anti-estrogen ICI 182,780 (1 nM) [44, 45] was added to cells growing in estrogen-free medium 2 days prior to the beginning of each experiment. Increases in G<sub>1</sub> cells (up to 85%) were noted, as described [46]. Arrested cells were compared to MCF-7 cells that were subsequently restimulated to enter the cell cycle by addition of 10 nM E<sub>2</sub> at the time of  $\beta$ -lap or TPT exposure (i.e., a 4-h pulse of either 8  $\mu$ M  $\beta$ -lap or 5  $\mu$ M TPT). Drugs were administered as short pulse treatments in order to determine if the rapid accumulation of hypophosphorylated pRb could be reversed after removal of  $\beta$ -lap or TPT. When used, ICI or E<sub>2</sub> was maintained in the medium.

MCF-7 cells treated with  $\beta$ -lap showed a dramatic loss of phosphorylated pRb within 6 h (compare lanes 3 and 4, Fig. 8), followed by general loss of the protein by 18 h after treatment (see lanes 10 and 13, Fig. 8); these data are consistent with earlier findings [24]. A similar loss of phosphorylated pRb was noted in MCF-7 cells after 5  $\mu$ M TPT; however, significant accumulation of hypophosphorylated pRb was not observed until 12 h after treatment (not shown), and complete loss was not noted until more than 18 h posttreatment (Fig. 8 and data not shown). In control cells, stimulation of arrested cells with estradiol led to an increase in the relative level of hyperphosphorylated pRb (by 6 to 18 h) compared to estrogen-deprived and/or ICI-treated cells (compare hypophosphorylated retinoblastoma protein (pRb) to hyperphosphorylated retinoblastoma protein (pRb-pp) levels in lanes 6, 9, and 12 to lane 3, Fig. 8). The change in phosphorylation status of pRb was accompanied by a dramatic increase in the proportion of cells in S phase by 18 h after E<sub>2</sub> stimulation (43% S phase with E<sub>2</sub>, 10% S phase without E<sub>2</sub>, compare lanes 12 and 9, Fig. 8). In both the E<sub>2</sub>- and the ICI-treated groups,  $\beta$ -lap exposure led to a complete loss of hyperphosphorylated pRb followed by an overall loss of all forms of pRb. Since estrogen-deprivation can cause an arrest in the cell cycle  $\sim$ 6 h from the restriction point in MCF-7 cells [47–49], possibly past the first cyclin D1–cdk2-dependent phosphorylation of pRb, the levels of hyperphosphorylated pRb in estrogen-deprived, anti-estrogen-treated MCF-7 cells were rather high (Fig. 8). In MCF-7 cells treated with either  $\beta$ -lap or TPT, PARP cleavage (atypical for  $\beta$ -lap, classic for TPT) was not apparent until 12–18 h after treatment (Fig. 8 for 18 h, and data not shown). Addition of E<sub>2</sub>, or maintenance of MCF-7 cells in estrogen-deprived medium (including ICI), had no effect on the appearance of PARP cleavage (see lanes 10 and 13, Fig. 8).

We performed a similar series of experiments using nocodazole to arrest cells during M phase. All MCF-7 groups examined showed a similar pattern of PARP



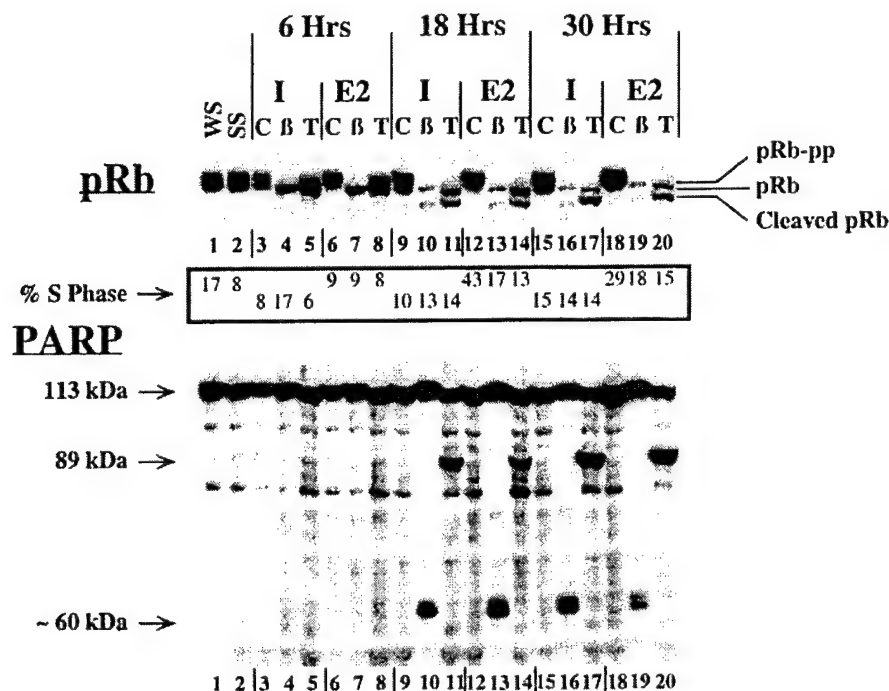


**FIG. 8.** Effect of  $\beta$ -lap or TPT on logarithmically growing or anti-estrogen-arrested MCF-7 cells. MCF-7 cells were estrogen-deprived for 6 days prior to seeding in estrogen-deprived medium containing 10 nM ICI 182,780 to ensure complete blockage of estrogen-stimulated growth. Cells were then treated with no drug (C), 5  $\mu$ M  $\beta$ -lap ( $\beta$ ), or 5  $\mu$ M TPT (T), in estrogen-free RPMI media supplemented with either 100 nM ICI (I) or 10 nM E<sub>2</sub> (E<sub>2</sub>). Whole-cell extracts were prepared at 6 and 18 h after treatment and changes in cell cycle distribution were monitored by flow cytometry, as described under Materials and Methods. For Western analyses, immunoblots were first probed with the C-2-10 anti-PARP monoclonal antibody, then stripped and reprobed with an anti-pRb monoclonal antibody which detected all forms of pRb. For controls, log-phase MCF-7 cells were grown continuously in medium containing whole serum (WS) or in medium containing estrogen-deprived serum (SS, for stripped serum) as described under Materials and Methods. Shown are three separate forms of the pRb protein: (a) pRb-pp, hyperphosphorylated pRb; (b) pRb, hypophosphorylated (nonphosphorylated) pRb; and (c) the cleaved form of pRb, in which 4 kDa of the C-terminus has been removed (Cleaved pRb). PARP protein forms included (a) the full-length PARP polypeptide of 113 kDa, (b) a caspase-mediated 89-kDa PARP fragment, and (c) an ~60-kDa atypical PARP cleavage polypeptide, which sometimes appears as a doublet at ~60 kDa. The Western blot shown is representative of at least three separate experiments.

cleavage after  $\beta$ -lap treatment (data not shown), supporting a cell-cycle-independent activation of apoptosis.

We [16], as well as others [50], showed that MCF-7 cells were devoid of caspase-3, due to a deletion in exon 3. To determine whether caspase-3 deficiency was responsible for atypical PARP cleavage, we isolated an MCF-7 clone that stably expressed full-length proform caspase-3 (Casp 3) (see Materials and Methods). A puromycin-resistant clone expressing empty vector (pBabe) was also analyzed. PARP, lamin B, and caspase-3 expression was monitored before or 24 h after  $\beta$ -lap treatment (2–10  $\mu$ M). Cells were treated for 4 h with 2–10  $\mu$ M  $\beta$ -lap and harvested 20 h later. As expected, Casp 3 cells expressed the 32-kDa proform of caspase-3, unlike MCF-7 cells transfected with the vector alone (Fig. 9, compare lanes 1 and 7). Atypical PARP cleavage was noted following  $\beta$ -lap treatment at similar levels in both transfected cell lines. Classic lamin B cleavage, presumably the result of caspase-6 activation [51, 52], was also observed. These data sug-

gest that expression of caspase-3 had no effect on apoptotic cleavage events in MCF-7 cells following various doses of  $\beta$ -lap. Interestingly, loss of procaspase-3 protein, in Casp 3 cells, mirrored cleavage of both PARP and lamin B. Importantly, the active p12 and p20 fragments of caspase-3 were not observed due to the lower affinity of this antibody to the processed forms of caspase-3. In contrast to  $\beta$ -lap treatments, Casp 3 cells showed an increased rate of apoptosis after exposure to TNF- $\alpha$  or granzyme B compared to MCF-7 cells transfected with pBabe/puro alone [16].

## DISCUSSION

We previously showed that  $\beta$ -lap killed a variety of cells by apoptosis. However, the mechanisms of specific proteolytic execution cascades that were activated by this compound remained unexplored.  $\beta$ -Lap induced apoptosis independent of p53 status and cell cycle distribution [18, 24]. In MCF-7 cells, the lethal effects of  $\beta$ -lap were accounted for solely by apoptosis. In this

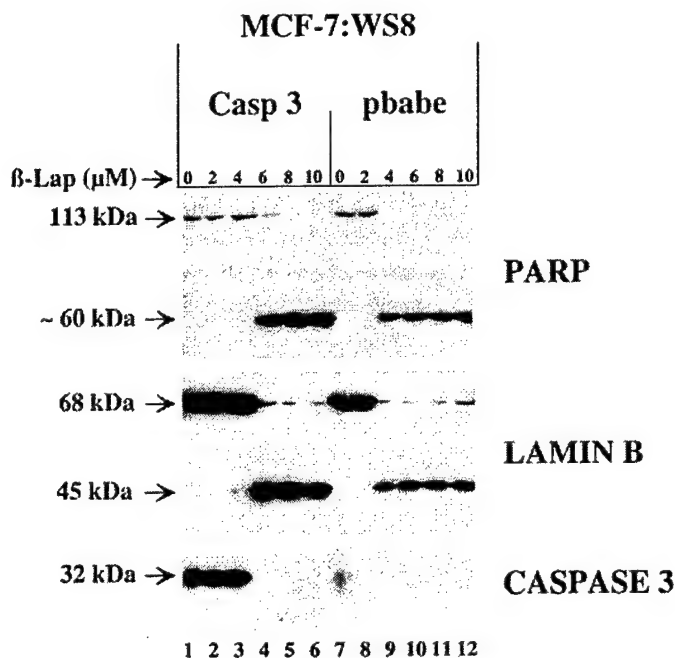


**FIG. 9.** Effect of caspase-3 expression on  $\beta$ -lap-mediated proteolysis. Caspase-3-negative MCF-7 cells were infected with a retroviral construct expressing full-length procaspase-3 (Casp 3) or vector alone (pbabe). Caspase 3 (full length is 32 kDa) expression is shown at the bottom. Cells were then treated with the designated concentrations of  $\beta$ -lap for 4 h, fresh medium was added, and whole-cell extracts were prepared 20 h later. Western immunoblots were then probed with the C-2-10 anti-PARP antibody, stripped, and reprobed with lamin B and later with caspase-3 antibodies. The Western blot shown is representative of at least three separate experiments.

study, we expanded our investigations to include the T47D cell line which has significant phenotypic and genotypic differences (Table 1). Using these cell lines (and others not shown here), we demonstrated that  $\beta$ -lap-mediated apoptosis did not require active ER and we confirmed that cell death was not dependent on wild-type p53 or cell-cycle status.

Our previous studies could not discern a cell cycle phase-specific apoptotic mechanism following  $\beta$ -lap exposure. In these studies, we utilized the estrogen-dependent  $G_1$  arrest characteristics of MCF-7 and T47D cells (~80% growth inhibition in  $E_2$ -deprived, compared to log-phase cells) to show that both cell lines were equally sensitive to  $\beta$ -lap or TPT, irrespective of their progression through the cell cycle (Fig. 2). When arrested cells were treated with either  $\beta$ -lap or TPT, the relative cytotoxicity was identical to that of log-phase cells. This result is in apparent conflict with the current paradigm for the mechanism of action of Topo I poisons, which suggested that the primary lethal event was the creation of DNA double-strand breaks following movement of the replication fork through the "cleavable complex." This mechanism has been used to describe the S-phase-specific killing of cancer cells by

TPT. Morris and Geller [53] also showed that CPT could induce apoptosis in postmitotic rat cortical neurons. Our data indicate that DNA synthesis may not be required for lethality or the stimulation of apoptosis in  $G_1$ -arrested breast cancer cells by  $\beta$ -lap or TPT. These data suggest that DNA-Topo I lesions caused by treatment may activate a nuclear signal (possibly originating from inhibited transcription) that triggers pRb dephosphorylation (see below) and downstream apoptotic reactions. Taken together, these results demonstrate that while actively growing cells may be killed more efficiently in some systems, arrested cells may also be sensitive to the toxic (i.e., apoptotic) effects of Topo I poisons. In comparison with  $\beta$ -lap, TPT was a less effective inducer of apoptosis, stimulating apoptotic reactions only at concentrations 20- to 100-fold over its  $IC_{50}$ .  $\beta$ -Lap killed cells by apoptosis at concentrations near its  $IC_{50}$ , as previously reported [24].

Using two methods of cell cycle arrest, estrogen deprivation (Figs. 2 and 9) and nocodazole administration (data not shown), we demonstrated that  $\beta$ -lap kills MCF-7 cells equally in all phases of the cell cycle. This would suggest that Topo II $\alpha$  does not play a central role in  $\beta$ -lap toxicity. Unlike Topo I, the expression of Topo II $\alpha$  is clearly cell cycle dependent ([26] and data not shown), and stages of the cell cycle in which Topo II $\alpha$  was not expressed (i.e.,  $G_0/G_1$ ) would be expected to be protected from  $\beta$ -lap toxicity, if Topo II $\alpha$  was a critical target. Conversely, stages of the cell cycle with highest Topo II $\alpha$  expression (i.e.,  $G_2/M$ ) would be expected to be more sensitive to  $\beta$ -lap. It is important to note that the  $\beta$ -lap/Topo II $\alpha$ -mediated cleavage has been observed using only *in vitro* assays, and  $\beta$ -lap/Topo II $\alpha$ -mediated DNA breaks have not been demonstrated in intact cells. Importantly, downstream consequences of DNA damage, such as p53 induction, have not been observed after  $\beta$ -lap treatment [24]. These data are in apparent conflict with the suggested role of Topo II $\alpha$  in  $\beta$ -lap-mediated toxicity as proposed by Frydman *et al.* [25].

**$\beta$ -Lap induces a novel apoptotic protease.** Exposure to  $\beta$ -lap gave rise to a unique pattern of proteolysis. At lower doses,  $\beta$ -lap treatment caused classic PARP cleavage. At higher doses, an ~60-kDa atypical PARP fragment was observed. The dose range over which this novel fragment appeared was quite sharp and correlated well with the notably sharp growth inhibition responses noted in Figs. 1 and 2 and previously described cytotoxicity [24]. Atypical PARP fragmentation was not simply the result of supra-lethal drug exposure, since cells treated with TPT at doses 200-fold greater than the  $IC_{50}$  of the drug did not show the same atypical cleavage pattern. Doses of  $\beta$ -lap necessary to induce atypical PARP cleavage were generally less than 5-fold over the  $IC_{50}$  for  $\beta$ -lap, depending upon the cell line examined and the method of treatment (i.e., continuous exposure or 4-h pulse). The lack of

observable atypical PARP cleavage at the  $IC_{50}$  dose was likely due to a relatively modest, but constant, loss of cells through apoptosis that does not result in the accumulation of enough cells containing cleaved PARP to be observed in Western analyses.

Previous reports have shown cleavage of PARP during necrosis, giving rise to a 50-kDa fragment [54]. However, the atypical PARP fragment observed in  $\beta$ -lap treated cells was ~60 kDa (Fig. 4). The demonstration of nuclear condensation, appearance of sub- $G_0/G_1$  cells [24], >90% TUNEL-positive cells (Fig. 6), and inhibition of apoptosis by EDTA and EGTA (Fig. 7B) leave little doubt that this response was apoptotic. Interestingly, in  $\beta$ -lap-treated cells, we have noted some unique characteristics that do not fit the "classic" definition of apoptosis. Further study of the action of this novel apoptosis-inducing agent may allow for elucidation of cell death processes which contain characteristics of apoptotic as well as necrotic proteolytic cascades. This agent may induce a heretofore uncharacterized apoptotic pathway that may be exploited for improved treatment of breast cancer. For example, this agent may be useful for treatment of breast cancer which has lost classic caspase-mediated apoptotic responses.

Atypical PARP cleavage observed in MCF-7 cells was not likely the result of caspase, granzyme B, cathepsins B or L, trypsin, or chymotrypsin-like proteases (see Fig. 5) [38]. However, the classic cleavage pattern observed in T47D cells after low-level  $\beta$ -lap exposures was prevented by 25  $\mu$ M zVAD-fmk, a general caspase inhibitor. Classic PARP cleavage induced by low-dose  $\beta$ -lap exposure was unaffected by other protease inhibitors, suggesting that a different member of the caspase family was responsible for apoptotic proteolysis in T47D cells. At higher doses of  $\beta$ -lap, T47D cells responded like MCF-7 cells, undergoing apoptosis and atypical PARP cleavage. Lack of inhibition of atypical PARP cleavage by zVAD-fmk in MCF-7 cells treated with  $\beta$ -lap strongly suggests that activation of the caspase pathway was not necessary for atypical PARP cleavage.

In  $\beta$ -lap-treated MCF-7 cells, atypical PARP fragmentation was blocked by iodoacetamide or *N*-ethylmaleimide, both cysteine-alkylating agents (data not shown). Additionally, atypical PARP cleavage was not inhibited by a battery of inhibitors (Fig. 5), each used at previously determined effective doses. These data suggest that atypical fragmentation of PARP *in vivo* was due to the activation of a cysteine protease which is apparently not a member of the caspase family of proteases. However, the nonspecific reactivity of iodoacetamide and *N*-ethylmaleimide does allow the possibility that the unknown protease may be indirectly activated after  $\beta$ -lap treatment by a factor which contains critical -SH groups. One protease which fits the available data could be the neutral calcium-dependent protease calpain. This possibility is further supported by the fact that p53 was cleaved in  $\beta$ -lap-treated MCF-7 cells, giving rise to fragments (Fig.

7A) which match those previously described as being the result of calpain activity [42, 43]. Furthermore, the time course of p53 cleavage was concomitant with the appearance of atypically cleaved PARP. Additionally, we provide evidence showing that the cysteine protease is  $Ca^{+2}$  dependent, since its activity (as measured by atypical PARP or p53 cleavage) was prevented by coadministration of EDTA or EGTA (Fig. 8B and data not shown). While these findings do not conclusively prove that calpain is responsible for this cleavage, they are suggestive. Our laboratory is currently in the process of definitively identifying the protease responsible for this cleavage of PARP. The use of caspase-3-expressing MCF-7 cells demonstrated that reexpression of caspase-3 did not lead to enhanced apoptosis or appearance of the caspase-mediated 89-kDa PARP fragmentation after  $\beta$ -lap exposure. In contrast, other studies have demonstrated enhanced apoptotic reactions in caspase-3-expressing MCF-7 cells after granzyme B or TNF- $\alpha$  treatments, compared to cells infected with the empty vector [16].

While  $\beta$ -lap treatment of MCF-7 cells appeared to activate a novel apoptotic pathway, classic lamin B cleavage (primarily due to the activation of caspase-6) was also observed ([24, 51] and Fig. 9). While caspase-6 is thought to be activated directly by caspase-3 [55, 56], our data suggest that either a distinct upstream protease can activate caspase-6 after  $\beta$ -lap treatment or an unknown,  $\beta$ -lap-activated protease can directly cleave lamin B, giving rise to fragments of size similar to those observed after caspase-6 cleavage. Our data suggest that once the apoptotic protease is activated, it dominates proteolysis in  $\beta$ -lap-treated MCF-7 cells, since visible classic PARP cleavage fragments were not observed. Interestingly, overexpression of caspase-3 in MCF-7 cells did not affect  $\beta$ -lap cytotoxicity, while increasing sensitivity to granzyme B or TNF- $\alpha$  [16].

Our studies demonstrate that  $\beta$ -lap can induce at least two independent apoptotic pathways in breast cancer cells. The apoptotic response seems to be independent of the *in vitro* observed  $\beta$ -lap/Topo II $\alpha$ -mediated DNA cleavage [25], since  $G_1$ -arrested cells (which contain very low Topo II $\alpha$  enzyme activity) were as effectively killed by  $\beta$ -lap as log-phase or  $G_2/M$ -arrested cells (which express high levels of Topo II $\alpha$  enzyme activity). Furthermore, the *in vivo* pathway activated by  $\beta$ -lap leading to apoptosis may also be independent of the Topo I inhibition observed *in vitro*. In some cells,  $\beta$ -lap mediates typical caspase activation, leading to the formation of the classic 89 kDa PARP cleavage fragment *in vivo* [57]. In other cells (specifically, MCF-7),  $\beta$ -lap activates a calcium-dependent, noncaspase cysteine protease. Interestingly, activation of this pathway of apoptosis (which may also result in midprotein cleavage of pRb) eventually occurred in MCF-7 and T47D breast cancer cells. An interesting profile of sensitivity of breast cancer cells to

$\beta$ -lap was observed. Sensitivity to this agent was very different from the cytotoxic responses observed following TPT treatment. In MCF-7 cells, the primary proteolytic events, which correlate directly with apoptosis induction and loss of survival, appear to be the result of this novel calcium-dependent noncaspase protease. Activation of this protease was not affected by inhibitors of a variety of proteases, most importantly the caspase inhibitors zVAD-fmk and DEVD-fmk. We hypothesize that this calcium-dependent, noncaspase cysteine protease is calpain. When this protease is activated, its novel apoptotic pathway may be a specific target for manipulation in the clinical treatment of breast cancer.

Funding for this work was provided to us by a grant from the United States Army Medical Research and Materiel Command Breast Cancer Initiative (DAMD17-98-1-8260 to D.A.B.) and by a Postdoctoral Fellowship from the U.S. Army (DAMD17-97-1-7221 to J.J.P.). We thank Dr. V. Craig Jordan for supplying us with the breast cancer cell lines and the anti-estrogen ICI 182,780 and Dr. Vishva Dixit for the caspase 3 cDNA. We thank Dr. William Bornmann for supplying us with  $\beta$ -lap and Dr. Nancy Oleinick for critically reviewing the manuscript. We are also grateful for support through the efforts of Mrs. Sara Hildebrand through the Breast Cancer Inspiration Fund and the Breast Cancer Research Fund. This work was also supported by the Arthritis Foundation-Illinois chapter (to C.J.F.). Finally, we are grateful to our many colleagues at the University of Wisconsin Comprehensive Cancer Center for their help in initiating these studies.

## REFERENCES

- Alnemri, E. S., Livingston, D. J., Nicholson, D. W., Salvesen, G., Thornberry, N. A., Wong, W. W., and Yuan, J. Y. (1996). Human Ice/Ced-3 protease nomenclature. *Cell* **87**, 171.
- Piedrafito, F. J., and Pfahl, M. (1997). Retinoid-induced apoptosis and Sp1 cleavage occur independently of transcription and require caspase activation. *Mol. Cell. Biol.* **17**, 6348–6358.
- Patel, T., Gores, G. J., and Kaufmann, S. H. (1996). The role of proteases during apoptosis. *FASEB J.* **10**, 587–597.
- Janicke, R. U., Walker, P. A., Lin, X. Y., and Porter, A. G. (1996). Specific cleavage of the retinoblastoma protein by an ICE-like protease in apoptosis. *EMBO J.* **15**, 6969–6978.
- An, B., and Dou, Q. P. (1996). Cleavage of retinoblastoma protein during apoptosis: An interleukin 1 beta-converting enzyme-like protease as candidate. *Cancer Res.* **56**, 438–442.
- Talanian, R. V., Quinlan, C., Trautz, S., Hackett, M. C., Manovich, J. A., Banach, D., Ghayur, T., Brady, K. D., and Wong, W. W. (1997). Substrate specificities of caspase family proteases. *J. Biol. Chem.* **272**, 9677–9682.
- Kaufmann, S. H., Desnoyers, S., Ottaviano, Y., Davidson, N. E., and Poirier, G. G. (1993). Specific proteolytic cleavage of poly(ADP-ribose) polymerase: An early marker of chemotherapy-induced apoptosis. *Cancer Res.* **53**, 3976–3985.
- Wang, X., Pal, J. T., Wiedenfeld, E. A., Medina, J. C., Slaughter, C. A., Goldstein, J. L., and Brown, M. S. (1995). Purification of an interleukin-1 beta converting enzyme-related cysteine protease that cleaves sterol regulatory element-binding proteins between the leucine zipper and transmembrane domains. *J. Biol. Chem.* **270**, 18044–18050.
- Squiter, M. K., Miller, A. C., Malkinson, A. M., and Cohen, J. J. (1994). Calpain activation in apoptosis. *J. Cell. Physiol.* **159**, 229–237.
- Wood, D. E., Thomas, A., Devi, L. A., Berman, Y., Beavis, R. C., Reed, J. C., and Newcomb, E. W. (1998). Bax cleavage is mediated by calpain during drug-induced apoptosis. *Oncogene* **17**, 1069–1078.
- Porn-Ares, M. I., Samali, A., and Orrenius, S. (1998). Cleavage of the calpain inhibitor, calpastatin, during apoptosis. *Cell Death Differ.* **5**, 1028–1033.
- Chandra, J., Niemer, I., Gilbreath, J., Kliche, K. O., Andreeff, M., Freireich, E. J., Keating, M., and McConkey, D. J. (1998). Proteasome inhibitors induce apoptosis in glucocorticoid-resistant chronic lymphocytic leukemic lymphocytes. *Blood* **92**, 4220–4229.
- McConkey, D. J. (1996). Calcium-dependent, interleukin 1-converting enzyme inhibitor-insensitive degradation of lamin B1 and DNA fragmentation in isolated thymocyte nuclei. *J. Biol. Chem.* **271**, 22398–22406.
- Shimizu, T., and Pommier, Y. (1997). Camptothecin-induced apoptosis in p53-null human leukemia HL60 cells and their isolated nuclei: Effects of the protease inhibitors Z-VAD-fmk and dichloroisocoumarin suggest an involvement of both caspases and serine proteases. *Leukemia* **11**, 1238–1244.
- Marthinuss, J., Andrade-Gordon, P., and Seiberg, M. (1995). A secreted serine protease can induce apoptosis in Pam212 keratinocytes. *Cell Growth Differ.* **6**, 807–816.
- Yang, X., Stennicke, H. R., Wang, B., Green, D. R., Janicke, R. U., Srinivasan, A., Seth, P., Salvesen, G. S., and Froelich, C. J. (1998). Granzyme B mimics apical caspases. Description of a unified pathway for trans-activation of executioner caspase-3 and -7. *J. Biol. Chem.* **273**, 34278–34283.
- Boothman, D. A., Trask, D. K., and Pardee, A. B. (1989). Inhibition of potentially lethal DNA damage repair in human tumor cells by beta-lapachone, an activator of topoisomerase I. *Cancer Res.* **49**, 605–612.
- Planchon, S. M., Wuerzberger, S., Frydman, B., Witiak, D. T., Hutson, P., Church, D. R., Wilding, G., and Boothman, D. A. (1995). Beta-lapachone-mediated apoptosis in human promyelocytic leukemia (HL-60) and human prostate cancer cells: A p53-independent response. *Cancer Res.* **55**, 3706–3711.
- Boothman, D. A., Wang, M., Schea, R. A., Burrows, H. L., Strickfaden, S., and Owens, J. K. (1992). Posttreatment exposure to camptothecin enhances the lethal effects of x-rays on radioresistant human malignant melanoma cells. *Int. J. Radiat. Oncol. Biol. Phys.* **24**, 939–948.
- Li, C. J., Averboukh, L., and Pardee, A. B. (1993). beta-Lapachone, a novel DNA topoisomerase I inhibitor with a mode of action different from camptothecin. *J. Biol. Chem.* **268**, 22463–22468.
- Boothman, D. A., and Pardee, A. B. (1989). Inhibition of radiation-induced neoplastic transformation by beta-lapachone. *Proc. Natl. Acad. Sci. USA* **86**, 4963–4967.
- Nelson, W. G., and Kastan, M. B. (1994). DNA strand breaks: The DNA template alterations that trigger p53-dependent DNA damage response pathways. *Mol. Cell. Biol.* **14**, 1815–1823.
- Boothman, D. A. (1994). Enhanced malignant transformation is accompanied by increased survival recovery after ionizing radiation in Chinese hamster embryo fibroblasts. *Radiat. Res.* **138**, S121–S125.
- Wuerzberger, S. M., Pink, J. J., Planchon, S. M., Byers, K. L., Bornmann, W. G., and Boothman, D. A. (1998). Induction of apoptosis in MCF-7/WS8 breast cancer cells by beta-lapachone. *Cancer Res.* **58**, 1876–1885.
- Frydman, B., Marton, L. J., Sun, J. S., Neder, K., Witiak, D. T., Liu, A. A., Wang, H. M., Mao, Y., Wu, H. Y., Sanders, M. M., and Liu, L. F. (1997). Induction of DNA topoisomerase II-mediated



- DNA cleavage by beta-lapachone and related naphthoquinones. *Cancer Res.* **57**, 620–627.
26. Larsen, A. K., Skladanowski, A., and Bojanowski, K. (1996). The roles of DNA topoisomerase II during the cell cycle. *Prog. Cell. Cycle. Res.* **2**, 229–239.
  27. D'Arpa, P., and Liu, L. F. (1989). Topoisomerase-targeting antitumor drugs. *Biochim. Biophys. Acta* **989**, 163–177.
  28. Slevin, M. L. (1991). The clinical pharmacology of etoposide. *Cancer* **67**, 319–329.
  29. Jonsson, E., Fridborg, H., Csoka, K., Dhar, S., Sundstrom, C., Nygren, P., and Larsson, R. (1997). Cytotoxic activity of topotecan in human tumour cell lines and primary cultures of human tumour cells from patients. *Br. J. Cancer* **76**, 211–219.
  30. Lamond, J. P., Wang, M., Kinsella, T. J., and Boothman, D. A. (1996). Radiation lethality enhancement with 9-aminocamptothecin: Comparison to other topoisomerase I inhibitors. *Int. J. Radiat. Oncol. Biol. Phys.* **36**, 369–376.
  31. Pink, J. J., Bilimoria, M. M., Assikis, J., and Jordan, V. C. (1996). Irreversible loss of the oestrogen receptor in T47D breast cancer cells following prolonged oestrogen deprivation. *Br. J. Cancer* **74**, 1227–1236.
  32. Pink, J. J., Jiang, S. Y., Fritsch, M., and Jordan, V. C. (1995). An estrogen-independent MCF-7 breast cancer cell line which contains a novel 80-kilodalton estrogen receptor-related protein. *Cancer Res.* **55**, 2583–2590.
  33. Pink, J. J., and Jordan, V. C. (1996). Models of estrogen receptor regulation by estrogens and antiestrogens in breast cancer cell lines. *Cancer Res.* **56**, 2321–2330.
  34. Labarca, C., and Paigen, K. (1980). A simple, rapid, and sensitive DNA assay procedure. *Anal. Biochem.* **102**, 344–352.
  35. Musgrove, E. A., and Sutherland, R. L. (1993). Acute effects of growth factors on T-47D breast cancer cell cycle progression. *Eur. J. Cancer* **29A**, 2273–2279.
  36. Musgrove, E. A., and Sutherland, R. L. (1991). Steroids, growth factors, and cell cycle controls in breast cancer. *Cancer Treat. Res.* **53**, 305–331.
  37. Pink, J. J., Fritsch, M., Bilimoria, M. M., Assikis, V. J., and Jordan, V. C. (1997). Cloning and characterization of a 77-kDa oestrogen receptor isolated from a human breast cancer cell line. *Br. J. Cancer* **75**, 17–27.
  38. Lotem, J., and Sachs, L. (1996). Differential suppression by protease inhibitors and cytokines of apoptosis induced by wild-type p53 and cytotoxic agents. *Proc. Natl. Acad. Sci. USA* **93**, 12507–12512.
  39. Li, X., Traganos, F., Melamed, M. R., and Darzynkiewicz, Z. (1995). Single-step procedure for labeling DNA strand breaks with fluorescein- or BODIPY-conjugated deoxynucleotides: Detection of apoptosis and bromodeoxyuridine incorporation. *Cytometry* **20**, 172–180.
  40. Zollner, H. (1993). "Handbook of Enzyme Inhibitors," pp. 728–730, VCH, Weinheim/New York.
  41. Waxman, L. (1981). Calcium-activated proteases in mammalian tissues. *Methods Enzymol.* **80**, 664–680.
  42. Kubbutat, M. H., and Vousden, K. H. (1997). Proteolytic cleavage of human p53 by calpain: A potential regulator of protein stability. *Mol. Cell. Biol.* **17**, 460–468.
  43. Parlat, M., Carillo, S., Molinari, M., Salvat, C., Debussche, L., Bracco, L., Milner, J., and Piechaczyk, M. (1997). Proteolysis by calpains: A possible contribution to degradation of p53. *Mol. Cell. Biol.* **17**, 2806–2815.
  44. Wakeling, A. E., and Bowler, J. (1992). ICI 182,780, a new antioestrogen with clinical potential. *J. Steroid Biochem. Mol. Biol.* **43**, 173–177.
  45. Pink, J. J., and Jordan, V. C. (1995). Molecular mechanisms of antiestrogen resistance. In "Drug and Hormonal Resistance in Breast Cancer: Cellular and Molecular Mechanisms" (R. B. Dickson and M. E. Lippman, Eds.), Ellis Horwood, Hemel Hempstead, UK.
  46. Musgrove, E. A., Sarcevic, B., and Sutherland, R. L. (1996). Inducible expression of cyclin D1 in T-47D human breast cancer cells is sufficient for Cdk2 activation and pRB hyperphosphorylation. *J. Cell. Biochem.* **60**, 363–378.
  47. Musgrove, E. A., and Sutherland, R. L. (1994). Cell cycle control by steroid hormones. *Semin. Cancer Biol.* **5**, 381–389.
  48. Musgrove, E. A., Wakeling, A. E., and Sutherland, R. L. (1989). Points of action of estrogen antagonists and a calmodulin antagonist within the MCF-7 human breast cancer cell cycle. *Cancer Res.* **49**, 2398–2404.
  49. Foster, J. S., and Wimalasena, J. (1996). Estrogen regulates activity of cyclin-dependent kinases and retinoblastoma protein phosphorylation in breast cancer cells. *Mol. Endocrinol.* **10**, 488–498.
  50. Li, F., Srinivasan, A., Wang, Y., Armstrong, R. C., Tomaselli, K. J., and Fritz, L. C. (1997). Cell-specific induction of apoptosis by microinjection of cytochrome c. Bcl-xL has activity independent of cytochrome c release. *J. Biol. Chem.* **272**, 30299–30305.
  51. Orth, K., Chinnaiyan, A. M., Garg, M., Froelich, C. J., and Dixit, V. M. (1996). The CED-3/ICE-like protease Mch2 is activated during apoptosis and cleaves the death substrate lamin A. *J. Biol. Chem.* **271**, 16443–16446.
  52. Takahashi, A., Alnemri, E. S., Lazebnik, Y. A., Fernandes-Alnemri, T., Litwack, G., Moir, R. D., Goldman, R. D., Poirier, G. G., Kaufmann, S. H., and Earnshaw, W. C. (1996). Cleavage of lamin A by Mch2 alpha but not CPP32: Multiple interleukin 1 beta-converting enzyme-related proteases with distinct substrate recognition properties are active in apoptosis. *Proc. Natl. Acad. Sci. USA* **93**, 8395–8400.
  53. Morris, E. J., and Geller, H. M. (1996). Induction of neuronal apoptosis by camptothecin, an inhibitor of DNA topoisomerase-I: Evidence for cell cycle-independent toxicity. *J. Cell Biol.* **134**, 757–770.
  54. Shah, G. M., Shah, R. G., and Poirier, G. G. (1996). Different cleavage pattern for poly(ADP-ribose) polymerase during necrosis and apoptosis in HL-60 cells. *Biochem. Biophys. Res. Commun.* **229**, 838–844.
  55. Faleiro, L., Kobayashi, R., Fearnhead, H., and Lazebnik, Y. (1997). Multiple species of CPP32 and Mch2 are the major active caspases present in apoptotic cells. *EMBO J.* **16**, 2271–2281.
  56. Hirata, H., Takahashi, A., Kobayashi, S., Yonehara, S., Sawai, H., Okazaki, T., Yamamoto, K., and Sasada, M. (1998). Caspases are activated in a branched protease cascade and control distinct downstream processes in Fas-induced apoptosis. *J. Exp. Med.* **187**, 587–600.
  57. Planchon, S. M., Wuerzberger-Davis, S. M., Pink, J. J., Robertson, K. A., Bornmann, W. G., and Boothman, D. A. (1999). Bcl-2 protects against  $\beta$ -lapachone-mediated caspase 3 activation and apoptosis in human myeloid leukemia (HL-60) cells. *Oncol. Rep.* **6**, 485–492.

Received August 11, 1999

Revised version received December 10, 1999



## NAD(P)H:Quinone Oxidoreductase Activity Is the Principal Determinant of $\beta$ -Lapachone Cytotoxicity\*

(Received for publication, October 13, 1999, and in revised form, December 7, 1999)

John J. Pink<sup>‡</sup>, Sarah M. Planchon<sup>‡</sup>, Colleen Tagliarino<sup>‡</sup>, Marie E. Varnes<sup>‡</sup>, David Siegel<sup>§</sup>,  
and David A. Boothman<sup>‡¶</sup>

From the <sup>‡</sup>Department of Radiation Oncology, Laboratory of Molecular Stress Responses, Ireland Comprehensive Cancer Center, Case Western Reserve University, Cleveland, Ohio 44106-4942 and the <sup>§</sup>Department of Pharmaceutical Sciences, School of Pharmacy and Cancer Center, University of Colorado Health Sciences Center, Denver, Colorado 80262

$\beta$ -Lapachone activates a novel apoptotic response in a number of cell lines. We demonstrate that the enzyme NAD(P)H:quinone oxidoreductase (NQO1) substantially enhances the toxicity of  $\beta$ -lapachone. NQO1 expression directly correlated with sensitivity to a 4-h pulse of  $\beta$ -lapachone in a panel of breast cancer cell lines, and the NQO1 inhibitor, dicoumarol, significantly protected NQO1-expressing cells from all aspects of  $\beta$ -lapachone toxicity. Stable transfection of the NQO1-deficient cell line, MDA-MB-468, with an NQO1 expression plasmid increased apoptotic responses and lethality after  $\beta$ -lapachone exposure. Dicoumarol blocked both the apoptotic responses and lethality. Biochemical studies suggest that reduction of  $\beta$ -lapachone by NQO1 leads to a futile cycling between the quinone and hydroquinone forms, with a concomitant loss of reduced NAD(P)H. In addition, the activation of a cysteine protease, which has characteristics consistent with the neutral calcium-dependent protease, calpain, is observed after  $\beta$ -lapachone treatment. This is the first definitive elucidation of an intracellular target for  $\beta$ -lapachone in tumor cells. NQO1 could be exploited for gene therapy, radiotherapy, and/or chemopreventive interventions, since the enzyme is elevated in a number of tumor types (*i.e.* breast and lung) and during neoplastic transformation.

$\beta$ -lap,<sup>1</sup> a novel 1,2-naphthoquinone, is a potent cytotoxic agent that demonstrates activity against various cancer cell lines (1–3). At lower doses, it is a radiosensitizer of a number of human cancer cell lines (4). We previously demonstrated that the primary mode of  $\beta$ -lap cytotoxicity is through the induction of apoptosis (1, 2). However, the clinical efficacy of this drug remains to be explored, and such studies await elucidation of its mechanism of action.

While a number of *in vitro* effects of  $\beta$ -lap have been described, the key intracellular target of  $\beta$ -lap remains unknown.

\* This work was supported by United States Army Medical Research and Materiel Command Breast Cancer Initiative Grant DAMD17-98-1-8260 (to D. A. B.) and Postdoctoral Fellowship DAMD17-97-1-7221 (to J. J. P.) and National Institutes of Health Grant CA51210 (to D. S.). The costs of publication of this article were defrayed in part by the payment of page charges. This article must therefore be hereby marked "advertisement" in accordance with 18 U.S.C. Section 1734 solely to indicate this fact.

¶ To whom correspondence should be addressed: Tel.: 216-368-0840; Fax: 216-368-1142; E-mail: dab30@po.cwru.edu.

<sup>1</sup> The abbreviations used are:  $\beta$ -lap,  $\beta$ -lapachone (3,4-dihydro-2,2-dimethyl-2H-naphtho[1,2-b]pyran-5,6-dione); xip-3, x-ray-inducible transcript-3; NQO1, NAD(P)H:quinone oxidoreductase, DT-diaphorase, xip-3 (EC 1.6.99.2); PARP, poly(ADP-ribose) polymerase; MMC, mitomycin C; TUNEL, terminal deoxynucleotidyl transferase-mediated dUTP nick end labeling.

$\beta$ -lap has many diverse effects *in vitro*, including (a) inhibition of DNA polymerase  $\alpha$  (5), (b) enhanced lipid peroxidation and free radical accumulation (6), (c) inhibition of DNA replication and thymidylate synthase activity (7), (d) inhibition of DNA repair (4, 8), (e) inhibition or activation of DNA topoisomerase I (1, 3), (f) oxidation of dihydrolipoamide (9), (g) induction of topoisomerase II $\alpha$ -mediated DNA breaks (10), (h) inhibition of poly(ADP-ribose) polymerase (11), and (i) inhibition of NF- $\kappa$ B activity (12). While these effects could be hypothetically linked to the cytotoxicity caused by  $\beta$ -lap administration, most have not been demonstrated *in vivo*, and none have led to elucidation of the drug's intracellular target.

Structural similarities between  $\beta$ -lap and other members of the naphthoquinone family, such as menadione (vitamin K<sub>3</sub>; 2-methyl-1,4 naphthoquinone), suggested that the enzyme, DT-diaphorase, quinone oxidoreductase, EC 1.6.99.2 (NQO1), may be involved in the activation or detoxification of  $\beta$ -lap (13–17). The x-ray-inducible nature of NQO1 (*i.e.* it was cloned by our laboratory as x-ray inducible transcript-3 (xip-3)) was also consistent with this compound's ability to sensitize irradiated cells (18).

NQO1 is a ubiquitous flavoprotein found in most eukaryotes. The human NQO1 gene encodes a 30-kDa protein that is expressed in most tissues but does show variable tissue-dependent expression. NQO1 is abundant in the liver of most mammals, except humans, where it is less abundant than in most other tissues (16, 19, 20). NQO1 knock-out mice show no detectable phenotype other than an enhanced sensitivity to menadione, suggesting that the principal function of NQO1 is the detoxification of quinone xenobiotics (21). Importantly, NQO1 is overexpressed in a number of tumors, including breast, colon, and lung cancers, compared with surrounding normal tissue (22–25). This observation, more than any other, suggests that drugs that are activated by NQO1 (*e.g.* MMC, streptozotocin, and EO9; see below) should show significant tumor-specific activity.

NQO1 catalyzes a two-electron reduction of various quinones (*e.g.* menadione), utilizing either NADH or NADPH as electron donors. Unlike most other cellular reductases, NQO1 reduces quinones directly to the hydroquinone, bypassing the unstable and highly reactive semiquinone intermediate. Semiquinones are excellent free radical generators, initiating a redox cycle that results in the generation of superoxide. Superoxide can dismutate to hydrogen peroxide, and hydroxyl radicals can then be formed by the iron-catalyzed reduction of peroxide via the Fenton reaction (26). All of these highly reactive species may directly react with DNA or other cellular macromolecules, such as lipids and proteins, causing damage. NQO1-mediated production of the hydroquinone, which can be readily conjugated and excreted from the cell, constitutes a protective mech-

anism against these types of damage (27). It is thought that the reducing activity of NQO1 protects cells from the toxicity of naturally occurring xenobiotics containing quinone moieties (14).

In addition to its protective effects, NQO1 can also reduce certain quinones to more reactive forms. The most well described of these compounds is MMC. It is through a two-electron reduction by NQO1 or through two separate one electron reductions by other reductases (such as NADH:cytochrome  $b_5$  reductase and NADPH:cytochrome P-450 reductase) that the alkylating activity of MMC is revealed (28–30). A correlation was observed between MMC sensitivity and NQO1 activity in a study using 69 cell lines from the NCI, National Institutes of Health, human tumor cell panel. These data suggested that NQO1 was a critical activator of MMC and probably other quinone-containing antitumor agents (31). Similarly, streptozotocin and EO9 can be activated by NQO1-catalyzed reduction (32).

Dicoumarol (3-3'-methylene-bis(4-hydroxycoumarin)) is a commonly used inhibitor of NQO1, which competes with NADH or NADPH for binding to the oxidized form of NQO1. Dicoumarol thereby prevents reduction of various target quinones (33, 34). Co-administration of dicoumarol significantly enhances the toxicity of a number of quinones, including menadione, presumably by increasing oxidative stress in the cell (35–37).

We demonstrate that NQO1 is an important activating enzyme for  $\beta$ -lap in breast cancer cells.  $\beta$ -lap cytotoxicity was significantly enhanced in breast cancer cells expressing NQO1. Conversely, cells that lacked this enzyme were more resistant to a short term exposure to the drug. Co-administration of dicoumarol protected NQO1-expressing cells from all downstream apoptotic responses and greatly enhanced survival. Stable transfection of NQO1-deficient, MDA-MB-468 cells, homozygous for a proline to serine substitution at amino acid 187, which leads to the synthesis of unstable protein (38), with human NQO1 cDNA sensitized these otherwise resistant cells and re-established apoptotic responses. As seen in other cells expressing endogenous NQO1, cytotoxicity was significantly inhibited by dicoumarol. Our data establish that NQO1 activity is an important determinant of  $\beta$ -lap cytotoxicity in breast cancer cells. A novel downstream apoptotic pathway induced by  $\beta$ -lapachone is also discussed.

#### EXPERIMENTAL PROCEDURES

**Cell Culture**—MCF-7:WS8 and T47D:A18 cells were obtained from V. Craig Jordan (Northwestern University, Chicago, IL). MDA-MB-468 cells were obtained from the American Type Culture Collection. All tissue culture components were purchased from Life Technologies, Inc. unless otherwise stated. Cells were grown in RPMI 1640 supplemented with 10% calf serum, 2 mM L-glutamine, 100 units/ml penicillin, and 100 mg/ml streptomycin. Cells were routinely passed at 1:5–1:20 dilutions once per week using 0.1% trypsin. All cells were grown in a 37 °C humidified incubator with 5% CO<sub>2</sub>, 95% air atmosphere. Tests for mycoplasma, using the Gen-Probe™ Rapid Detection Kit (Fisher), were performed quarterly, and all cell lines were found to be negative.

**Stable Transfection**—Cells were seeded into six-well dishes at  $2 \times 10^5$  cells/well and allowed to attach overnight. The following day, 1.0  $\mu$ g of BE8 plasmid DNA containing the human NQO1 cDNA in the pCDNA3 constitutive expression vector (39) was transfected into each of three wells using standard calcium phosphate methodology (40). After 2 days, cells were selected for growth in 350  $\mu$ g/ml Geneticin® (G418, Life Technologies, Inc.). A stable, pooled population was established after approximately 3 weeks, and subsequently clones were isolated by limiting dilution cloning, as described (41).

**Cell Growth Assays**—Cells were seeded into each well of a 96-well plate (1500 cells/well) in 0.2 ml of media on day 0. The following day (day 1), media were removed, and 0.2 ml of medium containing the appropriate compound(s) was added for 4 h. Drugs were then removed, control growth medium was added, and cells were allowed to grow for an additional 7 days. Stock solutions of  $\beta$ -lap (a generous gift from

William Bornmann, Sloan-Kettering Cancer Center, New York, NY) and menadione (Sigma) were dissolved in Me<sub>2</sub>SO and stored at –80 °C. Drugs were added to medium at a 1:1000 dilution immediately before administration to cells. Dicoumarol (Sigma) was suspended in water and solubilized using a minimal amount of NaOH. Dicoumarol was added at a 1:100 dilution to the appropriate medium. DNA content (a measure of cell growth) was determined by fluorescence of the DNA dye Hoechst 33258 (Sigma), using an adaptation of the method of Labarca and Paigen (42), and read in a Cytofluor fluorescence plate reader. Data were expressed as relative growth, T/C (treated/control) from three or more wells per treatment. Each experiment was repeated at least three times, and data were expressed as mean  $\pm$  S.E. Comparisons were performed using a two-tailed Student's *t* test for paired samples.

**Colony-forming Assays**—LD<sub>50</sub> survival determinations were calculated by clonogenic assays (4). Briefly, cells were seeded at various densities on 35-cm<sup>2</sup> tissue culture dishes and allowed 48 h to attach and initiate log phase growth. Drugs were added for 4 h at various concentrations and removed, as described above. Colonies from control or treated conditions were allowed to grow for 10 days. Colonies with 50 or more normal appearing cells were counted, and data were graphed as mean  $\pm$  S.E. Shown is a compilation of two independent experiments. Comparisons were performed using a two-tailed Student's *t* test for paired samples.

**Western Blot Analyses**—Whole cell extracts were prepared by direct lysis of scraped, PBS-washed cells (both floating and attached cells were pooled) in buffer composed of 6 M urea, 2% SDS, 10% glycerol, 62.5 mM Tris-HCl, pH 6.8, 5%  $\beta$ -mercaptoethanol, and 5  $\mu$ g/ml bromophenol blue followed by sonication. Equal amounts of protein were heated at 65 °C for 10 min and loaded into each lane of a 10% polyacrylamide gel with a 5% stacking gel. Following electrophoresis, proteins were transferred to Immobilon-P (Millipore Corp., Bedford, MA) using Multiphor II semi-dry electroblotting (Amersham Pharmacia Biotech) according to the manufacturer's directions. Loading equivalence and transfer efficiency were monitored by Ponceau S staining of the membrane. Standard Western blotting techniques were used, and the proteins of interest were visualized by incubation with Super Signal (Pierce) at 20 °C for 5 min. Membranes were then exposed to x-ray film for an appropriate time and developed. The C-2-10 anti-PARP antibody was purchased from Enzyme Systems Products (Dublin, CA). The anti-p53 antibody (DO-1) was purchased from Santa Cruz Biotechnology, Inc. (Santa Cruz, CA). NQO1 antibody was contained in medium from a mouse hybridoma clone A180 (43) and was used at a 1:4 dilution in 10% serum, 1 $\times$  PBS, 0.2% Tween 20 for Western blot analysis.

**Preparation of S9 Supernatants**—Cellular extracts for enzyme assays were prepared from cells in mid-log to late log phase growth. Cells were harvested by trypsinization (0.25% trypsin and 1 mM EDTA), washed twice in ice-cold, phenol red-free Hank's balanced salt solution, and then resuspended in a small volume of PBS, pH 7.2, containing 10  $\mu$ g/ $\mu$ l aprotinin. The cell suspensions were sonicated on ice four times, using 10-s pulses, and then centrifuged at 14,000  $\times$  g for 20 min. The S9 supernatants were aliquoted into microcentrifuge tubes and stored at –80 °C until used.

**Enzyme Assays**—Three enzymes were assayed as described by Fitzsimmons *et al.* (31) and Gustafson *et al.* (39). Reaction medium contained 77  $\mu$ M cytochrome *c* (practical grade; Sigma) and 0.14% bovine serum albumin in Tris-HCl buffer (50 mM, pH 7.5). NQO1 activity was measured using NADH (200  $\mu$ M) as the immediate electron donor and menadione (10  $\mu$ M) as the intermediate electron acceptor. Each assay was repeated in the presence of 10  $\mu$ M dicoumarol, and activity attributed to NQO1 was that inhibited by dicoumarol (44). NADH:cytochrome  $b_5$  reductase was measured using NADH (200  $\mu$ M) as the electron donor, and NADH:cytochrome P-450 reductase was measured using NADPH (200  $\mu$ M) as electron donor (45) in a Beckman DU 640 spectrophotometer (Beckman Coulter, Fullerton, CA). Reactions were carried out at 37 °C and were initiated by the addition of S9 supernatants. Varying amounts of supernatants, from 10 to 40  $\mu$ l, were used to ensure linearity of rates with protein concentration. Enzyme activities were calculated as nmol of cytochrome *c* reduced/min/mg of protein, based on the initial rate of change in OD at 550 nm and an extinction coefficient for cytochrome *c* of 21.1 mm<sup>2</sup>/cm. Results shown are the average enzyme activity for three separate cell extractions  $\pm$  S.D. or both values from duplicate experiments.

**NADH Recycling Assays**—Assays were performed with either purified NQO1 (46) or S9 extracts from MCF-7:WS8 cells. For the assay using purified NQO1, 1.5  $\mu$ g of recombinant human NQO1 was mixed with 200–500  $\mu$ M NADH in 50 mM potassium phosphate buffer, pH 7.0. Reactions were initiated by the addition of 2–20  $\mu$ M  $\beta$ -lap or menadione, and the change in absorbance at 340 nm was measured over time. For

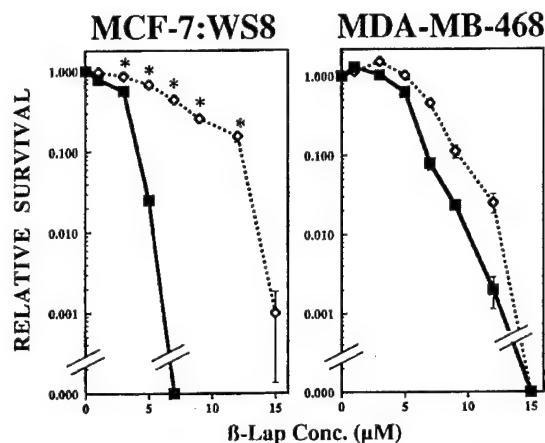


FIG. 1. Co-administration of dicoumarol protects MCF-7:WS8, but not MDA-MB-468, cells from  $\beta$ -lap-mediated cytotoxicity. Cells were seeded into 60-mm dishes (10,000 and 1000 cells/dish, in triplicate) and allowed to attach overnight. Cells were then exposed to a 4-h pulse of  $\beta$ -lap either alone (●) or with 50  $\mu$ M dicoumarol (◇). Media were removed, fresh drug-free media were added, and cells were allowed to grow for 10 days. Plates were then washed and stained with crystal violet in 50% methanol. Colonies of greater than 50 normal-appearing cells were then counted and plotted versus  $\beta$ -lap concentration. Shown is the mean  $\pm$  S.E. of triplicate plates from two independent experiments.

assays using MCF-7:WS8 S9 extracts, 5  $\mu$ l of extracts containing approximately 2000 units of NQO1/mg of protein were mixed with 200–500  $\mu$ M NADH in 50 mM Tris-HCl, pH 7.5, containing 0.14% bovine serum albumin. Reactions were initiated by the addition of 5–200  $\mu$ M  $\beta$ -lap or menadione, and change in absorbance at 340 nm was measured for 10 min. All reactions were also performed in the presence of 10  $\mu$ M dicoumarol, which inhibited all measurable NQO1 activity.

**Flow Cytometry and Apoptotic Measurements.**—Flow cytometric analyses were performed as described (1, 2). TUNEL assays, to measure DNA fragmentation during apoptosis, were performed using APO-DIRECT™ as described by the manufacturer (Phoenix Flow Systems, Inc., San Diego, CA). Samples were read in an EPICS Elite ESP flow cytometer using an air-cooled argon laser at 488 nm, 15 milliwatts (Beckman Coulter Electronics, Miami, FL). Propidium iodide was read at 640 nm using a long pass optical filter, and fluorescein isothiocyanate was read at 525 nm using a band pass filter. Analysis was performed using the Elite acquisition software provided with the instrument. All experiments were performed a minimum of three times.

## RESULTS

We previously showed that the naturally occurring 1,2-naphthoquinone,  $\beta$ -lap, induced apoptosis in a number of breast cancer cell lines (1, 2). We hypothesized that  $\beta$ -lap, as a member of the naphthoquinone family, may be a substrate for NQO1 and that its toxicity may be influenced by NQO1 expression. We therefore tested the effects of dicoumarol on  $\beta$ -lap-mediated cytotoxicity in MCF-7:WS8 or MDA-MB-468 breast cancer cell lines after a 4-h pulse of drug. Co-administration of 50  $\mu$ M dicoumarol during a 4-h pulse of  $\beta$ -lap caused a significant survival enhancement in MCF-7:WS8 cells (Fig. 1). While this protection was dramatic at  $\beta$ -lap doses of 4–12  $\mu$ M, the protective effects of dicoumarol were overcome by >14  $\mu$ M  $\beta$ -lap. In contrast, MDA-MB-468 cells were relatively resistant ( $LD_{50} \sim 8 \mu$ M, compared with MCF-7:WS8,  $LD_{50} \sim 4 \mu$ M) to  $\beta$ -lap alone and were not significantly protected by dicoumarol (Fig. 1). Since MDA-MB-468 cells do not express NQO1 (Table I and Fig. 3) and dicoumarol significantly protected NQO1-expressing MCF-7:WS8 cells (Table I and Fig. 3), these data suggested that NQO1 expression was a critical determining factor in  $\beta$ -lap-mediated cytotoxicity.

We then extended these studies to compare the relative toxicity of menadione (2-methyl-1,4-naphthoquinone) to  $\beta$ -lap, either alone or in the presence of dicoumarol. Three breast

TABLE I  
Endogenous reductase levels in breast cancer cell lines

Values represent averages for three or more separate S9 preparations  $\pm$  S.D. except as noted in Footnote c.

Cell line	Enzyme activities <sup>a</sup>		
	NQO1	NADH:cytochrome $b_5$ reductase	NADPH:cytochrome P-450 reductase
		nmol/min/mg	
MCF-7:WS8	2641 $\pm$ 555	81 $\pm$ 18	27 $\pm$ 5.0
T47D:A18	82 $\pm$ 17	131 $\pm$ 35	31 $\pm$ 1.0
MDA-MB-468	<10.0 <sup>b</sup>	93/108 <sup>c</sup>	26/36 <sup>c</sup>

<sup>a</sup> Units are nanomoles of cytochrome c reduced per min per mg of protein.

<sup>b</sup> <10.0\*\*, NQO1 activity not detected. The difference in the rate of cytochrome c reduction with and without dicoumarol was not statistically significant, based on Student's *t* test.

<sup>c</sup> Both values from separate S9 preparations are shown.

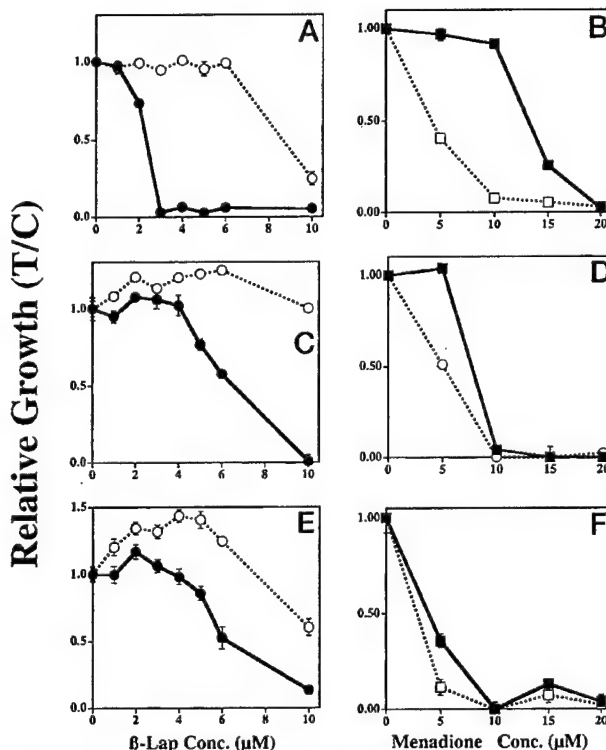
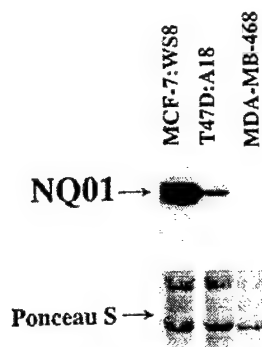


FIG. 2. Relative growth inhibition of various breast cancer cell lines by  $\beta$ -lap or menadione. Cells (MCF-7:WS8 (A and B), T47D:A18 (C and D) and MDA-MB-468 (E and F)) were seeded into 96-well plates (1500 cells/well) and allowed to attach overnight. Media containing drugs ( $\beta$ -lap in A, C, and E; menadione in B, D, and F), either alone ( $\beta$ -lap (●) or menadione (■)) or in the presence of 50  $\mu$ M dicoumarol ( $\beta$ -lap (○) or menadione (□)), were then added for 4 h. Media were then removed, fresh drug-free media were added, and the cells were allowed to grow for an additional 7 days. Relative DNA per well was then determined by Hoechst 33258 fluorescence, and relative growth (treated/control DNA) was plotted. Each point represents the mean of four independent wells  $\pm$  S.E.

cancer cell lines (T47D:A18, MDA-MB-468, and MCF-7:WS8) were treated with a 4-h pulse of drugs, and relative growth was measured 7 days later (Fig. 2). Dicoumarol significantly inhibited  $\beta$ -lap toxicity in MCF-7:WS8 and T47D:A18 cells. In contrast, dicoumarol showed little or no protective effect in MDA-MB-468 cells (compare graphs A, C, and E in Fig. 2).

In a parallel experiment using menadione, alone or with dicoumarol, the relative sensitivities of the cell lines to menadione were opposite those found with  $\beta$ -lap; MCF-7:WS8 cells were the most resistant to menadione, and MDA-MB-468 cells



**FIG. 3. NQO1 expression in various breast cancer cell lines.** Whole cell extracts were prepared from exponentially growing cell lines. Equal protein was loaded into each lane and confirmed by Ponceau S staining. Proteins were separated by standard 10% SDS-polyacrylamide gel electrophoresis, transferred to Immobilon P, and probed with medium from an anti-NQO1 hybridoma followed by horseradish peroxidase-conjugated anti-mouse secondary antibody. Signals were visualized using Super Signal reagent as described under "Experimental Procedures." Shown is a representative blot from experiments performed at least three times.

were the most sensitive. Co-administration of dicoumarol caused a significant sensitization of MCF-7:WS8 cells to menadione toxicity, with a decrease in the relative  $IC_{50}$  from 12 to 3  $\mu$ M. MDA-MB-468 cells, which were inherently more sensitive to menadione, were unaffected by dicoumarol co-administration. T47D:A18 cells were only minimally sensitized to menadione exposure when dicoumarol was co-administered (compare graphs B, D, and F; Fig. 2). These data were consistent with NQO1 expression (Fig. 3), where NQO1 protein levels were high in MCF-7:WS8 cells, moderate in T47D:A18 cells, and undetectable in MDA-MB-468 cells. NQO1 enzyme activities were consistent with protein levels (compare Fig. 3 and Table I). Using these cell extracts, we showed that  $\beta$ -lap could substitute for menadione in this *in vitro* assay, demonstrating that the compound was a suitable NQO1 substrate in intact cells (Fig. 9 and data not shown). These data demonstrated that both menadione and  $\beta$ -lap could serve as substrates for NQO1-mediated reduction and suggested that the end results of these reductions were opposite (*i.e.* menadione was inactivated by reduction, and  $\beta$ -lap was activated by reduction).

We previously showed that apoptosis in various human breast cancer cell lines induced by  $\beta$ -lap administration was unique, in that it caused a pattern of PARP and p53 cleavages distinct from that induced by other caspase-activating agents. After  $\beta$ -lap treatment, we observed a 60-kDa PARP fragment, which was probably due to the activation of a neutral, calcium-dependent protease with similar properties as calpain.<sup>2</sup> To investigate the effect of dicoumarol on this cleavage pattern in MCF-7:WS8 cells, we treated cells with a 4-h pulse of 8  $\mu$ M  $\beta$ -lap alone or in the presence of 50  $\mu$ M dicoumarol. Cells were lysed 20 h later, and PARP cleavage was monitored. We also investigated the effects of 1  $\mu$ M staurosporine treatment, in order to determine if dicoumarol could block classic apoptotic proteolysis or if it was specific for  $\beta$ -lap-induced apoptosis. As seen in Fig. 4, dicoumarol completely abrogated atypical PARP cleavage after  $\beta$ -lap exposure but had no effect on staurosporine-induced classic PARP cleavage (*i.e.* formation of an 89-kDa PARP fragment (47)) in MCF-7:WS8 cells. The fact that dicoumarol significantly protected NQO1-expressing cells from  $\beta$ -lap-mediated apoptosis strongly suggested a role for NQO1 in  $\beta$ -lap toxicity. However, previous studies indicated that dicou-

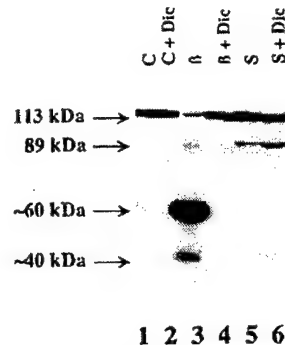


**FIG. 4. Dicoumarol inhibition of  $\beta$ -lap-induced atypical PARP cleavage.** MCF-7:WS8 cells were treated with a 4-h pulse of 8  $\mu$ M  $\beta$ -lap ( $\beta$ , lanes 3 and 4) or a 24-h pulse of 1  $\mu$ M staurosporine (S, lanes 5 and 6) either alone or with 50  $\mu$ M dicoumarol during the time of drug exposure. Untreated cells (C, lane 1) or cells treated only with 50  $\mu$ M dicoumarol (C + Dic, lane 2) were included as controls. Whole cell extracts were prepared at 24 h and analyzed using standard Western blot techniques as described for Fig. 3. The blot was probed with the C-2-10 anti-PARP monoclonal antibody followed by horseradish peroxidase-conjugated anti-mouse secondary antibody and visualized with Super Signal reagent. Shown is a representative blot from experiments performed at least three times.

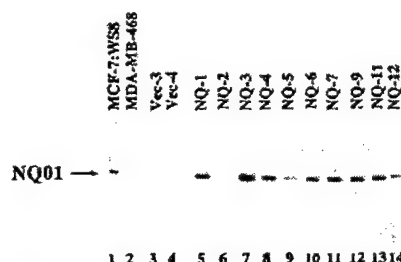


**FIG. 5. NQO1 protein expression in MDA-MB-468 transfectants.** Whole cell extracts were prepared from exponentially growing parental MCF-7:WS8 and MDA-MB-468 cells, two control vector alone MDA-MB-468 transfectants, and 10 NQO1 expression vector MDA-MB-468 transfectants. Equal amounts of protein were analyzed by standard Western blot techniques as described above using anti-NQO1 as described for Fig. 4. Shown is a representative blot from experiments performed at least three times.

marol may also inhibit other cellular enzymes (48).

In order to definitively demonstrate the role of NQO1 in  $\beta$ -lap toxicity, we utilized the NQO1-negative,  $\beta$ -lap-resistant, MDA-MB-468 cell line to determine if exogenous expression of NQO1 could sensitize these cells to  $\beta$ -lap. We stably transfected MDA-MB-468 cells with a constitutive NQO1 expression vector under the control of a cytomegalovirus promoter. We also performed a parallel transfection using the empty vector, pcDNA3. Following selection of a pooled population of G418-resistant cells, we isolated a number of clones by limiting dilution subcloning, as described under "Experimental Procedures." NQO1 expression in isolated clones was then determined by Western blot analyses (Fig. 5) and enzyme assays (Table II). In all cases, enzyme activity correlated with protein expression. As shown in Fig. 5 and Table II, the empty vector-containing clones did not demonstrate measurable NQO1 expression, as observed with parental, nontransfected cells (see lanes 2, 3, and 4). Of the 10 clones isolated from the NQO1 transfections, nine exhibited NQO1 expression. Clone NQ-2 (lane 6) showed no measurable NQO1 expression.

We tested a number of the clones for  $\beta$ -lap and menadione sensitivity. Growth inhibition was measured after a 4-h pulse of drugs, either alone or in the presence of 50  $\mu$ M dicoumarol. Relative growth of  $\beta$ -lap-treated compared with control cells ( $T/C$ ) was determined 7 days after drug exposures, using DNA

<sup>2</sup> J. J. Pink, S. Wuerzberger-Davis, C. Tagliarino, S. M. Planchon, X. Yang, C. J. Froelich, and D. A. Boothman (2000) *Exp. Cell Res.*, in press.



TABLE II  
NQO1 expression in MDA-MB-468 transfectants

Clone	NQO1 activity <sup>a</sup>
	nmol/min/mg
Vec-3	<10 <sup>b</sup>
NQ-1	6555/8264 <sup>c</sup>
NQ-2	<10 <sup>b</sup>
NQ-3	9276 $\pm$ 491 <sup>d</sup>
NQ-6	14,684/18,511 <sup>c</sup>
NQ-7	11,341/12,332 <sup>c</sup>

<sup>a</sup> Units are nmol of cytochrome c reduced per min per mg of protein.

<sup>b</sup> <10, NQO1 not detected. The difference in the rate of cytochrome c reduction with and without dicoumarol was not statistically significant, based on Student's *t* test.

<sup>c</sup> Both values from two separate S9 preparations.

<sup>d</sup> Average for three separate S9 preparations  $\pm$  S.D.

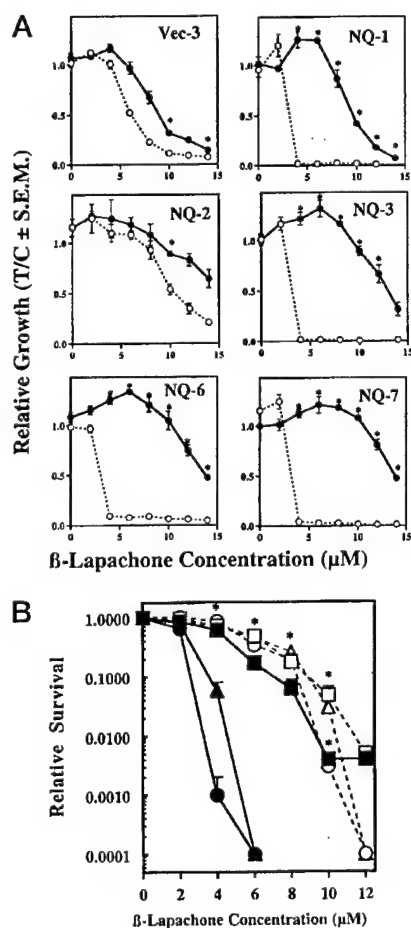


FIG. 6. NQO1 expression sensitizes cells to acute  $\beta$ -lap cytotoxicity. A, acute  $\beta$ -lap toxicity was determined using the control vector MDA-MB-468 transfectant (clone Vec-3) and five NQO1 vector-containing MDA-MB-468 transfectants, as described in Fig. 2. Note that clone NQ-2 showed no measurable NQO1 expression (Fig. 5 and Table II). Cells were exposed to a 4-h pulse of a range of  $\beta$ -lap doses either alone (●) or with 50  $\mu$ M dicoumarol (○) and then allowed to grow for an additional 7 days, at which time DNA content for treated (T) cells was measured and plotted relative to control (C) cells. B, Vec-3 (■, □), NQ-1 (▲, △), and NQ-3 (●, ○) cells were treated with a 4-h pulse of a range of  $\beta$ -lap doses alone (■, ▲, ●) or with 50  $\mu$ M dicoumarol (□, △, ○). Overall survival, as assessed by colony-forming ability, was measured after 10 days growth in control media. Shown is a representative graph from experiments performed at least three times with each group consisting of at least triplicate determinations. Differences between treatments were compared using a two-tailed Student's *t* test for paired samples and groups having *p* < 0.01 compared with  $\beta$ -lap or dicoumarol alone are indicated by an asterisk.

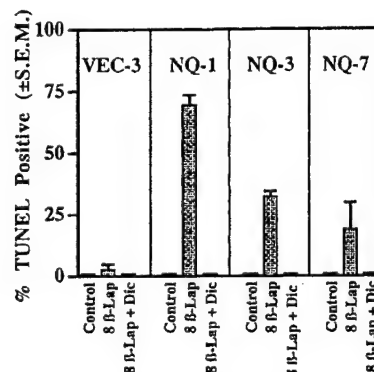


FIG. 7. Acute  $\beta$ -lap-mediated apoptosis requires NQO1 activity. DNA fragmentation was assessed using the TUNEL assay, as described under "Experimental Procedures." Cells were exposed to a 4-h pulse of  $\beta$ -lap alone or in combination with 50  $\mu$ M dicoumarol, and TUNEL assays were performed to monitor apoptosis 44 h later using the APO-DIRECT™ kit. Data were analyzed using an EPICS Elite ESP flow cytometer. Shown are the results of one experiment representative of at least three independent assays.

amount per well as an indicator of cell growth. In all cases, expression of NQO1 led to a marked increase in sensitivity to  $\beta$ -lap (see Fig. 6A). Co-administration of 50  $\mu$ M dicoumarol selectively inhibited  $\beta$ -lap toxicity in all clones that expressed NQO1. Dicoumarol did not affect the relatively more  $\beta$ -lap-resistant Vec-3 or NQ-2 clones, which did not express NQO1.

Opposite results were observed after menadione treatments. Cells expressing NQO1 were more resistant to menadione than NQO1-negative clones, and resistance could be ameliorated by dicoumarol co-administration (data not shown). To demonstrate that this effect was not due simply to transient growth inhibition, we also measured clonogenic survival of the Vec-3, NQ-3, and NQ-7 clones after a 4-h treatment with  $\beta$ -lap alone or in the presence of 50  $\mu$ M dicoumarol (Fig. 6B). Relative survival closely mimicked growth inhibition, demonstrating the sensitizing effect of NQO1 expression on  $\beta$ -lap cytotoxicity. These data clearly established that NQO1 activity was critical for the acute toxicity of  $\beta$ -lap.

To confirm that cell death occurred due to the induction of apoptosis in the NQO1 transfectants, we used TUNEL assays to measure DNA fragmentation due to apoptosis after  $\beta$ -lap treatment. Cells were treated with a 4-h pulse of 8  $\mu$ M  $\beta$ -lap alone or in combination with 50  $\mu$ M dicoumarol, harvested 48 h later, and monitored for apoptosis using TUNEL assays, where terminal deoxynucleotidyl transferase-mediated FITC-dUTP incorporation was measured. As shown in Fig. 7, Vec-3 cells showed less than 2% TUNEL-positive (apoptotic) cells after  $\beta$ -lap treatment. All NQO1-expressing clones showed between 30 and 70% TUNEL-positive cells. Dicoumarol co-administration completely blocked apoptosis-related DNA fragmentation in all of the NQO1-expressing MDA-MB-468 clones. These findings further demonstrated that while certain aspects of  $\beta$ -lap cytotoxicity were unique (e.g. atypical PARP cleavage), other aspects conform to the classic apoptotic pathway (e.g. DNA fragmentation, as measured by TUNEL assays and the presence of a sub-G<sub>0</sub>/G<sub>1</sub> cell population (2)).

We next utilized a number of the NQO1-expressing MDA-MB-468 clones to determine if cytotoxicity equated with corresponding increases in atypical apoptotic proteolysis, as measured by PARP and p53 cleavage. NQO1-expressing clones were exposed to 8  $\mu$ M  $\beta$ -lap for 4 h, and cell lysates were prepared 48 h later. As observed in Fig. 8A, clones with NQO1 expression (i.e. NQ-1, NQ-3, NQ-6, and NQ-7) demonstrated a prevalent 60-kDa PARP cleavage fragment after exposure to 8  $\mu$ M  $\beta$ -lap. The NQO1-negative clone, Vec-3, exhibited no PARP cleavage



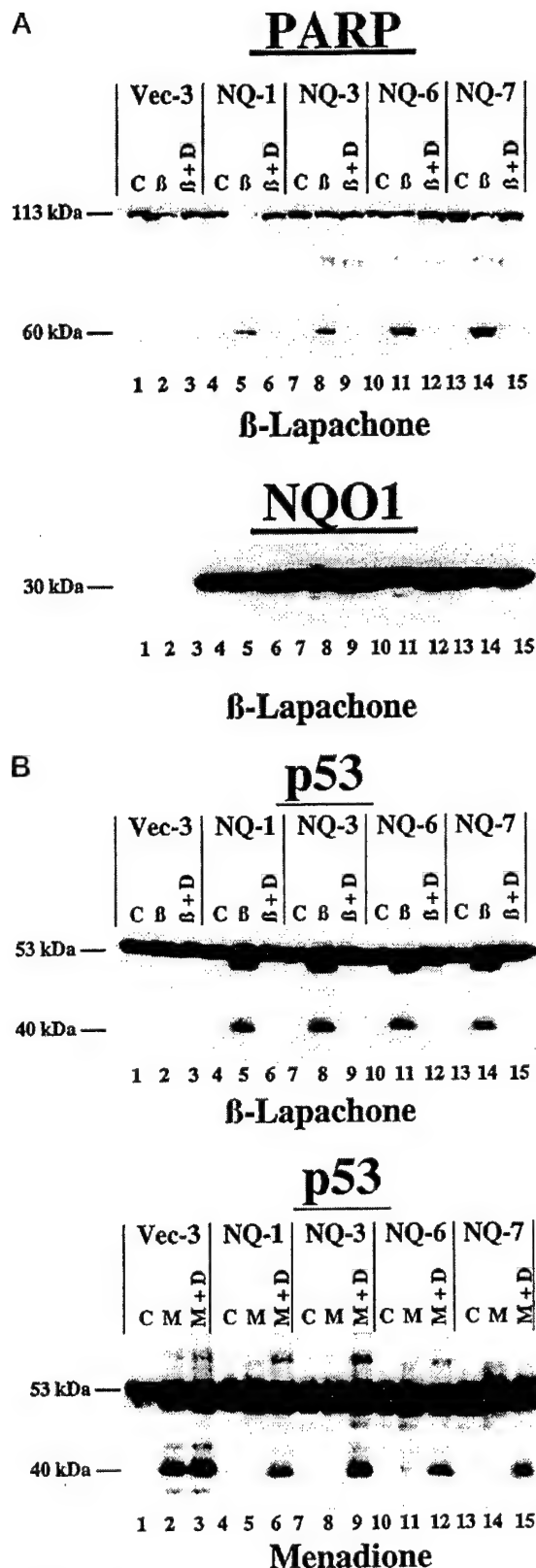


FIG. 8. NQO1 expression sensitizes cells to  $\beta$ -lap-mediated apoptotic proteolysis and inhibits menadione-mediated apoptotic proteolysis. Apoptotic proteolysis was measured in cells exposed to a 4-h pulse of 8  $\mu$ M  $\beta$ -lap alone ( $\beta$ ) or 8  $\mu$ M menadione alone (M) or in combination with 50  $\mu$ M dicoumarol ( $\beta$  + D and M + D, respectively). Whole cell extracts were prepared 44 h after drug treatment and ana-

lyzed using standard Western blot techniques. A, PARP cleavage was assessed using the C-2-10 monoclonal antibody, the blots were then stripped and reprobed with the anti-NQO1 antibody. B, cells were treated with either  $\beta$ -lap or menadione for 4 h and then probed with a p53 antibody (DO-1). Equal protein loading was assessed by Ponceau S staining as described under "Experimental Procedures." Shown is a representative blot from experiments performed at least three times.

at this  $\beta$ -lap dose. We noted cleavage of p53 (resulting in an ~40-kDa fragment) at the same  $\beta$ -lap dose that gave rise to the 60-kDa PARP fragment. Cells exposed to 10  $\mu$ M menadione with or without dicoumarol showed an opposite pattern, as monitored by p53 and PARP cleavage (Fig. 8B and data not shown). Dicoumarol enhanced p53 cleavage after menadione exposure. Importantly, NQO1 expression also led to resistance to menadione-induced p53 cleavage, which could be reversed by co-administration of dicoumarol. Previous studies from our laboratory suggested that both the PARP and p53 cleavage events were the result of activation of the calcium-dependent protease, calpain.<sup>2</sup>

To further characterize the nature by which  $\beta$ -lap could serve as a substrate for NQO1, we measured NADH oxidation using a modified *in vitro* assay. Using purified recombinant human NQO1 or cell extracts containing NQO1, we measured the oxidation of NADH in the presence of either menadione or  $\beta$ -lap. This assay was different from that used to measure NQO1 activity in cell lysates (described in Tables I and II), in that a terminal electron acceptor (*i.e.* cytochrome c) was not included in the reaction. If the substrates (menadione or  $\beta$ -lap) were utilized once in the enzyme reaction, the compounds could not reduce a terminal electron acceptor and would thereby presumably accumulate in their respective hydroquinone forms. This would result in oxidation of 1 mol of NADH/mol of quinone reduced. As expected, menadione reduction resulted in the oxidation of 1–3 mol of NADH/mol of menadione in 2 min and 3–4 mol of NADH/mol of menadione in 3 min using S9 extracts from MCF-7:WS8 or NQ-3 cells (Fig. 9 and data not shown).  $\beta$ -lap resulted in the oxidation of 10–20 mol of NADH/mol of  $\beta$ -lap in 2 min and 50–60 mol of NADH/mol of  $\beta$ -lap in 3 min (Fig. 9). The relative NADH oxidation with  $\beta$ -lap may be an underestimate of  $\beta$ -lap-mediated NADH oxidation, due to exhaustion of reduced NADH at later time points. Using purified NQO1, this effect was even more pronounced, giving rise to oxidation of 10 mol of NADH/mol of  $\beta$ -lap in 10 s and 100 mol of NADH/mol of  $\beta$ -lap in 10 min (data not shown). These results strongly suggest that the hydroquinone form of  $\beta$ -lap is unstable and rapidly undergoes autooxidation to the parent quinone, which can again serve as substrate for reduction by NQO1.

#### DISCUSSION

We demonstrated that  $\beta$ -lap cytotoxicity is dependent upon the expression of the obligate two-electron reductase, NQO1. Dicoumarol, an NQO1 inhibitor, significantly protected NQO1-expressing breast cancer cell lines against all tested aspects of  $\beta$ -lap toxicity, including cell death. Overall, NQO1 expression correlated well with sensitivity of various breast cancer cell lines to the effects of  $\beta$ -lap. Use of the redox cycling compound menadione, which is detoxified by NQO1, demonstrated that the protection offered by dicoumarol is not the result of a global apoptotic inhibition, since dicoumarol significantly enhanced the cytotoxicity of menadione, in cells that expressed NQO1 (Fig. 2). Dicoumarol also did not protect against staurosporine-induced apoptosis, instead demonstrating a very modest enhancement of PARP cleavage. The nature of this response is unknown but may involve signaling through the MEKK1 pathway, as recently described by Cross *et al.* (49). In addition, the relative sensitivities of the cell lines to menadione were oppo-

lyzed using standard Western blot techniques. A, PARP cleavage was assessed using the C-2-10 monoclonal antibody, the blots were then stripped and reprobed with the anti-NQO1 antibody. B, cells were treated with either  $\beta$ -lap or menadione for 4 h and then probed with a p53 antibody (DO-1). Equal protein loading was assessed by Ponceau S staining as described under "Experimental Procedures." Shown is a representative blot from experiments performed at least three times.

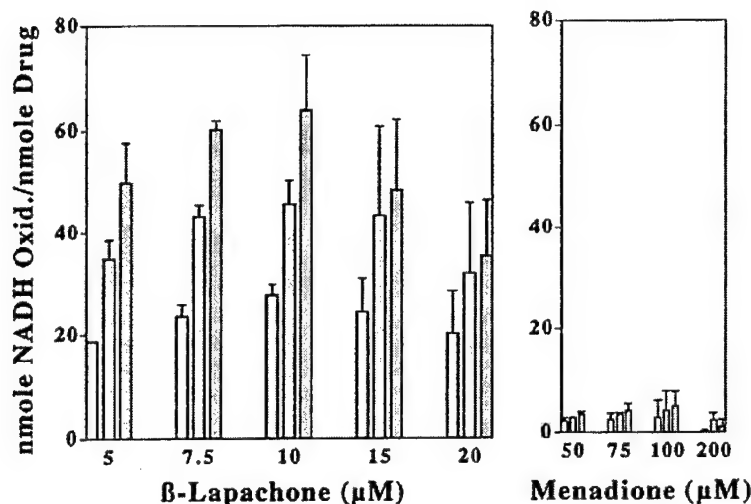


FIG. 9.  $\beta$ -lap-mediated NADH oxidation and futile cycling by NQO1-containing cell extracts. S9 extracts prepared from MCF-7:WS8 cells served as a source for NQO1 and were mixed with 500  $\mu$ M NADH in 50 mM Tris-HCl, pH 7.5, as described under "Experimental Procedures." Reactions were initiated by adding  $\beta$ -lap or menadione, and changes in absorbance at 340 nm (NADH absorbs at 340; NAD<sup>+</sup> does not) were measured over time for 3 min. Total loss of NADH was then calculated and divided by the concentration of  $\beta$ -lap or menadione used. This ratio was then plotted as a function of  $\beta$ -lap or menadione concentration after 1 (light bars), 2 (darker bars), and 3 (darkest bars) min. Shown is a representative graph from experiments repeated at least two times.

site those of  $\beta$ -lap, demonstrating that the  $\beta$ -lap-sensitive cells were not merely sensitive to unrelated cytotoxic compounds. Exogenous expression of NQO1, in NQO1-deficient MDA-MB-468 cells, shifted the LD<sub>50</sub> from >10  $\mu$ M to less than 4  $\mu$ M. While this shift may appear modest, the dose-response curves for both growth inhibition and survival after  $\beta$ -lap treatment were extremely steep. At 4  $\mu$ M  $\beta$ -lap, 60% of the NQO1-negative cells survived, whereas less than 0.05% survival was noted in cells transfected with NQO1. A similarly steep curve was noted with growth inhibition, where treatment with 4  $\mu$ M  $\beta$ -lap led to greater than 90% growth in the NQO1-negative cells and undetectable growth in the NQO1-expressing cells. In both survival and growth measurements, addition of 50  $\mu$ M dicoumarol protected NQO1-expressing cells completely and resulted in values nearly equal to that observed in untreated cells. While these findings suggest that  $\beta$ -lap should show considerable activity against NQO1 expressing tumors, the dose-response curves indicate that the overall drug exposure will undoubtedly need to be closely monitored if this drug is to prove clinically useful.

$\beta$ -lap may be activated by NQO1 in a manner analogous to that of MMC or EO9 (50, 51). However, unlike MMC (52), there is no indication of direct DNA damage by  $\beta$ -lap as assessed by p53 induction, alkaline or neutral filter elution, or covalent complex protein-DNA formation (2, 53, 54). Most specific demonstrations of  $\beta$ -lap activity have come from *in vitro* assays. For example, topoisomerase II $\alpha$ -mediated DNA damage has been observed *in vitro* after treatment with either  $\beta$ -lap or menadione (10). However, the expected downstream effects of this damage (e.g. p53 induction, DNA-topoisomerase II $\alpha$  complexes, etc.) have not been observed (1, 2). In addition, we previously showed that topoisomerase I could be inhibited or activated *in vitro* in a manner distinct from that of the classic topoisomerase I inhibitor, camptothecin (1). Neither "cleavable complex" formation (8) nor increases in the steady state levels of wild-type p53 were observed following  $\beta$ -lap treatment. In contrast, camptothecin or topoisomerase II $\alpha$  inhibitors caused a dramatic increase in p53, as previously reported (1, 55). The observations reported here suggest that  $\beta$ -lap must either be activated (reduced) to inhibit topoisomerases I or II $\alpha$  or that topoisomerase inhibition is not a necessary component of  $\beta$ -lap-mediated cytotoxicity.

One particularly unique aspect of  $\beta$ -lap toxicity is the apparent activation of a novel protease, which we first discerned by observation of an atypical cleavage pattern of the DNA repair protein and apoptotic substrate, PARP.<sup>2</sup> This pattern (giving rise to an ~60-kDa fragment instead of the classic 89-kDa fragment) was unique to  $\beta$ -lap-mediated apoptosis and correlated well with lethality. In addition, investigation of p53 proteolysis after  $\beta$ -lap treatment showed a fragment of ~40 kDa (Fig. 7B), which was similar to that previously attributed to calpain activation (56). Calpain has been implicated in apoptosis in a number of systems (57–59), and we hypothesize that calpain is the primary protease activated in  $\beta$ -lap-mediated cell death.<sup>2</sup> The data regarding the role of calpain as an inducer of apoptosis or simply a component of the execution phase of apoptosis appear to depend upon the cell type and method of apoptosis induction. The demonstration of menadione-induced p53 cleavage (Fig. 8) suggests that this proteolytic pathway is not unique to  $\beta$ -lap. Enhancement of menadione-mediated proteolysis by dicoumarol suggests that the hydroquinone form of menadione is a nontoxic species or is rapidly conjugated and excreted from the cell and does not activate this cell death pathway (60). However, when menadione is reduced to the semiquinone, in the absence of NQO1 activity, it can also undergo a futile cycle, leading to the loss of reduced NAD(P)H (61). This futile cycle is less potent than the  $\beta$ -lap futile cycling but can be activated by high concentrations of menadione in NQO1 expressing cells and lower menadione concentrations in cells lacking NQO1 activity.

While reduction of  $\beta$ -lap appears to be important for its cytotoxic effects against breast cancer cells, the mechanism by which reduction of  $\beta$ -lap leads to toxicity is still unresolved. Our findings regarding the futile cycling of  $\beta$ -lap suggest a possible component of the cytotoxic mechanism.  $\beta$ -lap-mediated exhaustion of NADH in the *in vitro* studies (Fig. 8) suggests that the hydroquinone form of  $\beta$ -lap is unstable and autoxidizes back to the parent compound. In an intact cell, this futile cycle would be expected to continue until one of the critical components of the reaction is exhausted (Fig. 10). Since NQO1 can utilize either NADH or NADPH as electron donors, this futile cycle could lead to a substantial loss of NADH and NADPH with a concomitant rise in NAD<sup>+</sup> and NADP<sup>+</sup> levels. This would have a dramatic effect on any cellular process

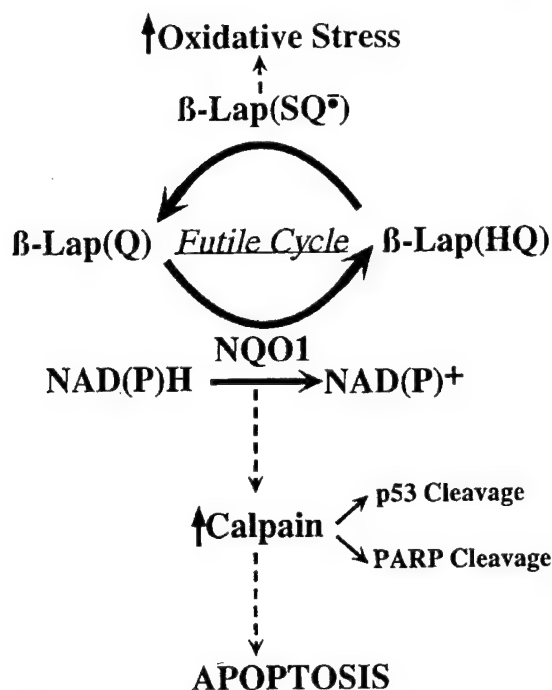


FIG. 10. Proposed model for  $\beta$ -lapachone-mediated cytotoxicity in cells expressing NQO1. In cells that express NQO1, the 1,2-naphthoquinone  $\beta$ -lap(Q) is reduced to the hydroquinone form ( $\beta$ -lap(HQ)) using one molecule of NADH per reaction. The hydroquinone form of  $\beta$ -lap is presumably unstable and spontaneously autoxidizes to its original parent form, probably through a semiquinone intermediate ( $\beta$ -lap(SQ)), which can cause redox cycling and oxidative stress. The regenerated parent compound can then serve as substrate for another round of reduction. This futile cycle causes a rapid and severe loss in reduced NAD(P)H, which ultimately activates calpain by mechanisms that are not completely understood at present.

requiring NADH or NADPH. It is likely that this exhaustion of reduced enzyme co-factors may be a critical factor for the activation of the apoptotic pathway after  $\beta$ -lap treatment. The downstream consequences of this futile cycle are currently under investigation in our laboratory.

At higher doses of  $\beta$ -lap ( $>10 \mu\text{M}$ ), NQO1-negative cells and NQO1-expressing cells treated with dicoumarol were killed by  $\beta$ -lap. This may be due to the production of oxidative stress, as a result of one electron reduction of  $\beta$ -lap by other enzymes, such as cytochrome  $b_5$  reductase and/or cytochrome P-450 reductase (62). One electron reduction of  $\beta$ -lap to the semiquinone would be expected to cause extensive redox cycling with the formation of various reactive oxygen species, and previous studies showed that  $\beta$ -lap caused oxygen radical formation in trypanosomes (63, 64). We speculate that  $\beta$ -lap-mediated free radical formation can be lethal to NQO1-deficient cells, as we previously reported with HL60 cells. The result in these studies was stimulation of a caspase-mediated death pathway (1). This hypothesis is supported by a recent study that showed that  $\beta$ -lap can induce apoptosis in HL-60 cells through peroxide production (65). Alternatively, other members of the NQO1 family that are insensitive to dicoumarol, such as NQO2 (66, 67), may be present and reduce (*i.e.* activate)  $\beta$ -lap when administered at high doses. However, we hypothesize that the production of cytosolic free radicals is not a primary mode of cell death in NQO1-expressing cells, since free radical scavengers (*e.g.*  $\alpha$ -tocopherol, *N*-acetyl-L-cysteine, or pyrrolidinedithiocarbamate) did not significantly affect lethality caused by  $\beta$ -lap exposure (data not shown). The free radical-driven path-

ways may predominate in NQO1-negative cells or in cells with inactivated NQO1. We propose that when active NQO1 is present, the pathway described in Fig. 10 is primarily responsible for cell death.

Our data identifying the intracellular target of  $\beta$ -lap as NQO1 may explain the myriad of *in vitro* and *in vivo* responses reported for this compound.  $\beta$ -lap exposure synergizes with MMS, ionizing radiation, and ultraviolet light irradiation damage (68). We speculate that the synergy between this compound and these DNA damaging agents is related to the induction of NQO1 (cloned as xip-3, an x-ray-inducible protein by our laboratory (18) and that of Fornace *et al.* (69)). This is further supported by the fact that only posttreatments of 4–5 h, and not pretreatments, with  $\beta$ -lap caused synergistic cell killing. Induction of  $\beta$ -lap's target may have been required for synergy, and the induction kinetics of NQO1/XIP3 after ultraviolet light or ionizing radiation exposures (*i.e.*  $\sim 2$  h) appear to fit this mechanism (18).  $\beta$ -lap exposure also prevented the formation of ionizing radiation-inducible secondary neoplastic transformants in Chinese hamster embryo fibroblasts (53). Since NQO1 expression is thought to increase during early stages of neoplastic initiation (possibly due to the permanent induction of a normal stress response, *i.e.* induction of NQO1) (70, 71), it is possible that  $\beta$ -lap administration selectively eliminates genetically damaged cells that constitutively overexpress this preneoplastic marker (*i.e.* NQO1). These data suggest that it may be possible to exploit this IR-inducible NQO1 target protein for improved radiochemotherapy, which would also result in a significantly lower level of IR-induced secondary carcinogenesis, as previously reported (53).

Thus, our data strongly suggest that NQO1 expression is an important determinant of  $\beta$ -lap-mediated apoptosis and lethality. The connection between the futile cycle of oxidation and reduction of  $\beta$ -lap by NQO1 and the activation of calpain-mediated apoptosis (Fig. 10) is currently under investigation in our laboratory. Investigation of this drug should shed light on calpain-mediated cell death processes and yield clinical regimens using  $\beta$ -lap or more efficient drugs in combination with DNA-damaging agents (*e.g.* radiotherapy). Use of this drug against tumors that overexpress NQO1, such as breast, colon, or lung cancers, is indicated. Identification of NQO1 as the intracellular target of  $\beta$ -lap also suggests the use of this compound for chemoprevention, since NQO1 is commonly elevated during neoplastic progression (43).

**Acknowledgments**—We thank Dr. Dan Gustafson and Dr. Charles Waldren for the NQO1 cDNA expression vector. We also thank Dr. Jill Kolesar and Peter Allen for helpful discussions and Dr. David Ross for critical reading of the manuscript.

#### REFERENCES

- Planchon, S. M., Wuerzberger, S., Frydman, B., Witiak, D. T., Hutson, P., Church, D. R., Wilding, G., and Boothman, D. A. (1995) *Cancer Res.* **55**, 3706–3711.
- Wuerzberger, S. M., Pink, J. J., Planchon, S. M., Byers, K. L., Bornmann, W. G., and Boothman, D. A. (1998) *Cancer Res.* **58**, 1876–1885.
- Li, C. J., Averboukh, L., and Pardee, A. B. (1993) *J. Biol. Chem.* **268**, 22463–22468.
- Boothman, D. A., Greer, S., and Pardee, A. B. (1987) *Cancer Res.* **47**, 5361–5366.
- Schuerch, A. R., and Wehrli, W. (1978) *Eur. J. Biochem.* **84**, 197–205.
- Docampo, R., Cruz, F. S., Boveris, A., Muniz, R. P., and Esquivel, D. M. (1979) *Biochem. Pharmacol.* **28**, 723–728.
- Boorstein, R. J., and Pardee, A. B. (1983) *Biochem. Biophys. Res. Commun.* **117**, 30–36.
- Boothman, D. A., Trask, D. K., and Pardee, A. B. (1989) *Cancer Res.* **49**, 605–612.
- Molina Portela, M. P., and Stoppani, A. O. (1996) *Biochem. Pharmacol.* **51**, 275–283.
- Frydman, B., Marton, L. J., Sun, J. S., Neder, K., Witiak, D. T., Liu, A. A., Wang, H. M., Mao, Y., Wu, H. Y., Sanders, M. M., and Liu, L. F. (1997) *Cancer Res.* **57**, 620–627.
- Vanni, A., Fiore, M., De Salvia, R., Cundari, E., Ricordi, R., Ceccarelli, R., and Degrossi, F. (1998) *Mutat. Res.* **401**, 55–63.
- Manna, S. K., Gad, Y. P., Mukhopadhyay, A., and Aggarwal, B. B. (1999)

- Biochem. Pharmacol. 57, 763-774
13. Robertson, N., Haigh, A., Adams, G. E., and Stratford, I. J. (1994) *Eur. J. Cancer* 30A, 1013-1019
14. Cadenas, E. (1995) *Biochem. Pharmacol.* 49, 127-140
15. Ross, D., Beall, H., Traver, R. D., Siegel, D., Phillips, R. M., and Gibson, N. W. (1994) *Oncol. Res.* 6, 493-500
16. Rauth, A. M., Goldberg, Z., and Misra, V. (1997) *Oncol. Res.* 9, 339-349
17. Ross, D., Siegel, D., Beall, H., Prakash, A. S., Mulcahy, R. T., and Gibson, N. W. (1993) *Cancer Metastasis Rev.* 12, 83-101
18. Boothman, D. A., Meyers, M., Fukunaga, N., and Lee, S. W. (1993) *Proc. Natl. Acad. Sci. U. S. A.* 90, 7200-7204
19. Chen, S., Knox, R., Lewis, A. D., Friedlos, F., Workman, P., Deng, P. S., Fung, M., Ebenstein, D., Wu, K., and Tsai, T. M. (1995) *Mol. Pharmacol.* 47, 934-939
20. Jaiswal, A. K., McBride, O. W., Adesnik, M., and Nebert, D. W. (1988) *J. Biol. Chem.* 263, 13572-13578
21. Radjendirane, V., Joseph, P., Lee, Y. H., Kimura, S., Klein-Szanto, A. J. P., Gonzalez, F. J., and Jaiswal, A. K. (1998) *J. Biol. Chem.* 273, 7382-7389
22. Marin, A., Lopez de Cerain, A., Hamilton, E., Lewis, A. D., Martinez-Penuela, J. M., Idoate, M. A., and Bello, J. (1997) *Br. J. Cancer* 76, 923-929
23. Malkinson, A. M., Siegel, D., Forrest, G. L., Gazdar, A. F., Oie, H. K., Chan, D. C., Bunn, P. A., Mabry, M., Dykes, D. J., Harrison, S. D., and Ross, D. (1992) *Cancer Res.* 52, 4752-4757
24. Belinsky, M., and Jaiswal, A. K. (1993) *Cancer Metastasis Rev.* 12, 103-117
25. Joseph, P., Xie, T., Xu, Y., and Jaiswal, A. K. (1994) *Oncol. Res.* 6, 525-532
26. Buettner, G. R. (1993) *Arch. Biochem. Biophys.* 300, 535-543
27. Ross, D., Thor, H., Orrenius, S., and Moldeus, P. (1985) *Chem. Biol. Interact.* 55, 177-184
28. Riley, R. J., and Workman, P. (1992) *Biochem. Pharmacol.* 43, 1657-1669
29. Siegel, D., Beall, H., Senekowitsch, C., Kasai, M., Arai, H., Gibson, N. W., and Ross, D. (1992) *Biochemistry* 31, 7879-7885
30. Prakash, A. S., Beall, H., Ross, D., and Gibson, N. W. (1993) *Biochemistry* 32, 5518-5525
31. Fitzsimmons, S. A., Workman, P., Grever, M., Paull, K., Camalier, R., and Lewis, A. D. (1996) *J. Natl. Cancer Inst.* 88, 259-269
32. Beall, H. D., Murphy, A. M., Siegel, D., Hargreaves, R. H., Butler, J., and Ross, D. (1995) *Mol. Pharmacol.* 48, 499-504
33. Hollander, P. M., and Ernster, L. (1975) *Arch. Biochem. Biophys.* 169, 560-567
34. Hosoda, S., Nakamura, W., and Hayashi, K. (1974) *J. Biol. Chem.* 249, 6416-6423
35. Duthie, S. J., and Grant, M. H. (1989) *Br. J. Cancer* 60, 566-571
36. Akman, S. A., Doroshow, J. H., Dietrich, M. F., Chlebowski, R. T., and Block, J. S. (1987) *J. Pharmacol. Exp. Ther.* 240, 486-491
37. Thor, H., Smith, M. T., Hartzell, P., Bellomo, G., Jewell, S. A., and Orrenius, S. (1982) *J. Biol. Chem.* 257, 12419-12425
38. Siegel, D., McGuinness, S. M., Winski, S. L., and Ross, D. (1999) *Pharmacogenetics* 9, 113-121
39. Gustafson, D. L., Beall, H. D., Bolton, E. M., Ross, D., and Waldren, C. A. (1996) *Mol. Pharmacol.* 50, 728-735
40. Sambrook, J., Fritsch, E. F., and Maniatis, T. (1989) *Molecular Cloning: A Laboratory Manual*, pp. 16.33-16.36, Cold Spring Harbor Laboratory, Cold Spring Harbor, NY
41. Pink, J. J., Bilimoria, M. M., Assikis, J., and Jordan, V. C. (1996) *Br. J. Cancer* 74, 1227-1236
42. Labarca, C., and Paigen, K. (1980) *Anal. Biochem.* 102, 344-352
43. Siegel, D., Franklin, W. A., and Ross, D. (1998) *Clin. Cancer Res.* 4, 2065-2070
44. Hollander, P. M., Bartfai, T., and Gatt, S. (1975) *Arch. Biochem. Biophys.* 169, 568-576
45. Strobel, H. W., and Dignam, J. D. (1978) *Methods Enzymol.* 52, 89-96
46. Beall, H. D., Mulcahy, R. T., Siegel, D., Traver, R. D., Gibson, N. W., and Ross, D. (1994) *Cancer Res.* 54, 3196-3201
47. Kaufmann, S. H., Desnoyers, S., Ottaviano, Y., Davidson, N. E., and Poirier, G. G. (1993) *Cancer Res.* 53, 3976-3985
48. Preusch, P. C., Siegel, D., Gibson, N. W., and Ross, D. (1991) *Free Radical Biol. Med.* 11, 77-80
49. Cross, J. V., Deak, J. C., Rich, E. A., Qian, Y., Lewis, M., Parrott, L. A., Mochida, K., Gustafson, D., Vande Pol, S., and Templeton, D. J. (1999) *J. Biol. Chem.* 274, 31150-31154
50. Siegel, D., Gibson, N. W., Preusch, P. C., and Ross, D. (1990) *Cancer Res.* 50, 7483-7489
51. Keyes, S. R., Fracasso, P. M., Heimbrook, D. C., Rockwell, S., Sligar, S. G., and Sartorelli, A. C. (1984) *Cancer Res.* 44, 5638-5643
52. Hess, R., Plaumann, B., Lutum, A. S., Haessler, C., Heinz, B., Fritsche, M., and Brandner, G. (1994) *Toxicol. Lett.* 72, 43-52
53. Boothman, D. A., and Pardee, A. B. (1989) *Proc. Natl. Acad. Sci. U. S. A.* 86, 4963-4967
54. Boothman, D. A., Wang, M., Schea, R. A., Burrows, H. L., Strickfaden, S., and Owens, J. K. (1992) *Int. J. Radiat. Oncol. Biol. Phys.* 24, 939-948
55. Nelson, W. G., and Kastan, M. B. (1994) *Mol. Cell. Biol.* 14, 1815-1823
56. Kubbutat, M. H., and Vousden, K. H. (1997) *Mol. Cell. Biol.* 17, 460-468
57. Squier, M. K., and Cohen, J. J. (1997) *J. Immunol.* 158, 3690-3697
58. Wood, D. E., and Newcomb, E. W. (1999) *J. Biol. Chem.* 274, 8309-8315
59. Squier, M. K., Sehnert, A. J., Sellins, K. S., Malkinson, A. M., Takano, E., and Cohen, J. J. (1999) *J. Cell. Physiol.* 178, 311-319
60. Wefers, H., and Sies, H. (1983) *Arch. Biochem. Biophys.* 224, 568-578
61. Bellomo, G., Jewell, S. A., and Orrenius, S. (1982) *J. Biol. Chem.* 257, 11558-11562
62. Iyanagi, T. (1990) *Free Radical Res. Commun.* 8, 259-268
63. Molina Portela, M. P., Fernandez Villamil, S. H., Perissinotti, L. J., and Stoppani, A. O. (1996) *Biochem. Pharmacol.* 52, 1875-1882
64. Docampo, R., Cruz, F. S., Boveris, A., Muniz, R. P., and Esquivel, D. M. (1978) *Arch. Biochem. Biophys.* 186, 292-297
65. Chau, Y. P., Shiah, S. G., Don, M. J., and Kuo, M. L. (1998) *Free Radical Biol. Med.* 24, 660-670
66. Zhao, Q., Yang, X. L., Holtzclaw, W. D., and Talalay, P. (1997) *Proc. Natl. Acad. Sci. U. S. A.* 94, 1669-1674
67. Jaiswal, A. K. (1994) *J. Biol. Chem.* 269, 14502-14508
68. Boorstein, R. J., and Pardee, A. B. (1984) *Biochem. Biophys. Res. Commun.* 118, 828-834
69. Fornace, A. J., Jr., Alamo, I., Jr., and Hollander, M. C. (1988) *Proc. Natl. Acad. Sci. U. S. A.* 85, 8800-8804
70. Williams, J. B., Wang, R., Lu, A. Y., and Pickett, C. B. (1984) *Arch. Biochem. Biophys.* 232, 408-413
71. Farber, E. (1984) *Can. J. Biochem. Cell Biol.* 62, 486-494

## Research Paper

# $\mu$ -Calpain Activation in $\beta$ -Lapachone-Mediated Apoptosis

Colleen Tagliarino

John J. Pink

Kathryn E. Reinicke

Sara M. Simmers

Shelly M. Wuerzberger-Davis

David A. Boothman

Departments of Radiation Oncology and Pharmacology, Case Western Reserve University, Cleveland, Ohio USA

\*Correspondence to: David A. Boothman, Ph.D.; Department of Radiation Oncology (BRB-326 East); Laboratory of Molecular Stress Responses; Case Western Reserve University; 10900 Euclid Ave.; Cleveland, Ohio 44106-4942 USA; Tel.: 216.368.0840; Fax 216.368.1142; E-mail: dab30@po.cwru.edu.

Received 12/02/02; Accepted 01/07/03

Previously published online as a CB&T "Paper in Press" at: <http://landesbioscience.com/journals/cbt/>

## KEY WORDS

$\beta$ -Lapachone, Apoptosis,  $Ca^{2+}$ , Calpain, Breast cancer

## ABBREVIATIONS

$\beta$ -Lap	$\beta$ -Lapachone
MCF-7	MCF-7/WS8
MDA-468	MDA-MD-468
NQO1	NAD(P)H:Quinone Oxidoreductase, DT-diaphorase (E.C. 1.6.99.2)
PARP	Poly(ADP-ribose) polymerase
TUNEL	Terminal deoxynucleotidyl transferase-mediated dUTP nick end labeling
ER	Endoplasmic reticulum
STS	Staurosporine
TPT	Topotecan
LD <sub>50</sub>	50 % lethal dose
IC <sub>50</sub>	50% inhibitory concentration
NF- $\kappa$ B	Nuclear transcription factor- $\kappa$ B
pRb	Retinoblastoma protein

This work was supported by United States Army Medical Research and Materiel Command Breast Cancer Initiative Grant DAMD17-98-1-8260 (to D.A.B.), Predoctoral Fellowship DAMD17-00-1-0194 (to C.T.), and Postdoctoral Fellowship DAMD-17-97-1-7221 (to J.J.P.). This work was also supported by an NIH R01 grant (CA92250) to D.A.B.

## ABSTRACT

$\beta$ -Lapachone ( $\beta$ -Lap) triggers apoptosis in a number of human breast and prostate cancer cell lines through a unique apoptotic pathway that is dependent upon NQO1, a two-electron reductase. Recently, our laboratory showed that  $\beta$ -lap-exposed MCF-7 cells exhibited an early increase in intracellular cytosolic  $Ca^{2+}$  from endoplasmic reticulum stores, and that BAPTA-AM (an intracellular  $Ca^{2+}$  chelator) blocked these early increases and partially inhibited all aspects of  $\beta$ -lap-induced apoptosis. We now show that exposure of NQO1-expressing breast cancer cells to  $\beta$ -lap stimulates a unique proteolytic apoptotic pathway involving  $\mu$ -calpain activation. No apparent activation of m-calpain was noted. Upon activation,  $\mu$ -calpain translocated to the nucleus concomitant with specific nuclear proteolytic events. Apoptotic responses in  $\beta$ -lap-exposed NQO1-expressing cells were significantly delayed and survival enhanced by exogenous over-expression of calpastatin, a natural inhibitor of  $\mu$ - and m-calpains. Furthermore, purified  $\mu$ -calpain cleaved PARP to a unique fragment (~60 kDa), not previously reported for calpains. We provide evidence that  $\beta$ -lap-induced,  $\mu$ -calpain-stimulated apoptosis does not involve any known apoptotic caspases; the activated fragments of caspases were not observed after  $\beta$ -lap exposures, nor were there any changes in the pro-enzyme forms as measured by Western blot analyses. The ability of  $\beta$ -lap to trigger an apparently novel, p53-independent, calpain-mediated apoptotic cell death further support the development of this drug for improved breast cancer therapy.

## INTRODUCTION

Apoptosis is an evolutionarily conserved pathway of biochemical and molecular events that underlie certain cell death processes involving the activation of intracellular zymogens. Once apoptosis is initiated, biochemical and morphological changes occur irreversibly that commit the cell to die. These changes include: DNA fragmentation, chromatin condensation, cytoplasmic membrane blebbing, cleavage of apoptotic substrates (e.g., PARP, lamin B), and loss of mitochondrial membrane potential with concomitant release of cytochrome c into the cytoplasm.<sup>1</sup>

Apoptosis is a highly regulated, active process that requires the participation of endogenous proteases that systematically dismantle the cell. The most well-characterized proteases in apoptosis are caspases, aspartate-specific cysteine proteases, that work through a cascade initiated by either:

- a. mitochondrial membrane depolarization leading to the release of cytochrome c and Apaf-1 into the cytoplasm,<sup>2</sup> that then activates caspase 9<sup>3</sup>; or
- b. activation of receptor-mediated caspase activation complexes (e.g., TRADD/MORT1) that initiate caspase pathways primarily via the activation of caspases 8 and 10 (reviewed in ref. 4).

In contrast, non-caspase-mediated pathways are less well understood and specific activation pathways have only been superficially described.

Calpains are a family of cysteine proteases existing primarily in two forms designated by the  $Ca^{2+}$  concentration needed for activation in vitro,  $\mu$ -calpain (calpain-I) and m-calpain (calpain-II). Each form is a heterodimer consisting of a large catalytic and a small regulatory subunit that are activated by increased intracellular  $Ca^{2+}$  concentrations. Calpains have been implicated in neutrophil apoptosis, glucocorticoid-induced thymocyte apoptosis, and adipocyte differentiation, but their patterns of activation are not well characterized.<sup>5-7</sup> Calpains are predominantly located in the cytoplasm,<sup>8,9</sup> but can translocate to cellular membranes where they can become activated.<sup>10</sup> Translocations to nuclear compartments have not been described in detail. Calpastatin is a specific, endogenous inhibitor of both m- and  $\mu$ -calpains. Calpastatin binds the catalytic subunits of calpains when associated



with the regulatory subunit and only in the presence of  $\text{Ca}^{2+}$ .<sup>11,12</sup> Calpastatin does not inhibit the muscle-specific calpain, p94, nor other known proteases (e.g., papains, trypsin).<sup>13-17</sup>

$\beta$ -Lapachone ( $\beta$ -Lap) is a naturally occurring quinone present in the bark of the South American Lapacho tree. The drug has anti-tumor activity against a variety of human cancers, including colon, prostate, promyelocytic leukemia, and breast.<sup>18-20</sup>  $\beta$ -Lap was an effective agent alone, and in combination with taxol, against human ovarian and prostate xenografts in mice, with low-level host toxicity.<sup>21</sup>  $\beta$ -Lap induced apoptosis in a number of cell lines as detected by the formation of a sub  $G_0$ - $G_1$  cell population visualized by propidium iodide staining,<sup>19</sup> acridine orange staining,<sup>22</sup> Annexin V staining,<sup>23</sup> nuclear condensation and DNA laddering.<sup>20,23</sup>

We recently demonstrated that  $\beta$ -lap killed human breast and prostate cancer cells by an apoptotic response significantly enhanced by NAD(P)H:quinone oxidoreductase (NQO1, E.C. 1.6.99.2) enzymatic activity.<sup>20,24</sup>  $\beta$ -Lap cytotoxicity was prevented by cotreatment with dicumarol (an NQO1 inhibitor) in NQO1-expressing breast and prostate cancer cells.<sup>20,24</sup> NQO1 is a cytosolic enzyme elevated in breast cancers<sup>25</sup> that catalyzes a two-electron reduction of quinones (e.g.,  $\beta$ -lap, menadione), utilizing either NADH or NADPH as electron donors. We recently showed that reduction of  $\beta$ -lap by NQO1 presumably led to a futile cycling of the compound, wherein the quinone and hydroquinone redox cycle with a net concomitant loss of reduced NAD(P)H.<sup>24</sup> Furthermore, elevated intracellular  $\text{Ca}^{2+}$  levels were critical for apoptosis induced by  $\beta$ -lap.<sup>26</sup> Increased cytosolic  $\text{Ca}^{2+}$ , due to ER  $\text{Ca}^{2+}$  pool depletion, led to loss of mitochondrial membrane potential, ATP depletion, specific and unique substrate proteolysis, DNA fragmentation, and cell death by apoptosis.<sup>26</sup>

We previously showed that apoptosis in human cancer cells following  $\beta$ -lap administration was unique, in that an ~60 kDa cleavage fragment of poly(ADP-ribose) polymerase (PARP), as well as a distinct intracellular proteolytic cleavage of p53, were observed in NQO1-expressing human breast or prostate cancer cells.<sup>20,24,26</sup> These cleavage events were distinct from those observed when caspases were activated by topoisomerase I poisons, staurosporine, or administration of Granzyme B.<sup>27,28</sup> Furthermore,  $\beta$ -lap-mediated cleavage events were blocked by dicumarol (an inhibitor of NQO1), global cysteine protease inhibitors, as well as both intra- and extracellular  $\text{Ca}^{2+}$  chelators.<sup>26,27</sup> Based on these data, we concluded that  $\beta$ -lap exposure of NQO1-expressing breast and prostate cancer cells elicited the activation of a  $\text{Ca}^{2+}$ -dependent protease with properties similar to calpain. In particular, the p53 cleavage pattern of  $\beta$ -lap-exposed cells<sup>24,27</sup> was remarkably similar to the pattern observed after calpain activation in various cell systems.<sup>29,30</sup>

In this study, we show that  $\beta$ -lap mediates a unique proteolytic apoptotic pathway in NQO1-expressing cells via  $\mu$ -calpain activation. Upon activation,  $\mu$ -calpain translocates to the nucleus where it can proteolytically cleave PARP and p53. We provide evidence that suggests that  $\beta$ -lap-induced,  $\mu$ -calpain stimulated, apoptosis does not involve any of the known caspases, including caspase 12; caspase 12 has been linked downstream of m-calpain activation in some studies.<sup>31</sup> Furthermore, the apoptotic responses in NQO1-expressing cells to  $\beta$ -lap can be significantly delayed, and survival enhanced via the exogenous over-expression of calpastatin, a natural calpain inhibitor.

## MATERIALS AND METHODS

**Reagents.**  $\beta$ -Lap (3,4-dihydro-2, 2-dimethyl-2H-naphtho [1,2b] pyran-5, 6-dione) was synthesized by Dr. William G. Bornmann (Memorial Sloan Kettering, NY, NY), dissolved in DMSO at 10 mM, and the concentration verified by spectrophotometric analyses as described.<sup>19,27</sup> Menadione, staurosporine, ionomycin, dicumarol, bovine serum albumin, saponin, and the acetyl-calpastatin peptide inhibitor (CN) were obtained from Sigma Chemical Co. (St. Louis, MO). PARP cDNA was a gracious gift from Dr. Xiaodong Wang (University of Texas Southwestern Medical School, TX) and was cloned into pcDNA3.1HisB (Invitrogen, Carlsbad, CA). Calpastatin cDNA was cloned into the mammalian expression vector pcDNA1-neo (Invitrogen) and was a gracious gift from Dr. Marc Piechaczyk (Institut de Genetique Moleculaire, Montpellier, France).

**Cell Culture.** MCF-7:WS8 (MCF-7) human breast cancer cells were obtained from Dr. V. Craig Jordan, (Northwestern University, Chicago, IL). NQO1-deficient MDA-MB-468 (MDA-468) cells were obtained from the American Type Culture Collection and stably transfected with the NQO1 cDNA in the pcDNA3 constitutive expression vector as described (MDA-468-NQ3).<sup>24</sup> Tissue culture components were purchased from Life Technologies, Inc., unless otherwise stated. Cells were grown in RPMI 1640 cell culture medium supplemented with 10% fetal bovine serum, in a 37°C humidified incubator with 5%  $\text{CO}_2$  and 95% air atmosphere as described.<sup>19,27</sup> For all experiments, log-phase MCF-7 breast cancer cells were exposed to 5  $\mu\text{M}$   $\beta$ -lap for 4 h and MDA-468-NQ3 breast cancer cells were exposed to 8  $\mu\text{M}$   $\beta$ -lap for 4 h. Fresh medium was then added and cells harvested at various times post-treatment.

**Stable Transfection.** MCF-7 cells were seeded at  $2.5 \times 10^5$  cells/well in 6-well plates and allowed to attach overnight. The following day, 1.0  $\mu\text{g}$  of plasmid DNA containing human calpastatin cDNA in the pcDNA1-Neo constitutive expression vector was added to each well using Effectene, as per manufacturer's instructions (Qiagen, Valencia, CA). Cells were selected for growth in 250  $\mu\text{g}/\text{ml}$  Geneticin® (G418, Life Technologies, Inc.) one day later. A stable, pooled population was established after approximately three weeks, and subsequent clones were isolated by limiting dilution cloning, as described.<sup>32</sup>

**Western Blot Analyses.** Whole cell extracts from DMSO control or  $\beta$ -lap-exposed breast cancer cells were prepared and analyzed by SDS-PAGE-Western blot analyses as described.<sup>19,27</sup> Loading equivalence and transfer efficiency were monitored by Western blot analyses of proteins known not to be altered in MCF-7 cells following  $\beta$ -lap exposures;<sup>19</sup> Ponceau S staining of the membrane was also used to verify loading. Probed membranes were then exposed to X-ray film for an appropriate time and developed. Dilutions of 1:7,000 for  $\alpha$ -PARP C2-10 antibody (Enzyme Systems Products; Livermore, CA); 1:5,000 for the  $\alpha$ -PARP H-250; and 1:2,000 for  $\alpha$ -p53 DO-1,  $\alpha$ -cyclin D1 HD11, and  $\alpha$ -lamin B (Santa Cruz; Santa Cruz, CA) antibodies were made. A 1:1,500 dilutions for  $\alpha$ -calpain small subunit MAB3083,  $\alpha$ -Calpastatin MAB3084,  $\alpha$ -m-calpain AB1625,  $\alpha$ - $\mu$ -calpain MAB3104 (Chemicon, Temecula, CA), and 1:2,000 for  $\alpha$ -actin (Amersham Pharmacia Biotech, Piscataway, NJ) were used as described.<sup>19,27</sup> The specificity of anti-calpain antibodies used were evaluated by Western blot analyses; antibodies to the catalytic subunit, anti-m-calpain AB1625, and anti- $\mu$ -calpain MAB3104 only recognized one polypeptide band, and the m-calpain antibody did not cross-react with the activated fragment of  $\mu$ -calpain, nor did it exhibit an activated fragment of its own (data not shown, Fig. 1 and Fig. 2).

**Caspase Activation.** Whole cell extracts from DMSO control,  $\beta$ -lap-, staurosporine (STS)-, or topotecan (TPT)-exposed MDA-468-NQ3 cells were prepared and analyzed by SDS-PAGE-Western blot analyses for specific loss of caspase pro-enzyme forms. The formation of corresponding cleavage fragments, indicative of active caspase enzymes, was also examined where applicable. Cells were exposed to a 4 h pulse of 8.0  $\mu\text{M}$   $\beta$ -lap or continuous exposures of 1.0  $\mu\text{M}$  STS or 10  $\mu\text{M}$  TPT for 24 h. Dilutions of 1:1,500 for  $\alpha$ -caspase 3 and  $\alpha$ -caspase 7 B-94-1 (Pharmingen, San Diego, CA), 1:1,500 for  $\alpha$ -caspase 8 1H10E4H10 and  $\alpha$ -caspase 10 25C2F2 (Zymed, San Francisco, CA), 1:1,000 for  $\alpha$ -caspase 6 K-20 (Santa Cruz, Santa Cruz, CA),

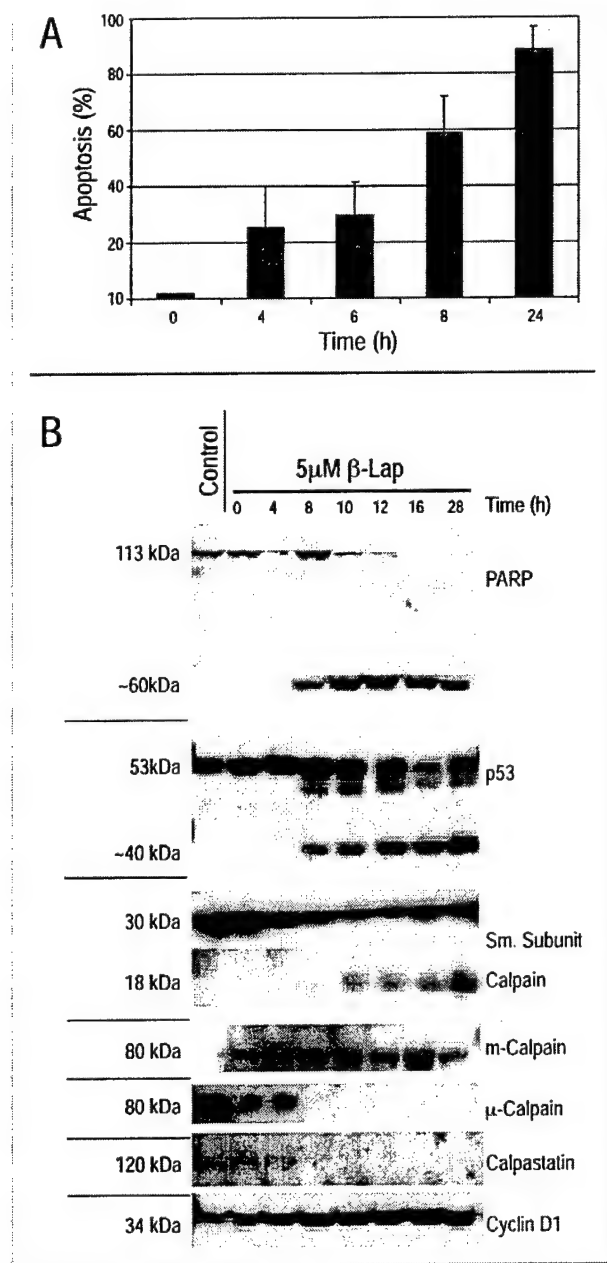


Figure 1. μ-Calpain activation in β-lap-mediated apoptosis. (A) TUNEL assays were performed to monitor DNA fragmentation at times indicated in MCF-7 cells after a 4 h pulse of 5 μM β-lap. Results are graphically summarized as the average of at least three independent experiments, mean ± S.E. (B) Apoptotic proteolysis was measured in MCF-7 cells exposed to a 4 h pulse of 5 μM β-lap, under identical conditions described in 1A. Whole cell extracts were prepared at the indicated times and analyzed using standard Western blotting techniques with antibodies to PARP, p53, the small subunit of calpains (2 different exposure times for full-length and cleavage fragment), m-calpain, μ-calpain, calpastatin, and cyclin D1. Shown are representative Western blots of whole cell extracts from experiments performed at least three times.

Table 1 β-LAP EXPOSURES DID NOT LEAD TO CASPASE ACTIVATION IN NQO1-EXPRESSING BREAST CANCER CELLS

Protease	STS	TPT	β-Lap
μ-Calpain	-	-	+
m-Calpain	-	-	-
Caspase 3	+	+	-
Caspase 6	-	+	-
Caspase 7	+	+	-
Caspase 8	+	+	-
Caspase 9	+	+	-
Caspase 10	+	+	-
Caspase 12	-	-	-

Western blot analyses were performed to assess protease activation of specific caspases determined by loss of pro-enzyme forms with concomitant appearance of cleavage fragments representative of active enzyme forms. NQO1-expressing MDA-468-NQ3 cells were exposed to either a 4 h pulse of 8 μM β-lap or to continuous exposure with 1 μM STS or 10 μM TPT. Cells were then harvested at 24 h following STS or TPT treatments and at 6, 8, 10, 12 and 24 h after exposure to β-lap. Experiments were performed at least twice.

2.0 μg/ml for α-caspase 9 96-2-22 (Upstate Biotechnology, Lake Placid, NY), and 1.0 μg/ml for α-caspase 12 NT (Exalpha Biologicals, Boston, MA) were used as recommended by the corresponding manufacturer.

**TUNEL Assays.** MCF-7 and MDA-468-NQ3 cells were seeded at 1 x 10<sup>6</sup> cells per 10 cm<sup>2</sup> tissue culture dish. Log-phase cells were then treated for 4 h with β-lap, as described above. Medium was collected from experimental as well as control conditions at times indicated, and attached along with floating cells were monitored for apoptosis using TUNEL 3'-biotinylated DNA end labeling via the APO-DIRECT kit (Pharmingen, San Diego, CA) as described.<sup>24</sup> Apoptotic cells were analyzed and quantified using an EPICS XL-MCL flow cytometer that contained an air-cooled argon laser at 488 nm, 15 mW (Beckman Coulter Electronics; Miami, FL) and XL-MCL acquisition software provided with the instrument.

**Calpain Cleavage Assay.** PARP protein was translated using an in vitro transcription and translation TNT-coupled Reticulocyte Lysate system (Promega, Madison, WI) according to manufacturer's instructions. <sup>35</sup>S-Methionine-labeled protein (1–2 μl) was incubated with either 0.05 U of recombinant human erythrocyte μ-calpain (Calbiochem, San Diego, CA), 20 U of recombinant caspase 3 (BioMol, Plymouth, PA), or 30 μg of cell lysate from control or β-lap-treated cells, unless otherwise indicated, in 100 μM CaCl<sub>2</sub>. Reactants were incubated at 37°C for 1 h. The reaction mix was then treated 1:1 with 2X SDS-loading buffer, boiled for 5 min at 90°C, and proteins separated by 9% SDS-PAGE. Gels were fixed and proteins were visualized by autoradiography. MCF-7 or MDA-468-NQ3 cells were separately treated for 4 h with β-lap (indicated above), or with 25 μM Menadione or continuously with 10 μM ionomycin. Cells were harvested at 8 h or 10 h, respectively, in lysis buffer (10 mM HEPES pH 7.4, 5 mM MgCl<sub>2</sub>, 42mM KCl and 0.32 M sucrose) unless otherwise indicated, and sonicated. Protein concentrations were determined using Bradford assays (Bio-Rad, Hercules, CA) using a BSA standard curve as described.<sup>33</sup>

**Colony-Forming Assays.** Cells were seeded into 60-mm dishes (2000 cells/dish in duplicate) and allowed to attach overnight to initiate log-phase growth. Cells were then exposed to a 4 h pulse of β-lap (1.5 μM or 3 μM) or DMSO. Medium was removed, fresh medium was added, and cells were allowed to grow for seven days. Plates were then washed and stained with crystal violet in 50% methanol. Colonies of >50 normal-appearing cells were then counted and data graphed and analyzed as described.<sup>20,24</sup>

**Confocal Microscopy.** Cells were plated on a 6-well microscope slide and allowed to attach and reach log-phase growth. MCF-7 or MDA-468-NQ3 cells were treated for 4 h with 25 μM menadione, 5 μM or 8 μM β-lap, respectively, or continuously with 1 μM STS or 3 μM ionomycin.

Where indicated, dicumarol (50  $\mu$ M) was concomitantly added with  $\beta$ -lap for 4 h. MCF-7 or MDA-468-NQ3 cells were fixed at 8 h or 10 h, respectively, in 3.7% formaldehyde for 5 min. Cells were left overnight at 4°C in PBS and indirect immunofluorescent staining performed after cells were permeabilized in 100% methanol for 10 min at -20°C. Cells were incubated in primary antibody for 2 h at 37°C at dilutions of 1:100 for  $\alpha$ - $\mu$ -calpain 9A4H8D3 (Alexis Corp., San Diego, CA), 1:75 for  $\alpha$ -calpastatin MAB3084 (Chemicon, Temecula, CA), and 1:50  $\alpha$ -NQO1 that was contained in medium from mouse hybridoma clone A180;<sup>34</sup> all antibodies were diluted in 1% BSA and 0.005% saponin in PBS. Cells were then washed twice for 30 min each in 0.005% saponin in PBS and incubated for 1 h at room temp in secondary FITC-anti-mouse (Vector, Burlingame, CA) at a dilution of 1:50 in antibody diluting buffer. Cells were then washed twice for 30 min each in wash buffer and incubated overnight in fresh wash buffer at 4°C. Slides were coated with mounting medium containing propidium iodide (Vector, Burlingame, CA) for 5 min and imaged with a Bio-Rad MRC-600 confocal microscope (Hercules, CA) equipped with a 63X N.A. 1.25 oil immersion plan-neofluor objective at room temp. Confocal images were collected using dual excitation at 488 nm and 568 nm from a krypton/argon laser. The epitope for the  $\alpha$ - $\mu$ -calpain antibody recognizes amino acids 465-520 (domain III of the catalytic subunit) of human  $\mu$ -calpain; domain III is the least homologous domain between  $\mu$ - and m-calpain. The  $\alpha$ - $\mu$ -calpain antibody did not cross-react with m-calpain or calpastatin, nor did the  $\alpha$ -m-calpain antibody cross-react with  $\mu$ -calpain. There was no change in m-calpain immunoreactivity after drug exposures (see Results).

## RESULTS

**Exposure of MCF-7 Cells to  $\beta$ -Lap Resulted in  $\mu$ -Calpain Activation in a Temporal Manner Corresponding to Cell Death.** Log-phase MCF-7 cells were treated for 4 h with 5  $\mu$ M  $\beta$ -lap, at which time fresh medium was added. Cells were harvested at the indicated times and analyzed for substrate proteolysis,  $\mu$ - and m-calpain activation (via western blot analyses), and apoptosis. Treatment of MCF-7 cells with  $\beta$ -lap resulted in ~25% apoptotic cells at 4–6 h post-treatment, ~60% apoptosis at 8 h, and >90% apoptotic cells by 24 h, as measured by TUNEL analyzes (Fig. 1A). TUNEL data was correlated with morphological analyses via phase contrast microscopy and Hoechst staining for nuclear condensation as described,<sup>20</sup> indicating that TUNEL data was representative of apoptotic cells. Treatment of MCF-7 cells with  $\beta$ -lap also resulted in PARP and p53 proteolysis 8 h post-treatment, and complete loss of full-length PARP protein by 16 h post-treatment (Fig. 1B). Proteolysis of the 113 kDa full-length PARP protein to an ~60 kDa cleavage fragment was distinct from that observed after caspase activation (e.g., 89 and 24 kDa fragments) and occurred at the same time p53 was cleaved to a characteristic calpain cleavage fragment of ~40 kDa (Fig. 1B).<sup>29,30,35</sup> Calpain activation was assessed using autolysis of the regulatory (30 kDa full-length protein to an 18 kDa fragment), as well as the catalytic subunit of  $\mu$ -calpain (80 kDa full-length protein to 76 or 78 kDa fragments).<sup>10,30</sup> PARP and p53 underwent proteolysis in a temporal manner corresponding to autolysis of the regulatory subunit of calpain and loss of full-length  $\mu$ -calpain (Fig. 1B). Calpastatin, an endogenous inhibitor of calpains, was degraded by 8 h post-treatment at the same time the small subunit of calpain underwent autolysis and full-length  $\mu$ -calpain was cleaved (Fig. 1B), further implicating calpain activation in  $\beta$ -lap-induced apoptosis. Apoptotic and calpain substrate proteolysis were observed at the same time >50% of cells exposed to  $\beta$ -lap exhibited apoptosis (8 h), as determined by DNA fragmentation measured by the TUNEL assay (Fig. 1A). The other ubiquitously expressed form of calpain, m-calpain, was not lost (80 kDa) nor cleaved to a fragment (76 kDa) indicative of activation. These data indicate that m-calpain was not activated in NQO1-expressing cells after  $\beta$ -lap exposures (Fig. 1B). Similarly, cyclin D1 levels remained unchanged in  $\beta$ -lap-treated MCF-7 cells, as previously described.<sup>19</sup> Consistent with previous results, neither calpain activation nor cell death (loss of survival) occurred in NQO1-deficient cells following a 4 h, 8  $\mu$ M  $\beta$ -lap exposure (data not shown, ref. 24).

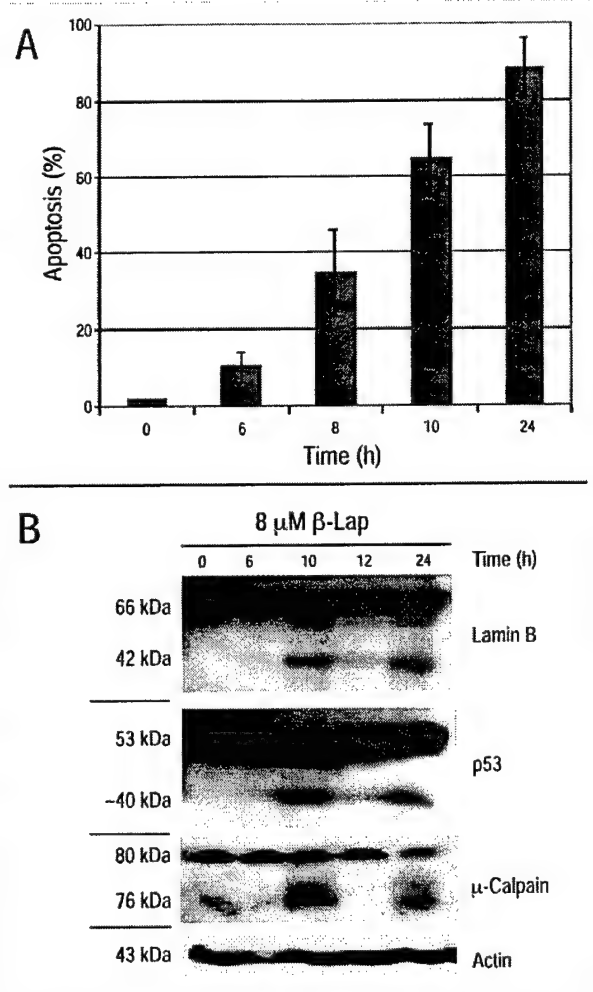


**Figure 2.**  $\mu$ -Calpain activation, but not caspase activation, during  $\beta$ -lap-mediated apoptosis in NQO1-expressing MDA-468-NQ3 cells. (A) TUNEL assays were performed to monitor DNA fragmentation in MDA-468-NQ3 cells at the times indicated after a 4 h pulse of 8  $\mu$ M  $\beta$ -lap. Results are graphically summarized as the average of at three independent experiments, mean  $\pm$  S.E. (B) Apoptotic proteolysis was measured in MDA-468-NQ3 cells exposed to a 4 h pulse of 8  $\mu$ M  $\beta$ -lap. Whole cell extracts were prepared at the indicated times and analyzed using standard Western blotting techniques using antibodies to lamin B, p53,  $\mu$ -calpain and actin. Shown is a representative Western blot of whole cell extracts from experiments performed at least three times.

**$\mu$ -Calpain Activation Occurred Independent of Caspases, in NQO1-expressing Breast Cancer Cells After  $\beta$ -Lap Exposure.** Caspase activation was assessed, as previously described, using SDS-PAGE western immunoblot analyses via the formation of the active fragment from the full-length pro-enzyme (Table 1).<sup>36</sup> Since MCF-7 cells lack caspase 3, caspase 3-containing MDA-468 cells transfected with NQO1 (MDA-468-NQ23) to sensitize them to  $\beta$ -lap were used, as described.<sup>24,27</sup> A nominal level of apoptosis (~15%) was observed 6 h after exposure to 8  $\mu$ M  $\beta$ -lap (for 4 h), increasing to ~38% by 8 h, and ~65% by 10 h (Fig. 2A). By 24 h, >80% apoptotic cells were noted (Fig. 2A). Furthermore, MDA-468-NQ3 cells elicited the same apoptotic proteolysis as MCF-7 cells, but at a later time; 10 h vs. 8 h in MCF-7 cells (Fig. 2B and Fig. 1B, respectively and data not

shown). Lamin B and p53 cleavages were observed 10 h after  $\beta$ -lap treatment (Fig. 2B). Autolysis (i.e., activation) of  $\mu$ -calpain corresponded in a temporal fashion to proteolysis (Fig. 2B), as well as to the level of apoptosis: at 10 h > 60% of the cells were apoptotic when  $\mu$ -calpain activation and substrate proteolysis were observed (Fig. 2A). It was interesting to note in Figure 2B, that Lamin B and p53 proteolysis occurred concurrent with  $\mu$ -calpain activation, further suggesting that the apoptotic proteolysis observed in cells after exposure to  $\beta$ -lap was indeed due to  $\mu$ -calpain activation; Lamin B and p53 proteolysis were diminished concurrently with decreased  $\mu$ -calpain activation at 12 h. The inactivation of  $\mu$ -calpain at 12 h was not observed in all experiments, but the absence of proteolytic cleavages at 12 h in this experiment further supports the role of calpain in substrate cleavages in these cells in response to  $\beta$ -lap.

We then examined activation of known apoptotic caspases in MDA-468-NQ3 cells 8–24 h following a 4 h pulse of 8  $\mu$ M  $\beta$ -lap. Known apoptotic-inducing agents, topotecan (TPT) and staurosporine (STS), were used as positive controls for caspase activation. None of the caspases examined (3, 6, 7, 8, 9, 10, and 12), nor m-calpain, were activated in MDA-468-NQ3 cells following  $\beta$ -lap treatment (Table 1). In contrast,  $\mu$ -calpain was cleaved to its active form following  $\beta$ -lap exposures (Fig. 2B and Table 1). Additionally, the proteolytic events (Lamin B, PARP and p53 cleavage events) observed after  $\beta$ -lap treatment were not blocked by pan-caspase peptide inhibitors, zVAD, DEVD, or YVAD (Ref. 20,27 and data not shown). Thus,  $\mu$ -calpain, but not caspase, activation was the predominant event in NQO1-expressing breast cancer cells after  $\beta$ -lap treatment.

**Purified  $\mu$ -Calpain Elicited the Same PARP Cleavage Fragment Observed in NQO1-Expressing Breast Cancer Cells Exposed to  $\beta$ -Lap.** It was previously reported that  $\mu$ -calpain could cleave PARP yielding an ~40 kDa fragment in vivo in SH-SY5Y human neuroblastoma cells during maitotoxin-induced necrosis,<sup>37</sup> or when using purified  $\mu$ -calpain isolated from calf thymus yielding ~42 kDa, 55 kDa and 67 kDa cleavage fragments.<sup>38</sup> However, the proteolysis of PARP was not reported to be accompanied by p53 cleavage nor apoptosis, nor was it identical to proteolysis observed in NQO1-expressing cells after  $\beta$ -lap exposure (~60 kDa).<sup>27</sup> To directly observe  $\beta$ -lap-mediated activated  $\mu$ -calpain activity from treated cells using PARP as a substrate, <sup>35</sup>S-methionine-labeled PARP was generated by coupled in vitro transcription and translation of full-length human PARP cDNA, and then incubated with various cell extracts or purified enzymes. Using this in vitro cleavage assay, we examined whether purified  $\mu$ -calpain could cleave in vitro transcribed/translated <sup>35</sup>S-met-PARP to similar polypeptide fragments as observed in NQO1-expressing breast cancer cells exposed to  $\beta$ -lap. Log-phase MCF-7 or MDA-468-NQ3 cells were treated with  $\beta$ -lap for 4 h and harvested at 8 or 10 h, respectively (corresponding to Western blot analyses of  $\mu$ -calpain activation and proteolysis after exposure to  $\beta$ -lap, Fig. 1B and Fig. 2B), to assess enzymatic activity using <sup>35</sup>S-met-PARP. Cell extracts or purified enzyme ( $\mu$ -calpain or caspase 3, used as controls) were incubated with <sup>35</sup>S-met-PARP for 1 h at 37°C. Caspase 3 cleaved PARP to the expected 89 and 24 kDa fragments (Figs. 3A–3B, lane 2 and data not shown). Purified  $\mu$ -calpain cleaved PARP to ~60 kDa and ~50 kDa fragments (Figs. 3A–3B, lane 3 and data not shown). The PARP cleavage fragment observed after  $\beta$ -lap-treated cell extracts were incubated with <sup>35</sup>S-met-PARP was the same as that elicited by recombinant  $\mu$ -calpain (Figs. 3A, lanes 3 and 6–8, 11–12 and Fig. 3B, lanes 3 and 4–7 and 11). This was most apparent when <sup>35</sup>S-met PARP substrate was cleaved by purified  $\mu$ -calpain and analyzed with  $\beta$ -lap-treated cell extracts on the same gel (Fig. 3B lanes 3–7).  $\beta$ -Lap-treated cell extracts cleaved PARP in a protein concentration-dependent manner (Fig. 3A lanes 5–8 and Fig. 3B lanes 4–7); increasing concentrations of protein extract were added to the same amount of <sup>35</sup>S-met PARP substrate to observe the activity of the extract.  $\beta$ -Lap-treated cell extracts also cleaved PARP in a time-dependent manner (Fig. 3A lanes 10–12 and Fig. 3B lanes 9–11) corresponding to Western blot analyses (Fig. 1B and Fig. 2B), further implicating  $\mu$ -calpain activation in  $\beta$ -lap-induced apoptosis. DMSO-treated cell extracts did not exhibit any cleavage of PARP in this assay (Fig. 3A lane 4 and Fig. 3B lane 8). Proteolytic activity in cell extracts (control or  $\beta$ -lap-treated conditions)

could not be stimulated by addition of 100  $\mu$ M Ca<sup>2+</sup> alone, suggesting that the enzymatic activity was inherent to the  $\beta$ -lap-treated extract upon harvest (data not shown).

To further support the role of  $\mu$ -calpain in  $\beta$ -lap-induced apoptosis, menadione-treated cells, the only other known agent to stimulate a similar cell death pathway as  $\beta$ -lap,<sup>24,26</sup> were also examined. In contrast to extracts from untreated cells, extracts from menadione-exposed cells elicited cleavage of <sup>35</sup>S-met-PARP resulting in fragments similar to those generated by purified  $\mu$ -calpain or  $\beta$ -lap-treated cell extracts (~60 kDa) (Fig. 3A, lanes 3, 6–8 and 11–13 and Fig. 3B, lanes 3, 4–7, and 11–12). Ionomycin is a calcium ionophore reported to activate  $\mu$ -calpain.<sup>5,39,40</sup> Ionomycin-treated MDA-468-NQ3 cell extracts also elicited the same PARP cleavage pattern (Fig. 3B, lanes 13–14), as did pure  $\mu$ -calpain, menadione, and  $\beta$ -lap-exposed cell extracts (Fig. 3B, lanes 3, 12, and 4–7 and 11). Interestingly, ionomycin did not elicit PARP cleavage in MCF-7 cells (Fig. 3A, lane 14).

**Calpastatin, A Modulator of  $\beta$ -Lap-Mediated Apoptosis Involving Calpain Activation.** We noted that MDA-468-NQ3 cells expressed higher levels of endogenous calpastatin than MCF-7 cells (Fig. 4B). We hypothesized that levels of this endogenous calpain inhibitor may explain the slower responses of MDA-468-NQ3 cells (in terms of substrate proteolysis and apoptosis) compared to MCF-7 cells that contained far less calpastatin (10 h vs. 8 hr, Fig. 1, Fig. 2 and data not shown). In addition, the aforementioned data suggested a correlation between PARP and p53 cleavage with  $\mu$ -calpain activation. To further investigate whether calpain was indeed involved in apoptotic substrate proteolysis after  $\beta$ -lap-exposure, we examined the effects of a calpastatin peptide containing the inhibitory sequence of calpastatin, as well as stable overexpression of calpastatin in MCF-7 cells. Calpastatin is a specific endogenous inhibitor of calpains, and does not inhibit other proteases (e.g., cathepsins, caspases).<sup>41,42</sup> A calpastatin peptide containing the domain sequence of the calpastatin protein that can inhibit 1 mole of calpain per domain sequence was used (Fig. 4A); calpastatin contains four inhibitory domains and thus is able to inhibit 4 moles of calpain per mole of calpastatin (Fig. 4A).<sup>15,43,44</sup> In the in vitro cleavage assay, the calpastatin peptide inhibitor (CN) blocked purified  $\mu$ -calpain-mediated <sup>35</sup>S-met-PARP cleavage, but not caspase 3-mediated <sup>35</sup>S-met-PARP cleavage (Fig. 4A, lanes 2–5). The CN peptide alone did not have any effect on the integrity of the <sup>35</sup>S-met PARP substrate (data not shown). DMSO-treated cell extracts also did not exhibit any PARP cleavage activity (Fig. 4A lane 6). Cell extracts generated from MCF-7 cells treated with a 4 h pulse of 5  $\mu$ M  $\beta$ -lap and extracted 4 h post-treatment elicited PARP cleavage activity yielding an ~60 kDa fragment (Fig. 4A, lane 7). In contrast,  $\beta$ -lap-exposed MCF-7 cell extracts co-incubated with increasing concentrations of the CN peptide, exhibited a decreased amount of the PARP cleavage fragment in a concentration-dependent manner (0–25  $\mu$ M CN peptide) (Fig. 4A lanes 8–10) compared to  $\beta$ -lap-exposed cell extracts containing no peptide treatment (lane 7). Thus, <sup>35</sup>S-met-PARP cleavage, mediated by  $\beta$ -lap treated cell extracts, was inhibited in a concentration-dependent manner by the calpastatin inhibitory peptide (Fig. 4A, lanes 8–10). Furthermore, in Western blot analyses 8 h after  $\beta$ -lap exposure, the calpastatin peptide inhibitor slightly diminished PARP cleavage and loss of the small subunit of calpain in a dose-dependent manner. Interestingly, the peptide had a greater effect on the enzymatic activity in menadione-treated cells (data not shown).

To further support the role of  $\mu$ -calpain activation in  $\beta$ -lap-induced apoptosis, MCF-7 cells were transfected with calpastatin and clones selected by limiting dilution cloning (Fig. 4B–4E). Two clones with varying levels of calpastatin, MCF-7 CN1 (CN1) and MCF-7 CN2 (CN2), were selected for subsequent analyses. The two MCF-7 calpastatin clones selected expressed intermediate levels of calpastatin, compared to MCF-7 or MDA-468-NQ3 cells (Fig. 4B). CN1 cells expressed higher levels of calpastatin than MCF-7 or CN2 cells, but less than MDA-468-NQ3 cells (Fig. 4B). CN2 cells expressed a much lower level of calpastatin than CN1, but a higher level than MCF-7 cells (Fig. 4B). The molecular weight difference between endogenous and exogenous calpastatin in the MCF-7 clones compared to MCF-7 parental cells is presumably due to the lack of exon 1 in exogenous calpastatin (sequence analysis). Exon 1 encodes part of domain L of calpastatin;

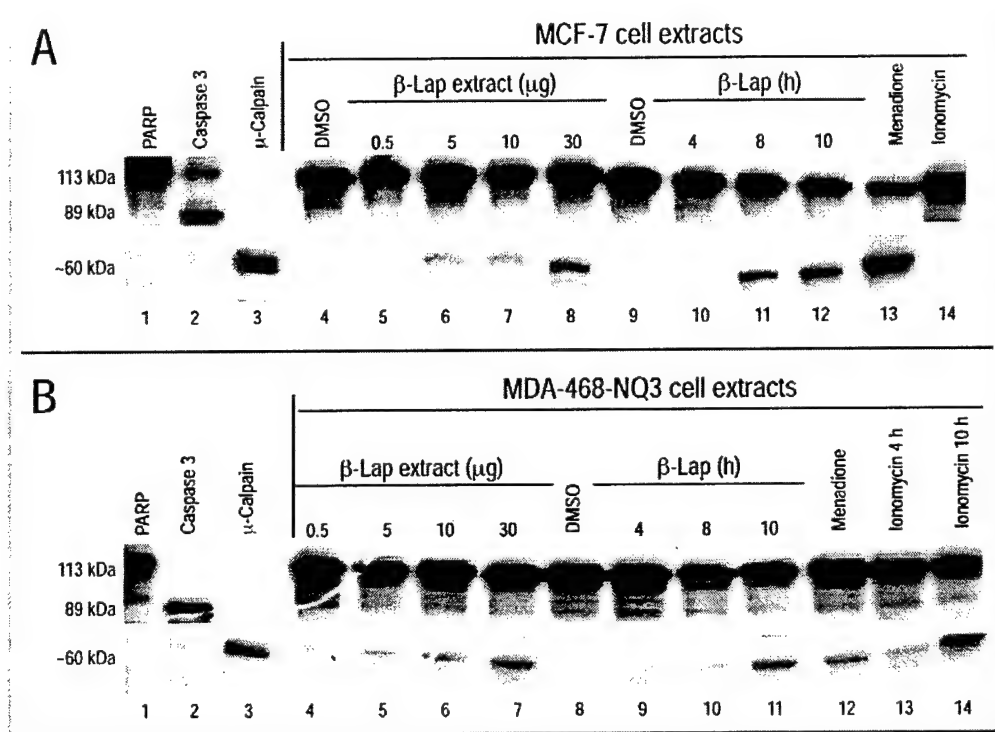


**Figure 3.** Purified  $\mu$ -calpain cleaved PARP to the same fragment size as did NQO1-expressing breast cancer cells exposed to  $\beta$ -lap. PARP protein was translated using an in vitro transcription and translation TNT-coupled Reticulocyte lysate system.  $^{35}$ S-methionine-labeled protein was incubated with 100  $\mu$ M  $\text{CaCl}_2$  and either 0.05 U of recombinant human erythrocyte  $\mu$ -calpain, 20 U of recombinant caspase 3, or 30  $\mu$ g of cell lysate, unless otherwise indicated. The reaction mix was incubated at 37°C for 1 h. (A) MCF-7 cells were treated for 4 h with 5  $\mu$ M  $\beta$ -lap or 25  $\mu$ M menadione or continuously with 10  $\mu$ M ionomycin, and harvested at 8 h, unless otherwise indicated. Lanes 5–8 are increasing protein concentrations of  $\beta$ -lap-treated cell extracts incubated with labeled PARP protein and lanes 9–12 are DMSO control or time-course analyses of  $\beta$ -lap-treated cell extracts, respectively, incubated with labeled PARP protein. (B) MDA-468-NQ3 cells were treated for 4 h with 8  $\mu$ M  $\beta$ -lap or 25  $\mu$ M menadione or continuously with 10  $\mu$ M ionomycin, and harvested at 10 h post-treatment, unless otherwise indicated. Sample proteins were separated on a 9% SDS-PAGE gel and  $^{35}$ S-met-PARP was visualized via autoradiography. Lanes 4–7 are increasing protein concentrations of  $\beta$ -lap-treated cell extracts incubated with labeled PARP protein and lanes 8–11 are DMSO control or time-course analyses of  $\beta$ -lap-treated cell extracts, respectively, incubated with labeled PARP protein. Shown is a representative exposure of whole cell extracts from experiments performed at least three times.

the function of domain L remains unknown and alternative first exons have been shown to lead to four calpastatin isoforms with distinct amino-terminal sequences resulting in protein sizes ranging from 60–120 kDa via western blot analyses.<sup>45</sup> It is important to note that endogenous calpastatin was not detected at the higher molecular weight in these clones (Fig. 4B). Calpastatin contains four repetitive and homologous domains (not encoded by exon 1) that each inhibit both m- and  $\mu$ -calpain; each domain is a functioning unit of calpastatin and can bind one calpain molecule and inhibit its activity.<sup>15,43,44</sup> Other inhibitors have been used to inhibit calpain activity, however, these inhibitors are less useful due to their poor solubilities, intracellular uptake, and non-specific ability to inhibit other proteases and/or the proteasome (e.g., cathepsins B and L, papains, etc.).<sup>46–49</sup>

Log-phase MCF-7, MDA-468-NQ3, CN1 and CN2 cells were treated for 4 h with 1.5  $\mu$ M or 3  $\mu$ M  $\beta$ -lap, at which time fresh medium was added. Clonogenic survival was determined seven days later. At 1.5  $\mu$ M  $\beta$ -lap, increasing survival after  $\beta$ -lap exposure correlated with the level of calpastatin expressed in each cell line; MCF-7 cells (low calpastatin) exhibited ~30% survival, CN2 cells (intermediate calpastatin) exhibited ~60% survival, and CN1 cells (high calpastatin) exhibited ~100% survival (Fig. 4C). At 3  $\mu$ M  $\beta$ -lap, no difference in survival was observed indicating that the inhibitory affects of calpastatin could be overcome with higher drug concentrations (Fig. 4C); binding of calpains to calpastatin is reversible and does not result in any lingering loss of calpain activity.<sup>50</sup>

To examine proteolysis during  $\beta$ -lap-mediated cell death in CN1 and CN2 cell clones, cells were harvested at the indicated times for Western blot and apoptosis analyses. MCF-7 cells expressed low levels of calpastatin and exhibited ~50% apoptosis at 8 h, increasing to >90% cells staining TUNEL positive at 24 h. In contrast,  $\beta$ -lap-treated CN1 and CN2 cells that possessed higher levels of calpastatin exhibited less apoptosis than MCF-7 cells at 8, 10 and 12 h after 5  $\mu$ M  $\beta$ -lap exposures (Fig. 4D). At 24 h, no difference was observed between the cell lines, indicating that the inhibitory affects of calpastatin could be overcome with time following a 4 h, 5  $\mu$ M  $\beta$ -lap exposure (Fig. 4D), and corresponding to cell survival data at 3  $\mu$ M (Fig. 4C).

Specific proteolytic events in cells with varied calpastatin levels were then examined following  $\beta$ -lap exposure.  $\beta$ -Lap-exposed MCF-7 cells expressed low levels of calpastatin and exhibited apoptotic-substrate proteolysis, specifically PARP cleavage to a distinct ~60 kDa fragment at 8 h, with complete loss of full-length protein by 16 h (Fig. 1B). In contrast,  $\beta$ -lap-treated MDA-468-NQ3 cells that possessed higher levels of calpastatin, exhibited apoptotic-substrate proteolysis at 10 h (Fig. 2B). Loss of PARP protein also corresponded with cleavage of both the small subunit of calpains and  $\mu$ -calpain (Fig. 1B and 2B and data not shown), indicative of calpain activation.<sup>10,30</sup> In MCF-7 clones stably expressing calpastatin,  $\beta$ -lap-induced apoptosis and calpastatin levels were inversely correlated (Fig. 4D and Fig. 4E). CN2 cells expressed low levels of calpastatin and exhibited a similar time-course of



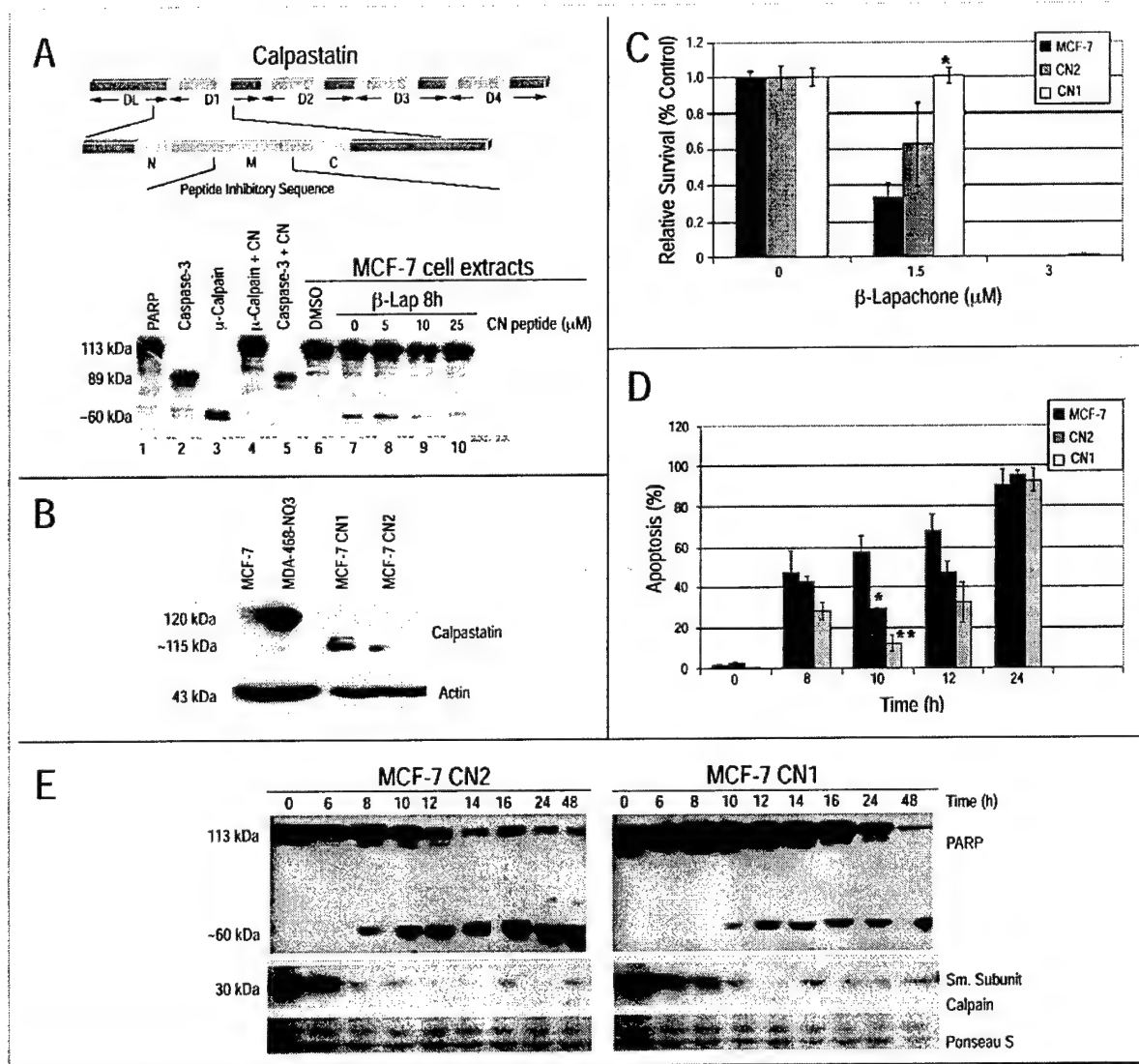


Figure 4. Calpastatin inhibits or delays substrate proteolysis, apoptosis and survival after exposure to β-lap. (A) A diagram of calpastatin protein structure and the location of the inhibitory peptide sequence. <sup>35</sup>S-methionine-labeled protein was incubated with 0.05 U recombinant μ-calpain, 20 U recombinant caspase 3, or 30 μg cell lysate. MCF-7 cells were treated for 4 h with 5 μM β-lap and where indicated, with a calpastatin peptide inhibitor (CN), and harvested at 8 h. Purified caspase 3 and μ-calpain were incubated with 25 μM CN. Samples were run on a 9% SDS-PAGE gel and <sup>35</sup>S-met-PARP was visualized via autoradiography. Shown is a representative blot from experiments performed at least twice. (B) Whole cell extracts were collected and Western blot analyses performed using a calpastatin primary antibody to determine relative calpastatin levels in MCF-7, MDA-468-NQ3, and MCF-7 cells stably expressing calpastatin. (C) Cells were seeded into 60-mm dishes (2000 cells/dish in duplicate) and allowed to attach overnight. Cells were then exposed to a 4 h pulse of β-lap. Medium was removed, fresh medium was added, and cells were allowed to grow for 7 days. Plates were then washed and stained with crystal violet in 50% methanol. Colonies of >50 normal-appearing cells were then counted. Results were graphically summarized as the average of two independent experiments performed in duplicate, mean ± S.E. Student's t test for paired samples, experimental group compared to MCF-7 cells treated with β-lap were indicated (\*, p<0.01). (D) At times indicated, TUNEL assays were performed to monitor apoptotic DNA fragmentation in cells after a 4 h pulse of 5 μM β-lap. Results were graphically summarized as the average of two independent experiments, mean ± S.E. Student's t test for paired samples, experimental group compared to MCF-7 cells treated with β-lap were indicated (\*, p<0.1 and \*\*, p<0.05). (E) Apoptotic proteolysis was measured in the various cell lines exposed to a 4 h pulse of 5 μM β-lap. Whole cell extracts were prepared at the indicated times and analyzed using standard Western blotting techniques with antibodies to PARP and the small subunit of calpains. Shown is a representative Western blot of whole cell extracts from experiments performed at least three times with Ponceau S staining of the membrane for protein loading.

PARP and small subunit of calpain proteolysis at 8 h, to that observed in MCF-7 cells (Fig. 4E). In contrast, CN1 cells that expressed high levels of calpastatin showed a more delayed time-course of proteolysis following

β-lap exposure similar to that of MDA-468-NQ3 cells; PARP cleavage occurred at 10–12 h (Fig. 4E). Furthermore, the small subunit of calpain was lost much earlier in CN1 cells than in MDA-468-NQ3 cells, but later

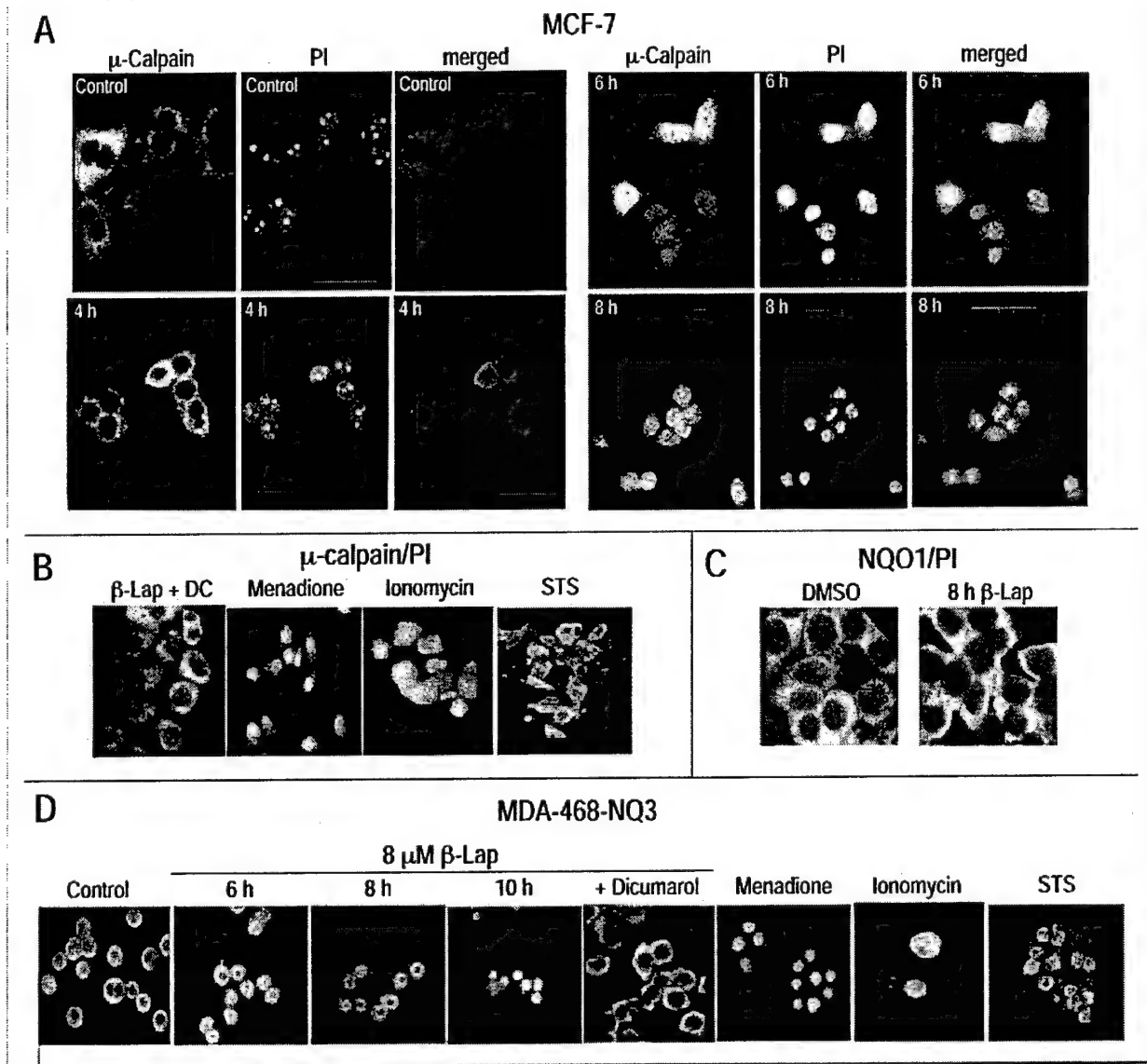


Figure 5. μ-Calpain translocated to the nucleus after exposure to β-lap. (A) MCF-7 cells were treated for 4 h with 5 μM β-lap and cells were fixed at the indicated times for analyses. Indirect immunofluorescent staining of fixed cells was performed using a primary antibody for μ-calpain and secondary FITC-anti-mouse antibody (green). Slides were coated with mounting medium containing propidium iodide for DNA/nuclear staining (red) and analyzed. Confocal images were collected using dual excitation at 488 nm and 568 nm from a krypton/argon laser. Nuclear translocation was indicated by yellow fluorescence from the merging of red DNA/nuclear staining and green protein staining. (B) MCF-7 cells were treated for 4 h with 5 μM β-lap concomitantly with dicumarol (50 μM), 4 h with 25 μM menadione or continuously with 3 μM ionomycin or 1 μM STS, respectively. MCF-7 cells were fixed at 8 h for analyses. Cells were stained as described in (A). (C) MCF-7 cells were treated for 4 h with 5 μM β-lap and fixed at 8 h for analyses. Indirect immunofluorescent staining of fixed cells was performed using a primary antibody for NQO1 with secondary FITC-anti-mouse antibody (green). Slides were coated with mounting medium containing propidium iodide for DNA/nuclear staining (red) and analyzed. (D) MDA-468-NQ3 cells were treated for 4 h with 8 μM β-lap, 25 μM menadione, or continuously with 3 μM ionomycin or 1 μM STS, respectively. Dicumarol (50 μM) was added concomitantly with β-lap for 4 h where indicated. MDA-468-NQ3 cells were fixed at 10 h for analyses, unless otherwise indicated. Indirect immunofluorescent staining of fixed cells was performed as described in (A). All images were taken at magnification of 63X, except (C) where they were taken at 100X. The image width is indicated in all images in (A), scale bar = 50 μm.

than MCF-7 or CN2 cells (Fig. 4E, Fig. 1B, Fig. 2B and data not shown). These data strongly suggest that calpastatin levels can influence the responses

of NQO1-expressing cells to β-lap-induced, μ-calpain-mediated apoptosis and survival.

**$\mu$ -Calpain Translocated to the Nucleus in NQO1-Expressing Breast Cancer Cells After  $\beta$ -Lap Exposure-** PARP and p53 are nuclear proteins and  $\mu$ -calpain is reported to primarily reside in the cytoplasm.<sup>9,51</sup> Confocal microscopic analyses were performed to examine  $\mu$ -calpain localization after  $\beta$ -lap treatment. Log-phase MCF-7 or MDA-468-NQ3 cells were treated for 4 h with  $\beta$ -lap (5  $\mu$ M or 8  $\mu$ M, respectively) and fixed for indirect immunofluorescent staining at 8 h or 10 h, unless otherwise indicated. Cells were stained with a primary antibody specific for  $\mu$ -calpain and a FITC-conjugated secondary antibody (green). Slides were then mounted in medium containing propidium iodide for DNA/nuclear staining (red). Cells exhibited  $\mu$ -calpain translocation to the nucleus (Fig. 5A;  $\mu$ -calpain staining is green, DNA is red, and nuclear translocation of  $\mu$ -calpain is indicated by yellow fluorescence) at a time concomitant with  $\mu$ -calpain activation after  $\beta$ -lap treatment (Figs. 1B and Fig. 2B). In MCF-7 cells,  $\mu$ -calpain exhibited minimal nuclear translocation at 4 h increasing to almost 100% by 8 h, consistent with substrate proteolysis in Fig. 1B (Fig. 5A). In MDA-468-NQ3 cells,  $\mu$ -calpain did not exhibit nuclear translocation until 10 h, corresponding to substrate proteolysis in these cells (Figs. 5D and Fig. 2B). In addition, translocation of  $\mu$ -calpain to the nucleus was concomitant with overall loss of calpastatin immunofluorescence and protein expression, as determined by Western blot analyses, after exposure to  $\beta$ -lap (Fig. 1 and data not shown). Translocation of  $\mu$ -calpain was NQO1-dependent, since it was prevented by coadministration of 50  $\mu$ M dicumarol (Fig. 5B and Fig. 5D), and did not occur in cells that lacked NQO1 enzymatic activity (i.e., in MDA-468 cells not transfected with NQO1 sequence (vector alone, data not shown)).

Translocation of  $\mu$ -calpain to the nucleus in NQO1-expressing,  $\beta$ -lap-treated cells, was a specific event that did not occur due to nuclear membrane breakdown. Proteins residing in the cytoplasm (NQO1) did not translocate to the nucleus, and proteins that reside in the nucleus (Ku70/Ku80) did not diffuse out into the cytoplasm at the times  $\mu$ -calpain was observed to translocate to the nucleus (Fig. 5C and data not shown); Ku70/Ku80 is a heterodimeric nuclear protein required for non-homologous DNA double strand break repair.<sup>52</sup> Also, consistent with Western blot analyses in Figure 1,  $\mu$ -calpain immunoreactivity did not change after exposure of NQO1-expressing breast cancer cells to  $\beta$ -lap (data not shown), further implicating  $\mu$ -calpain activation specifically in  $\beta$ -lap-induced apoptosis.

Other agents (e.g., menadione) that cause the same cell death pathway as  $\beta$ -lap also induced  $\mu$ -calpain translocation to the nucleus at times concomitant with PARP and p53 proteolysis, while agents that elicit caspase-mediated cell death (e.g., staurosporine) did not elicit changes in  $\mu$ -calpain localization (Fig. 5B and Fig. 5D). Ionomycin, a  $\text{Ca}^{2+}$  ionophore, activated calpain in some cells.<sup>53,40</sup> Consistent with these data,  $\mu$ -calpain translocated to nuclei after treatment with ionomycin in MCF-7 and MDA-468-NQ3 cells (Fig. 5B and Fig. 5D). Translocation of  $\mu$ -calpain after ionomycin was more prominent in MDA-468-NQ3 cells than in MCF-7 cells, corresponding to the ability of each cell line to elicit PARP (Fig. 3A and Fig. 3B, lane 14) or p53 (not shown) cleavage. Menadione elicited a similar cell death pathway as did  $\beta$ -lap, and in a similar manner to  $\beta$ -lap-exposed cells. For example, menadione-treated cells caused translocation of  $\mu$ -calpain to the nucleus at times concomitant with PARP and p53 substrate proteolysis (Fig. 3 and ref. 24). In contrast to  $\beta$ -lap exposures, there was no observed change in  $\mu$ -calpain localization in staurosporine (STS)-exposed MCF-7 or MDA-468-NQ3 cells (Fig. 5B and Fig. 5D); STS is a protein kinase inhibitor<sup>53</sup> that initiates apoptosis via a caspase-mediated pathway.<sup>54</sup> Collectively, these data implicate  $\mu$ -calpain activation in  $\beta$ -lap-mediated apoptosis and  $\mu$ -calpain translocation to the nucleus upon its activation. These data are consistent with the essential role of  $\text{Ca}^{2+}$  release in  $\beta$ -lap-induced apoptosis as previously demonstrated.<sup>26,27</sup>

## DISCUSSION

We previously demonstrated that treatment of NQO1-expressing breast cancer cells with  $\beta$ -lap exposure caused increases in intracellular  $\text{Ca}^{2+}$  levels that were critical for apoptosis and cell death.<sup>26</sup> Calpain is a  $\text{Ca}^{2+}$ -activated protease implicated in a number of apoptotic pathways.<sup>5,6,49,55,56</sup> Our results indicate that  $\mu$ -calpain is activated after  $\beta$ -lap-induced apoptosis by cleavage of the catalytic subunit, as well as the regulatory subunit of calpains, to fragment sizes indicative of calpain activation (Fig. 1 and Fig. 2). Purified  $\mu$ -calpain was also able to cleave in vitro <sup>35</sup>S-met-PARP to the same fragment size as observed in  $\beta$ -lap-treated MCF-7 or MDA-468-NQ3 cell extracts (Fig. 3). Furthermore, extracts from  $\beta$ -lap-treated MCF-7 cells were also able to cleave <sup>35</sup>S-met PARP to the same cleavage fragments as observed with PARP substrate incubated with purified calf thymus  $\mu$ -calpain. Finally, cleavage of p53 in  $\beta$ -lap-exposed cells to fragments indicative of  $\mu$ -calpain activation further suggests  $\mu$ -calpain activation in these cells.<sup>29,30</sup>

We used calpastatin, the specific endogenous inhibitor of calpains, to assay calpain's role in  $\beta$ -lap-mediated apoptosis. Since many calpain inhibitors can also inhibit the proteasome, cathepsins, other cysteine proteases, or inhibit entirely different enzymes (for example, a protein tyrosine phosphatase),<sup>57,58</sup> the use of exogenous calpastatin expression to delay/inhibit  $\beta$ -lap-mediated apoptosis has significant advantages over the exclusive use of inhibitors. A peptide comprised of the inhibitory domain of calpastatin was able to block purified  $\mu$ -calpain-mediated PARP cleavage, as well as the ability of  $\beta$ -lap-treated cell extracts to cleave PARP both in vitro and in vivo (Fig. 4 and data not shown). Furthermore, stable over-expression of the calpastatin protein in MCF-7 cells, which possess low levels of calpastatin compared to MDA-MB-468 cells, delayed  $\beta$ -lap-mediated apoptotic events and protected against cell death at 1.5  $\mu$ M  $\beta$ -lap in clonogenic assays (Fig. 4C).

Calpain has two distinct sites for association with calpastatin, one at the active site and another at the EF-hand domain;<sup>10</sup> it is believed that calpain interacts with substrates through these two sites. Binding of calpains to calpastatin is reversible and does not result in irreversible loss of calpain activity.<sup>50</sup> Therefore, the ability of calpain activation to overcome the inhibitory effects of calpastatin was not surprising. The delay of calpain activation observed in cells over-expressing calpastatin after  $\beta$ -lap exposure could be due to the dissociation of calpastatin, or the eventual degradation of calpastatin by initial minimal calpain activation, thus explaining the rather moderate survival and apoptotic inhibition caused by this exogenous natural inhibitor. The degradation of calpastatin after calpain activation is supported by the loss of calpastatin protein observed in Western blot as well as confocal analyses (Fig. 1B and data not shown). It is also possible that calpastatin has a lower affinity for calpain than calpain substrates. These data suggest a role for calpain in the effector phase of the apoptotic pathway induced by  $\beta$ -lap.

The role of calpains in apoptosis has been widely discussed, but their patterns of activation are not well characterized.<sup>5-7</sup> Thus, elucidation of calpain activation after exposure of NQO1-expressing breast cancer cells to  $\beta$ -lap, and the potential role of caspases in regulating  $\beta$ -lap-mediated apoptosis was critical to evaluate.  $\mu$ -Calpain was activated in a temporal manner corresponding to proteolytic cleavage events, apoptosis, and its apparent translocation to the nucleus from the cytoplasm (Figs. 1–5). Known apoptotic caspases (3, 6, 7, 8, 9, 10 and 12) were not activated after treatment of NQO1-expressing cells with  $\beta$ -lap, suggesting a role for  $\mu$ -calpain

in this apoptotic response independent of caspase activation (Table 1). Other caspases (1, 4, 5, 11 and 13) were not assayed for activation after  $\beta$ -lap exposures because they are not associated with most apoptotic pathways, but rather, are implicated in inflammation processes.<sup>59,60</sup> Killer/DR5, a death-domain containing pro-apoptotic receptor, mRNA was reported to be upregulated after  $\beta$ -lap-exposures in colon cancer cell lines, however, neither downstream receptor activation nor caspase activation were assayed in these cells.<sup>61</sup> Since caspases 8 and 10 are important for receptor-mediated apoptosis, through their association with death domains (e.g., FADD),<sup>62</sup> and neither caspase was activated after  $\beta$ -lap exposures in MDA-468-NQ3 cells (Table 1), our data would strongly suggest that receptor-mediated pathways are not involved in  $\beta$ -lap-induced apoptosis. Furthermore, pan-caspase inhibitors did not prevent apoptotic proteolytic substrate cleavages, nor cell death induced by  $\beta$ -lap.<sup>20,27</sup> In contrast,  $\text{Ca}^{2+}$  chelators and calpastatin, the endogenous inhibitor of calpains, did prevent and/or delay proteolytic cleavage events, as well as apoptosis induced by  $\beta$ -lap (Refs. 26,27 and Fig. 4), further implicating a role for calpains in apoptosis independent of caspase activation. Together with the rather dramatic loss of ATP in  $\beta$ -lap-exposed cells,<sup>26</sup> these data strongly suggest that caspases are not involved in cell death induced by this cytotoxic agent.

Determining whether caspases were involved in  $\beta$ -lap induced apoptosis was essential since caspases are known to be involved in a number of classic apoptotic pathways.<sup>2-4</sup> In addition, calpain activation in apoptosis is usually linked upstream or downstream of caspase activation, or in a parallel pathway alongside caspase activation.<sup>63-65</sup> In studies described above, we demonstrated that calpains were activated in human breast cancer cells during  $\beta$ -lap-mediated apoptosis, while caspase activation was not apparent (Fig. 1-4, Table 1). In addition, caspase inhibitors did not have any effect on the apoptotic morphology or survival of NQO1-expressing cells exposed to  $\beta$ -lap.<sup>20,27</sup> This may suggest a redundancy of apoptotic proteases, as well as a novel proteolytic pathway for calpains. Furthermore, although calpain is activated, this protease may either be one of a family of proteases activated in response to  $\beta$ -lap, or simply represent a mechanism for eliminating badly damaged cells. This conclusion is supported by the fact that calpain inhibitors (chemicals or endogenous calpastatin expression) only slightly delayed apoptotic responses triggered by  $\beta$ -lap.

Endonuclease activation is a critical step in the apoptotic pathway culminating in DNA fragmentation. Many DNases are known to exist, some of which are involved in apoptosis, such as  $\text{Ca}^{2+}/\text{Mg}^{2+}$ -dependent endonucleases (e.g., DNase I, DNase gamma),  $\text{Mg}^{2+}$ -dependent endonucleases (CAD/DFF40), and the cation-independent endonucleases (DNase II).<sup>66</sup> Caspase 3 usually mediates cleavage of DFF45/ICAD (a DNase inhibitor) allowing for translocation and activation of DFF40/CAD that mediates DNA fragmentation.<sup>67</sup> Since caspases were not activated in  $\beta$ -lap-mediated apoptosis and DNA fragmentation was observed via the TUNEL assay (Figs. 1-4 and Table 1), three potential pathways for endonuclease activation in  $\beta$ -lap-mediated apoptosis are possible:

1. Calpains directly activate an endonuclease;
2. Calpains activate another protease that then activates an endonuclease; or
3. Calpains are not involved in endonuclease activation, and  $\text{Ca}^{2+}$  alone may activate an endonuclease.

In some apoptotic pathways, calpain inhibitors blocked all aspects of apoptosis, including DNA fragmentation.<sup>5,55</sup> These data imply that calpain activation led to endonuclease activation either directly, or

indirectly, and it is unclear whether this is through activation of a caspase, another protease, or directly by calpains. Our data suggest that either calpain directly activates an endonuclease or that calpain activates another protease (independent of caspases) that then activates an endonuclease, since calpastatin over-expression can delay the onset of DNA fragmentation and calpastatin protein levels were inversely proportional to the time and amount of DNA fragmentation observed after  $\beta$ -lap exposure (Fig. 4). Calpastatin should not affect the levels of  $\text{Ca}^{2+}$  in the cell and thus should not affect endonuclease activation by  $\text{Ca}^{2+}$  alone. However, although calpastatin is not known to inhibit any other proteases, it may inhibit another yet unknown protease that is involved in endonuclease activation. We have preliminary evidence that DFF45 was cleaved concomitantly with PARP and p53 proteolysis, as well as calpain activation in vivo in MDA-468-NQ3 cells exposed to 8  $\mu\text{M}$   $\beta$ -lap and by purified  $\mu$ -calpain in vitro (Tagliarino et al., unpublished results). These data suggest that calpain might directly activate the DFF40/CAD endonuclease.

Calpains are not only suggested to be involved in DNA fragmentation (via endonuclease activation), but are also effector proteases that cleave cellular proteins involved in DNA repair (e.g., PARP), membrane associated proteins (e.g.,  $\alpha$ -spectrin and actin) and other homeostatic regulatory proteins (e.g., c-FOS, C-JUN, p53).<sup>5,10,29,37,68,69</sup> Calpain substrate cleavage does not involve a specific primary cleavage site, but rather, is dependent upon the secondary structure of the substrate, making calpains a class of proteases different from the aspartate-specific caspases.<sup>68,70-72</sup> We demonstrated that  $\beta$ -lap-induced activation of  $\mu$ -calpain in human breast cancer cells mediated cleavage of p53 in a manner similar to that previously reported.<sup>29,30</sup> Loss of p53 may further promote apoptosis by preventing anti-apoptotic pathways or cell cycle arrest to allow for cell repair. PARP is a caspase 3 substrate, and a widely used indicator of apoptosis when cleaved to a characteristic 89 kDa fragment from its 113 kDa full-length protein. PARP was previously reported to be cleaved by calpains to a 40 kDa fragment during maitotoxin-induced necrosis.<sup>37</sup> PARP was also cleaved by calpains purified from calf thymus to ~42 kDa, ~55 kDa (doublet) and ~67 kDa (triplet) fragments.<sup>38</sup> Here, we show a novel cleavage of PARP to an ~60 kDa polypeptide fragment, mediated by  $\mu$ -calpain in  $\beta$ -lap-treated, NQO1-expressing breast cancer cells during apoptosis, as well as by purified active human erythrocyte  $\mu$ -calpain (Figs. 1-4).

**$\mu$ -Calpain Translocated to the Nucleus Upon Activation in  $\beta$ -Lap-Induced Apoptosis.** Both m- and  $\mu$ -calpains are predominantly cytoplasmic.<sup>51,73-75</sup> However, some immunoreactivity towards calpains has been localized at the cell membrane,<sup>76</sup> at cell-substrate attachment plaques in cultured cells,<sup>77</sup> at the I-band in muscle cells,<sup>78</sup> or around and within the nucleus.<sup>30,35,51,79,80</sup> Calpains can exhibit diffuse cytoplasmic staining with no change after activation by certain agents.<sup>9</sup> Conversely, calpains have also been shown to undergo redistribution from the cytosol to the plasma membrane upon activation by other agents.<sup>81</sup> This suggests a complex activation process for calpains that is agent- and cell type-specific. While calpains have been reported to cleave a number of nuclear proteins (e.g., p53, PARP) there is negligible data that calpains may be localized to the nucleus, and translocation to the nucleus upon activation has only been suggested.<sup>30,51</sup> Interestingly, one group showed that  $\mu$ -calpain immunoreactivity transiently accumulated in cell nuclei concomitant with proteolysis of p53 in late G<sub>1</sub> phase.<sup>35</sup> Mellgren et al.<sup>80</sup> also demonstrated nuclear transport of purified calpains in permeabilized cells; fluorescein-tagged,

μ-calpain was transported into nuclei in an ATP-dependent fashion and calpastatin did not block m-calpain translocation. Here, we demonstrate the ability of m-calpain to translocate to the nucleus in NQO1-expressing breast cancer cells after exposure to β-lap that is presumably ATP-independent (Fig. 5); ATP levels in the cell are depleted prior to nuclear translocation of μ-calpain.<sup>26</sup> μ-Calpain translocated to the nucleus concomitant with its own activation, apoptotic proteolytic cleavage events, and DNA fragmentation (Figs. 1–2 and Fig. 5). This translocation would allow calpain to proteolytically cleave the nuclear substrates, PARP and p53, as well as potentially activate an endonuclease.

In conclusion, we demonstrated that μ-calpain was activated in NQO1-expressing breast cancer cells exposed to β-lap. Its activation involved an apoptotic signal transduction pathway leading to cell death independent of caspase activation and sensitive to calpastatin expression (Figs. 1–4 and Table 1). We also demonstrated a novel translocation of μ-calpain to the nucleus upon its activation in β-lap- and menadione-mediated apoptosis (Fig. 5). However, to unambiguously prove the essential role of calpains in β-lap-induced apoptosis, NQO1-expressing cells deficient in calpain enzymatic activity compared with calpain containing cells after exposure to β-lap would be paramount.

#### Acknowledgements

The authors would like to thank Rich Tarin for his technical assistance, as well as R. Michael Sramkoski, B.S. MT(ASCP)H for aid with flow cytometry analyses. We are grateful to Dr. William G. Bornmann for synthesizing β-lapachone, and to Philip A. Verhoef for critical review of this manuscript. Finally, we are indebted to Mrs. Sarah Hildebrand for her enduring support of our research.

#### References

- Patel T, Gores GJ, Kaufmann SH. The role of proteases during apoptosis. *FASEB J* 1996; 5:587-97.
- Li P, Nijhawan D, Budihardjo I, Srinivasula SM, Ahmad M, Alnemri ES, et al. Cytochrome c and dATP-dependent formation of Apaf-1/caspase-9 complex initiates an apoptotic protease cascade. *Cell* 1997; 91:479-89.
- Eguchi Y, Srinivasan A, Tomaselli KJ, Shimizu S, Tsujimoto Y. ATP-dependent steps in apoptotic signal transduction. *Cancer Res* 1999; 59:2174-81.
- Nagata S. Apoptosis by death factor. *Cell* 1997; 88:355-65.
- Squier MK, Cohen JJ. Calpain, an upstream regulator of thymocyte apoptosis. *J Immunol* 1997; 158:3690-7.
- Squier MK, Schnert AJ, Sellins KS, Malkinson AM, Takano E, Cohen JJ. Calpain and calpastatin regulate neutrophil apoptosis. *J Cell Physiol* 1999; 178:311-9.
- Patel YM, Lane MD. Role of calpain in adipocyte differentiation. *Proc Natl Acad Sci USA* 1999; 96:1279-84.
- Banik NL, DeVries GH, Neuberger T, Russell T, Chakrabarti AK, Hogan EL. Calcium-activated neutral proteinase (CANP; calpain) activity in Schwann cells: immunofluorescence localization and compartmentation of mu- and mCANP. *J Neurosci Res* 1991; 29:346-54.
- Yoshimura N, Hatanaka M, Kitahara A, Kawaguchi N, Murachi T. Intracellular localization of two distinct Ca<sup>2+</sup>-proteases (calpain I and calpain II) as demonstrated by using discriminative antibodies. *J Biol Chem* 1984; 259:9847-52.
- Kawasaki H, Kawashima S. Regulation of the calpain-calpastatin system by membranes (review). *Mol Membr Biol* 1996; 13:217-24.
- Crawford C, Brown NR, Willis AC. Studies of the active site of m-calpain and the interaction with calpastatin. *Biochem J* 1993; 296:135-42.
- Cottin P, Vidalenc PL, Ducastraing A. Ca<sup>2+</sup>-dependent association between a Ca<sup>2+</sup>-activated neutral proteinase (CaANP) and its specific inhibitor. *FEBS Lett* 1981; 136:221-4.
- Croall DE, McGrody KS. Domain structure of calpain: mapping the binding site for calpastatin. *Biochemistry* 1994; 33:13223-30.
- Sorimachi H, Kinbara K, Kimura S, Takahashi M, Ishiura S, Sasagawa N, et al. Muscle-specific calpain, p94, responsible for limb girdle muscular dystrophy type 2A, associates with connexin through IS2, a p94-specific sequence. *J Biol Chem* 1995; 270:31158-62.
- Maki M, Bagci H, Hamaguchi K, Ueda M, Murachi T, Hatanaka M. Inhibition of calpain by a synthetic oligopeptide corresponding to an exon of the human calpastatin gene. *J Biol Chem* 1989; 264:18866-9.
- Maki M, Takano E, Osawa T, Ooi T, Murachi T, Hatanaka M. Analysis of structure-function relationship of pig calpastatin by expression of mutated cDNAs in *Escherichia coli*. *J Biol Chem* 1988; 263:10254-61.
- Kawasaki H, Emori Y, Imajoh-Ohmi S, Minami Y, Suzuki K. Identification and characterization of inhibitory sequences in four repeating domains of the endogenous inhibitor for calcium-dependent protease. *J Biochem (Tokyo)* 1989; 106:274-81.
- Planchon SM, Wuerzberger S, Frydman B, Witak DT, Hutson P, Church DR, et al. β-lapachone-mediated apoptosis in human promyelocytic leukemia (HL-60) and human prostate cancer cells: a p53-independent response. *Cancer Res* 1995; 55:3706-11.
- Wuerzberger SM, Pink JJ, Planchon SM, Byers KL, Bornmann WG, Boothman DA. Induction of apoptosis in MCF-7/WS8 breast cancer cells by β-lapachone. *Cancer Res* 1998; 58:1876-85.
- Planchon SM, Pink JJ, Tagliarino C, Bornmann WG, Varnes ME, Boothman DA. β-lapachone-induced apoptosis in human prostate cancer cells: involvement of nqo1/xip3. *Exp Cell Res* 2001; 267:95-106.
- Li CJ, Li YZ, Pinto AV, Pardee AB. Potent inhibition of tumor survival in vivo by β-lapachone plus taxol: combining drugs imposes different artificial checkpoints. *Proc Natl Acad Sci USA* 1999; 96:13369-74.
- Don MJ, Chang YH, Chen KK, Ho LK, Chau YP. Induction of CDK inhibitors (p21(WAF1) and p27(Kip1)) and Bak in the β-lapachone-induced apoptosis of human prostate cancer cells. *Mol Pharmacol* 2001; 59:784-94.
- Li Y, Li CJ, Yu D, Pardee AB. Potent induction of apoptosis by β-lapachone in human multiple myeloma cell lines and patient cells. *Mol Med* 2000; 6:1008-15.
- Pink JJ, Planchon SM, Tagliarino C, Varnes ME, Siegel D, Boothman DA. NAD(P)H:Quinone oxidoreductase activity is the principal determinant of β-lapachone cytotoxicity. *J Biol Chem* 2000; 275:5416-24.
- Marin A, Lopez de Cerain A, Hamilton E, Lewis AD, Martinez-Penuela JM, Idoate MA, et al. DT-diaphorase and cytochrome B5 reductase in human lung and breast tumours. *Br J Cancer* 1997; 76:923-9.
- Tagliarino C, Pink JJ, Dubyak GR, Nieminen AL, Boothman DA. Calcium Is a Key Signaling Molecule in β-Lapachone-mediated Cell Death. *J Biol Chem* 2001; 276:19150-9.
- Pink JJ, Wuerzberger-Davis S, Tagliarino C, Planchon SM, Yang X, Froelich CJ, et al. Activation of a cysteine protease in MCF-7 and T47D breast cancer cells during β-lapachone-mediated apoptosis. *Exp Cell Res* 2000; 255:144-55.
- Froelich CJ, Hanna WL, Poirier GG, Duriez PJ, D'Amours D, Salvesen GS, et al. Granzyme B/perforin-mediated apoptosis of Jurkat cells results in cleavage of poly(ADP-ribose) polymerase to the 89-kDa apoptotic fragment and less abundant 64-kDa fragment. *Biochem Biophys Res Commun* 1996; 227:658-65.
- Pariat M, Carillo S, Molinari M, Salvat C, Debussche L, Bracco L, et al. Proteolysis by calpains: a possible contribution to degradation of p53. *Mol Cell Biol* 1997; 17:2806-15.
- Kubbutat MH, Vousden KH. Proteolytic cleavage of human p53 by calpain: a potential regulator of protein stability. *Mol Cell Biol* 1997; 17:460-8.
- Nakagawa T, Yuan J. Cross-talk between two cysteine protease families. Activation of caspase-12 by calpain in apoptosis. *J Cell Biol* 2000; 150:887-94.
- Pink JJ, Bilimoria MM, Assikis J, Jordan VC. Irreversible loss of the oestrogen receptor in T47D breast cancer cells following prolonged oestrogen deprivation. *Br J Cancer* 1996; 74:1227-36.
- Bradford MM. A rapid and sensitive method for the quantitation of microgram quantities of protein utilizing the principle of protein-dye binding. *Anal Biochem* 1976; 72:248-54.
- Siegel D, Franklin WA, Ross D. Immunohistochemical detection of NAD(P)H:quinone oxidoreductase in human lung and lung tumors. *Clin Cancer Res* 1998; 4:2065-70.
- Zhang W, Lu Q, Xie ZJ, Mellgren RL. Inhibition of the growth of WI-38 fibroblasts by benzyloxycarbonyl-Leu-Leu-Tyr diazomethyl ketone: evidence that cleavage of p53 by a calpain-like protease is necessary for G1 to S-phase transition. *Oncogene* 1997; 14:255-63.
- Janicke RU, Ng P, Sprengart ML, Porter AG. Caspase-3 is required for alpha-fodrin cleavage but dispensable for cleavage of other death substrates in apoptosis. *J Biol Chem* 1998; 273:15540-5.
- McGinnis KM, Gnegy ME, Park YH, Mukerjee N, Wang KK. Procaspase-3 and poly(ADP-ribose) polymerase (PARP) are calpain substrates. *Biochem Biophys Res Commun* 1999; 263:94-9.
- Buki KG, Bauer PI, Kun E. Isolation and identification of a proteinase from calf thymus that cleaves poly(ADP-ribose) polymerase and histone H1. *Biochim Biophys Acta* 1997; 1338:100-6.
- Shea TB. Restriction of microM-calcium-requiring calpain activation to the plasma membrane in human neuroblastoma cells: evidence for regionalized influence of a calpain activator protein. *J Neurosci Res* 1997; 48:543-50.
- Nagao S, Saido TC, Akita Y, Tsuchiya T, Suzuki K, Kawashima S. Calpain-calpastatin interactions in epidermoid carcinoma KB cells. *J Biochem (Tokyo)* 1994; 115:1178-84.
- Suzuki K, Imajoh S, Emori Y, Kawasaki H, Minami Y, Ohno S. Calcium-activated neutral protease and its endogenous inhibitor. Activation at the cell membrane and biological function. *FEBS Lett* 1987; 220:271-7.
- Mohan PS, Nixon RA. Purification and properties of high molecular weight calpastatin from bovine brain. *J Neurochem* 1995; 64:859-66.
- Maki M, Takano E, Mori H, Sato A, Murachi T, Hatanaka M. All four internally repetitive domains of pig calpastatin possess inhibitory activities against calpains I and II. *FEBS Lett* 1987; 223:174-80.



44. Emori Y, Kawasaki H, Imaoh S, Minami Y, Suzuki K. All four repeating domains of the endogenous inhibitor for calcium-dependent protease independently retain inhibitory activity. Expression of the cDNA fragments in *Escherichia coli*. *J Biol Chem* 1988; 263:2364-70.
45. Takano J, Watanabe M, Hitomi K, Maki M. Four types of calpastatin isoforms with distinct amino-terminal sequences are specified by alternative first exons and differentially expressed in mouse tissues. *J Biochem (Tokyo)* 2000; 128:83-92.
46. Sasaki T, Kishi M, Saito M, Tanaka T, Higuchi N, Kominami E, et al. Inhibitory effect of di- and tripeptidyl aldehydes on calpains and cathepsins. *J Enzyme Inhib* 1990; 3:195-201.
47. Rock KL, Gramm C, Rothstein L, Clark K, Stein R, Dick L, et al. Inhibitors of the proteasome block the degradation of most cell proteins and the generation of peptides presented on MHC class I molecules. *Cell* 1994; 78:761-71.
48. Schoenwaelder SM, Burridge K. Evidence for a calpeptin-sensitive protein-tyrosine phosphatase upstream of the small GTPase Rho. A novel role for the calpain inhibitor calpeptin in the inhibition of protein-tyrosine phosphatases. *J Biol Chem* 1999; 274:14359-67.
49. Spinelli A, Oliverio S, Di Sano F, Piacentini M. Calpain involvement in calphostin C-induced apoptosis. *Biochem Pharmacol* 1998; 56:1489-92.
50. Kapprell HP, Goll DE. Effect of  $\text{Ca}^{2+}$  on binding of the calpains to calpastatin. *J Biol Chem* 1989; 264:17888-96.
51. Lane RD, Allan DM, Mellgren RL. A comparison of the intracellular distribution of  $\mu$ -calpain, m-calpain, and calpastatin in proliferating human A431 cells. *Exp Cell Res* 1992; 203:5-16.
52. Yang CR, Leskov K, Hosley-Eberlein K, Criswell T, Pink JJ, Kinsella TJ, Boothman DA. Nuclear clusterin/XIP8, an x-ray-induced Ku70-binding protein that signals cell death. *Proc Natl Acad Sci USA* 2000; 97:5907-12.
53. Combadiere C, Pedrucci E, Hakim J, Perianin A. A protein kinase inhibitor, staurosporine, enhances the expression of phorbol dibutyrate binding sites in human polymorphonuclear leucocytes. *Biochem J* 1993; 289:695-701.
54. Tang D, Lahti JM, Kidd VJ. Caspase-8 activation and bid cleavage contribute to MCF7 cellular execution in a caspase-3-dependent manner during staurosporine-mediated apoptosis. *J Biol Chem* 2000; 275:9303-7.
55. Squier MK, Miller AC, Malkinson AM, Cohen JJ. Calpain activation in apoptosis. *J Cell Physiol* 1994; 159:229-37.
56. Waterhouse NJ, Finucane DM, Green DR, Elce JS, Kumar S, Alnemri ES, et al. Calpain activation is upstream of caspases in radiation-induced apoptosis. *Cell Death Differ* 1998; 5:1051-61.
57. Tenev T, Marani M, McNeish I, Lemoine NR. Pro-caspase-3 overexpression sensitizes ovarian cancer cells to proteasome inhibitors. *Cell Death Differ* 2001; 8:256-264.
58. Barrett AJ, Kembhavi AA, Brown MA, Kirschke H, Knight CG, Tamai M, et al. L-trans-Epoxy succinyl-leucylamido(4-guanidinyl)butane (E-64) and its analogues as inhibitors of cysteine proteinases including cathepsins B, H and L. *Biochem J* 1982; 201:189-98.
59. Thornberry NA, Lazebnik Y. Caspases: enemies within. *Science* 1998; 281(5381):1312-6.
60. Nicholson DW. Caspase structure, proteolytic substrates, and function during apoptotic cell death. *Cell Death Differ* 1999; 6:1028-42.
61. Meng RD, El-Deiry WS. p53-independent upregulation of KILLER/DR5 TRAIL receptor expression by glucocorticoids and interferon-gamma. *Exp Cell Res* 2001; 262:154-69.
62. Zheng TS, Hunor S, Kuida K, Flavell RA. Caspase knockouts: matters of life and death. *Cell Death Differ* 1999; 6:1043-53.
63. Ruiz-Vela A, Gonzalez de Buitrago G, Martinez AC. Implication of calpain in caspase activation during B cell clonal deletion. *Embo J* 1999; 18:4988-98.
64. Wood DE, Newcomb EW. Caspase-dependent activation of calpain during drug-induced apoptosis. *J Biol Chem* 1999; 274:8309-15.
65. Wang KK, Posmantur R, Nadimpalli R, Nath R, Mohan P, Nixon RA, et al. Caspase-mediated fragmentation of calpain inhibitor protein calpastatin during apoptosis. *Arch Biochem Biophys* 1998; 356:187-96.
66. Counis MF, Torriglia A. DNases and apoptosis. *Biochem Cell Biol* 2000; 78(4):405-14.
67. Liu X, Zou H, Widlak P, Garrard W, Wang X. Activation of the apoptotic endonuclease DFF40 (caspase-activated DNase or nuclease). Oligomerization and direct interaction with histone H1. *J Biol Chem* 1999; 274:13836-40.
68. Nath R, Raser KJ, Stafford D, Hajimohammadreza I, Posner A, Allen H, et al. Non-erythroid alpha-spectrin breakdown by calpain and interleukin 1 beta-converting-enzyme-like protease(s) in apoptotic cells: contributory roles of both protease families in neuronal apoptosis. *Biochem J* 1996; 319:683-90.
69. McGinnis KM, Whittom MM, Gnegy ME, Wang KK. Calcium/calmodulin-dependent protein kinase IV is cleaved by caspase-3 and calpain in SH-SY5Y human neuroblastoma cells undergoing apoptosis. *J Biol Chem* 1998; 273:19993-20000.
70. Croall DE, Morrow JS, DeMartino GN. Limited proteolysis of the erythrocyte membrane skeleton by calcium-dependent proteinases. *Biochim Biophys Acta* 1986; 882:287-96.
71. Sakai K, Akanuma H, Imahori K, Kawashima S. A unique specificity of a calcium activated neutral protease indicated in histone hydrolysis. *J Biochem (Tokyo)* 1987; 101(4):911-8.
72. Wang KK, Villalobo A, Roufogalis BD. Calmodulin-binding proteins as calpain substrates. *Biochem J* 1989; 262:693-706.
73. Murachi T, Tanaka K, Hatanaka M, Murakami T. Intracellular  $\text{Ca}^{2+}$ -dependent protease (calpain) and its high-molecular-weight endogenous inhibitor (calpastatin). *Adv Enzyme Regul* 1980; 19:407-24.
74. Kleese WC, Goll DE, Edmunds T, Shannon JD. Immunofluorescent localization of the  $\text{Ca}^{2+}$ -dependent proteinase and its inhibitor in tissues of *Crotalus atrox*. *J Exp Zool* 1987; 241:277-89.
75. Murachi T. Calcium-dependent proteinases and specific inhibitors: calpain and calpastatin. *Biochem Soc Symp* 1984; 49:149-67.
76. Schollmeyer JE. Calpain II involvement in mitosis. *Science* 1988; 240:911-3.
77. Beckerle MC, Burridge K, DeMartino GN, Croall DE. Colocalization of calcium-dependent protease II and one of its substrates at sites of cell adhesion. *Cell* 1987; 51:569-77.
78. Yoshimura N, Murachi T, Heath R, Kay J, Jasani B, Newman GR. Immunogold electron-microscopic localisation of calpain I in skeletal muscle of rats. *Cell Tissue Res* 1986; 244:265-70.
79. Barney S, Zipser Y, Glaser T, Grimberg Y, Kosower NS. Association of calpain ( $\text{Ca}^{2+}$ -dependent thiol protease) with its endogenous inhibitor calpastatin in myoblasts. *J Cell Biochem* 1999; 74:522-31.
80. Mellgren RL, Lu Q. Selective nuclear transport of  $\mu$ -calpain. *Biochem Biophys Res Commun* 1994; 204:544-50.
81. Tullio RD, Passalacqua M, Averna M, Salamino F, Melloni E, Pontremoli S. Changes in intracellular localization of calpastatin during calpain activation. *Biochem J* 1999; 343:467-72.
82. Arthur JS, Elce JS, Hegadorn C, Williams K, Greer PA. Disruption of the murine calpain small subunit gene, *Capn4*: calpain is essential for embryonic development but not for cell growth and division. *Mol Cell Biol* 2000; 20:4474-81.
83. Azam M, Andrabi SS, Sahr KE, Kamath L, Kuliopulos A, Chishti AH. Disruption of the mouse  $\mu$ -calpain gene reveals an essential role in platelet function. *Mol Cell Biol* 2001; 21:2213-20.